



Exploring new reactions with Organic Electron Donors and the complexities of the Birch reduction

Jonathan Chua, MSci


A thesis submitted to the University of Strathclyde in part fulfilment of regulations for the degree of PhD in Chemistry

WestChem, Department of Pure & Applied Chemistry, University of Strathclyde,
Thomas Graham Building, 295 Cathedral Street, Glasgow G1 1XL

Declaration of Authenticity and Author's Rights

'This thesis is the result of the author's original research. It has been composed by the author and has not been previously submitted for examination which has led to the award of a degree.'

'The copyright of this thesis belongs to the author under the terms of the United Kingdom Copyright Acts as qualified by University of Strathclyde Regulation 3.50. Due acknowledgement must always be made of the use of any material contained in, or derived from, this thesis.'

Signed: 

Date: 30/01/2016

Acknowledgements

I would like to thank Professor John A. Murphy for granting me the opportunity to pursue a Ph.D under your guidance and supervision. Your patience, motivation and encouragement have been helpful throughout the course of my studies.

To Doni and Steve O'Sullivan, you have both been a tremendous help especially when I first started the Ph.D. Not forgetting all the past and present JAM group members who have made my Ph.D experience most memorable.

I must thank Dr Sheng-ze Zhou for all his invaluable help practically and for all the important discussions we have had on the various research projects. Thanks for your patience in explaining new concepts and for all your advice.

I am grateful for all the assistance given to me by the technicians including Gavin Bain, Craig Irvine (NMR instrumentation), and Pat Keating (mass spectrometry analysis).

For funding my studies, I would like to thank WestCHEM, the University of Strathclyde and my parents.

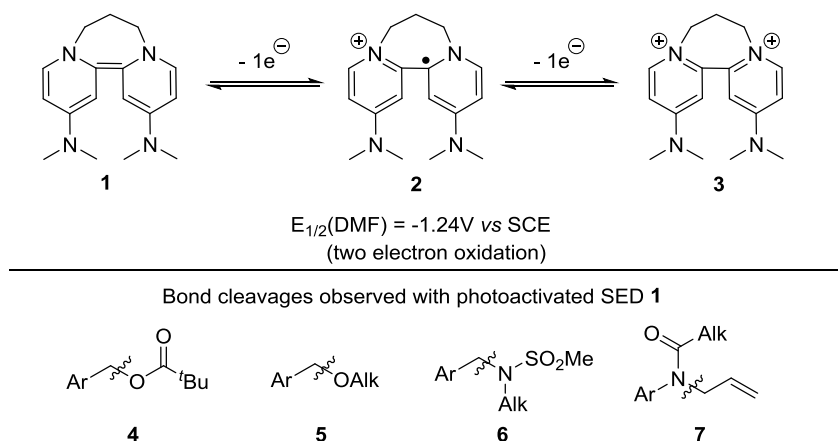
I wish to thank Kellie Bracegirdle at the University Chaplaincy centre. You have been very kind in allowing me to access the seminar room especially in the evening so that I could write this thesis with few distractions.

To my wife Jhenath, thank you for being a great help and support especially during this Ph.D programme. You have been there through the difficult times and I am very grateful for that. Thanks for always reminding me to look on the bright side of life!

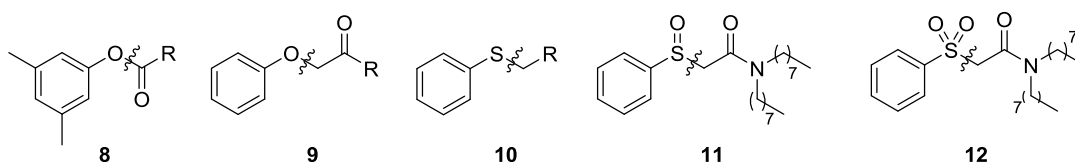
Outside university life, I would like to express thanks to my dear friend David. The care and kindness that you have shown to me since I first arrived in Glasgow has really made me feel at home.

Abstract

Reductive σ -bond cleavages of challenging substrates under metal-free, mild conditions have recently been achieved with photoactivated super-electron donor (SED) **1**. These include (but are not limited to) C-O bonds of benzylic ethers and esters i.e. **4** and **5**, C-N bonds of benzylic sulfonamides **6** and aromatic amides **7**.

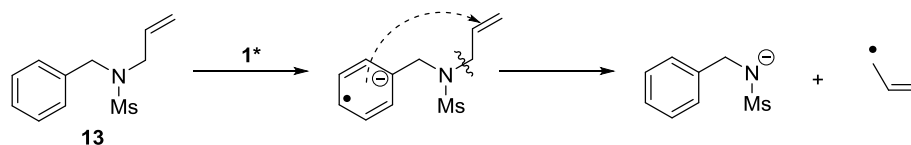


This work has successfully widened the substrate scope of reduction by SED **1** to include i) the C-O bond cleavages of phenolic esters **8** and aryl ethers **9** and ii) the C-S bond cleavages of aromatic sulfides **10**, sulfoxides **11** and sulfones **12**.

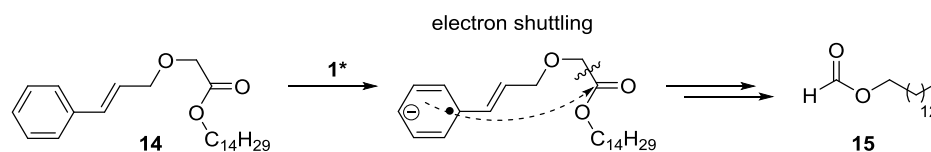


Previously, it was also discovered that the X-N bond of several amides e.g. **13** were reductively cleaved *via* intramolecular electron-shuttling instead of the more conventional through-bond electron transfer.

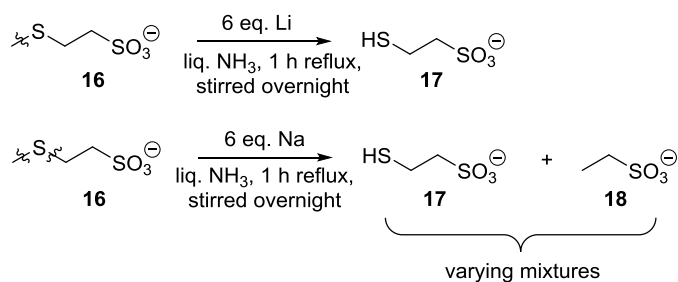
Previously disclosed intramolecular electron-shuttling effect



This mode of reduction by SED **1** is not well-explored. To this end, several ester and amide-based substrates were synthesised in an attempt to expand the scope of this electron-shuttling mechanism induced by SED **1**. This study has also been successful, with the electron-shuttling effect thought to be responsible for the C-C bond cleavage of **14**, resulting in the production of **15**.



Perhaps the most powerful reducing agent in synthetic chemistry is the “solvated electron” which is conveniently prepared during the Birch reduction. In this work, the Birch reduction conditions were successfully applied, in an unprecedented way, to the C-S bond cleavage of methyl-coenzyme M **16** (MeCoM). The experimental results have the potential to contribute significantly towards our current understanding of MeCoM reductase activity.



This study has also highlighted the complex nature of the Birch reduction; by simply switching from sodium to lithium, reactivity and regioselectivity could be significantly altered. Presently, some details of the mechanism for the observed reduction(s) remain unresolved.

Table of Contents

Abbreviations	3
Chapter 1: C-O bond cleavages.....	9
1.1 Benzylic ethers and alcohols	9
1.2 Aryl ethers	15
1.3 Benzoates.....	22
Chapter 2: C-S bond cleavages	25
2.1 Reductive cleavage.....	25
2.2 Oxidative cleavage	29
2.3 Biological relevance of C-S bond cleavage - Methanogenesis	32
2.3.1 Crystal structures of Methyl coenzyme M Reductase (MCR).....	33
2.3.2 Binding mode of coenzyme F ₄₃₀	37
2.3.3 Binding mode of coenzyme M (CoM).....	38
2.3.4 Binding mode of coenzyme B (CoB)	39
2.3.5 Conformational changes of CoB and CoM.....	40
2.3.6 Nucleophilic substitution mechanism.....	42
2.3.7 Radical-mediated mechanism	44
Chapter 3 Organic molecules as electron donors.....	47
Chapter 4 Organic molecules as super-electron donors.....	55
4.1 The development of DMAP-based super-electron donor.....	55
4.2 Reductions with Photoactivated SED 4.1.15	57
4.2.1 Benzylic C-O bond cleavages.....	57
4.2.2 C-N bond cleavages of activated amines and amides.....	61
4.2.3 Diphenyl Cyclopropanes C-C bond cleavage.....	64
4.3 Project Aims.....	66
Chapter 5 Results and Discussion – C-O bond cleavages.....	67
5.1 C-O bond cleavage of esters with extended conjugation.	67
5.2 C-O & C-C bond cleavages of esters and amides with aromatic auxiliaries....	81
5.3 C-O bond cleavage of phenolic esters.....	101

5.4 C-O bond cleavage of aryl ethers.....	115
Chapter 6 Results and Discussion - C-S bond cleavages.....	125
6.1 C-S bond cleavage of aromatic sulfur compounds.....	125
6.1.1 Aromatic sulfides.....	125
6.1.2 C-S bond cleavage of aromatic sulfoxides and sulfones.....	133
6.2 C-S Bond cleavage of non aromatic sulfides.....	143
Chapter 7 Experimental.....	171
7.1 General information.....	171
7.2 General procedures.....	173
7.3 Experimental for Chapter 5.1.....	174
7.4 Experimental for Chapter 5.2.....	188
7.5 Experimental for Chapter 5.3.....	208
7.6 Experimental for Chapter 5.4.....	222
7.7 Experimental for Chapter 6.1.....	234
7.8 Experimental for Chapter 6.2.....	255
Chapter 8 References.....	275

Abbreviations

°C	Degrees Celsius
A	Ampere
Ac	Acetyl
Å	Ångstrom
AIBN	Azobisisobutyronitrile
Anhy.	Anhydrous
APCI	Atmospheric pressure chemical ionisation
Aq.	Aqueous
Ar	Aryl
BMEA	Bismethoxyethylamine
bpy	2,2'-Bipyridine
Bu	Butyl
cat.	Catalyst
Cgr	Control gate electrode
CI	Chemical ionisation
cm	Centimetre
CoB	Coenzyme B
COD	Cyclooctadiene
CoM	Coenzyme M
CP	Cyclopropane

Cyp	Cyclopentyl
Cy	Cyclohexyl
d	Doublet
DBB	di- <i>tert</i> -Butylbiphenyl
DBD	Doubly-bridged donor
DBU	1,8-Diazabicycloundec-7-ene
DCE	1,2-Dichloroethane
DCM	Dichloromethane
de	Diastereomeric excess
Decomp.	Decomposed
DEAD	Diethyl azodicarboxylate
DET	Double electron transfer
DIBAL-H	Diisobutylaluminium hydride
DIPEA	<i>N,N</i> -diisopropylethylamine
DMA	Dimethylacetamide
4-DMAP	4 Dimethylaminopyridine
DME	1,2-Dimethoxyethane
DMF	<i>N,N</i> -Dimethylformamide
DMSO	Dimethyl sulfoxide
DP	Diarylpropanes
e ⁻	Electron
e.g.	exempli gratia (for example)

EI	Electron ionisation
eq.	Equivalent (s)
ESI	Electrospray ionisation
ESR	Electron spin resonance
g	Gram(s)
GC	Gas-phase chromatography
h	Hour
HMPA	Hexamethylphosphoramide
HNESF	high resolution nano-electrospray
HOMO	Highest occupied molecular orbital
h ν	Irradiation
Hz	Hertz
i.e.	<i>id est</i> (that is)
IR	Infrared
J	Coupling constant
Kcal	kilocalories
KHMDS	Potassium bis (trimethylsilyl) amide
L	Ligand
LDA	Lithium diisopropylamide
LED	Light-emitting diode
Liq.	Liquid
LUMO	Lowest unoccupied molecular orbital

<i>m</i>	Meta
Mol	Molar (mole/litre)
<i>m</i> -CPBA	<i>meta</i> -Chloroperbenzoic acid
MCR	Methyl coenzyme M reductase
MeCoM	methyl coenzyme M
mg	Milligram
min	Minute
mL	Millilitre
mol	Mole
M.pt.	Melting point
MPM	Mole percentage of metal
Ms	Mesyl (methanesulfonyl)
MS	Mass spectrometry
NAD	Nicotinamide adenine dinucleotide
NADH	Reduced nicotinamide adenine dinucleotide
NBS	<i>N</i> -Bromosuccinimide
NHE	Normal hydrogen electrode
nm	nanometre
NMP	<i>N</i> -Methyl-2-pyrrolidone
NMQ	<i>N</i> -Methylquinolinium
NMR	Nuclear magnetic resonance
<i>nOe</i>	Nuclear Overhauser effect

<i>o</i>	<i>Ortho</i>
<i>p</i>	<i>Para</i>
PET	Photo-induced electron transfer
Ph	Phenyl
Piv	Pivaloyl
PMB	<i>para</i> -methoxybenzyl
ppm	Parts per million
ppy	2-Phenylpyridine
Pr	Propyl
<i>p</i> TSA	<i>para</i> -Toluenesulfonic acid
q	Quartet
RB	Round-bottomed
r.t.	Room temperature
s	Singlet
sat.	Saturated
SCE	Saturated calomel electrode
SED	Super-electron donor
SET	Single electron transfer
SHE	Standard hydrogen electrode
S.M.	Starting material
t	Triplet
TDAE	1,1,2,2-Tetra(dimethylamino)ethene

TEMPO	(2,2,6,6-tetramethylpiperidiny-1-yl)oxidanyl
THF	Tetrahydrofuran
TLC	Thin layer chromatography
TMEDA	Tetramethylethylenediamine
TTF	Tetrathiafulvalene
UV	Ultra-violet
<i>vs.</i>	Versus
V	Volt
δ	Chemical shift

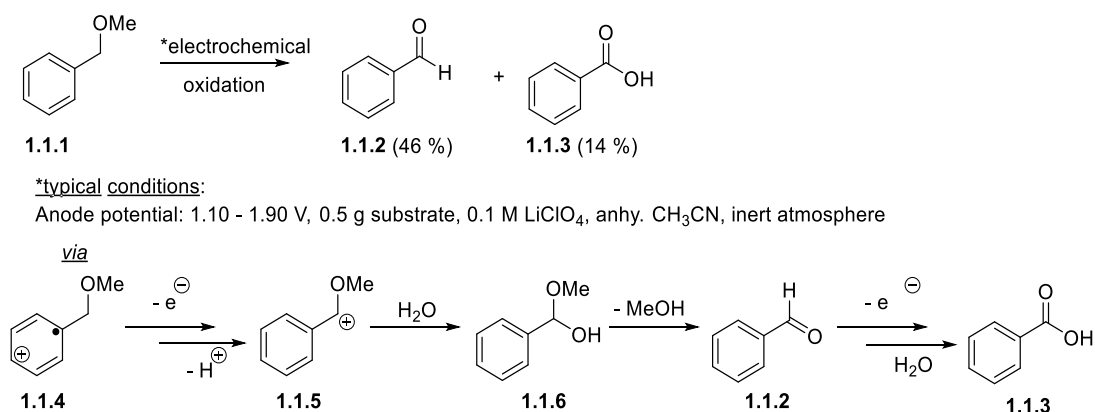
Chapter 1: C-O bond cleavages

Part of this Ph.D. project involved the exploration of reductive C-O bond cleavages using a super electron donor. This being the case, a review on the current methods for C-O bond reduction is provided.

1.1 Benzylic ethers and alcohols

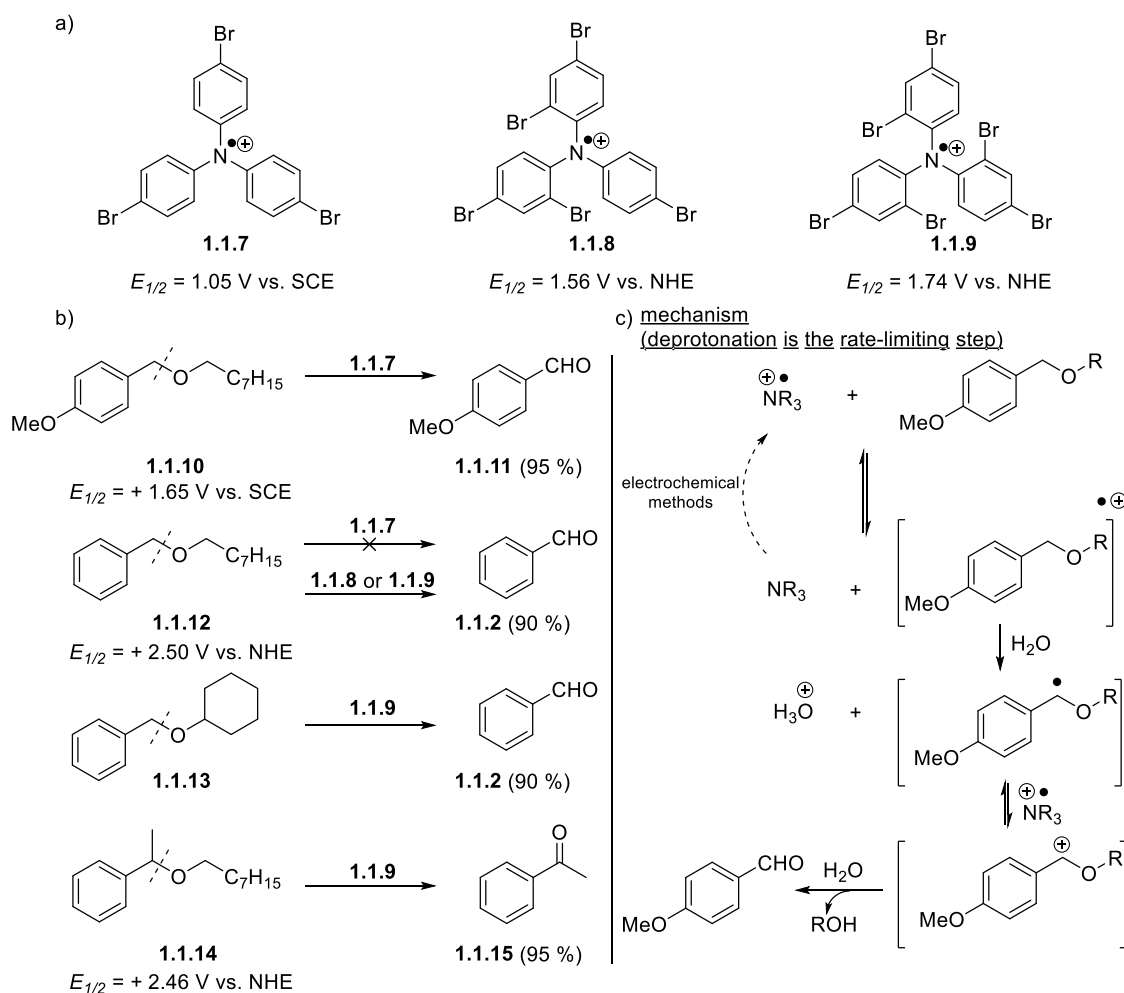
Benzylic ethers are common functional groups employed for the protection of the corresponding alcohols.¹ It is therefore not surprising that there are numerous methods for their cleavage.² For a long time, strong acids e.g. HI, HBr,³ cerium ammonium nitrate⁴⁻⁶ i.e. $\text{Ce}(\text{NH}_4)_2(\text{NO}_3)_6$, 2,3-dichloro-5,6-dicyano-1,4-benzoquinone⁷ i.e. DDQ, organo-alkali metals⁸⁻⁹ various electrochemical methods¹⁰ and hydrogenolysis¹¹ were routinely employed. More recently, reagents which are more selective or that can be used under more benign conditions have been developed for this purpose.

Early research in this field had shown that the benzylic C-O oxidative cleavage was possible using strictly controlled anodic oxidation (Scheme 1.1.1).¹²⁻¹³ However, there were major setbacks in this technique including: i) the appreciable drop in reactivity upon compromise of the anode. This passivation of the anode was inevitable during the course of the reaction and led to irreproducible or inconsistent experimental results. ii) the over-oxidation of the substrate. Although benzylic ethers e.g. **1.1.1** were found to be easily oxidised under such conditions, these were routinely oxidised further to give mixtures of aldehydes e.g. **1.1.2** and acids e.g. **1.1.3**



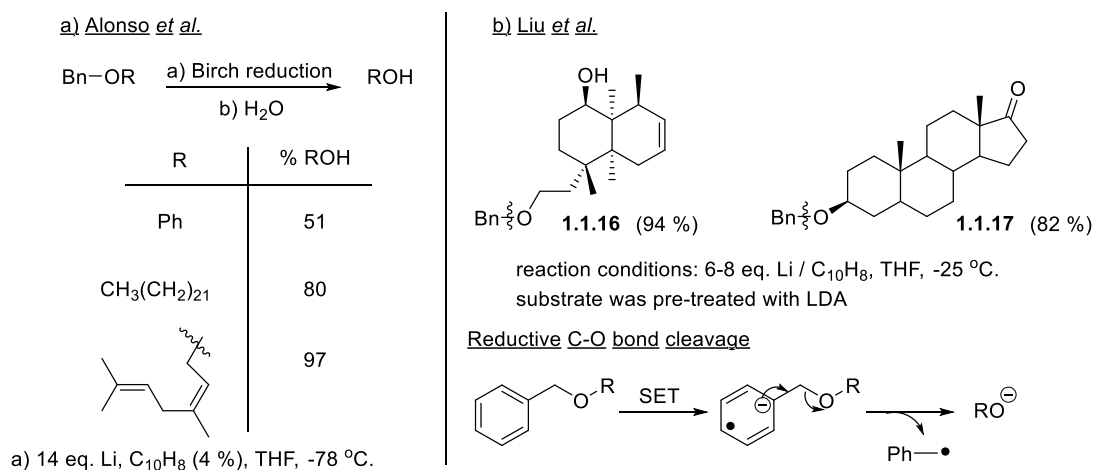
Scheme 1.1.1 Oxidative cleavage of benzylic ethers using electrochemical methods.

Steckhan *et al.*¹⁴ provided an alternative method which involved homogeneous electron transfer from the substrate to tertiary amine radical cations. The parent amine, which is relatively easy to synthesise¹⁴⁻¹⁶ can then be electrochemically oxidised to obtain the reactive oxidant (Scheme 1.1.2). These amines could be exploited as suitable reagents because of their relatively high redox potential and so are able to facilitate SET from the ether substrate. Aminium salt **1.1.7** specifically cleaves PMB ethers even in the presence of benzylic ethers.¹⁴ In contrast, aminium salts **1.1.8** or **1.1.9** which have higher reduction potentials can accomplish oxidative C-O bond cleavages¹⁷⁻¹⁹ of more challenging substrates (Scheme 1.1.2 b). The mechanism consisted of a stepwise SET, deprotonation, SET and hydrolysis (Scheme 1.1.2 c).



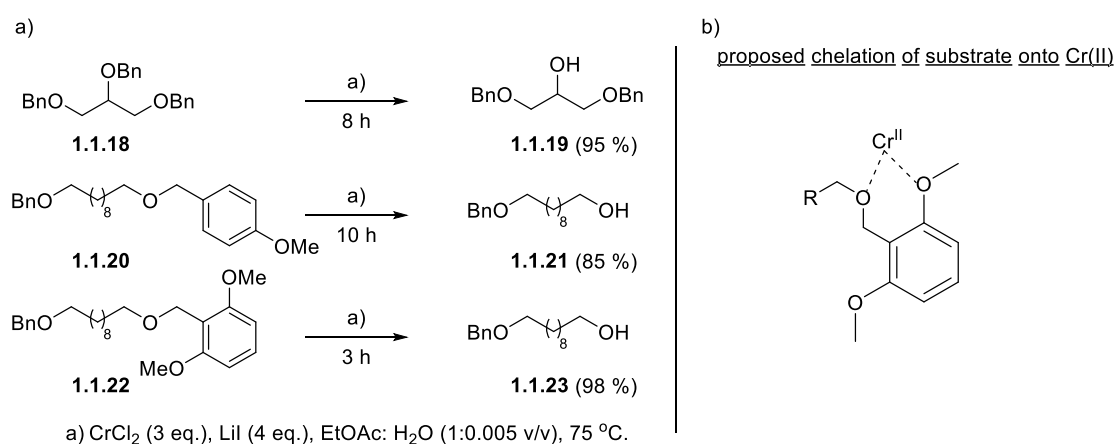
Scheme 1.1.2. Oxidative C-O bond cleavage of benzylic ethers was possible using amine radical cations as redox partners as shown by Steckhan *et al.*¹⁸

Benzylic C-O bond cleavage is not limited to oxidative methods as shown above; the modified Birch reduction has also been successfully employed for this transformation. Lithium naphthalenide, generated *in situ* from lithium powder and naphthalene dissolved in liquid NH₃, was developed by Alonso *et al.*⁹ and then later exploited by Liu *et al.* for selective debenylation in their studies on terpenes²⁰ (Scheme 1.1.3).



Scheme 1.1.3. Birch reduction using lithium naphthalenide was utilised by Alonso *et al.*⁹ and Liu *et al.*²⁰

Benzylic C-O cleavage can also be conducted using lithium iodide in combination with salts of transition²¹ or rare earth metals²² that have the ability to coordinate with oxygen. Upon coordination with the benzylic fragment of the substrate, the C-O bond weakens and a subsequent attack by a suitable nucleophile results in the observed debenylation (Scheme 1.1.4).

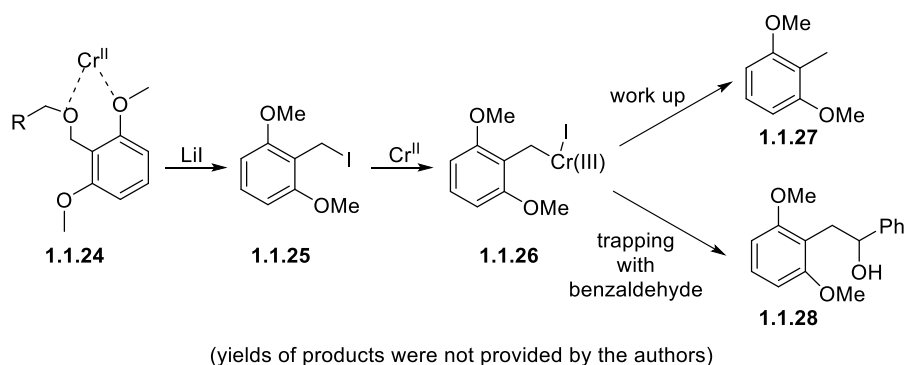


Scheme 1.1.4. a) C-O cleavage of benzylic ethers was achieved using CrCl₂ as shown by Falck *et al.*²³ b) A cyclic intermediate was proposed for the bond-cleavage mechanism.

A versatile method was developed by Falck *et al.*²³ in which a mixture of CrCl₂ and LiI in moist EtOAc was successfully employed to specifically mono-debenzylate a wide range of substrates (Scheme 1.1.4).

Falck *et al.* further observed that selective debenzylation occurred at the 2,6-dimethoxy-type fragment in the case of **1.1.22** which suggested that a chelation mechanism was involved during the reaction (Scheme 1.1.4 b). The 2,6-dimethoxy fragment provided more extensive coordination with the chromium centre, hence the observed selectivity.

The proposed mechanism was also supported by the successful conversion of the 2,6-dimethoxybenzyl iodide by-product **1.1.25** to its organometallic Cr^{III} species which was then trapped with benzaldehyde or isolated as 2,6-dimethoxytoluene **1.1.27** upon work up with water (Scheme 1.1.5).²⁴

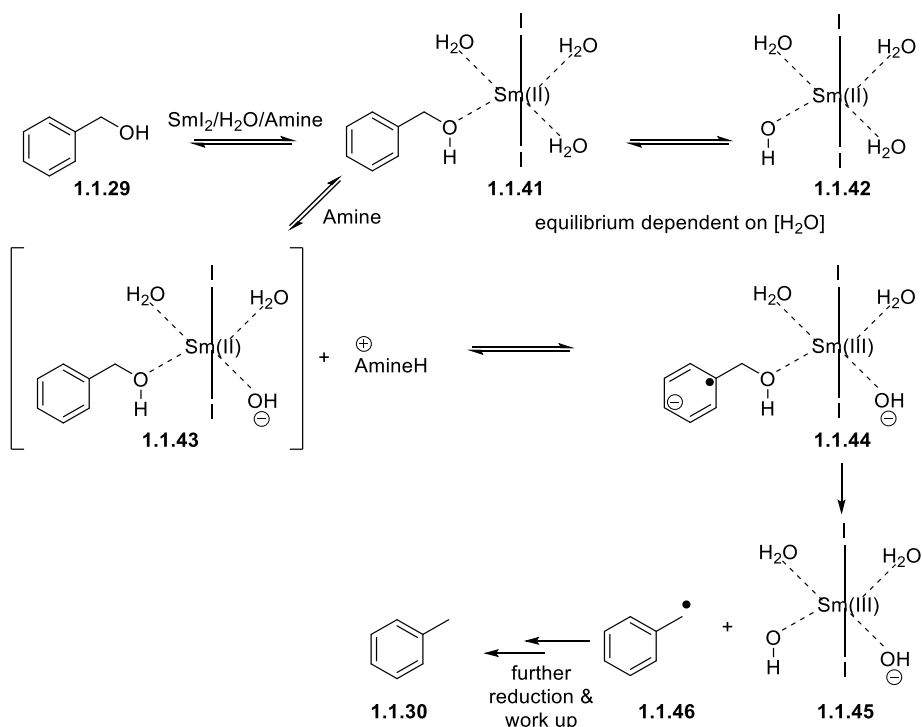
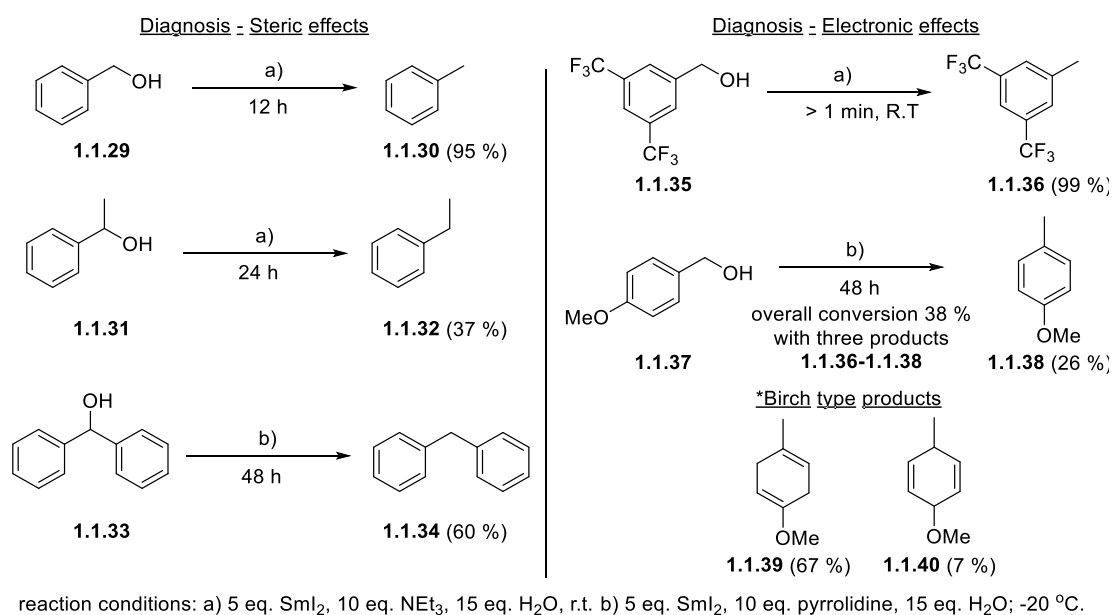


Scheme 1.1.5. Further evidence for the proposed mechanism stemmed from the successful trapping of the benzyl iodide fragment **1.1.25** with benzaldehyde to yield **1.1.28**.

This methodology tolerated several functional groups including alkenes, silanes, esters and acetals, thereby proving to be an attractive alternative to other conventional debenzylation methods including the Birch reduction, H₂/Pd and Me₃SiI.²⁵ Indeed, Piancatelli specially chose the CrCl₂/LiI methodology in the synthesis of isoxazole-containing natural products.²⁶

Samarium-based reagents have also shown to be a versatile reagent for this chemistry. It has been previously reported that pre-activated C-O bonds cleaved readily when SmI₂ was used with a suitable proton source.²⁷⁻²⁹ More recently, Hilmersson and Ankner refined this chemistry further³⁰ and developed a reagent mixture

(SmI₂/H₂O/amine) which could reductively cleave C-O bonds of benzylic alcohols without any prior activation of the substrate. It was discovered that both steric and electronic factors were crucial for the success of the cleavage (Scheme 1.1.6 a).



Scheme 1.1.6. a) Samarium-based reagents could reductively cleave benzylic C-O bonds. Both electronic and steric effects were important. b) The reduction proceeded *via* inner sphere electron transfer from Sm to the benzylic moiety.

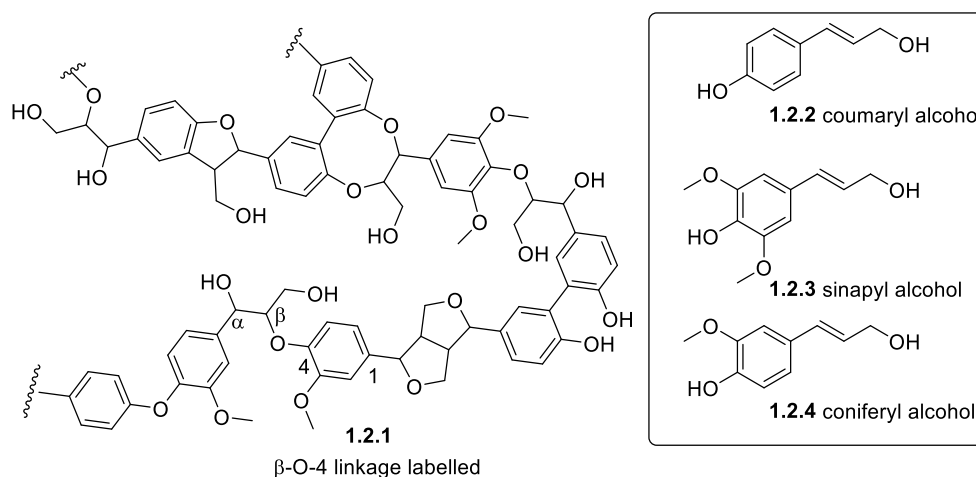
The team conducted kinetic studies which further revealed that the reaction was heavily dependent on the concentration of water present in the reaction. At low concentrations (24-300 mM) the rate order fluctuated; as the concentration was increased a steady first-order rate was achieved and upon increasing the concentration further a zero rate order was measured. Increasing the concentration even further ($[\text{H}_2\text{O}] > 300 \text{ mM}$) saw a dramatic drop in the rate.

These results reflected the importance of controlled coordination of water to the metal centre. As water is a stronger ligand than benzyl alcohol, increasing its concentration would result in it out-competing the alcohol for complexation with samarium, thereby stalling the reaction. Furthermore, the requirement for the benzyl alcohol to coordinate with the metal centre meant that the reaction proceeded *via* an inner-sphere electron transfer process (Scheme 1.1.6 b).

1.2 Aryl ethers

One of the key developing applications for C-O bond cleavage of organic molecules is in lignin degradation. This class of natural product (Figure 1.2.1) is the second most abundant source of renewable carbon after cellulose. During the production of bioethanol from cellulose, large amounts of lignin are generated as a by-product which, to date, has very little use. This has encouraged researchers to develop methods to exploit this highly abundant natural resource. Research efforts so far have their focus heavily on the controlled depolymerisation of lignin.³¹ When successfully applied, the products afforded from lignin are compounds which could be used as fine chemicals.³² Alternatively, the aromatic ether units in lignin can be used as high energy fuel stock.³³⁻³⁵ However, depolymerisation of this natural heterobiopolymer suffers greatly from the lack of selectivity and requires both high temperature and pressure, thereby making this methodology industrially unattractive and costly.^{31,34}

Figure 1.2.1. Polymeric structure of lignin. Inset: the three most prevalent biosynthetic precursors in lignin.

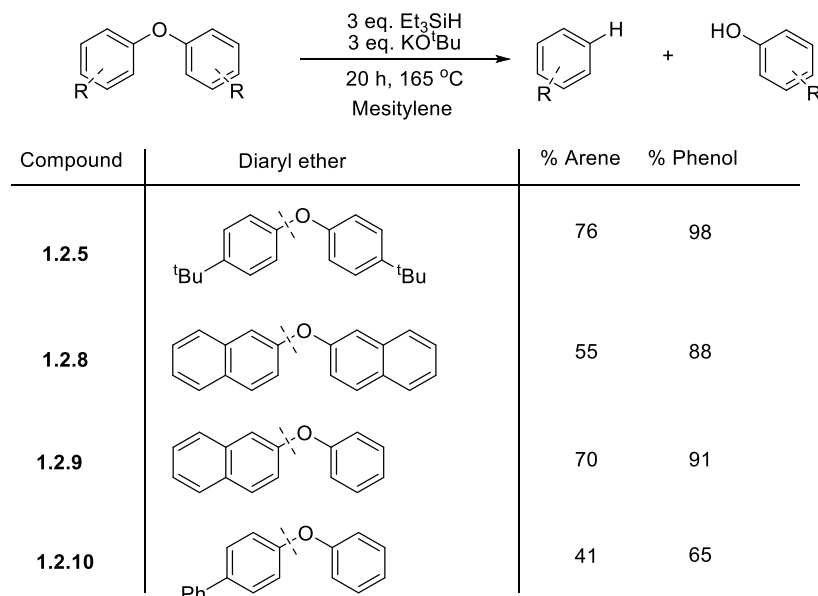


Essentially lignin derives from three types of phenylpropanols; coumaryl, sinapyl and coniferyl alcohols (Figure 1.2.1, **1.2.2-1.2.4**). Selective C-O bond cleavage must be achieved in order to obtain derivatives of these alcohols.³⁵⁻³⁶

Aryl C-O bond cleavage can be challenging due to the strength and stability of the bond. Several research groups have successfully employed reductants for such cleavages which broadly fall under metal-based or metal-free reaction conditions.

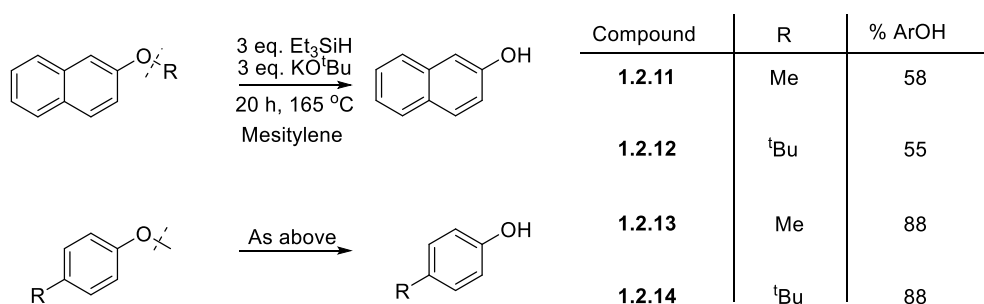
In a separate account, Grubbs *et al.*⁴¹ developed reaction conditions which purportedly created a powerful silane-based reductant that efficiently cleaved C_{Ar}-O bonds (Table 1.2.3).

Table 1.2.3. Ar(C)-O bond cleavage of biphenyl ethers proceeded in good yields using a silane-based reductant.⁴¹



While expanding the scope of silane-based reduction to alkyl aryl ethers (Table 1.2.4), it was also discovered that the alkyl C-O bond scission was preferred – this is in contrast to the results from Sergeev’s work when the nickel carbene was utilised (see Table 1.2.2 b).

Table 1.2.4. Reductive cleavage of alkyl aryl ethers using Et₃SiH under basic conditions showed regioselectivity.⁴¹

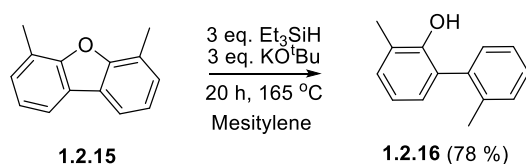


The reaction mechanism is yet to be firmly established. However, it was inferred that reactivity is not *via* a benzyne mechanism. This was shown by the successful C-O bond reduction of **1.2.15** to yield **1.2.16** in good yield (Scheme 1.2.5). This reduction

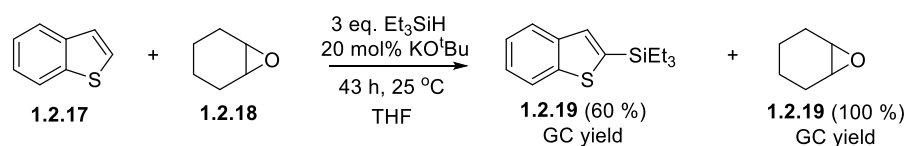
is thought to proceed *via* SET onto the substrate. Moreover, the reaction mixtures during the reaction were found to be ESR active thus indicating the possibility of a radical mechanism.

In a later study,⁴² epoxide **1.2.18** did not undergo ring-opening thereby indicating that silyl anions were not present⁴³ (Scheme 1.2.5 b). Considering these factors, it was possible that the reduction involved the initial attack of a silyl radical (generated *in situ*) with a suitable aryl partner which, upon subsequent deprotonation, forms a reductant e.g. **1.2.21** that readily transferred an electron onto the ether substrate **1.2.22** (Scheme 1.2.5 c).

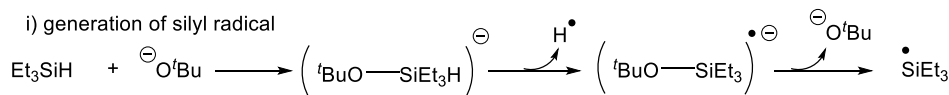
a) benzyne-based mechanism is not involved



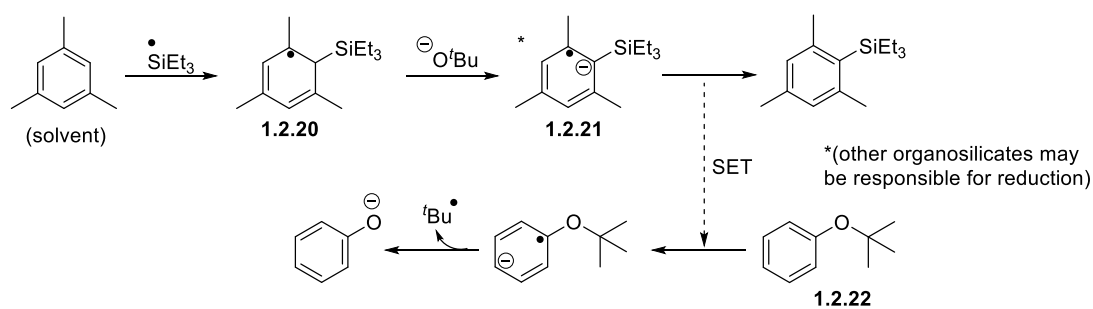
b) nucleophilic silates are also not involved



c) possible radical mediated pathway



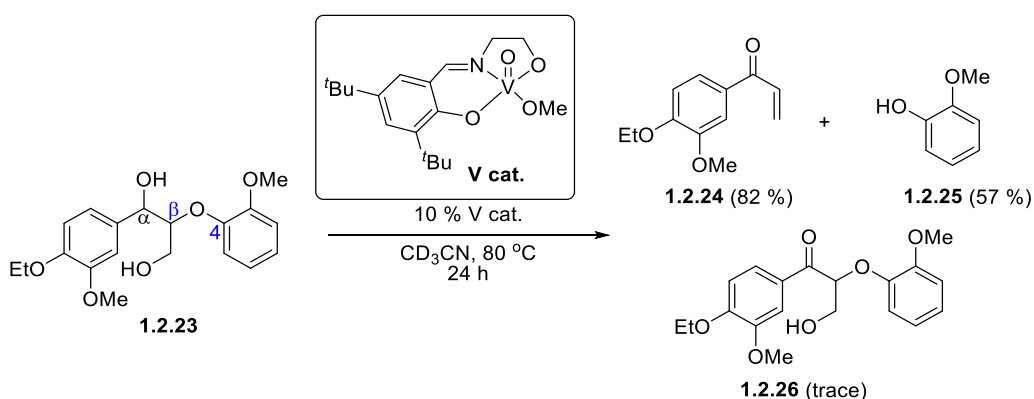
ii) reductive C-O bond cleavage mediated by silyl radical



Scheme 1.2.5. a) Benzyne and b) Silyl anions were not responsible for the observed reactivity. c) A SET radical-based mechanism could account for the observed C-O bond cleavage.

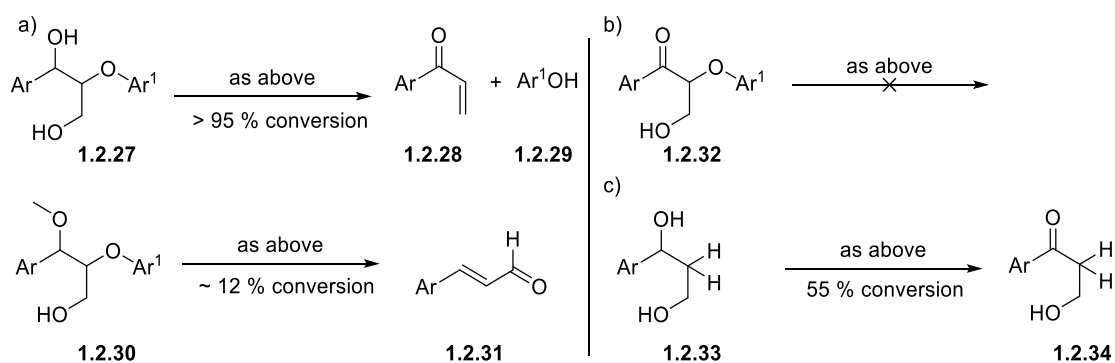
Son and Toste⁴⁴ focused their research on lignin degradation on a particular template **1.2.23** which contained the β -O-4 linkage commonly found in lignin (Scheme 1.2.6).

In so doing, they successfully developed a method which utilised a vanadium catalyst to facilitate the redox-neutral cleavage of **1.2.23** in good yields. The exclusion of oxygen was found to be detrimental for the reaction.



Scheme 1.2.6. A vanadium catalyst was used by Son and Toste to reductively cleave the ArO-C bond in **1.2.23**.⁴⁴

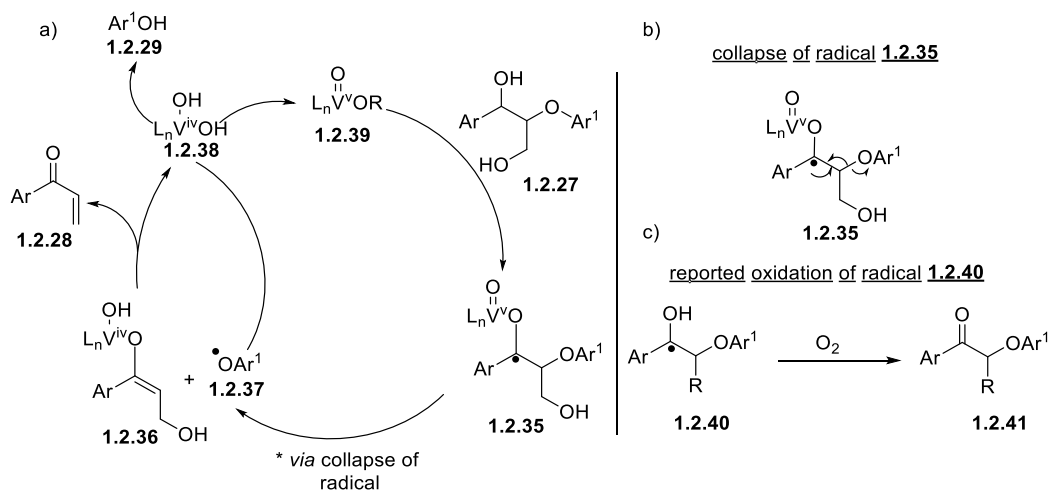
Further mechanistic studies also revealed several key parameters for the reaction: i) a benzylic alcohol was essential as this allowed coordination with the catalyst (Scheme 1.2.7 a.). ii) the reaction did not proceed *via* oxidation to a ketone prior to C-O bond cleavage (Scheme 1.2.7 b.). iii) the Ar¹O- fragment is necessary for the C-O cleavage; its absence led to **1.2.34** as the sole product (Scheme 1.2.7 c).



Scheme 1.2.7. Test substrates provided mechanistic details for the observed C-O bond cleavage.

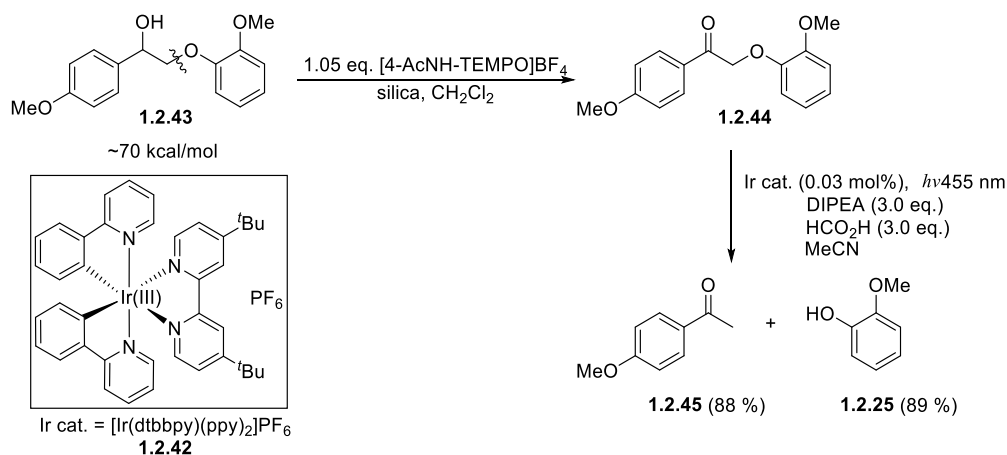
A catalytic cycle was proposed as shown in Scheme 1.2.8 a. The key to this reaction was the formation of radical **1.2.35** which preferentially collapsed to expel the phenyl radical. This remains contentious as the radical **1.2.40** was reported, in a separate account, to oxidise under aerobic conditions to yield the corresponding ketone **1.2.41** (Scheme 1.2.8 c.).⁴⁵ Nevertheless, another useful methodology for

quantitative and selective C-O cleavage of lignin has been developed using a homogeneous vanadium catalyst.



Scheme 1.2.8. a) The proposed catalytic vanadium cycle. b) The collapse of benzylic radical **1.2.35** is crucial in this mechanism. c) Radical **1.2.40** was reported to preferentially oxidise to the ketone instead of fragmenting.⁴⁵

In recent years, photoredox catalysis has come to the fore in research.⁴⁶⁻⁴⁸ In particular, this powerful technique allows chemical transformations to proceed under benign conditions that are often chemo- and regioselective.⁴⁹ Stephenson *et al.*³⁶ employed **1.2.43** in a reductive photoredox catalytic fashion when conducting studies on lignin degradation (Scheme 1.2.9).

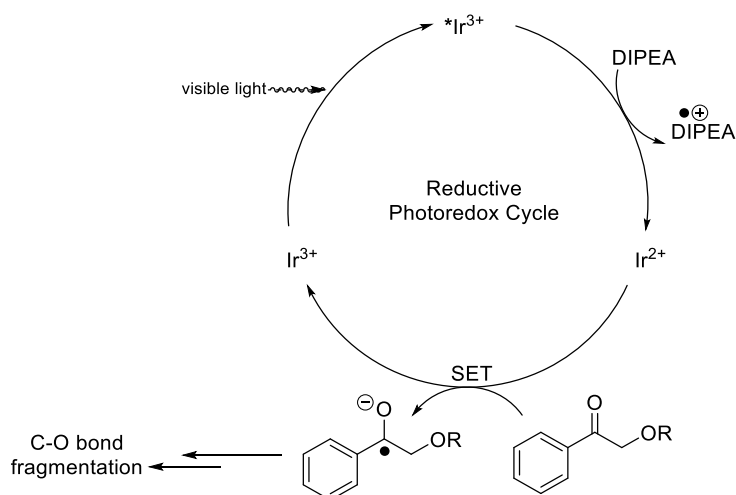


Scheme 1.2.9. Photoredox catalysis using the iridium(III) complex **1.2.42** successfully reduced **1.2.43** in good yield.³⁶

This method was even more powerful when coupled with the flow-technique which improved the yields and minimised solvent usage. Conducting the reaction at room

temperature also suppressed the undesired degradation of both the substrates and reagents.

The proposed mechanism³⁶ (Scheme 1.2.10) involved the initial excitation of the Ir(III) catalyst *via* metal-to-ligand charge transfer. The excited catalyst proceeded to accept an electron from the amine DIPEA, in the process creating a strong reductant ($[\text{Ir}]^{2+}$ $E_{1/2} = -1.51$ vs. SCE) which could reduce the aryl ether substrate.



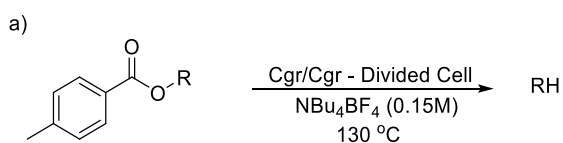
Scheme 1.2.10. The proposed catalytic cycle involved in the reductive C-O bond cleavage of lignin-based substrates.³⁶

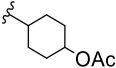
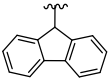
Although lignin degradation remains a formidable challenge on an industrial scale, this subject has continued to arouse interest among researchers. With increasing pressure to develop more sustainable and environmentally friendly processes, attractive methods toward lignin degradation may require transition metal-free and redox-neutral catalysis.

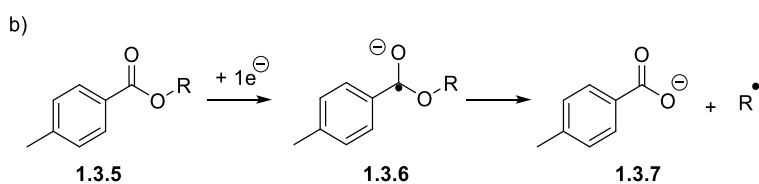
1.3 Benzoates

Besides ethers, esters can also be subjected to reductive C-O bond cleavages as shown by Marko *et al.*⁵⁰⁻⁵² The team successfully developed a methodology to reduce esters using a divided H-type cell with graphite electrodes. The *p*-toluate functional group was selected for its accessible redox potential under the electrochemical conditions employed ($E_{1/2} = -2.60$ V vs Ag/AgCl). The method involved a custom-made electrochemical cell which allowed for a refluxing system of NMP/THF mixture (optimal temperature of 100 °C). When employed, a wide range of toluates were reduced in moderate to good yields (Table 1.3.1 a).

Table 1.3.1. a) Electrochemical methods were employed in the reductive C-O bond cleavage of toluates.⁵¹ b) Fragmentation of radical anion 1.3.6 afforded the benzoate 1.3.7 and its corresponding alkyl radical.



Entry	R	RH (%)
1.3.1	1-Adamantyl	85
1.3.2		72
1.3.3	${}^n\text{C}_{22}\text{H}_{45}$	41
1.3.4		38



Cyclic voltammetry studies indicated that it was most likely for the C-O bond cleavage to occur at the stage of the radical anion **1.3.6** (Table 1.3.1 b). Further studies also revealed that the reduction rate was heavily dependent on the stability of the resulting radical fragment.

Very recently, it was shown by Reiser *et al.* that photoredox catalysis could also reductively cleave the C-O bond of 3,5-bis(trifluoromethyl) benzoates.⁵³ By

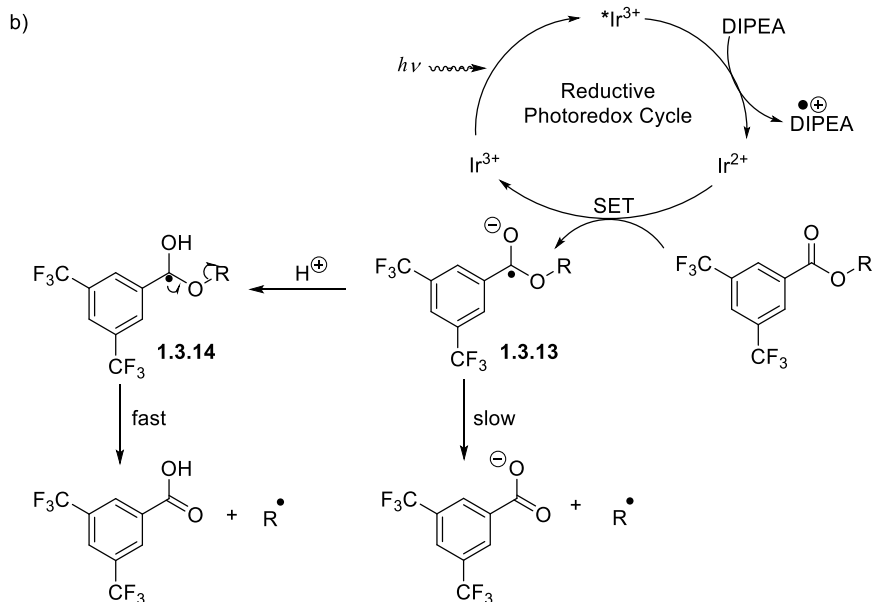
photoexciting Ir[(dtbbpy)(ppy)₂](PF₆) **1.2.42** with blue light, a wide range of benzoates was reduced in good yields (Table 1.3.2 is not exhaustive).

Table 1.3.2. a) Several benzoates were successfully reduced by employing photoredox catalysis with the iridium complex 1.2.42. b) Proposed mechanism for the reductive C-O bond cleavage of the benzoates.⁵³

a)

R	% RH
	91 %
	87 %
	86 %
	99 %

Ir cat. **1.2.42**



Further studies suggested that the reaction proceeded *via* a reductive quenching cycle of the photocatalyst (Table 1.3.2 b). Based on computational investigations it was

also discovered that protonation of radical anion **1.3.13** would significantly speed up the reaction as the spin density of radical **1.3.14** was now shifted onto the C-O σ^* orbital.

This chapter has illustrated several different methods and conditions (metal-based and metal-free) to cleave C-O bonds contained in different functional groups under reductive and oxidative conditions. The bond itself can also be reduced in more than one fashion and the challenge therefore, is to achieve good regioselectivity in the cleavage. The methods disclosed in this chapter highlight the recent progress made by different research groups to achieve regioselective reduction.

A potentially very important application of C-O bond cleavages has been described. In the case of lignin degradation, greener and more benign reaction conditions are still being sought. To date, redox catalysis has shown to be a useful methodology in this field. Ultimately, a metal-free, catalytic method, which can proceed under benign conditions would be very attractive.

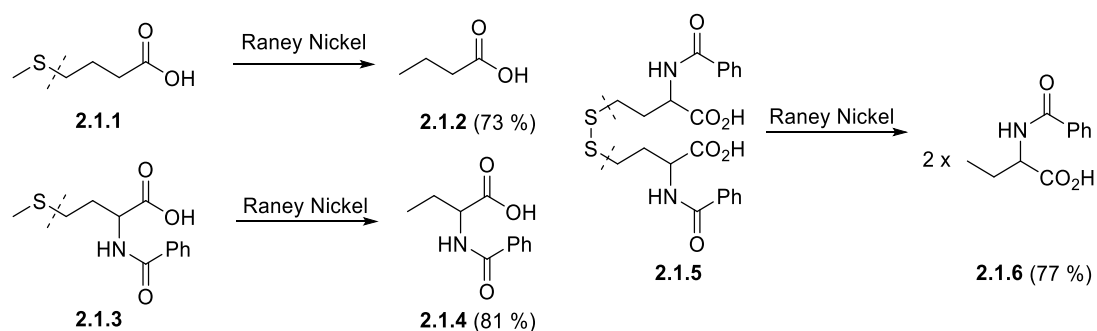
Chapter 2: C-S bond cleavages

2.1 Reductive cleavage

i) Nickel-based reagents

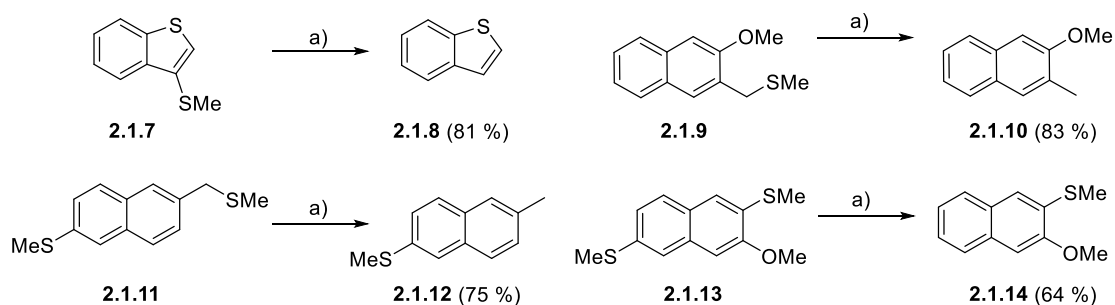
Of the three Group 10 elements (Ni, Pd, Pt), nickel is the most redox active (over a potential range of 1.5 volts)⁵⁴ and displays the widest range of coordination geometries.⁵⁵ The metal coordinates well with heteroatoms in different geometries, with square planar, square pyramidal and octahedral environments commonly adopted. Not surprisingly, nickel chemistry is very versatile and has been used both in nature and in research for a variety of redox reactions.

For a long time⁵⁶ (reports on such reactivity came to the fore in the 1940s) poisoned catalysts were reactivated by employing Raney nickel. Some of these poisons were later discovered to be sulfur-containing compounds. While attempting to understand the fate of these sulfur compounds, Mozingo *et al.*⁵⁶ demonstrated that Raney nickel was a versatile reductant for a wide range of sulfur compounds, both aromatic and aliphatic and of various oxidation states. Sulfur-containing amino acid derivatives also showed good reactivity (Scheme 2.1.1).



Scheme 2.1.1. Raney Nickel can be used to reductively cleave C-S bonds.⁵⁶

Recently, Martin *et al.*⁵⁷ further demonstrated that Raney nickel could be replaced with a combination of Ni(COD)₂ and Me₂EtSiH (as the hydride source) for desulfurization under milder conditions. Their work focused on the reduction of the methyl thioether functional group, showcasing both regioselectivity and chemoselectivity towards reductive C-SMe cleavage (Scheme 2.1.2). In all cases, the selectivity observed in the bond cleavages led to more stable products.

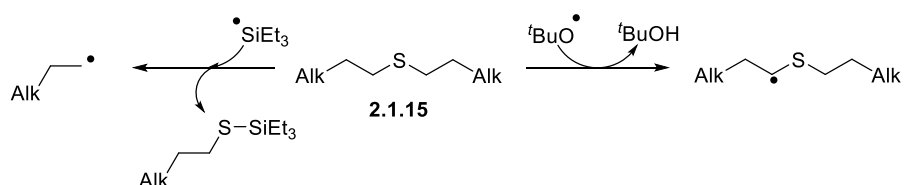


reaction conditions a) 10 mol % Ni(COD)₂, 2 eq. Me₂EtSiH, 90-110 °C, Toluene

Scheme 2.1.2. Selective C-SMe bond cleavage was achieved by employing Ni(COD)₂ and Me₂EtSiH.⁵⁷

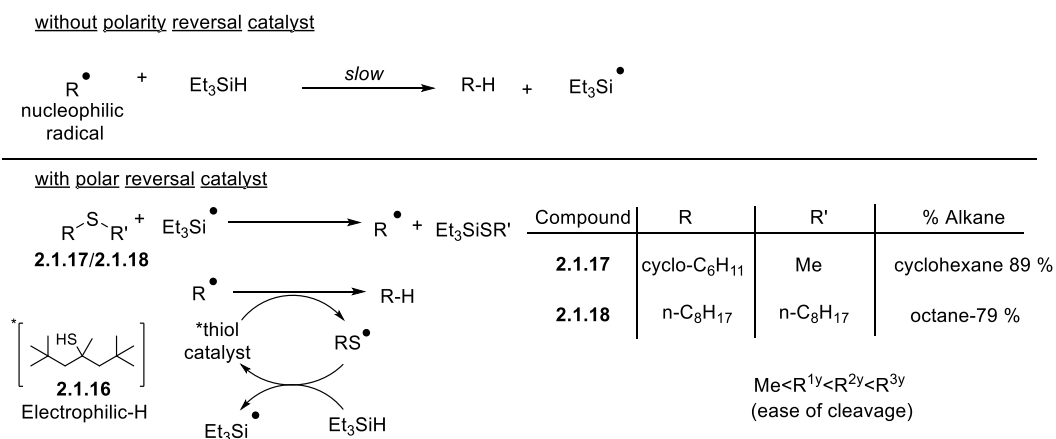
ii) Silanes⁵⁸

During a comparative study on silyl and oxygen-centred radicals, Roberts and Gara⁵⁹ discovered that the triethylsilyl radical would selectively dealkylate dialkyl sulfide **2.1.15** while the oxyl radical abstracted a hydrogen radical (Scheme 2.1.3).



Scheme 2.1.3. Silyl and oxygen-centred radicals reacted with sulfide **2.1.15** in different fashions.⁵⁹

This reactivity observed with the triethylsilyl radical was later exploited when used in combination with a thiol as a polarity reversal catalyst (PRC) (Scheme 2.1.4).⁶⁰



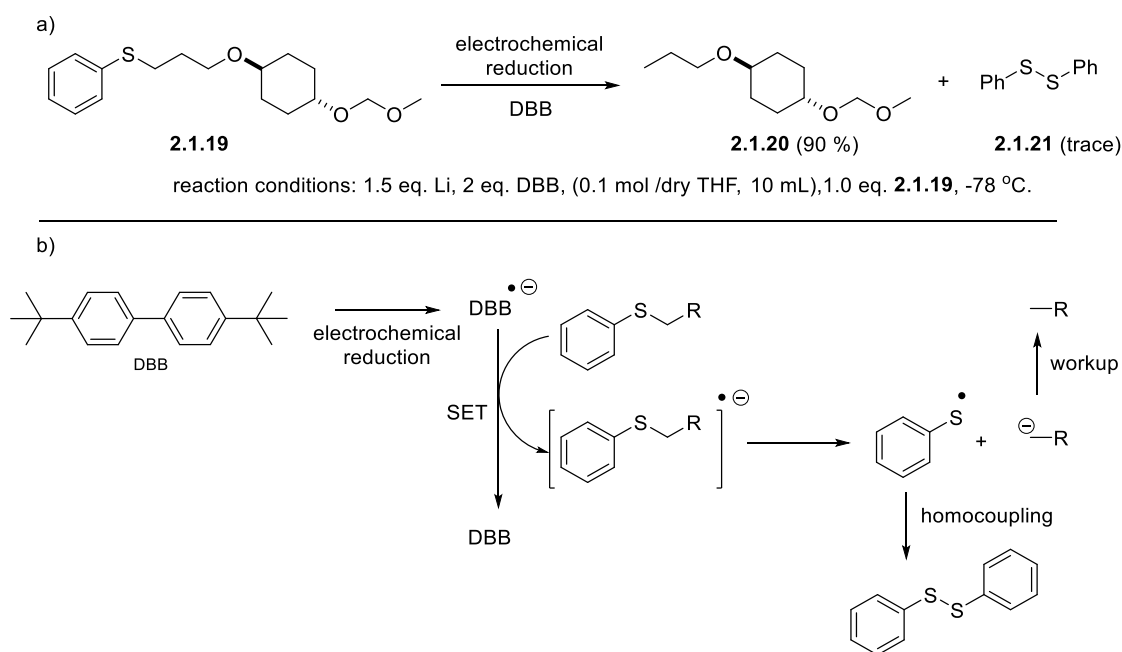
Scheme 2.1.4. Dialkyl sulfide reduction was achieved using a mixture of thiol catalyst and triethylsilane.

In the absence of the thiol catalyst, the nucleophilic alkyl radical must abstract a hydrogen from the nucleophilic triethylsilane; this process is sluggish (Scheme 2.1.4). However, by adding the thiol catalyst, polar effects will now favour the hydrogen abstraction from the catalyst and the reaction rate is enhanced.⁶¹ The sulfide reduction follows the order of the resulting stability of the alkyl radical (Me < 1^y < 2^y < 3^y) although sterically hindered alkyl groups were found to offset the general trend.

This silane-based methodology for the production of alkyl radicals from sulfides can replace the use of the Barton-McCombie reaction which generates alkyl radicals from thiocarbonyl derivatives using tributyltin hydride.⁶²

iii) Electrochemical methods

Direct electrochemical reduction of aromatic sulfides,⁶³⁻⁶⁵ such as **2.1.19** (Scheme 2.1.5), was achieved quantitatively upon generation of its radical anion. However, this process usually required high potentials (**2.1.19** $E_{1/2} \approx -3.53$ V vs Fc/Fc⁺PF₆⁻)⁶⁶ and often resulted in the competing decomposition of the substrate.



Scheme 2.1.5. a) Quantitative reduction of **2.1.19** was possible using electrochemical methods. b) By using DBB as the electron transfer mediator, milder reaction conditions could be employed.⁶³

To improve the reaction profile and lower the required reduction potential, Compton *et al.*⁶³ employed electron transfer mediators under cryoelectrochemical conditions; the most successful mediator was found to be 4,4'-di-*tert*-butyl-1,1'-biphenyl, DBB (Scheme 2.1.5). Unlike direct electrochemical reduction, the reduction of aromatic sulfide **2.1.19** now proceeded efficiently *via* SET from the mediator DBB. The low temperature was required for the stabilisation of the radical anion species formed from the mediator; otherwise the formation of its dianion would shut down reactivity since proton abstraction (from the solvent) would be more favourable.

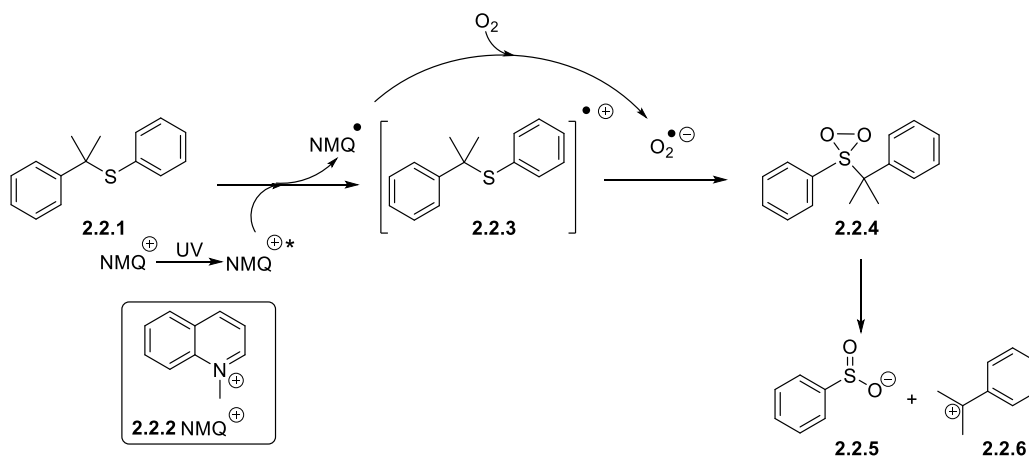
The dimer, diphenyl disulfide **2.1.21**, was isolated in trace amounts upon the reduction of **2.1.19**. Further tests confirmed that this product was not due to aerial oxidation but from radical coupling. This led to the proposal that the radical anion formed upon SET from the mediator would cleave to yield the phenylthiyl radical and the corresponding alkyl anion (Scheme 2.1.5 b).

2.2 Oxidative cleavage

C-S bond cleavages of sulfides have also been conducted *in situ via* the formation of radical cations. One such methodology was developed by Baciocchi *et al.*⁶⁷ when it was discovered that oxidative C-S bond cleavage was greatly enhanced by conducting the reactions with photoexcitation of a fluorescent sensitizer, N-methyl quinolium tetrafluoroborate **2.2.2** (NMQ⁺), in oxygen-enriched solvents (Scheme 2.2.1).

The key step was determined to be the reaction of the O₂^{•-} superoxide with the sulfide radical cation. **2.2.3** By conducting laser flash photolysis experiments with benzoquinone (known to readily trap O₂^{•-}), it was found that the quantum yields in the photolysis of the sulfide-based substrates significantly decreased, thereby confirming that the O₂^{•-} species was responsible for the observed cleavage of the sulfides.

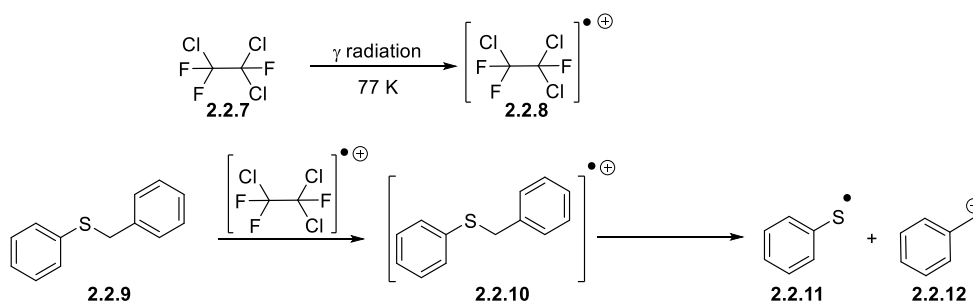
Singlet oxygen was not responsible for the observed reactivity since experiments conducted using Rose Bengal (for the conversion of ³O₂ to ¹O₂) did not result in any reaction even after extended reaction times.



Scheme 2.2.1 Oxidative C-S bond cleavage using photoactivated NMQ.⁶⁸

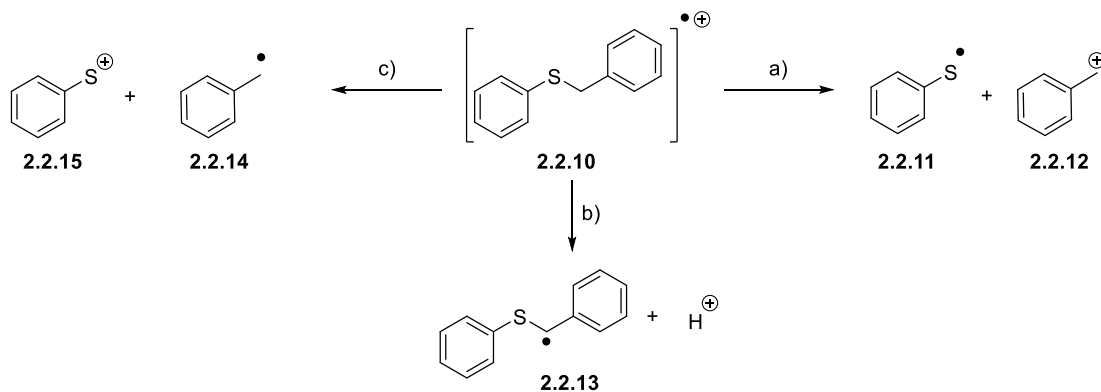
In a separate study, specifically on aromatic sulfide **2.2.9**, Faucitano *et al.*⁶⁹ were able to generate its radical cation **2.2.10** by radiation in a chlorofluorocarbon matrix (Scheme 2.2.2). The high ionisation energy of the chlorofluorocarbon matrix (12 eV)

encourages the electron transfer from the sulfide to the electron deficient matrix thereby leading to the oxidative cleavage.



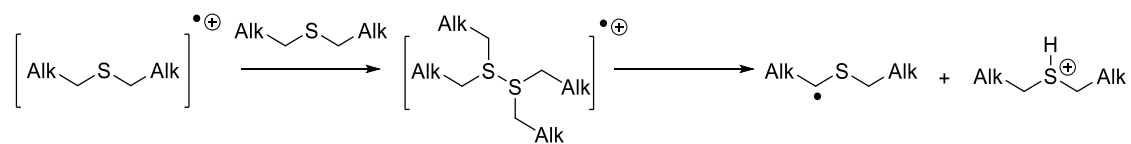
Scheme 2.2.2. Oxidative C-S bond cleavage using a chlorofluorocarbon matrix.⁶⁹

In theory, **2.2.10** would be presented with three modes of C-S bond cleavage (Scheme 2.2.3). By employing computational methods (DFT B3LYP/N07D, gas phase and toluene), the ESR spectra of the stabilised radicals resulting from cleavage were generated and compared with experimental data. The result showed that only the computer-simulated data for the phenylthiyl radical **2.2.11** agreed well with the experimental data. Moreover, the expected major couplings (one for **2.2.13** and two for **2.2.14**) were not present in the ESR data acquired from the reaction. These results further confirmed the proposed cleavage route for the radical cation **2.2.10**.



Scheme 2.2.3. Three modes of cleavage were available to 2.2.10. Using computer-generated data, it was possible to confirm the cleavage resulted in 2.2.11 and 2.2.12 i.e. pathway a).⁶⁹

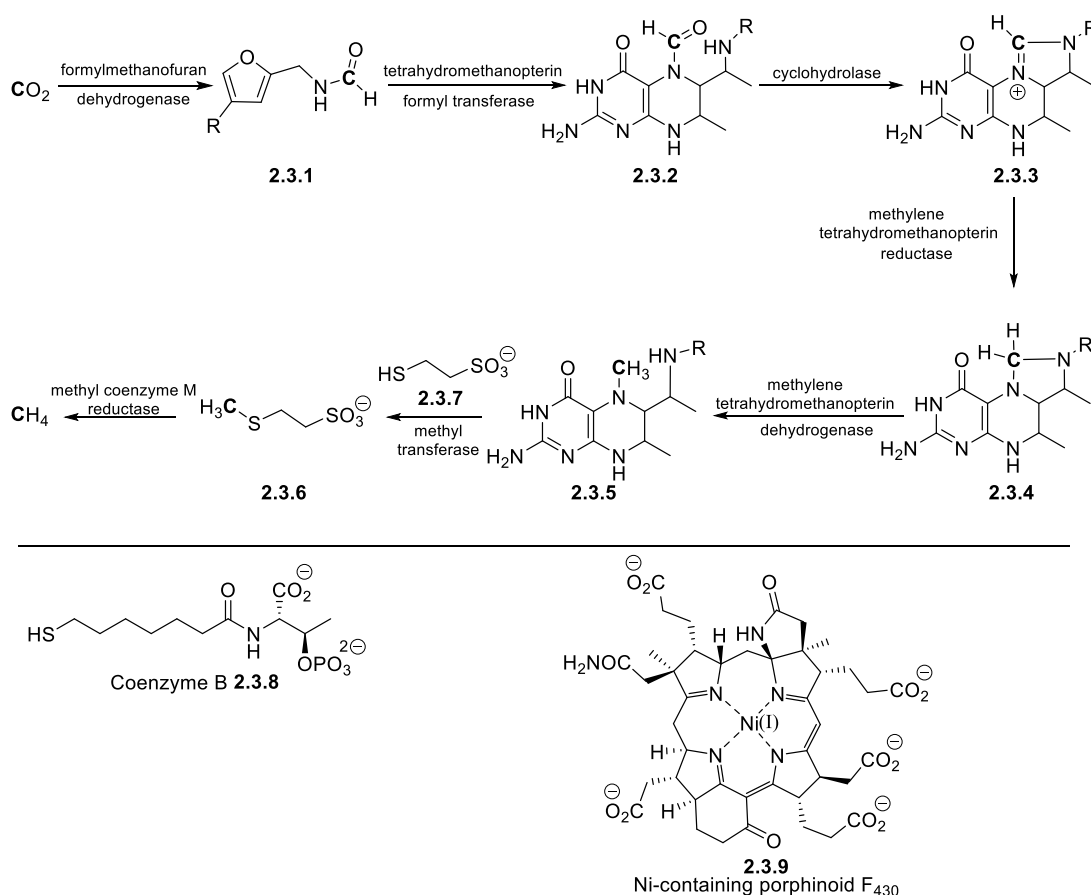
This reactivity is limited to aromatic sulfides, with radical cations of dialkyl sulfides preferentially dimerising with their parent molecules followed by decomposition to yield α -alkyl thioether radicals (Scheme 2.2.4).



Scheme 2.2.4. Radical cations of dialkyl sulfides generated in the chlorofluorocarbon matrix do not readily undergo C-S bond cleavage.

2.3 Biological relevance of C-S bond cleavage - Methanogenesis

Methanogenesis begins with carbon dioxide as the starting material and requires seven subsequent steps for its complete reduction to methane (Scheme 2.3.1).⁷⁰⁻⁷² This important biological process is carried out by methanogens under strictly anaerobic conditions.



Scheme 2.3.1. a) Methanogenesis involves seven consecutive steps to reduce CO_2 to CH_4 , commonly known as the Wolfe cycle.⁷³ b) Structures of coenzyme B and nickel-containing porphinoid F_{430}

The final step involves the reductive C-S bond cleavage of methyl coenzyme M (MeCoM) with protonation or hydrogen abstraction to yield methane.⁷⁴ The reductase, methyl coenzyme M reductase (MCR), responsible for this reaction utilises coenzyme B, **2.3.8** (N^7 -mercaptoheptanoyl threonine phosphate - hereafter abbreviated as CoB) and a nickel-containing porphinoid (F_{430}) **2.3.9** for activity (Scheme 2.3.1 b).⁷⁵ Only one class of microorganisms – *methanogenic archaea* – is known to efficiently perform this reaction.⁷⁴

MCR is highly specific⁷⁶ and fairly efficient as reflected by its high turnover rate (100 s^{-1}) with $k_{cat}/K_m(\text{MeCoM}) \approx 1.9 \times 10^4 \text{ M}^{-1} \text{ s}^{-1}$ at $65 \text{ }^\circ\text{C}$.⁷⁷⁻⁷⁹

About 10^9 tons of methane is released into the atmosphere every year.⁸⁰ With the increase in agricultural and industrial activities globally, it is further estimated that atmospheric methane levels have exceeded 1.7 ppm which is a growing concern since methane is a greenhouse gas. As such, research interest in methanogenesis has grown and this section serves to highlight the current understanding of this important biological process.

2.3.1 Crystal structures of Methyl coenzyme M Reductase (MCR)

MCR was first characterised by Wolfe and Ellefson⁸¹ as a yellow protein comprising of three different subunits arranged in a $\alpha_2\beta_2\gamma_2$ fashion with two independent and identical active sites 50 \AA apart (Figure 2.3.2). Since then, several crystal structures^{75,82} of the heterodimer have been elucidated using cells from *methanobacterium thermoautrophicum* in different oxidation states of nickel. Four main crystal structures have been relied upon for the proposed mechanisms for MCR activity. By employing EPR spectroscopy techniques, these four crystal structures were assigned based on the oxidation states of the resident nickel atom in F₄₃₀ and provide key information on several steps involved in the reduction sequence.⁸³⁻⁸⁷

Figure 2.3.2 MCR is a heterodimer with three different subunits; substrates at the active sites are shown in yellow (pdb 1HBN). Cartoons were reprinted with permission from AAAS.⁸⁸



a) MCR_{silent}

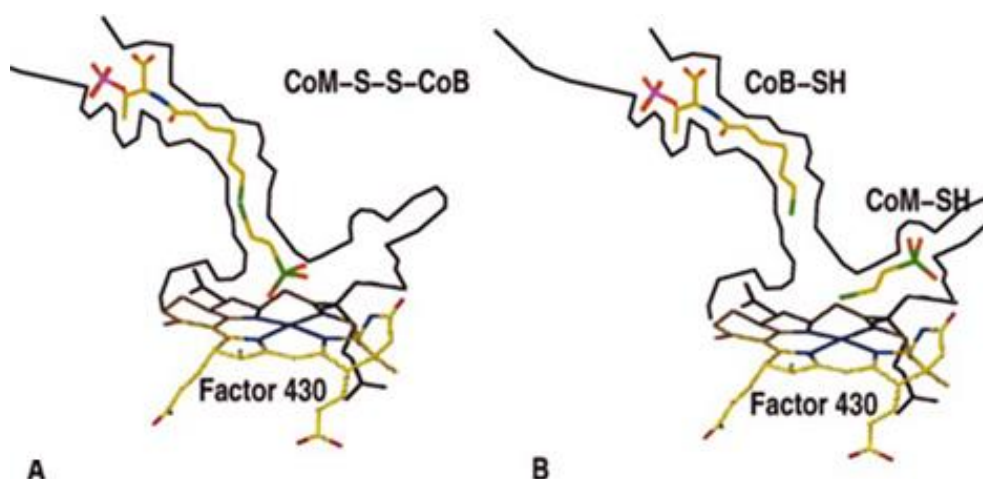
To obtain crystals in this state,^{82,89} the cells were grown in a H₂/CO₂ enriched environment. These cells were EPR silent and the crystal structure of the enzyme was found to contain CoM and CoB in its oxidised disulfide form (Figure 2.3.3 a), in coordination with the central nickel atom through the sulfonate terminus group. Being EPR silent strongly indicated that the diamagnetic Ni(II) oxidation state was present. In this state, the enzyme activity could be partially restored upon addition of a reducing mixture consisting of Ti(III) citrate, cobalamin and dithiothreitol.⁹⁰

It is thought that the crystal structure of this species is reflective of the final resting state of MCR upon the evolution of CH₄. Since, MCR_{silent} shows Ni(II) strongly coordinated to the sulfonate fragment of the heterodisulfide, a subsequent reaction would be required to complete the catalytic cycle with the restoration of Ni(I) and expulsion of the products.

b) MCR_{ox1-silent}

The crystal structure in this state revealed two moles of F₄₃₀, reduced CoM and reduced CoB.⁸⁸⁻⁹² The major difference between MCR_{ox1-silent} and MCR_{silent} lies in the conformations of CoM and CoB. This is discussed in fuller detail later (see Section 2.3.5).

Figure 2.3.3. Cartoons depicting a) MCR_{silent} (pdb 1HBN) and b) MCR_{ox1-silent} (pdb 1MRO). Cartoons were reprinted with permission from AAAS.⁸⁸

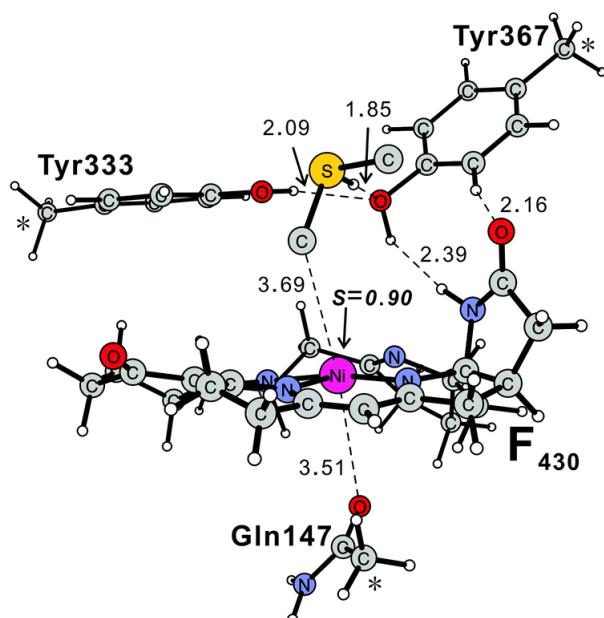


c) MCR_{red1}

When the cells were treated with 100 % H₂ prior to harvest, the enzyme was found to be ESR active with its spectrum closely similar to the non-protein bound Ni(I)F₄₃₀ ESR spectrum. This correlation indicated that MCR_{red1} contained Ni(I) in its active state (Figure 2.3.4).^{82,93-95}

Upon exposure to oxygen, activity was rapidly lost as reflected by the fast decay in EPR activity. The succeeding state of the enzyme was therefore annotated as MCR_{red1-silent}. The loss of activity could indicate that a radical-based mechanism was present, in which case the introduction of molecular oxygen would readily decrease enzyme activity.

Figure 2.3.4. Optimised structure of MCR_{red1} showing a Ni(I) active site (calculated spin = 0.90) binding loosely to MeCoM. Structure reprinted with permission from AAAS.⁹⁶

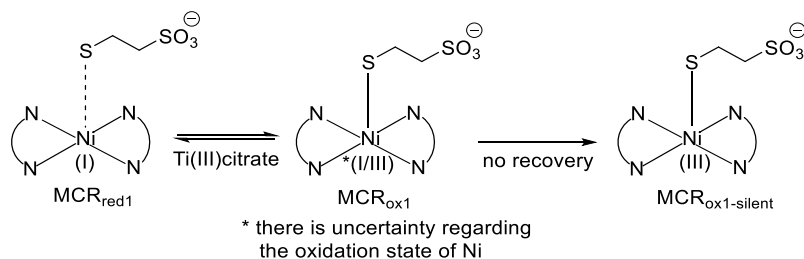


d) MCR_{ox1}

By treating the cells with 80 % CO₂/ 20 % N₂ before harvesting, another EPR active state was detected with its spectrum significantly different from that of MCR_{red1}.^{74,97-}

⁹⁸ As with the case of MCR_{red1} cells, activity decreased with time but in this case, could be effectively restored using only Ti(III) citrate as the reductant which was an indication that this species was different from MCR_{silent}.⁹⁹ The resulting ESR spectrum after recovery revealed that the cells were now MCR_{red1}. If recovery of

activity was not attempted, the cells eventually lost all EPR activity and this gives rise to the $\text{MCR}_{\text{ox1-silent}}$ state (Scheme 2.3.5).



Scheme 2.3.5. MCR_{ox1} can be reduced to MCR_{red1} . If no recovery is attempted $\text{MCR}_{\text{ox1-silent}}$ results.¹⁰⁰

In contrast to MCR_{red1} , MCR_{ox1} did not show instantaneous loss of EPR activity when oxygen was introduced. Rather, it was discovered that the decay rate of MCR_{ox1} was identical under aerobic and anaerobic conditions. This discovery then led to the proposal that a non-radical, Ni(III) based mechanism could be responsible for MCR activity.⁷⁴

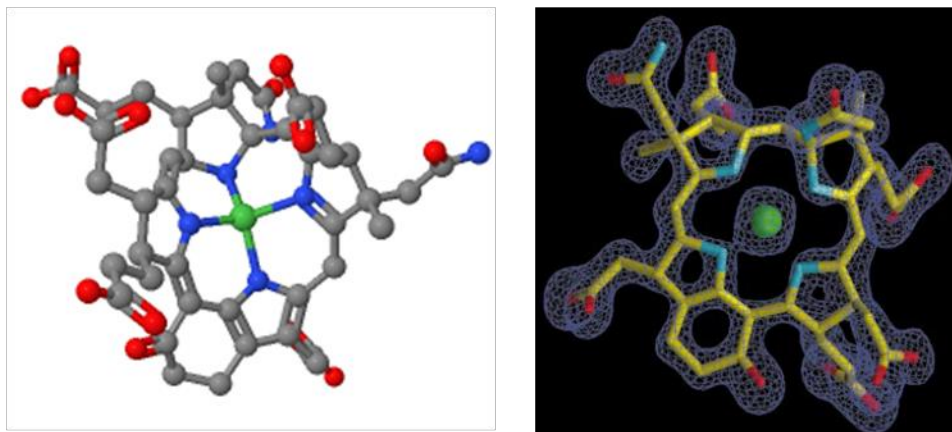
However, Tesler *et al.* later provided an alternative view on the slow decay of MCR_{ox1} by proposing that CoB could be acting as a radical scavenger. By residing at the top of the active site, CoB effectively prevents rapid oxidation of Ni(I). As such, Ni(III) is arguably not present.⁹⁷

To date, there is still uncertainty with regard to the oxidation state of nickel in MCR_{ox1} . The evidence that MCR_{red1} could be obtained upon reduction of MCR_{ox1} using Ti(III) citrate certainly suggested that a two electron reduction had occurred on the oxidised species. However, the ultra violet/visible and EPR spectra of the non-enzyme bound Ni(III) F_{430} cofactor was found to be significantly different from that obtained from the enzyme in the MCR_{ox1} state. This could imply that Ni(I) was already present in this state and the reduction upon treatment with Ti(III) citrate occurred on the ligand(s) and not on the metal.⁹⁹

2.3.2 Binding mode of coenzyme F₄₃₀

The MCR_{ox1-silent} state revealed that the F₄₃₀ is buried deep in the active site with the tunnel itself measuring 30 Å in depth.¹⁰¹ In this state, the nickel atom adopts an octahedral coordination geometry and resides in a pseudo planar position (Figure 2.3.6) with the porphinoid (0.16 Å above the plane).⁹²

Figure 2.3.6. MCR_{ox1-silent} state revealed that the nickel atom is pseudo-planar with the porphinoid. Both cartoons were reprinted with permission from Elsevier.⁸⁸



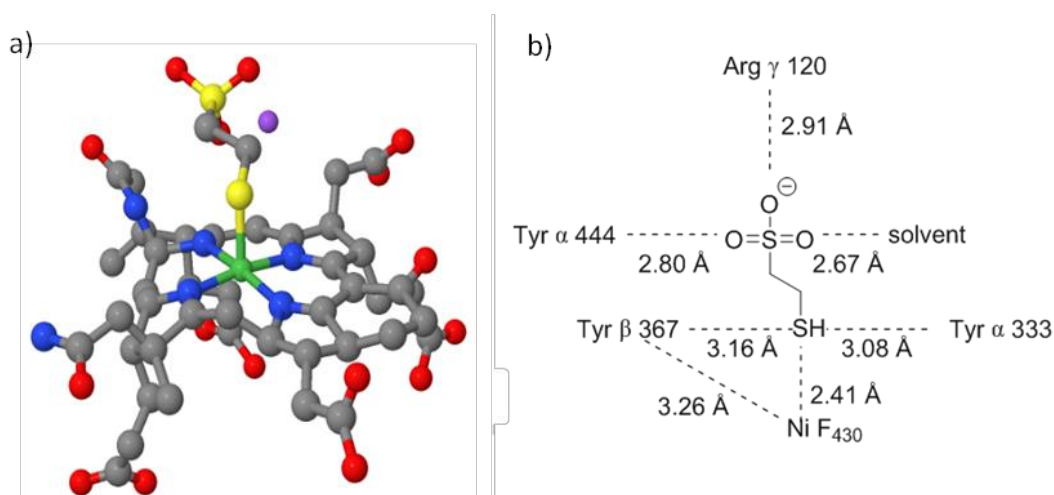
The porphinoid itself is both highly planar and flexible which is attributed to its highly reduced form.⁸⁸ To date, this porphinoid is the most reduced tetrapyrrole that is known to be present in biological systems.⁹¹ In total, it has five double-bonds with four of these forming a conjugated system.⁷⁴ The four equatorial nitrogen atoms are approximately 1.99 – 2.10 Å from the central nickel atom⁸⁸ with the oxygen of side-chain Gln^{α147} as the rear axial ligand and the thiol group of CoM occupying the frontal axial coordination site. In the MCR_{silent} state, it is the oxygen of the sulfonate terminus in CoB that acts as the sixth ligand.⁸⁸

Although no covalent interactions exist between the porphinoid and the enzyme, ionic interactions (between carboxylate anions of F₄₃₀ and the protein) and extensive hydrogen bonding ensure that F₄₃₀ is firmly positioned at the apex of the channel.⁹² Hydrophobic interactions between the tetrapyrrole rings and protein side chains further assist in keeping F₄₃₀ firmly in place (see Figure 2.3.3).¹⁰¹

2.3.3 Binding mode of coenzyme M (CoM)

In its demethylated form, $\text{MCR}_{\text{ox1-silent}}$ revealed that the thiol group binds axially to the nickel atom (Figure 2.3.7 a). CoM is kept in position mainly by interactions between its electron-rich sulfonate tail and the reductase (Figure 2.3.7 b).

Figure 2.3.7. a) Crystal structure of $\text{MCR}_{\text{ox1-silent}}$ showing binding of thiol group to nickel (pdb 1MRO). Cartoon was reprinted with permission from AAAS.⁸² b) Sulfonate tail of CoM interacts with surrounding residues. Reprinted with permission from Elsevier.⁸⁸



Important interactions between the substrate and the reductase include the salt bridge to Arg $^{\gamma 120}$, the hydrogen bond with the main chain nitrogen of Tyr $^{\alpha 444}$ and the hydrogen bond with a resident water molecule thought to be present in the enzyme (Figure 2.3.7 b).⁸⁸ At the sulfhydryl head of CoM, hydrogen bonds with Tyr $^{\alpha 333}$ and Tyr $^{\beta 367}$ help stabilise the substrate further. A water molecule is thought to be present in the $\text{MCR}_{\text{ox1-silent}}$ state, which serves as a bridge between CoM and CoB.⁸² It has been suggested that this single water molecule must be expelled upon entry of the bulky MeCoM, thereby favouring methane formation in an ideal hydrophobic environment.

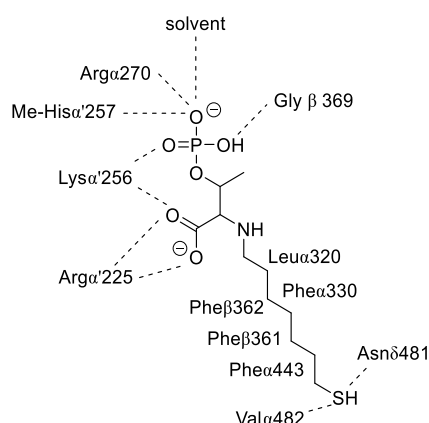
Additionally, a hydrophobic environment will also favour the formation of radical intermediates, which has been proposed.⁸² However, there is still uncertainty if it is indeed a water molecule residing in the highly hydrophobic region of the cavity between CoM and CoB. In his later work, Ermler *et al.* has suggested that this solvent molecule could actually be trapped methane (not water) based on the poor electron density in that location.⁸⁸

Finally, the ethyl fragment of CoM is specifically and favourably sandwiched between the lactam ring of F₄₃₀ and the phenyl ring of Phe^{α443}.⁸⁸

2.3.4 Binding mode of coenzyme B (CoB)

CoB binds at the narrow, top region of the pocket (Figure 2.3.3).⁸² The binding is “head-in” with the thiol directed into the apex while the threonine phosphate resides at the entrance of the channel. Binding is favourable in this setup with the anionic threonine phosphate moiety accessible to the bulk solvent (Figure 2.3.8).

Figure 2.3.8. Binding of CoB depicted in sketch. Sketch was reproduced with permission from Elsevier.⁸⁸



The ionic tail interacts with the reductase by salt bridges with amino acids - Arg^{α270}, Lys^{α256} and methyl-His^{α257}. This conformation essentially caps the active site, preventing polar solvent molecules from entering and thereby maintaining a hydrophobic environment. Importantly, the binding position of CoB indicated that the delivery of CoB and MeCoM was sequential i.e., it is necessary that MeCoM entered the active site before the “lid shutting” action of CoB.

The thiol head has up to three key interactions; i) the side-chain nitrogen of Asn^{δ481}, ii) the main chain peptide nitrogen of Val^{α482} and iii) possibly, a bridging water molecule which brings CoM and CoB into close proximity (6.2 Å). The middle aliphatic region is stabilised by van der Waals contacts with several hydrophobic residues (Figure 2.3.8)

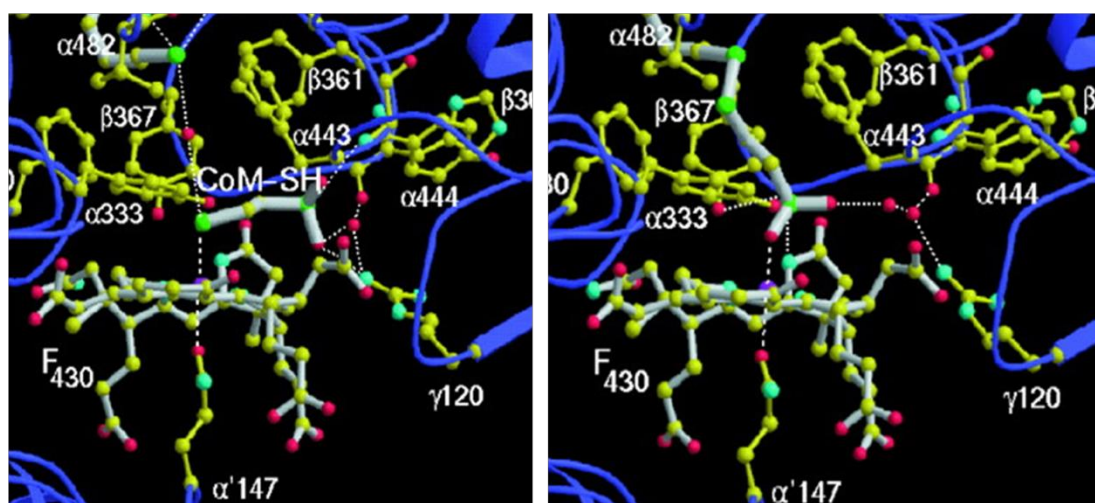
Significantly, MCR_{ox1} reveals that the heptanoyl arm of CoB, which protrudes into the narrow pocket is not long enough to allow any direct reaction with the nickel

centre (8.7 Å between thiol and nickel).¹⁰² Clearly this crystal structure discounts any mechanism which proposes direct interaction between nickel and CoB.¹⁰³

2.3.5 Conformational changes of CoB and CoM

Conformational changes can be inferred from the crystal structures of MCR_{silent}, MCR_{ox1-silent}. Of the three participants, it is CoM which undergoes major conformational changes during the demethylation process. Both the F₄₃₀ and CoB structures experience only minor perturbations based on comparisons of the crystal structures.⁸²

Figure 2.3.9. Cartoons depicting the 90° rotation of the sulfonate fragment upon demethylation of MeCoM. Reproduced with permission from AAAS.⁸²



The superimposition of MCR_{ox1-silent} (which reflects spatial conformations before demethylation) onto MCR_{silent} (the oxidised disulfide after demethylation of MeCoM) reveals that the thiol group has rotated through 90°.⁸² This causes one of the oxygens of the sulfonate fragment to adopt the axial coordination site of the nickel atom (Figure 2.3.9).

X-ray crystal structures have assisted researchers immensely in their understanding of MCR activity but there are still discrepancies. To date, there are two mutually exclusive mechanisms proposed with further variations within each of them.

Whatever the mechanism, several parameters have been established based on evidence gathered mainly from the crystal structures and isotopic labelling studies:

- i) Ni(I) is essential for activity.^{93-95,104} The Ni centre rests in its pentavalent state, with one coordination site vacant for binding with substrate.
- ii) The demethylation process cannot proceed unless both MeCoM and CoB are bound to the enzyme.^{78,105} Theoretically, demethylation of Me-CoM can proceed without CoB. However, as revealed by steady state studies, CoB is required for reactivity.^{78,105-107}
- iii) Me-CoM must enter the reductase before CoB which then blocks off the narrow channel leading to the Ni active site.¹⁰⁵ With this pre-organisation, there is enhanced substrate specificity. Indeed, MCR is known only to convert two other substrate analogues but with much poorer efficiency; namely ethyl coenzyme M¹⁰⁷ and trifluoromethyl coenzyme M.⁸²
- iv) There must be stereoinversion of the carbon bearing the methyl group. This was realised with studies using chiral ethyl coenzyme M. The resulting ethane from substrate reduction was converted into acetate and the configuration was determined, revealing stereoinversion at the chiral carbon atom.⁷⁶

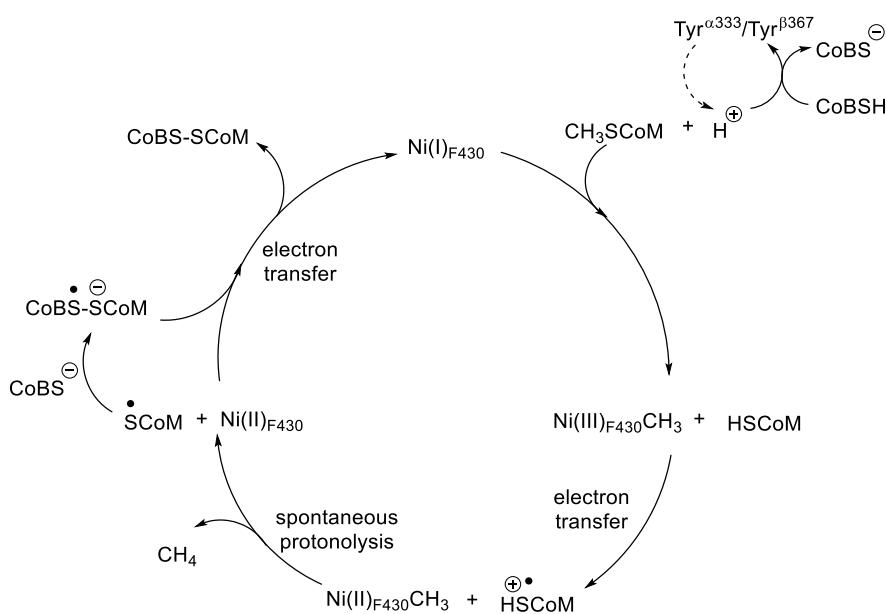
2.3.6 Nucleophilic substitution mechanism

Mechanistic investigations supporting this mechanism stem from *in vitro* studies of isolated F₄₃₀.⁷⁴ Jaun *et al.*¹⁰⁸ had successfully shown that the free Ni(I) F₄₃₀ readily underwent nucleophilic substitution with conventional electrophilic methyl donors including methyl iodide, methyl triflate and methyl tosylate.

In all these cases, only the Ni(II)-CH₃ species could be detected after the reaction, which is thought to have resulted from the rapid reduction of the unstable Ni(III)-CH₃ species. This was based on the measured redox potential of the Ni(III)_{F430}/Ni(II)_{F430} couple ($E_0 = +0.825$ V vs. Fc⁺/Fc) and the related Ni(III)-CH₃/Ni(II)-CH₃ is expected to be similar.¹⁰³ It was also observed that the nucleophilicity of Ni(I) was enhanced in a protic acidic medium which further suggested that methane formation proceeded *via* initial protonation of MeCoM to yield the highly reactive sulfonium cation.

To ascertain the source of hydrogen for methane formation, further experiments were conducted in (CH₃)₂CHOD and (CH₃)₂CDOH separately.¹⁰⁸ Deuterium incorporation in methane was observed only with isopropanol-OD (> 85 %) which was strongly suggestive that protonation and not hydrogen abstraction was involved.

Figure 2.3.10 The nucleophilic mechanism involves the generation of the Ni(III) complex. Recent computational investigations predict an excessively high energy barrier for its formation.¹⁰⁹



These findings led Thauer *et al.*⁷⁴ to refine the nucleophilic model by introducing a transition state involving the protonation of Me-CoM. The proton source⁸² could be from CoB *via* transfer between neighbouring amino acids (Tyr^{α333} and Tyr^{β367}). The resulting sulfonium cation is now poised for nucleophilic attack by Ni(I). The resulting CH₃-Ni(III) complex is a strong one-electron oxidant which rapidly reduces upon electron transfer with CoM (suitable redox partner); this in turn creates a strongly-acidic CoMH radical cation which spontaneously protonates CH₃-Ni(II) thereby generating CH₄ (Figure 2.3.10).

The methane formation step is irreversible and drives the subsequent formation of the disulfide radical anion which has a sufficiently negative redox potential to reduce Ni(II) to Ni(I), thereby completing the cycle.¹⁰⁹

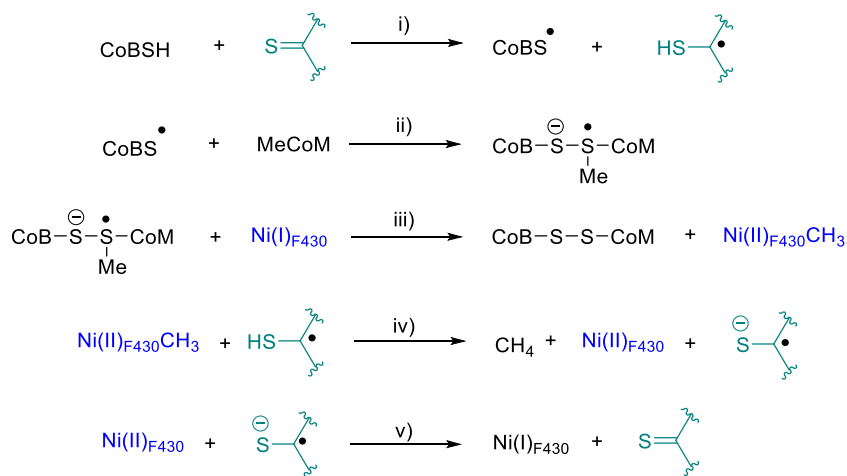
This proposed mechanism agrees well with the information provided by the crystal structures. Importantly, the electron transfer from the disulfide radical anion¹¹⁰ is energetically feasible with the possibility of the modified Gly^{α445} (a thioglycine) present at the active site acting as the mediator.¹¹¹

However this mechanism has one major drawback; it implies that the absence of CoB would shut down the cycle rapidly and this deactivation would be detected by a rapid decay of EPR activity. Experimentally this was not the case, with EPR activity of MCR_{red1} found to be stable even after deletion of CoB.⁹⁴

Further concerns have been raised when this model was revisited using computational analysis. The formation of the proposed Ni(III)-CH₃ complex formation is highly endergonic ($\approx 23.5 \text{ kcal mol}^{-1}$)^{109,112} and DFT calculations also revealed that the Ni(III)-C bond is very weak or almost non-existent.¹¹³ In view of these computational results, a different mechanistic pathway which is more thermodynamically feasible should be considered. One solution was to envisage the Ni(I) complex -in its radical capacity- attacking the sulfur centre of MeCoM to generate a Ni(II)-SCoM adduct. This alternative view is attractive as it has a relatively lower activation energy along with the formation of a stronger Ni-S bond.

2.3.7 Radical-mediated mechanism

It was mentioned earlier that the highly hydrophobic channel was suggestive of a radical-based reaction over a polar mechanism. To circumvent the highly endergonic formation of the Ni(III) species, several radical-based mechanisms have been proposed in which Ni(I) reacts using its unpaired electron (Scheme 2.3.11).^{103,108,114}

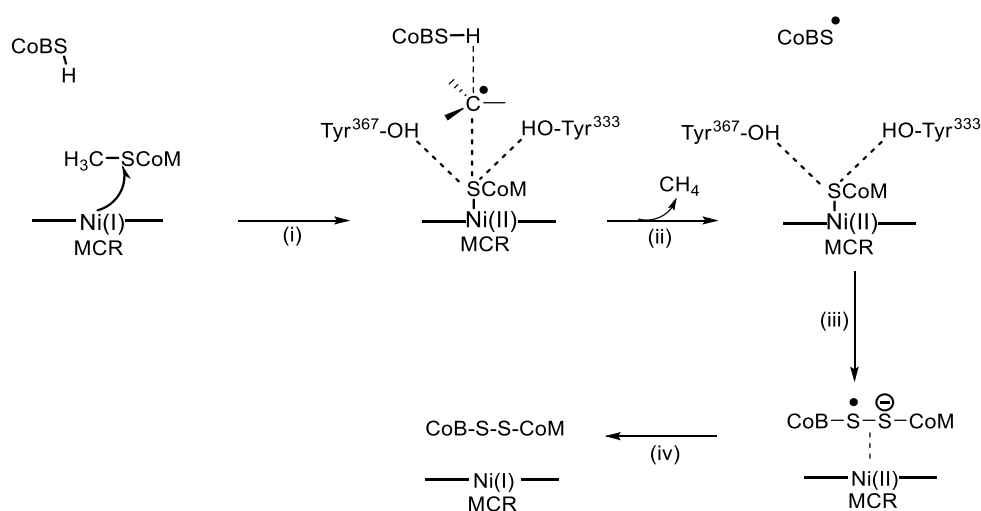


Scheme 2.3.11. An early model for the proposed radical mechanism involves modified Gly^{a445} as a redox participant.¹¹⁵

One such model^{93,111,116} postulates that a second redox couple, possibly involving the proximal thioglycine, initiates the reaction (Scheme 2.3.11 step i).^{74,103,110} The initiation provides the source of the CoBS radical which then proceeds to react with Me-CoM to form the sulfuranyl radical anion (Scheme 2.3.11 step ii). This is followed by methyl transfer between the disulfide and the Ni(I) centre. The cycle comes to completion with methane production after a couple of redox reactions between thioglycine and the Ni(II) complex. (Scheme 2.3.11 steps iv and v).

This model relies heavily on the modified Gly^{a445} for activity which may seem precarious considering that little research has been done to substantiate the importance of this modified amino acid. Furthermore, little is known about the feasibility of the first step proceeding in biological systems and the later reduction of thioglycine to its radical anion is also unfavourable (≈ -1.4 V vs. NHE). These factors raised concerns regarding the viability of this model.

More recently, a joint study by Chen and Siegbahn¹¹² resulted in another radical mediated mechanism which did not rely heavily on the modified glycine (Scheme 2.3.12). The authors disclosed that it was overall energetically feasible for the three coenzymes to react without assistance from Gly^{α445} and that the rate-limiting step in this pathway (Scheme 2.3.12 step i) required just 15 kcal/mol for the Ni(II)-S bond formation. Further refinement using quantum chemical methods actually predicted an even lower energy barrier (5.5 kcalmol⁻¹) resulting from stabilising hydrogen bonds with the proximal tyrosine residues at the active site.

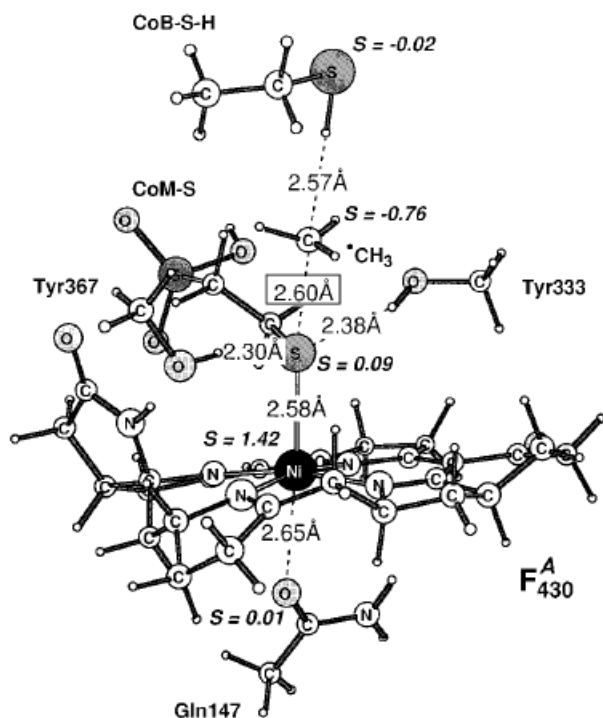


Scheme 2.3.12. A later model of a radical-base mechanism was proposed by Chen and Siegbahn.^{96,112}

Although the reaction is not concerted, the free methyl radical is very short-lived and rapidly abstracts a hydrogen from CoB. It is also thought that the abstraction occurs faster than the possible rotation of the methyl radical. It was also suggested that the long S-S distance (6.0 Å) between CoB and CoM was optimal (Figure 2.3.13) for the transfer of the methyl radical.

A strongly coordinated disulfide radical anion formed after methane evolution then proceeds to reduce Ni(II) to its required active state thereby completing the catalytic cycle (Scheme 2.3.12 step iv).

Figure 2.3.13. Computationally generated structures suggested that the long S-S distance is optimal for the transfer of the methyl radical. Reproduced with permission from the American Chemical Society.¹⁰⁹



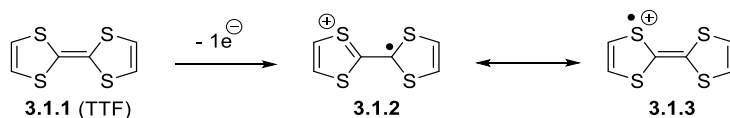
Despite the wealth of data available through research, the mechanism of MCR still remains a mystery. It is also noteworthy that no reports have proven the significance, if any, of the five modified amino acids located at the active site namely 1-*N*-methyl-His^{α257}, 4-methyl-Arg^{α271}, 2-methyl-Gln^{α400}, S-methyl-Cys^{α452} and particularly Gly^{α445} (the carbonyl oxygen is substituted by sulfur); perhaps owing to the difficulty in breeding stable site-specific protein variants. Certainly, it has been suggested that these modifications might serve some purpose either structurally or electronically.⁸²

“In chemistry, the reductive cleavage of an inert thioether is a highly complicated reaction, requiring harsh conditions”.¹¹⁵ This is possibly the reason for the significant lack of non-enzymatic experimental benchwork towards understanding MCR reactivity. Certainly, there is much scope that remains unexplored and this has led to new adventures in the reduction of sulfides during the course of this Ph.D. project. The ground-breaking results from this project will be presented and discussed later.

Chapter 3 Organic molecules as electron donors

With a better understanding of the behaviour of radicals in recent years, scientists have begun to uncover the hidden potentials of utilising radicals in useful chemical transformations. Particularly in the field of functional group reduction and transformation, radical-based reactions have been well developed, most of which are metal-based (e.g. Sn and Sm). Even more exciting and challenging would be to utilise metal-free organic molecules to perform (or even outperform) these chemical reactions.

In this section, it will be shown how the careful design of organic frameworks has assisted researchers in the development of moderate-to-powerful electron donors with reactivity that parallels metal-based reductants. These developments can be traced back to tetrathiafulvalene (TTF) **3.1.1** as the lead compound.¹ At the outset, Wudl¹¹⁷ reported that this electron-rich compound was observed to oxidise readily to its radical cation ($E_{1/2}^1(\text{MeCN}) = +0.32 \text{ V vs. SCE}$).¹¹⁸ The stabilisation of the resulting radical cation from the electron-rich sulfur atoms and the gain in aromaticity make the oxidation process favourable (Scheme 3.1.1).



Scheme 3.1.1. Tetrathiafulvalene (TTF) readily loses one electron. In doing so, partial aromaticity and stabilisation of the radical cation by the heteroatoms are achieved.

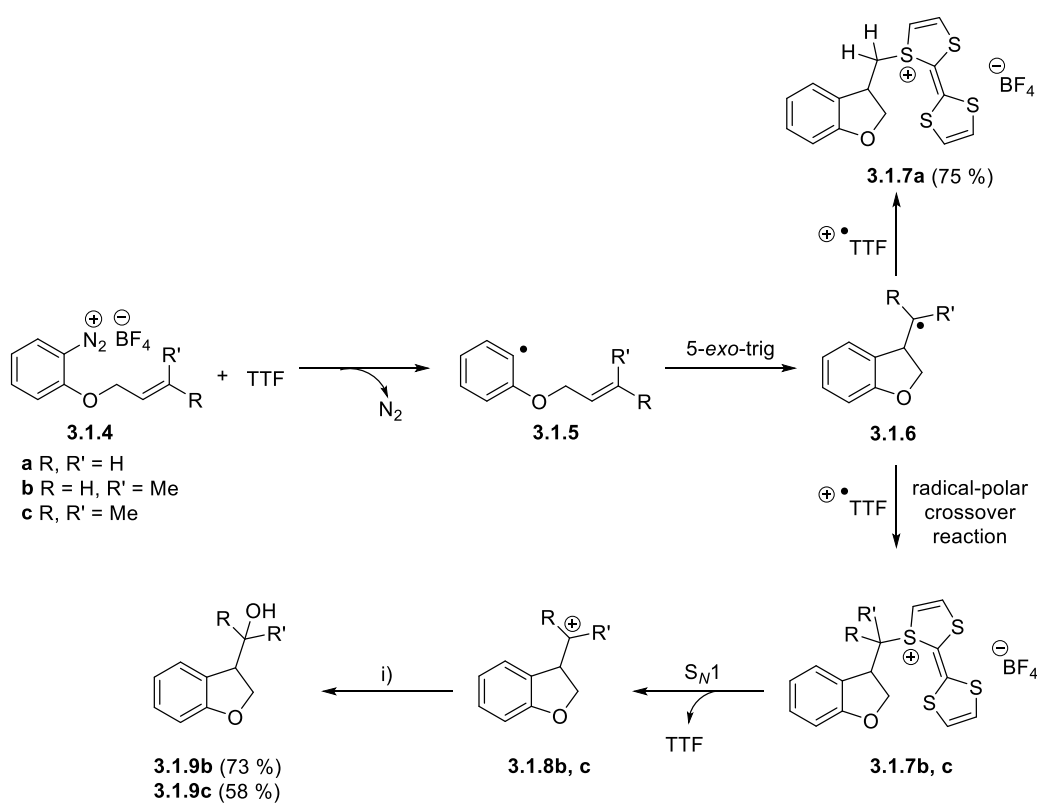
Later, Neiland *et al.* proceeded to show that TTF readily reduces arenediazonium salts to aryl radicals with the liberation of dinitrogen serving as a powerful driving force for the process.¹¹⁹

The usage of TTF as an electron donor was further developed by Murphy *et al.* who utilised this chemistry to perform intramolecular Meerwein cyclisations in good yields without the conventional use of copper salts. Thorough experimental

¹ Although TTF was not the first organic reductant to be synthesised, more research had been conducted on it than tetrakis(dimethylamino)ethylene (TDAE) which predates TTF by 30 years. TDAE is discussed later in the chapter.

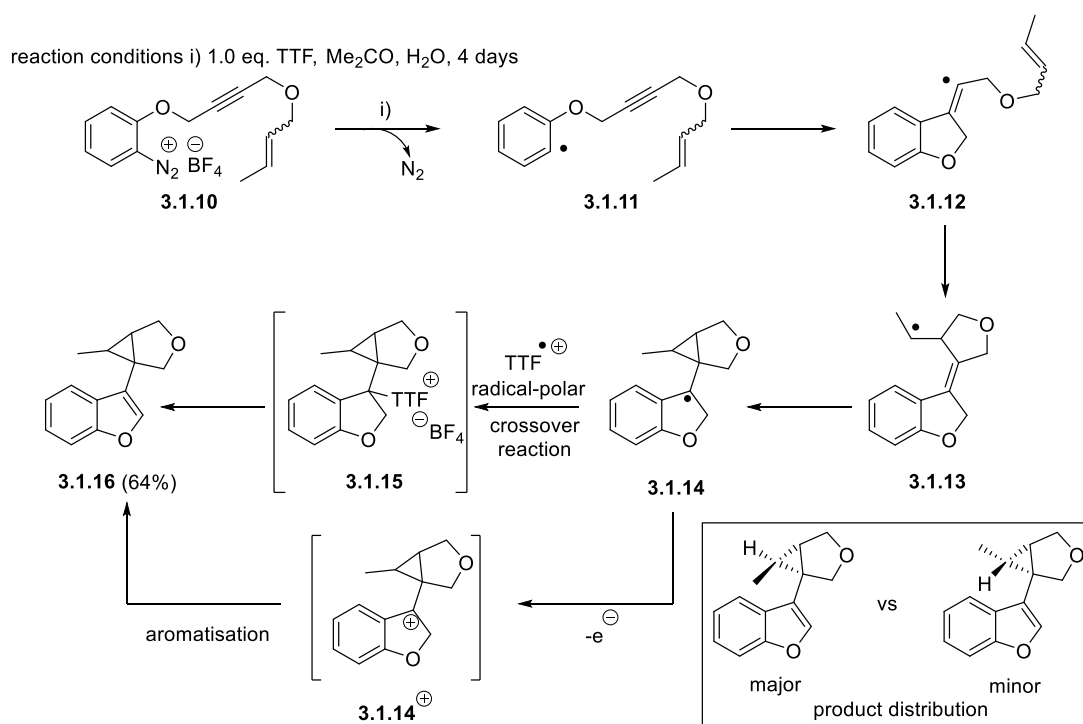
investigations revealed that the reaction involved the formation of the sulfonium salt **3.1.7a-c** (**3.1.7c** was not characterised but its formation was inferred from the detection of **3.1.7a** and **3.1.7b**). In the case of **3.1.7a**, the salt was found to be highly stable and would not undergo further reaction. The other analogues **3.1.7b** and **3.1.7c** were more reactive and dissociated to their stabilised cations **3.1.8 b** and **c** which then proceeded to form the alcohol products **3.1.9 b** and **c**, either by direct reaction with trace amounts of water in the acetone or with the solvent itself followed by hydrolysis (Scheme 3.1.2).

The observed reactivity between TTF and diazonium salts is conveniently described as the radical-polar crossover reaction since it begins with a radical cyclisation and then switches over to the polar S_N1 reaction upon trapping of the TTF radical cation.



Scheme 3.1.2. Intramolecular Meerwein cyclisation of diazonium salt using TTF proceeded smoothly. In this instance, the TTF radical cation is trapped by 3.1.6 and its dissociation from 3.1.7b and 3.1.7c ultimately led to alcohols 3.1.9b and 3.1.9c.

Since the aryl radical cyclisation was found to proceed faster than the trapping of the TTF radical cation, the methodology was successfully extended to include more elaborate cascade cyclisations (Scheme 3.1.3).

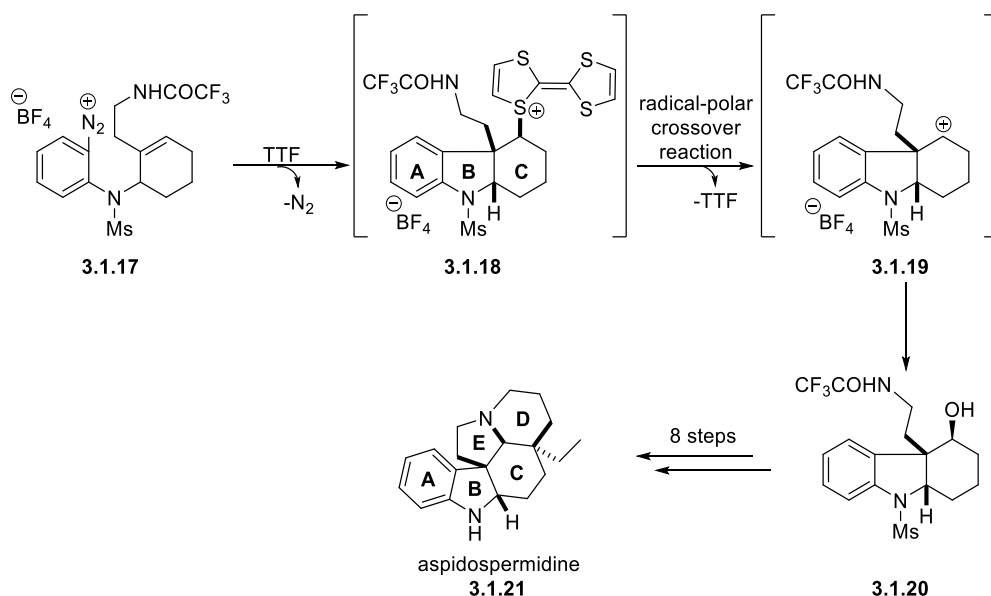


Scheme 3.1.3. The radical polar cross-over reaction was employed by Murphy *et al.* in the synthesis of tricyclic **3.1.16**.¹²⁰

In the event, the radical **3.1.11** generated from diazonium salt **3.1.10** underwent three consecutive cyclisations to give **3.1.14**. This tricyclic radical is thought to couple with the TTF radical cation *via* the radical-polar crossover reaction. The gain in aromaticity drives the reaction to completion resulting in **3.1.16**. Since **3.1.15** was not isolated during the reaction, it was also possible that the tricyclic radical **3.1.14** could have transferred an electron to the TTF radical cation or the diazonium salt **3.1.10**, after which the resulting cation proceeds to aromatises to yield the observed product **3.1.16**.

Having uncovered the hidden potential for cascading cyclisations, Murphy *et al.* proceeded to apply the radical-polar crossover reaction to the synthesis of aspidospermidine **3.1.21** (Scheme 3.1.4).¹²¹ This synthesis requires the installation of up to four stereocentres on ring C. By employing radical chemistry in the first step,

the initial *cis*-ring junction can be installed along with the correct stereochemistry at the quaternary carbon.

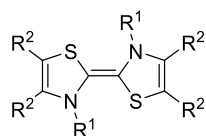


Scheme 3.1.4. Application of the radical-polar crossover reaction to the synthesis of aspidospermidine by Murphy *et al.*¹²¹

As shown from previous examples, the radical-polar crossover reaction naturally allows for the formation of the tertiary carbocation which comes in useful for further transformations to obtain the final product. This methodology is more attractive than the more conventional polar chemistry as the latter suffers from steric problems when installing the stereocentres. (In the case of radical reactions, reactive centres readily adopt early transition states which are less affected by steric effects than for polar reactions).

Drawing from the reactivity of TTF, one strategy to increase an organic molecule's reducing power is to replace the sulfur atoms with nitrogen atoms (Figure 3.1.5).

Figure 3.1.5. Electrochemical studies on diazadithiafulvalenes showed that these species would oxidise more readily than TTF.



3.1.22a (R¹ = Me, R² = COOMe), E¹_{1/2} = + 0.06 V, E²_{1/2} = + 0.41 V

3.1.22b (R¹ = Ph, R² = COOMe), E¹_{1/2} = + 0.15 V, E²_{1/2} = + 0.62 V

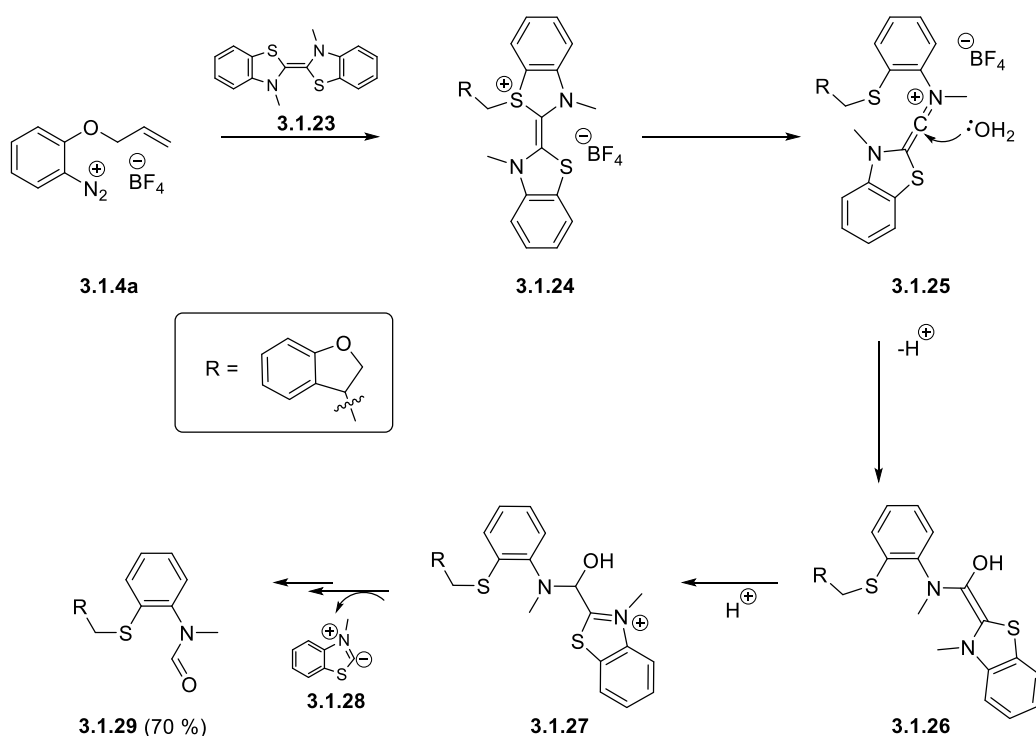
TTF, E¹_{1/2} = + 0.35 V, E²_{1/2} = + 0.71 V

All CV studies measured against SCE,
1,2 dichloroethane used as solvent

Not only is nitrogen electron-rich (possessing a lone pair), it also allows for better π -overlap with the adjacent carbon, which in turn enhances stabilisation of the resulting

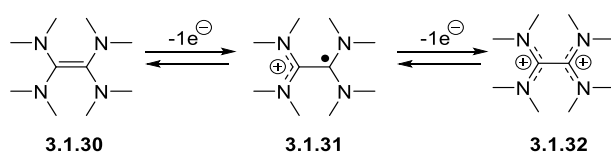
cationic species. This was shown by Tormos *et al.* who investigated the electrochemical properties of diazadithiafulvalenes **3.1.22a** and **3.1.22b** (Figure 3.1.5) and discovered that these compounds indeed had lower redox potentials than TTF.¹²²

Murphy *et al.* further discovered that diazadithiafulvalene **3.1.23** could also initiate the radical-polar crossover sequence efficiently. In contrast with the reactivity observed with TTF, the present case resulted in the isolation of formamide **3.1.29**. This was due to the spontaneous ring-opening of salt **3.1.24** since greater positive charge stabilisation was afforded by the nitrogen atom which is not present in TTF (Scheme 3.1.6).



Scheme 3.1.6. The radical polar cross-over reaction of diazonium salt **3.1.4a** proceeded in good yield with **3.1.22** as the electron donor. Fragmentation of **3.1.24** was the preferred route due greater stability of the positive charge afforded by the nitrogen atom.

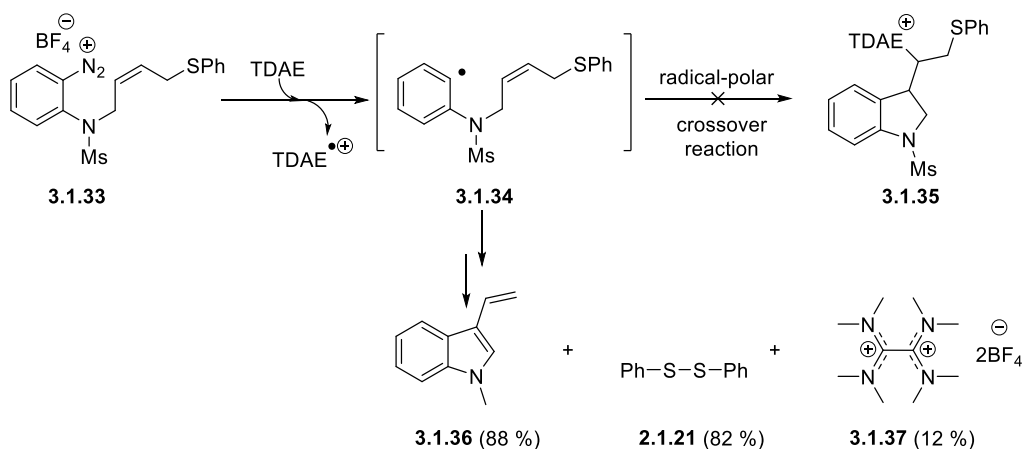
It should follow that the replacement of all four sulfur atoms on TTF should afford organic electron donors that are even more powerful than diazadithiafulvalenes. Earlier on, a team in Du Pont investigated the possibility of reacting chlorotrifluoroethylene with excess dimethyl amine under metal-free reaction conditions. In so doing, it was shown that tetrakis(dimethylamino)ethene (TDAE) **3.1.30** was synthesised and this compound was reported as “strongly luminescent in contact with air”.¹²³



Scheme 3.1.7. TDAE readily oxidises due to the resulting stability of the cationic species.

The ability for TDAE to behave as an organic electron donor at that time was not investigated but its redox potential was later measured by Burkholder *et al.* [$E^1_{1/2}(\text{MeCN}) = -0.78 \text{ V vs SCE}$] and [$E^2_{1/2}(\text{MeCN}) = -0.61 \text{ V vs SCE}$]¹²⁴ This indicated that TDAE could oxidise more readily than TTF and diazadithiafulvalenes. Indeed, the potential for TDAE to behave as an electron donor was later discovered through the experimental work of various groups. Suitable substrates included polyfluorinated hydrocarbons,¹²⁵ electron-deficient nitrobenzyl chlorides¹²⁶ and α -bromoketones.¹²⁷

In a study comparing the reactivity profile of TDAE and TTF, Murphy *et al.*¹²⁸ reported the ability of TDAE to reduce arenediazonium salts but without the subsequent radical-polar crossover reaction (Scheme 3.1.8).



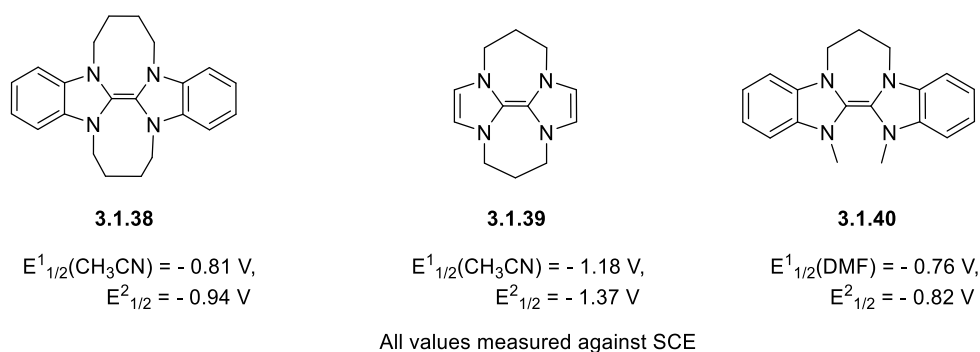
reaction conditions: 1.0 eq. TDAE, Me_2CO , 25 °C, 5 min.

Scheme 3.1.8. TDAE was successfully employed in the reduction of arenediazonium salts. Substituted indoles were conveniently synthesised using this methodology.¹²⁸

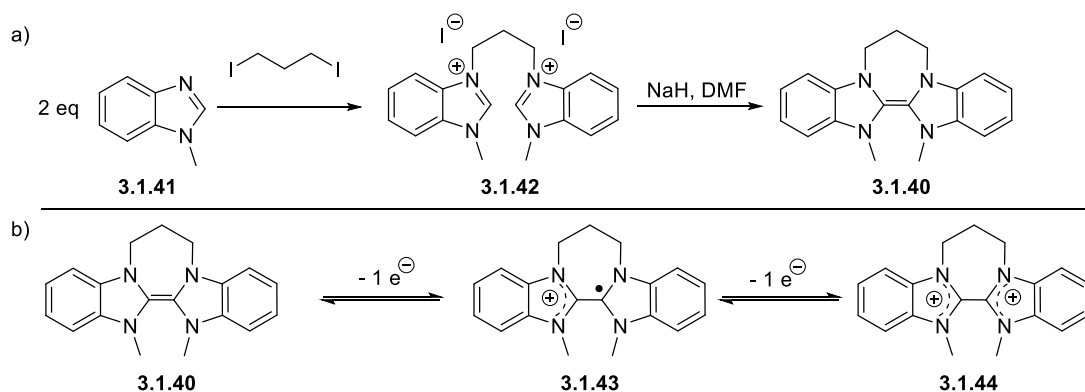
With TDAE, hydrogen abstraction after cyclisation was the favoured termination route. Alternatively, elimination of a suitably positioned leaving group, if present, was preferred (e.g. phenylthiyl radical in the case of **3.1.33**). This reactivity was further exploited for the synthesis of indoles.¹²⁸

It has been shown that the generation of aromaticity and the nature of the heteroatom(s) can influence the oxidation potential of an organic molecule. Candidates **3.1.38–3.1.40** can be considered to be a result of combining these two concepts (Figure 3.1.9). These imidazole-based compounds have been synthesised previously and their redox potentials were also measured.¹²⁹⁻¹³²

Figure 3.1.9. Imidazole-based molecular frameworks were synthesised and characterised by several research groups. These compounds were found to readily undergo oxidation.¹²⁹⁻¹³²

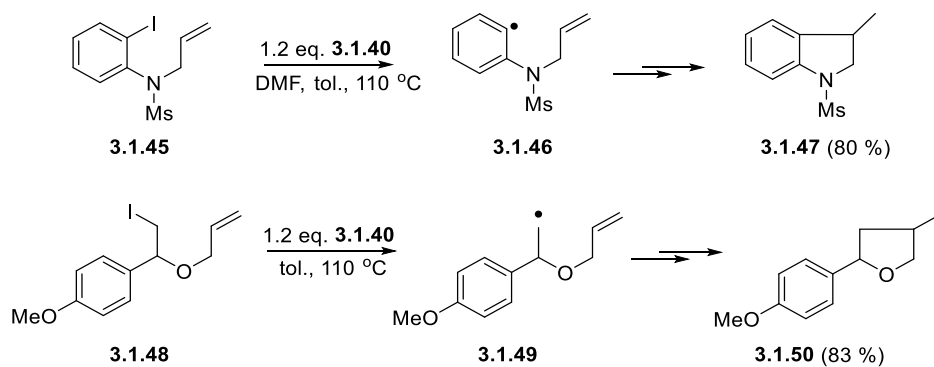


Although **3.1.38** and **3.1.39**, have more negative redox potentials than TDAE **3.1.30** thereby indicating that these were stronger electron donors, only the mono-bridged **3.1.40** was easy to synthesise and isolate (Scheme 3.1.10 a) while the other two molecules required longer reaction time for the installation of the second alkyl bridge (the challenges in synthesising **3.1.39** are discussed in chapter 4).



Scheme 3.1.10 a) Synthesis of 3.1.40 followed a two-step route, firstly with installation of the alkyl bridge and then deprotonation of the disalt to yield the electron donor 3.1.40. b) Aromaticity and stabilisation of the positive charge(s) are driving forces for the oxidation of 3.1.40.

Importantly, **3.1.40** was shown to be the first ground-state organic electron donor that was sufficiently powerful to reduce aryl iodides and alkyl iodides to their corresponding radicals (Scheme 3.1.11).¹³³

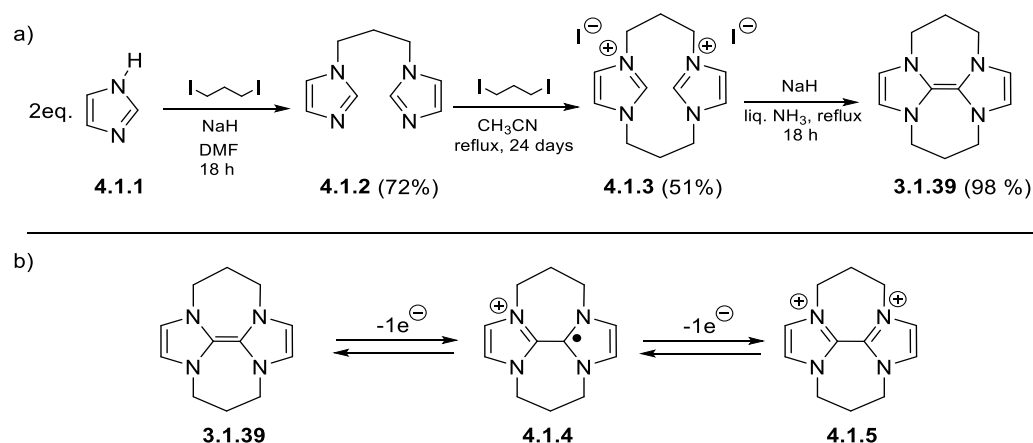


Scheme 3.1.11. Reduction with subsequent ring closures of aryl and alkyl iodides were possible with **3.1.40**.

Chapter 4 Organic molecules as super-electron donors

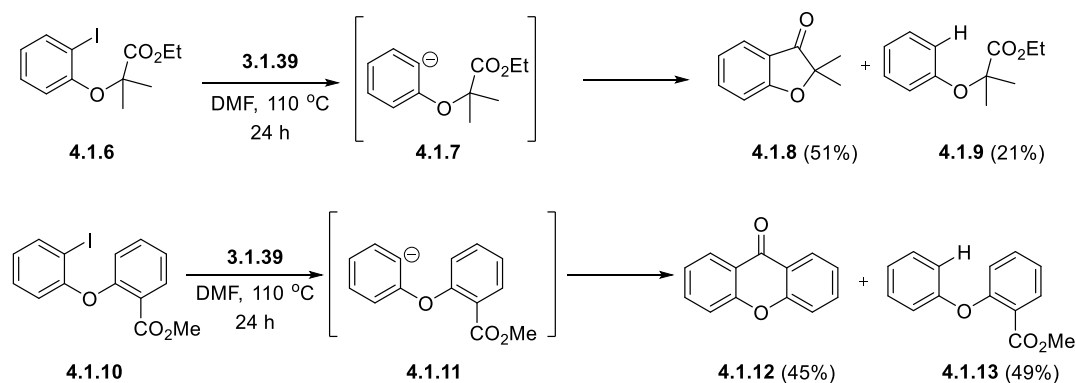
4.1 The development of DMAP-based super-electron donor

Super electron donors (SED)s are defined as organic molecules which are able to reduce aryl iodides e.g. **4.1.6** to aryl anions e.g. **4.1.7** (i.e. a two-electron reduction is required). As such, the benzimidazole-based donor **3.1.40** discussed in the previous chapter would not be considered a SED. However, the imidazole-based donor **3.1.39**, with a more negative redox potential,¹³⁴ indicates that this molecule might qualify as a SED.



Scheme 4.1.1. a) Electron donor **3.1.39** possesses four electron-rich nitrogen atoms. b) Two-electron oxidation of **3.1.39** would result in the formation of two aromatic rings.

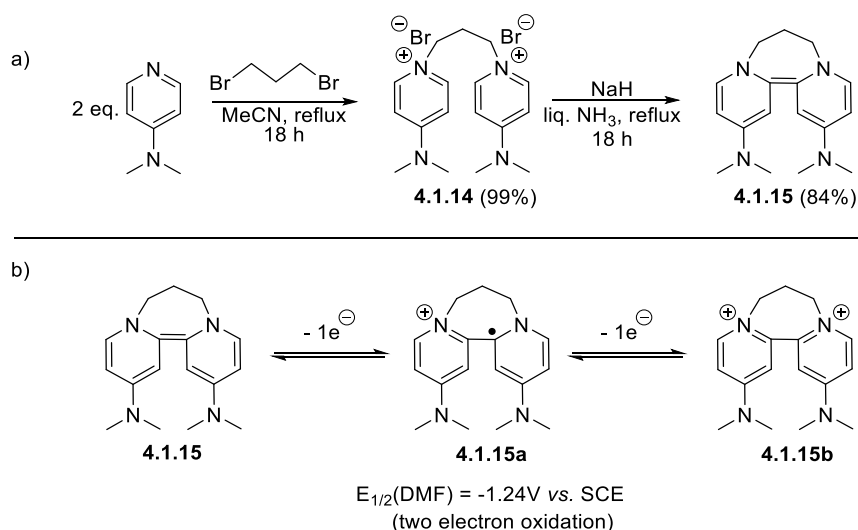
In the event, experiments conducted on aryl iodides **4.1.6** and **4.1.10** by Murphy *et al.* confirmed that **3.1.39** was reducing iodoarene substrates to their aryl anion states (Scheme 4.1.2).^{134, 135}



Scheme 4.1.2. Electron donor **3.1.39** was able to reduce aryl iodides to its anion states.^{134, 135}

This was based on the knowledge that aryl anions, and not radicals, nucleophilically attack esters leading to the cyclic products **4.1.8** and **4.1.12**. In both instances, the dehalogenated products were also isolated.

The drawback with using **3.1.39** as a super-electron donor (SED) concerns its synthesis; particularly the second step is quite time consuming due to the difficulty in installing the second trimethylene bridge. It would be synthetically more attractive if SEDs could be more easily obtained. To this end, Murphy and co-workers turned their attention to the synthesis of the DMAP-derived SED **4.1.15**. Starting with cheap and commercially available DMAP, the two-step synthesis of **4.1.15** was found to be high yielding and less time consuming since there was no requirement to install a second trimethylene bridge (Scheme 4.1.3 a).



Scheme 4.1.3. a) The synthesis of DMAP-derived donor **4.1.15** was straightforward and high yielding. b) SED **4.1.15** displayed a reversible two-electron redox potential at -1.24 V vs. SCE .¹³⁷

When subjected to electrochemical studies¹³⁷ it was found that **4.1.15** possessed a two electron reversible wave at a potential of $[E_{1/2}(\text{DMF}) = -1.69\text{V vs. Fc/Fc}^+]$ ¹³⁸ which would equate to -1.24V vs. SCE ; $[E_{1/2}(\text{DMF})_{\text{Fc/Fc}^+} = 0.45\text{V vs. SCE}]$.¹³⁷ These measurements indicated that **4.1.15** was comparable with the imidazole-based SED **3.1.39**.

4.2 Reductions with Photoactivated SED 4.1.15

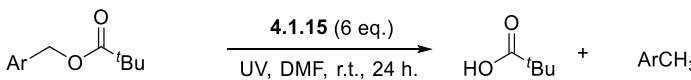
In recent years, the scope of reduction using **4.1.15** has expanded widely to include more challenging functional groups when it was discovered that this deep purple material could be photoexcited at 345 nm (commercial UV bulbs with 365 nm could be conveniently used). Challenging reductions included those of aromatic amides, benzylic ethers and esters, and malononitriles. This section highlights the recent success of these reductions.

4.2.1 Benzylic C-O bond cleavages.

Benzylic ethers and esters are common functional groups employed for the protection of the corresponding alcohols and carboxylic acids. It is not surprising that there are numerous methods for their cleavage. These include the use of heterogeneous catalysts in hydrogenolysis, the Birch reduction and electrolytic methods. This transformation can now be accomplished using **4.1.15** under photoactivated conditions.¹³⁹ Thorough experimental investigations confirmed that two different mechanisms were responsible for the observed reductions of esters and ethers.

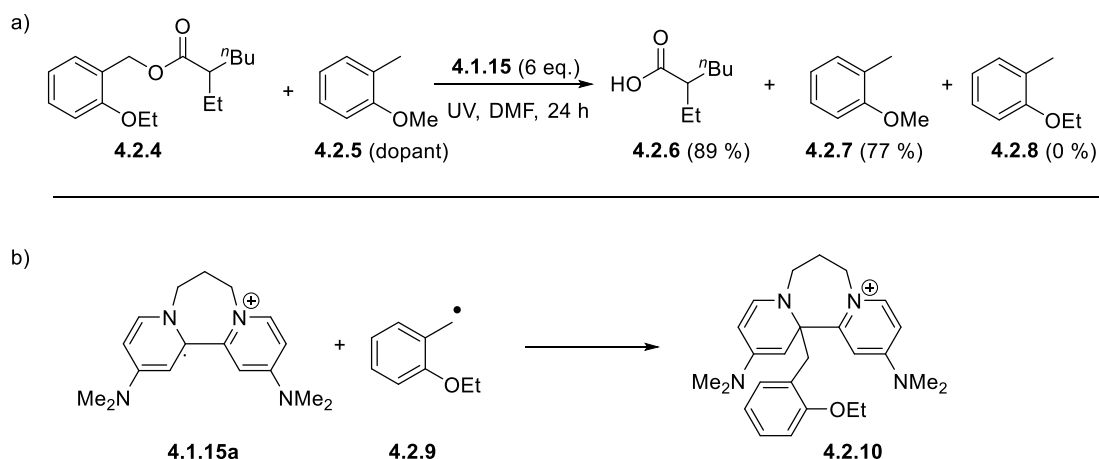
When benzylic esters **4.2.1-4.2.3** were treated with photoactivated **4.1.15**, good yields of the corresponding acids were isolated (Table 4.2.1). In every case, the disparity between the yields of the acid and the partnering toluene-type fragment, ArCH₃ led to the proposal that cleavage occurred at the radical anion stage leading to the carboxylate anion and the toluyl radical which was readily trapped by the radical cation **4.1.15a** (Scheme 4.2.2 b).

Table 4.2.1. Benzylic C-O bond cleavage of esters proceeded in good yields using photoactivated 4.1.15.



Substrate	Ar	Carboxylic acid (%)	Ar CH ₃ (%)
4.2.1	2-(MeO)C ₆ H ₄	90	0
4.2.2	3,5-(MeO) ₂ C ₆ H ₃	78	9
4.2.3	4-(CF ₃)C ₆ H ₄	88	trace

A doping experiment (Scheme 4.2.2 a) was therefore conducted with **4.2.4** which confirmed that the low yields of the toluene-type fragment from the reductions **4.2.1-4.2.3** were not due to volatility. Rather, the poor recovery was consistent with trapping by the donor radical cation **4.1.15a**, with the resulting salt **4.2.10** readily partitioning into the aqueous phase upon workup, rendering it irrecoverable (Scheme 4.2.2 b).



Scheme 4.2.2. a) Doping experiment using ester **4.2.4** revealed that absence of **4.2.8** was not due to volatility issues. b) Radical trapping by the donor radical cation **4.1.15a** is proposed to result in toluene-type fragments being irretrievable upon workup.

Impressively, C-O bond reduction of benzylic ethers could also be achieved with photoactivated **4.1.15** albeit the yields of the isolated alcohols were generally lower when compared to the carboxylic acids arising from reduction of the esters. Interestingly, most ether substrates were yielding at least moderate percentages of their toluene partners after reductive cleavage (Table 4.2.3).

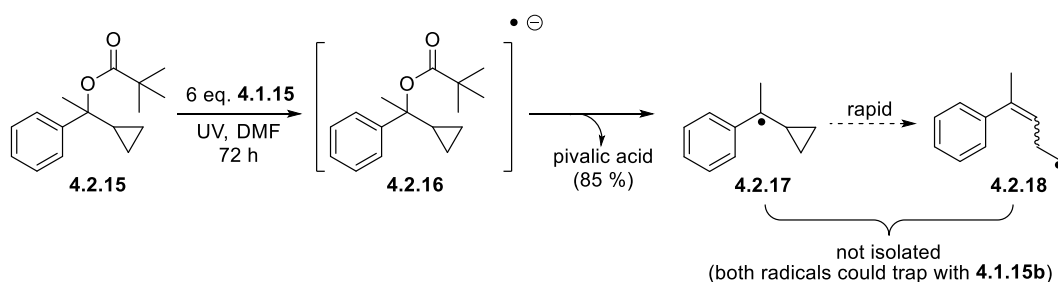
Table 4.2.3. Benzylic ethers could also be cleaved by photoactivated **4.1.15**.

Substrate	$\text{Ar}-\text{CH}_2-\text{OR} \xrightarrow[\text{UV, DMF, r.t., 24h.}]{\text{4.1.15 (6 eq.)}} \text{ArCH}_3 + \text{ROH}$		Ar CH ₃ (%)	ROH(%)	S.M.(%)
	Ar	R			
4.2.11	2-(MeO)C ₆ H ₄		23	73	8
4.2.12	2-(MeO)C ₆ H ₄	C ₁₀ H ₂₁	20	71	8
4.2.13	3,5-(MeO) ₂ C ₆ H ₃	C ₁₀ H ₂₁	27	60	11
4.2.14	4-(CF ₃)C ₆ H ₄	C ₁₁ H ₂₃	0	0	4

It was suspected that the reductive cleavage of ethers required two electrons as this would result in two anionic fragments that would not be susceptible to trapping with the radical cation **4.1.15b**. A possible mechanism involves the initial fragmentation of the radical anion followed by the rapid transfer of a second electron onto the radical fragment thus resulting in two anionic fragments. To determine if this mechanism was involved, **4.2.1** was subjected to photoactivated reduction with excess **4.1.15** (6 eq.) and with extended reaction times (72h). Under these conditions, the toluene-based fragment was present only in trace amounts (2 %) which indicated that the further reduction of the benzyl radical to its anion was not possible even with longer reaction times. This would rule out the likelihood of the fragmentation of benzylic ethers proceeding at the radical anion stage.

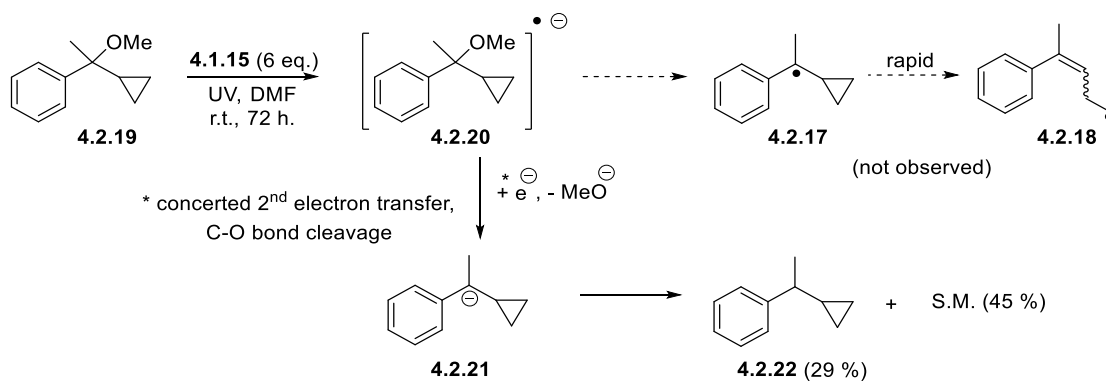
It was also unlikely that a highly unstable anti-aromatic arene dianion should be involved. Therefore, an alternative mechanism would be for the C-O bond cleavage and the second electron transfer to proceed in a concerted fashion. To determine if this could account for the formation of the two anionic fragments, **4.2.15** (Scheme 4.2.4) and **4.2.19** (Scheme 4.2.5) were subjected to reduction with photoactivated **4.1.15**.

In the event, **4.2.15** underwent quantitative reductive cleavage at the radical anion state to afford pivalic acid (85 %) as the sole product following workup. The radical partner **4.2.17** was expected to rapidly ring-open¹⁴⁰ with both radicals **4.2.17** and **4.2.18** being trapped by radical cation **4.1.15b**.



Scheme 4.2.4. The cyclopropyl-bearing ester **4.2.15** underwent quantitative C-O bond reduction at the radical anion stage. The radical fragment **4.2.17** would readily ring-open and both radical species would be trapped with **4.1.15b**.

In contrast, the reduction of the related ether **4.2.19** yielded a different result (Scheme 4.2.5). In this case, the cyclopropyl fragment **4.2.22** was isolated, which indicated that the related radical **4.2.17** was not involved in this mechanism. This comparative study confirmed that the C-O cleavage of the ether proceeded from a concerted second electron transfer.

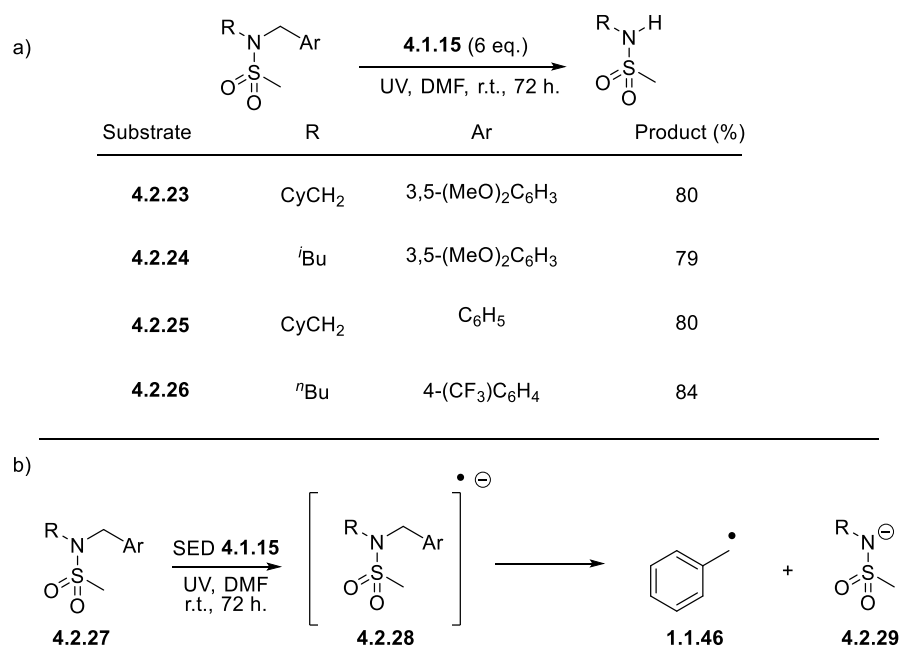


Scheme 4.2.5. The cyclopropyl probe **4.1.15** helped to determine that reduction of benzylic ethers required two electrons from **4.2.15**.

4.2.2 C-N bond cleavages of activated amines and amides

Recently, it has also been reported that benzylic and allylic sulfonamides undergo cleavage of their benzylic and allylic units using photoactivated **4.1.15** (Scheme 4.2.6 a).¹⁴¹

Scheme 4.2.6. a) Photoactivated 4.1.15 accomplished the cleavage of benzylic C-N bonds of sulfonamides. b) Mechanistic studies revealed that the reductions proceeded *via* fragmentation of the radical anion with regioconservation of spin.

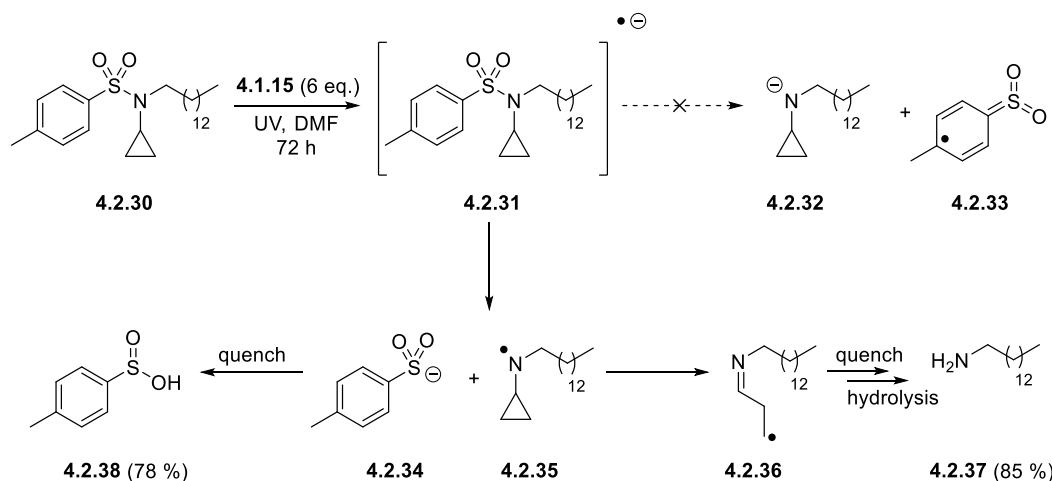


By employing computational methods, it was predicted that the debenzoylation proceeded from the radical anion and that the ensuing fragmentation should lead favourably to the formation of the resonance-stabilised sulfonamide anion and the corresponding toluenyl radical (Scheme 4.2.6 b).¹⁴²

It was also predicted computationally that the LUMO of these benzylic sulfonamides resided on the aromatic fragments and it followed that the SET event would initially occur in this region. This would account for the observed chemoselectivity such that no demethylated products were observed (i.e. no competing N-S bond cleavage).

Tosylamides e.g. **4.2.30** could also be reductively cleaved upon generation of its radical anion. Here, the electron was initially captured by the tosyl fragment and subsequently transferred to the N-S bond whereupon fragmentation occurred. In this case, the bond cleavage resulted in the toluenesulfinate anion **4.2.34** and the aminyl

radical fragment **4.2.35** which underwent ring-opening to yield the iminyl radical **4.2.36**. The iminyl radical in turn was quenched and hydrolysed upon workup to yield the amine **4.2.37** good yield. If the fragmentation had instead, yielded the aminyl anion **4.2.32**, then the cyclopropyl would remain intact and its protonated form would have been the observed product (Scheme 4.2.7).



Scheme 4.2.7. Reduction by **4.1.15** led to the N-S bond cleavage of **4.2.31**, resulting in fragments **4.2.35** and **4.2.36**.

To extend the scope of C-N bond reductions, aniline-based substrates were also tested with photoactivated **4.1.15** (Table 4.2.8).

Table 4.2.8. a) C-N bond cleavage on aniline-based substrates using photoactivated **4.1.15** was possible. b) Allylic sulfonamides were also reduced by photoactivated **4.1.15**.

a)				b)			
Substrate	R	S.M (%)	Product (%)	Substrate	R	S.M (%)	Product (%)
4.2.39	Me	62	6	4.2.43	C ₁₂ H ₂₅	32	63
4.2.40	COMe	59	33	4.2.44	<i>i</i> pentyl	38	50
4.2.41	CO ^t Bu	8	83	4.2.45	C ₆ H ₅ (CH ₂) ₂	57	41
4.2.42	CO ₂ Et	37	58	4.2.46	C ₆ H ₅ (CH ₂) ₃	47	42

In this case, the electron-rich aniline should be less susceptible to reduction to its corresponding radical anion. To compensate for this, electron-withdrawing

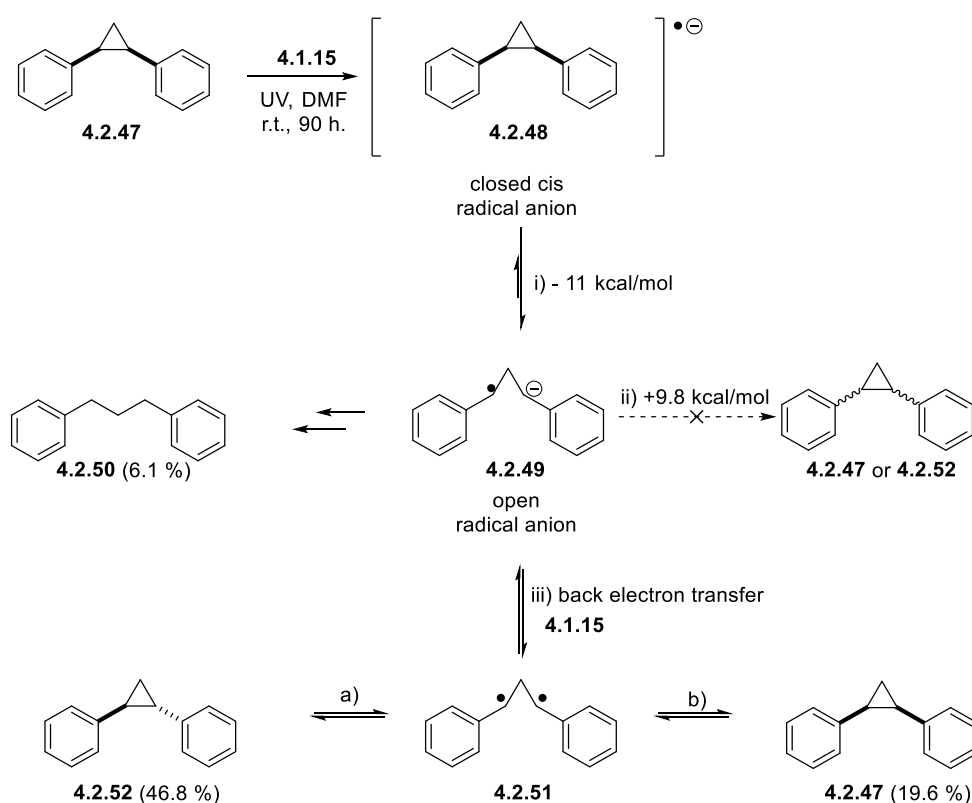
substituents which can lower the LUMO energy were installed into the substrates. In the event, cleavage of the allyl group proceeded with amides **4.2.39–4.2.42**, with pivalamide **4.2.41** being the most successful (Table 4.2.8).

Having showcased the ability of **4.1.15** to reductively cleave C-N bonds of benzyl methanesulfonamides and aniline-based substrates, even more challenging C-N bond cleavages were attempted. By simply replacing the benzyl group with an allylic group, the LUMO energy was expected to be markedly increased.

Remarkably, reductive cleavage was still possible as seen from substrates **4.2.43–4.2.46**; albeit with slightly diminished yields which would reflect the increased difficulty in generating the radical anion (Table 4.2.9). The results from substrates **4.2.45** and **4.2.46** merit attention because they demonstrated that intramolecular electron shuttling from the benzene ring (where the LUMO resided) to the allylic fragment could have occurred to account for the observed cleavage (more details of this mechanism is provided later in Chapter 5.1 – Conclusion and Future work).

4.2.3 Diphenyl Cyclopanes C-C bond cleavage

Benzene ($E^0 = -3.42$ V vs. SCE)¹⁴³, LUMO = -0.393 eV,¹⁴⁴ is notoriously difficult to reduce and this often requires powerful metals including sodium, lithium, calcium, and lately, a combination of SmI₂ and amine has also shown success.³⁰ To determine the reductive ability of photoactivated **4.1.15** towards benzene, related substrates must be carefully selected such that they do not possess significant activation e.g. electron-withdrawing or donating substituents. Therefore, diphenylcyclopropane **4.2.47** was selected as one of the suitable probes; with its calculated LUMO energy (-0.587 eV)¹⁴⁵ comparatively similar to that of benzene.

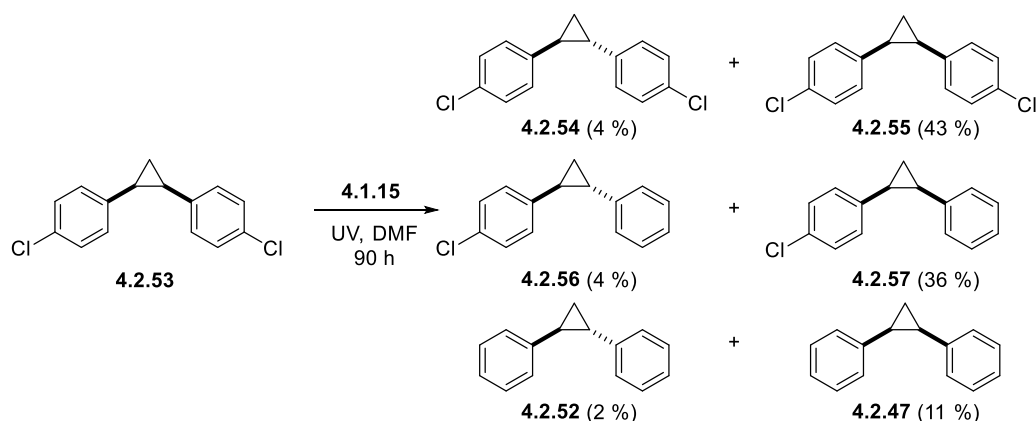


Scheme 4.2.9. Diphenyl cyclopropane **4.2.47** was successfully reduced by **4.1.15** resulting in C-C bond cleavage and stereomutation. Energy values were calculated using UB3LYP/6-31+6(d) level of theory.

When tested for reduction with photoactivated **4.1.15**, compounds **4.2.47**, **4.2.50**, and **4.2.52** were obtained (Scheme 4.2.9). The ring-opened product **4.2.50** confirmed that C-C bond reduction had occurred. It was clear from the products obtained that stereomutation of the starting material had occurred which further indicated that ring-opening of the starting material had taken place.

Computational investigations revealed that ring opening of the radical anion **4.2.49** was spontaneous and exothermic (Scheme 4.2.9, step i, $-11 \text{ kcal mol}^{-1}$). It also indicated that the subsequent stereo-mutation upon ring closure did not occur at the radical anion stage as this was too energetically demanding (Scheme 4.2.9, step ii, $+9.8 \text{ kcal mol}^{-1}$). To circumvent this energy barrier, it was likely that the radical anion underwent back electron-transfer to the radical cation of SED **4.1.15**. By doing so, the singlet biradical **4.2.51** can be obtained (Scheme 4.3.9, step iii) which would readily proceed with ring closure.

Further evidence for radical anion formation derived from the reaction involving chloro-containing substrate **4.2.53** (Scheme 4.2.10). In this case, products resulting from reductive dehalogenation were also observed; a process possible only upon generation of the precursor radical anions.



Scheme 4.2.10. Photactivated **4.1.15** was sufficiently powerful to reduce diphenylcyclopropanes thus indicating the donor's ability to reduce benzene.

4.3 Project Aims

In the preceding introductory chapters, several methods for C-O and C-S bond cleavages have been showcased. Additionally, an outline on the development of super-electron donors and the impressive reactivity of SED **4.1.15** was shown. This Ph.D. programme was aimed at exploring:

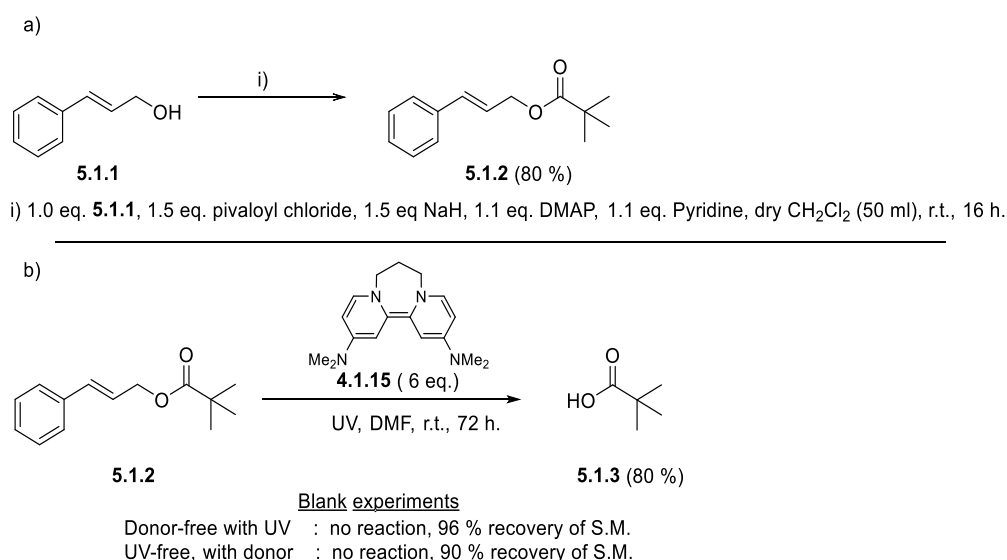
1. The reductive C-O bond cleavages of non-benzylic esters and ethers using photoactivated **4.1.15**.
2. The reduction of challenging C-C bonds of amides and esters afforded by photoactivated **4.1.15**.
3. C-S bond reductions of aromatic sulfides, sulfoxides and sulfones by employing photoactivated **4.1.15**.
4. The possibility of applying the Birch reduction to non-aromatic sulfides and its significance towards understanding methanogenesis.

Chapter 5 Results and Discussion – C-O bond cleavages

In Chapter 4.2.1, it was shown that photoactivated **4.1.15** could reduce benzylic C-O bonds in very good yields. Blank reactions had confirmed that thermal activation did not account for the observed reactivity. The high efficiency in these reductions strongly suggested that this reactivity was not limited to benzylic-based substrates. Because of this, experiments were conducted to investigate the threshold of the C-O bond cleavage afforded by photoactivated **4.1.15**.

5.1 C-O bond cleavage of esters with extended conjugation

A simple modification that could be made on benzylic esters involved extending the conjugation between the benzene ring and the C-O bond. Beginning with cinnamyl alcohol **5.1.1**, the required ester **5.1.2** was synthesised in good yield and tested for reduction (Scheme 5.1.1).



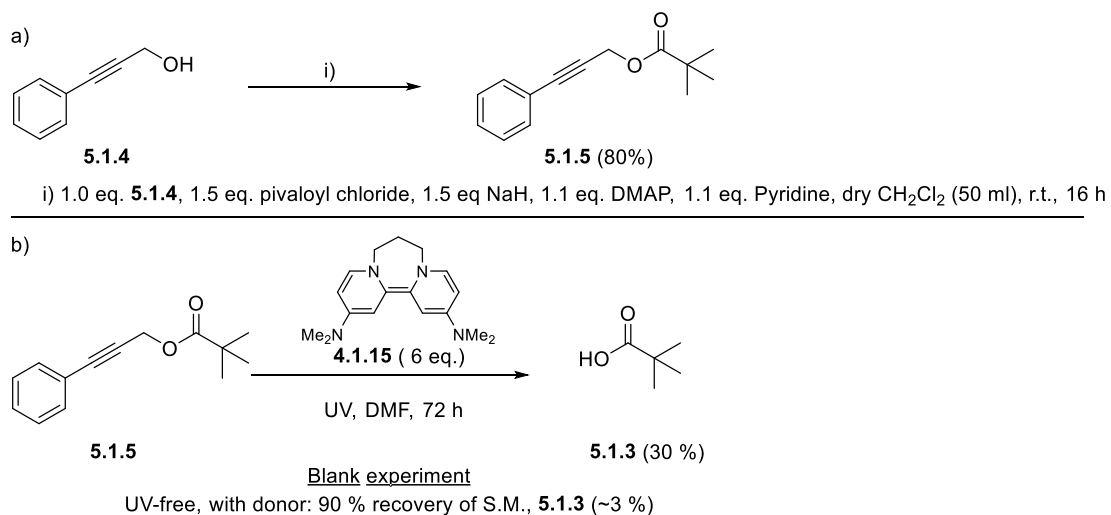
Scheme 5.1.1. a) Synthesis of ester **5.1.2** from cinnamyl alcohol proceeded in high yield. b) C-O bond cleavage was observed when **5.1.2** was subjected to reduction with photoactivated **4.1.15**.

Previously, UV-studies had indicated that **4.1.15** was photoexcitable at three different wavelengths - 260, 345 and 520 nm.¹⁴⁶ As such, experiments requiring photoactivation of **4.1.15** could be conveniently achieved with two focused Blak-ray B-100 series lamps (365 nm) which were purchased from UVP Ltd. These lamps were positioned opposite each other with the reaction flask clamped equidistant between the two bulbs.

Impressively, the photoreduction proceeded efficiently, with pivalic acid **5.1.3** isolated in good yield (80 %). To confirm that the observed C-O bond cleavage required photoexcitation of the super-electron donor, two types of blank experiments were conducted. In the first instance, the reaction involving **4.1.15** and **5.1.2** was conducted without the UV bulbs. In a separate experiment, **5.1.2** was dissolved in DMF and the flask was then clamped between the two UV bulbs; this was to determine if the observed C-O bond cleavage was due to photoexcitation of the substrate (as opposed to the super-electron donor).

Pleasantly, no reactivity was observed with these blank reactions confirming that the photoactivated **4.1.15** was required for the reduction.

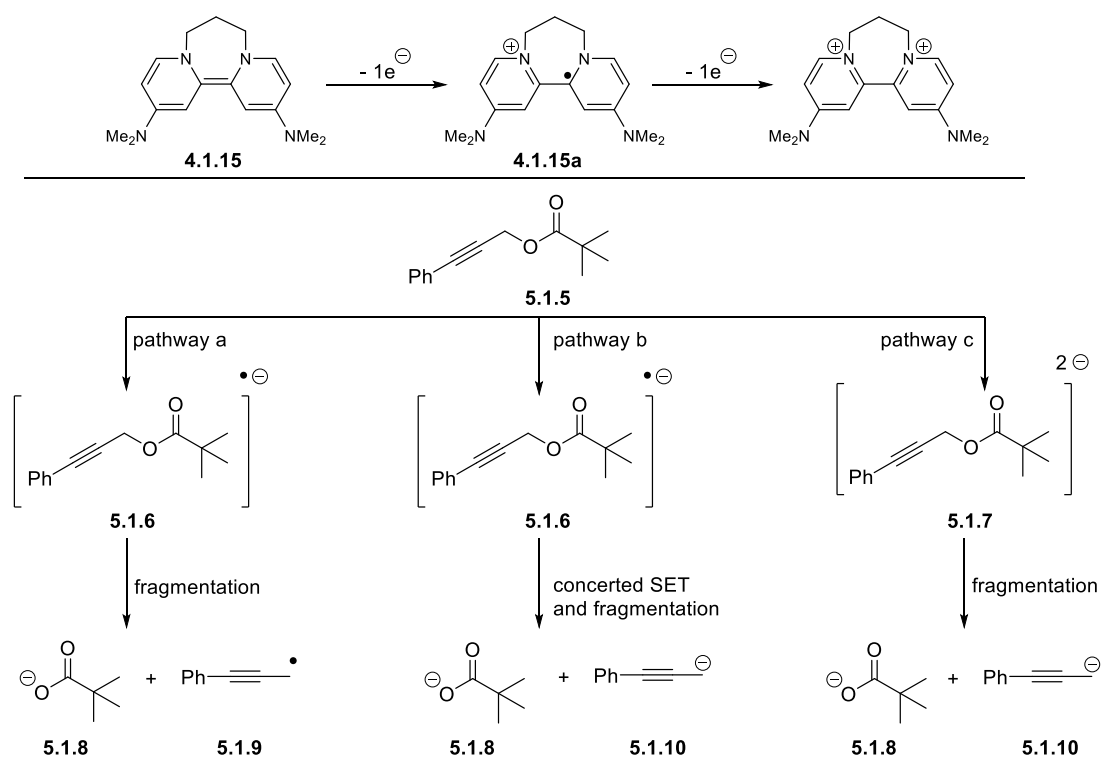
This led on to the design and synthesis of propargylic ester **5.1.5** (Scheme 5.1.2 a) which was then subjected to reduction conditions with photoactivated **4.1.15**. In the event, the yield of the pivalic acid isolated after the reaction was low (30 %); highly indicative that the reduction was not as efficient as that of the related cinnamate ester **5.1.2** (Scheme 5.1.2 b). A blank experiment consisting of non-photactivated **4.1.15** and the substrate led to excellent recovery of the starting material thus confirming that the observed reduction required photoactivation of the donor.



Scheme 5.1.2. a) Synthesis of propargylic ester **5.1.5** from propargylic alcohol proceeded in high yield. b) C-O bond cleavage was observed to a small extent when **5.1.5** was subjected to reduction with photoactivated **4.1.15**.

At this stage, it was important to ascertain the reduction mechanism. In this regard, there were at least three theoretical explanations for the observed reactivity. These are illustrated in Scheme 5.1.3, with substrate **5.1.5** as an example.

It could be that a single electron transfer (SET) event from the super-electron donor to the ester resulted in the generation of the corresponding radical anion which spontaneously fragmented (Scheme 5.1.3, path a). Alternatively, it may be that the fragmentation of the ester required two electrons (at its dianion state), in which case, double electron transfer (DET) from the super-electron donor was necessary and was possible. Two scenarios could arise for DET process; it might result in the formation of a dianion before fragmentation (Scheme 5.1.3, path c) or, the second electron transfer and the bond cleavage was concerted (Scheme 5.1.3, path b).

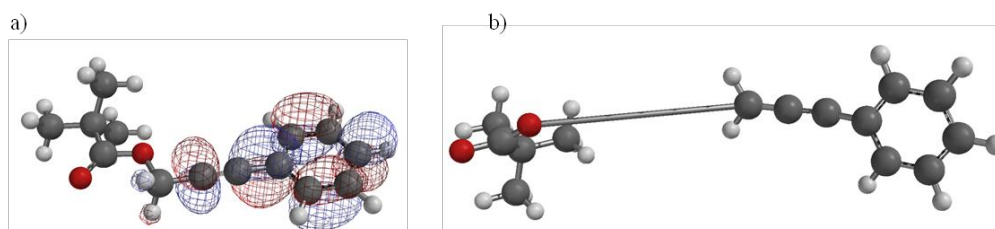


Scheme 5.1.3. Three possible mechanisms could account for the observed C-O bond cleavage of **5.1.5**. Pathway a predicts reductive bond cleavage upon formation of the radical anion. Pathways b and c postulates the requirement of DET for fragmentation. If so, SED **4.1.15** is sufficiently reactive to provide two electrons.

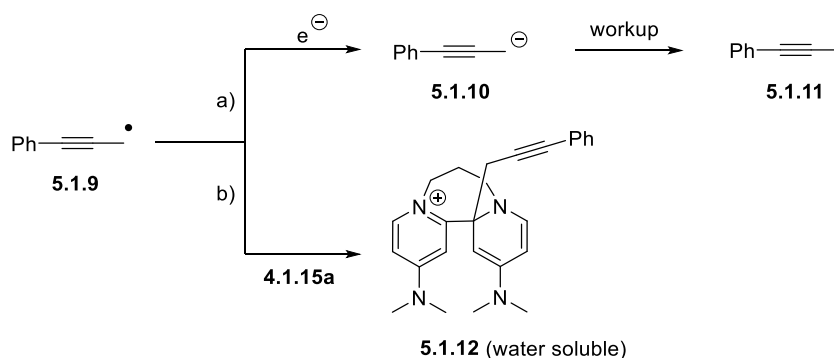
To investigate the possibility of the C-O bond cleavage proceeding to yield two anionic products (paths b and c), the reductions of esters **5.1.2** and **5.1.5** were both repeated with photoactivated **4.1.15**. The crude products were then analysed by ^1H

NMR immediately after acidic quenching and workup. In all cases, the NMR spectrum revealed that the aromatic fragments were absent, with pivalic acid as the major product in both cases. The absence of the aryl-containing fragment was highly indicative that it had undergone trapping as a radical with the radical cation **4.1.15a**, derived from the super-electron donor. Further support for the radical anion fragmentation (pathway a) stemmed from computational investigations. The optimisation of the radical anion **5.1.6** was attempted (DFT, B3LYP, 6-31G(d,p) was employed) but failed to converge and indicated that spontaneous bond cleavage would likely occur without any energy barrier to attain more stable products (Figure 5.1.4). Therefore, a second electron was not required for C-O bond cleavage.

Figure 5.1.4. a) The calculated LUMO of **5.1.5** resided mainly on the aryl moiety. b) Spontaneous C-O bond cleavage was predicted when energy minimisation was attempted on the radical anion of **5.1.5**. Note that the elongated line does not represent a bond. (Spartan 2010 version, DFT, B3LYP, 6-31G(d,p) in DMF was employed).

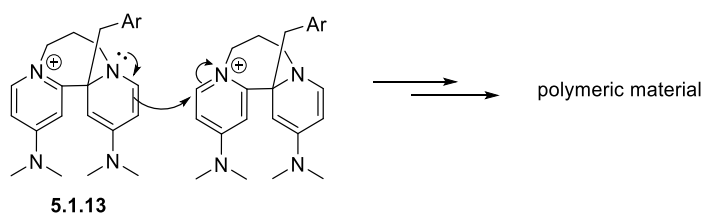


Finally, the fate of the resulting aryl-containing fragments in the reduction of **5.1.2** and **5.1.5** are addressed. Following the proposal that the C-O bond cleavage proceeded at the radical anion stage, it would have meant that the aryl-containing fragment was expelled as a radical as opposed to an anion. This would also allow for regioconservation of spin.¹⁴² In theory, the radical can be further reduced to its anion (Scheme 5.1.5, pathway a).



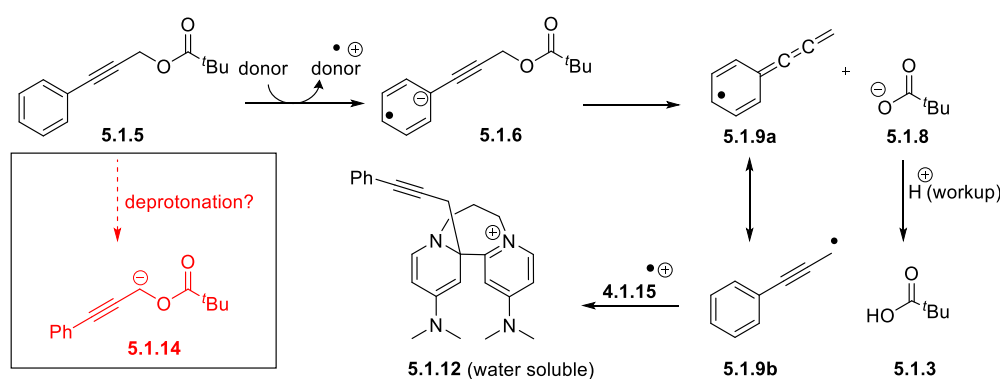
Scheme 5.1.5. Two possible fates of the radical fragment **5.1.9**

Experimentally this was not detected and, considering that the reaction was conducted for 72 hours with excess **4.1.15**, it was clear that further reduction of the aryl radical was not possible. This was also previously established in the study of C-O bond cleavages of benzylic esters (see Chapter 4.2.1). It was more likely that the radical fragment proceeded to couple with the radical cation of the super-electron donor **4.1.15a**. The resulting cation would readily partition into the aqueous layer upon workup (Scheme 5.1.5, pathway b). As part of his Ph.D. studies, Steven O'Sullivan had recently attempted to track down the fate of similar aromatic radical fragments. This proved extremely challenging with the proposed cationic product undetected. A possible reason was that the cation itself could have reacted further through its enamine moiety leading to polymerisation (Scheme 5.1.6).



Scheme 5.1.6. Cation **5.1.13** was thought to undergo further polymerisation, making isolation and characterisation challenging.

Piecing all the information together, it was highly likely that the reductive C-O bond cleavage began with the initial generation of the radical anion **5.1.6**, followed by its fragmentation, resulting in the radical residing on the aryl-containing fragment and the corresponding pivalic acid anion (Scheme 5.1.7).

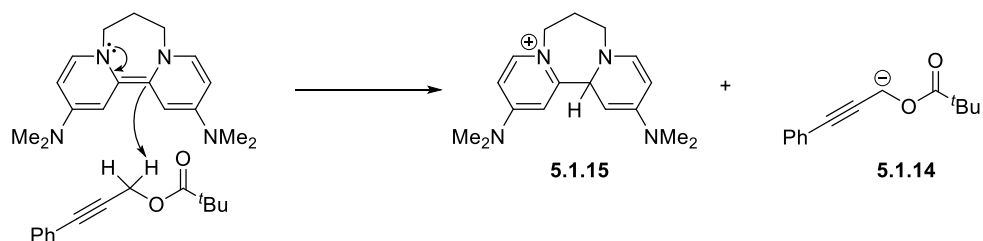


Scheme 5.1.7. A proposed mechanism to account for the absence of the aromatic fragment **5.1.9** upon reductive cleavage of the parent substrate. Inset: deprotonation of **5.1.5** by **4.1.15** cannot be ruled out at this stage.

Although no firm evidence could be provided to explain the fate of radical fragment, there were strong indications that **5.1.9** was trapped by the radical cation **4.1.15a**

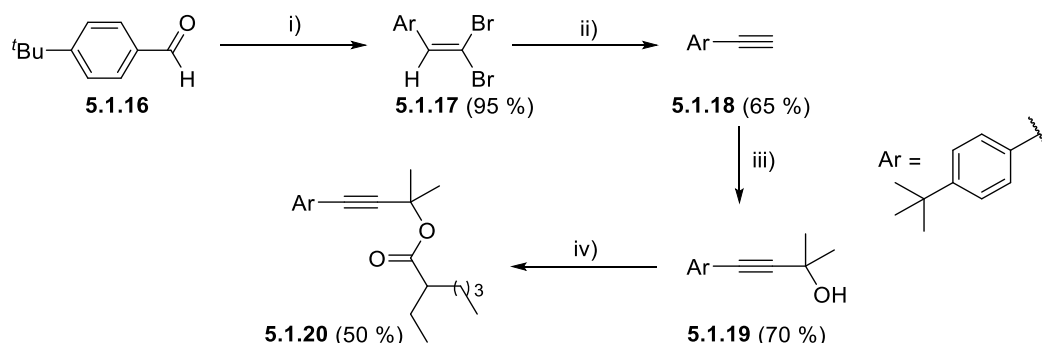
(Scheme 5.1.7 illustrates the mechanism with propargylic **5.1.5** but would also apply to the cinnamyl-based **5.1.2**).

Previously, **4.1.15** was discovered to be sufficiently basic to deprotonate acetonitrile¹⁴⁷ and so it was possible that a similar reaction was competing with the reduction (Scheme 5.1.8).



Scheme 5.1.8. Deprotonation of **5.1.5** by the super-electron donor could be operative and competing with the reductive cleavage.

To address this concern, substrate **5.1.20** was designed and synthesised. The installation of the required alkyne fragment was possible by employing the Corey-Fuchs¹⁴⁸ reaction (Scheme 5.1.9).



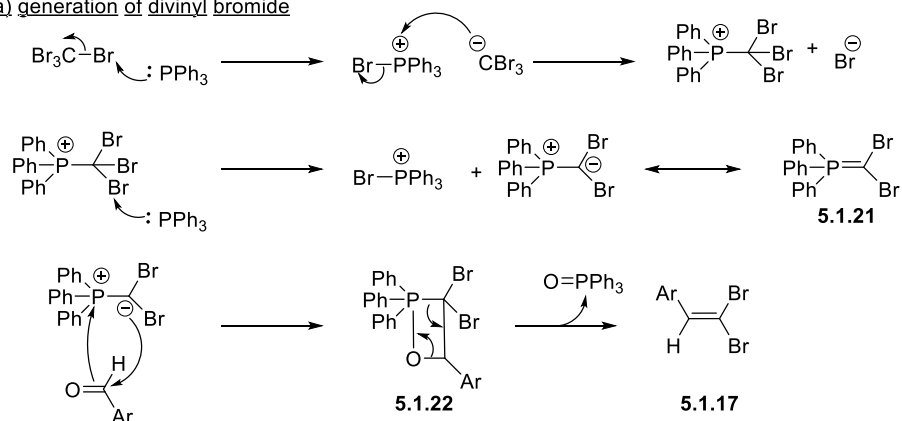
- i) 1.0 eq. **5.1.16**, 1.5 eq. CBr_4 , 2.5 eq. PPh_3 , dry CH_2Cl_2 , $0\text{ }^\circ\text{C} \rightarrow \text{r.t.}$, 48 h.
- ii) 1.0 eq. **5.1.17**, 3.0 eq. $n\text{-BuLi}$ (2.2 M), dry THF (10 ml), $-78\text{ }^\circ\text{C} \rightarrow 0\text{ }^\circ\text{C}$, 2 h.
- iii) 1.0 eq. **5.1.18**, 1.1 eq. $n\text{-BuLi}$ (2.2 M), 5.0 eq. dry acetone, dry THF (10 ml), $-78\text{ }^\circ\text{C} \rightarrow \text{r.t.}$, 16 h.
- iv) 1.0 eq. **5.1.19**, 1.5 eq. NaH , 2.2 eq. 2-ethylhexanoyl chloride, excess pyridine, 1.1 eq. 4-DMAP, dry CH_2Cl_2 (15 ml), r.t. , 16 h.

Scheme 5.1.9. Synthesis of **5.1.20** comprised of four steps including the use of of the Corey-Fuchs reaction to obtain the terminal alkyne **5.1.18**.

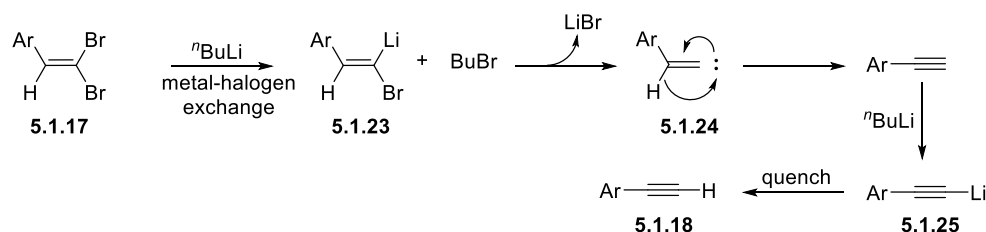
In the first of the multi-step synthesis, the vinyl dibromide **5.1.17** was obtained in 95 % yield. The two reagents are thought to react with each other through a series of nucleophilic attacks and displacements of leaving group (Scheme 5.1.10 a). This would result in the formation of phosphonium ylide **5.1.21**. The propensity for

phosphorus to form bond(s) with oxygen would set up the succeeding reaction with the aldehyde, with the resulting oxaphosphetane rapidly collapsing to yield **5.1.17**.

a) generation of divinyl bromide

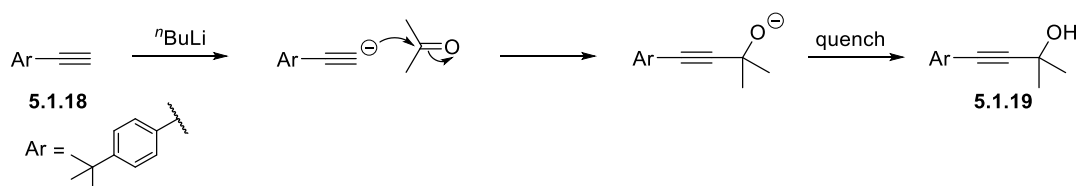


b) generation of terminal alkyne



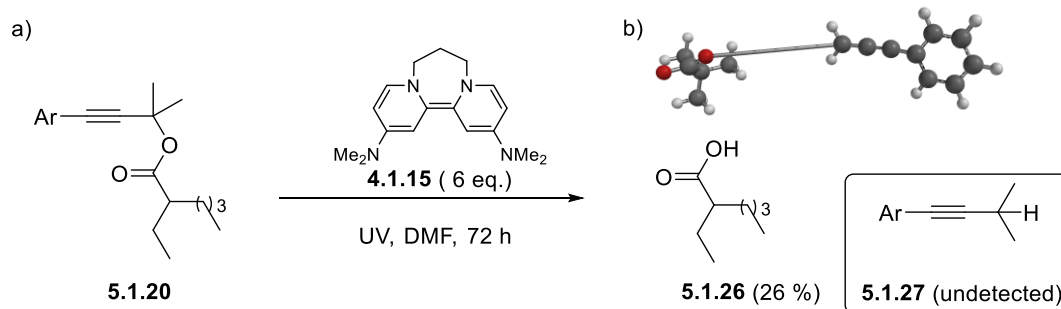
Scheme 5.1.10. a) Mechanistic details on the formation of divinyl bromide **5.1.17**. b) Treatment of **5.1.17** with $n\text{BuLi}$ allowed access to the terminal alkyne **5.1.18**.¹⁴⁸

By treating **5.1.17** with excess $n\text{BuLi}$, a metal-halogen exchange takes place. The loss of the second halide from **5.1.23** would then result in the formation of an unstable carbene **5.1.24** which would rearrange to yield the terminal alkyne.¹⁴⁸ Under the basic conditions employed, the alkyne would exist in its lithium salt-form **5.1.25** and acidic quenching should then allow protonation to finally yield **5.1.18**. Installation of the gem-dimethyl fragment involved deprotonation of **5.1.18** and nucleophilic attack onto acetone (Scheme 5.1.11). Quenching the reaction afforded the tertiary alcohol which was then used in a straightforward esterification with commercially available 2-ethylhexanoyl chloride to obtain the final product **5.1.20**.



Scheme 5.1.11. Tertiary alcohol **5.1.19** was obtained by reacting **5.1.18** with acetone.

When **5.1.20** was tested for reduction with photoactivated **4.1.15**, 2-ethylhexanoic acid **5.1.26** was isolated in low yield (Scheme 5.1.12 a). Similar to the previous experiments with **5.1.2** and **5.1.5**, the aryl-containing fragment **5.1.27** remained undetected. A repeat of the reaction yielded consistent results, indicating that the aryl fragment was being trapped by the radical cation of **4.1.15**. As seen previously with **5.1.5**, computational investigations indicated that C-O bond cleavage of **5.1.20** would be spontaneous upon generation of its radical anion (Scheme 5.1.12 b).



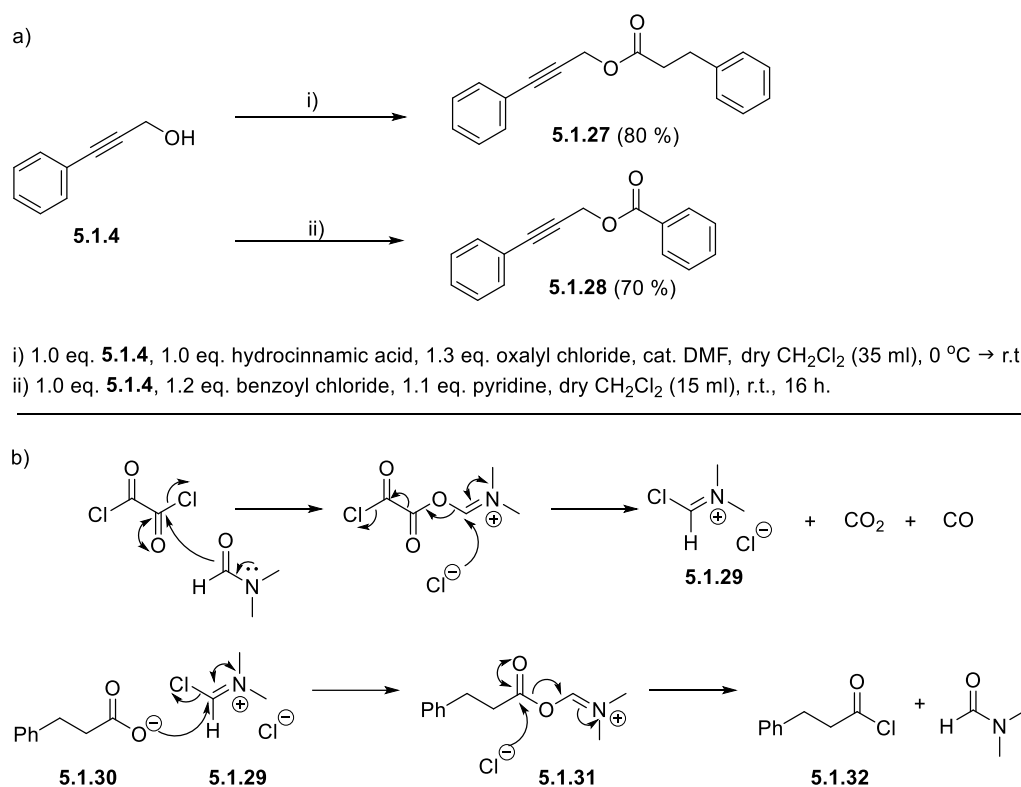
Scheme 5.1.12. a) C-O bond cleavage of **5.1.20** was observed when tested with photoactivated **4.1.15**. b) Computational calculations revealed that there was no energy barrier for the cleavage of the C-O bond in the radical anion state of **5.1.20** (Spartan 2010 version, DFT, B3LYP, 6-31G(d,p) in DMF was employed).

Testing **5.1.20** for reduction with photoactivated **4.1.15** was with a view to deducing if deprotonation of propargylic protons was undermining the efficiency in reductive bond cleavage. This issue can now be addressed.

Broadly speaking, the yields of 2-ethylhexanoic acid **5.1.26** and pivalic acid **5.1.3** obtained after the reduction of their parent esters were not drastically different. If, in the event that deprotonation of propargylic protons was impeding the reduction of the substrate, then a significant increase in the yield of carboxylic acid **5.1.26** should have been observed. Additionally, **5.1.26** (b.pt: 70 °C at 0.1 Torr i.e., 228.1 °C at 760 Torr)¹⁴⁹ was expected to be non-volatile under the workup and purification conditions. Yet, the isolated yield was similar to that of pivalic acid obtained from the reduction of **5.1.5**. Therefore, it can be concluded that the reductive cleavage of propargylic esters was inherently more challenging than the corresponding cinnamyl-based ester **5.1.2** (average yield of pivalic acid was 80 %).

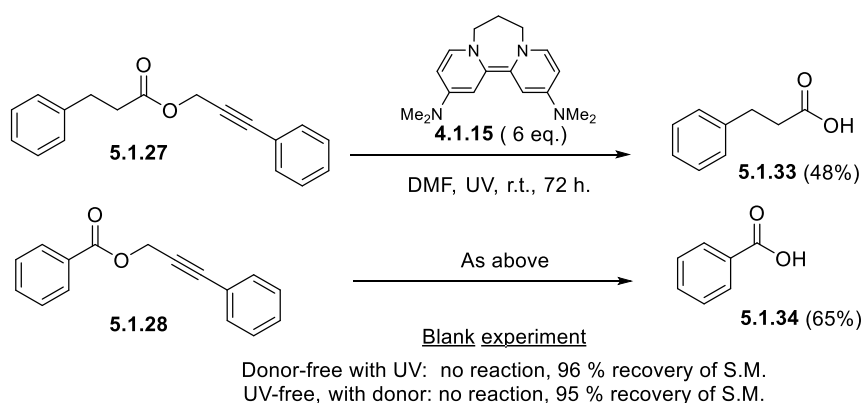
In an attempt to broaden the substrate scope of the newly discovered reduction, aromatic alkynes **5.1.27** and **5.1.28** were prepared by simple esterification (Scheme

5.1.13). In the case of **5.1.27**, *in situ* generation of hydrocinnamoyl acyl chloride was conducted using oxalyl chloride and catalytic amounts of DMF (Scheme 5.1.13 b).



Scheme 5.1.13. a) Synthesis of propargylic-based esters **5.1.27** and **5.1.28**. b) Proposed mechanism for the generation of **5.1.32** using oxalyl chloride and DMF.¹⁵⁰

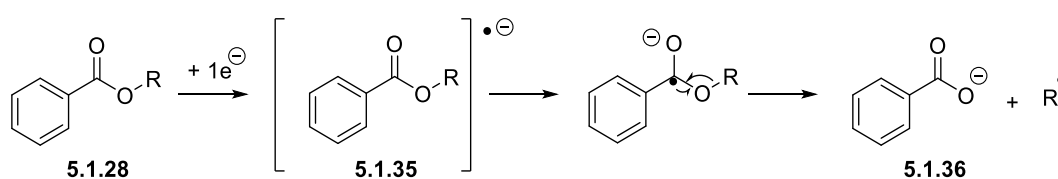
It was pleasing to observe that the reduction of these substrates was possible with photoactivated **4.1.15** as evidenced by the successful isolation of their carboxylic acid fragments (Scheme 5.1.14).



Scheme 5.1.14. Substrates **5.1.27** and **5.1.28** both experienced reductive C-O bond cleavage with photoactivated **4.1.15**.

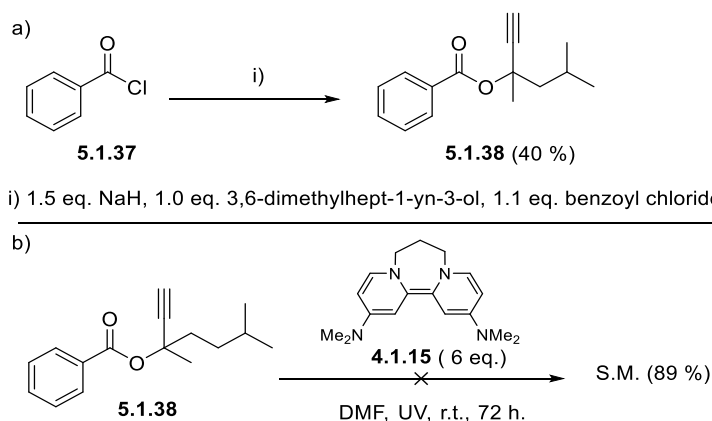
It has been deduced (*vide supra*) that the aromatic alkyne-based esters were inherently more difficult to reduce than for example, the cinnamyl-based substrates; this makes **5.1.28** an outlier since the yield of benzoic acid **5.1.34** was suspiciously high. Intrigued by the observed enhanced reactivity, it was thought that a different mechanism was afforded to this benzoate candidate.

In theory, the observed C-O bond cleavage of **5.1.28** by photoactivated **4.1.15** could have resulted from reduction of the benzoate moiety to its radical anion (Scheme 5.1.15).



Scheme 5.1.15. Reduction of the benzoate **5.1.28** could have proceeded without any participation from the aromatic alkyne fragment.

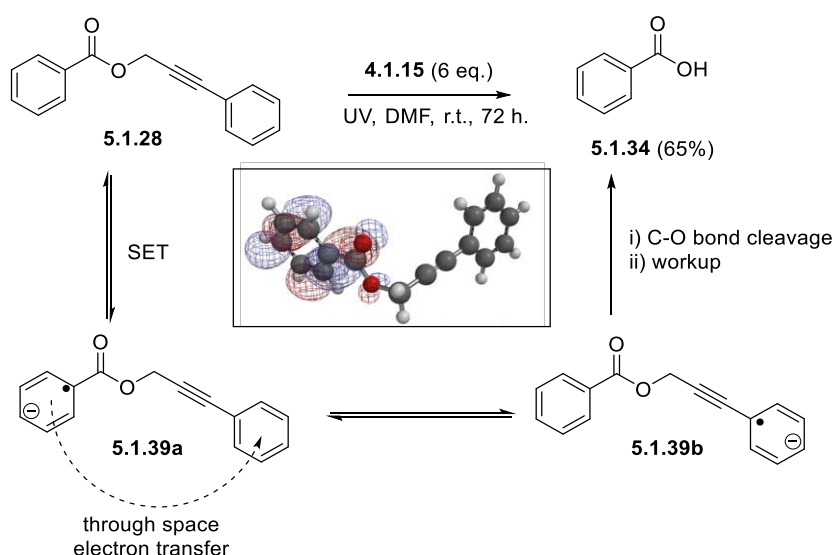
To test this hypothesis, benzoate **5.1.38** was synthesised in which the aromatic ring attached to the alkyne was eliminated and at the same time, ensuring that there were no acidic protons present. When tested for reduction, no reactivity was observed (Scheme 5.1.16). Therefore, reduction of the benzoate moiety by photoactivated **4.1.15** can be ruled out.



Scheme 5.1.16. a) To test for the possibility of benzoate reduction by **4.1.15**, benzoate **5.1.38** was synthesised and subjected to reduction. b) Benzoate **5.1.38** did not undergo C-O bond cleavage and was recovered in 89 % yield.

The enhanced reactivity of benzoate **5.1.28** must derive from an alternative mechanism. An important clue stemmed from computational investigations which predicted that the LUMO of **5.1.28** actually resided on the benzoate and not on the aromatic alkyne fragment (Scheme 5.1.17, inset). Since it has been shown experimentally that benzoates cannot be reductively cleaved, it is proposed that intramolecular electron transfer was operative.

Essentially, the benzoate fragment served as an electron reservoir for **5.1.39** upon reduction by the photoactivated **4.1.15**. The electron then proceeded to “hop” onto the aromatic alkyne fragment with the subsequent C-O bond cleavage proceeding to yield the benzoic acid anion and its radical partner. As with previous cases, the radical partner is thought to couple with the radical cation **4.1.15a**.

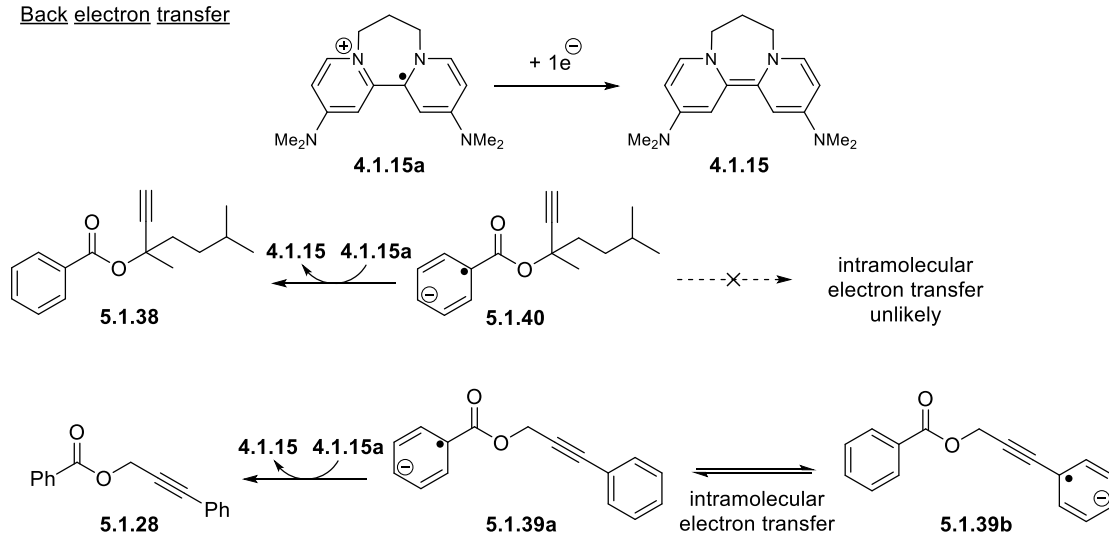


Scheme 5.1.17. Proposed mechanism for the observed enhanced reductive cleavage of benzoate **5.1.28**.

It cannot be discounted that back electron transfer was also operative in the case of benzoates **5.1.28** and **5.1.38**. For **5.1.38**, back electron transfer from its stable radical anion to **4.1.15a** would regenerate the starting material and the super-electron donor, thus allowing good recovery of the unreacted starting material.

In the case of **5.1.28**, it might be that electron shuttling was more efficient and so more C-O bond cleavage was observed (Scheme 5.1.18).

Back electron transfer



Scheme 5.1.18. Back electron transfer reactions could have been operative for benzoates **5.1.28** and **5.1.38**.

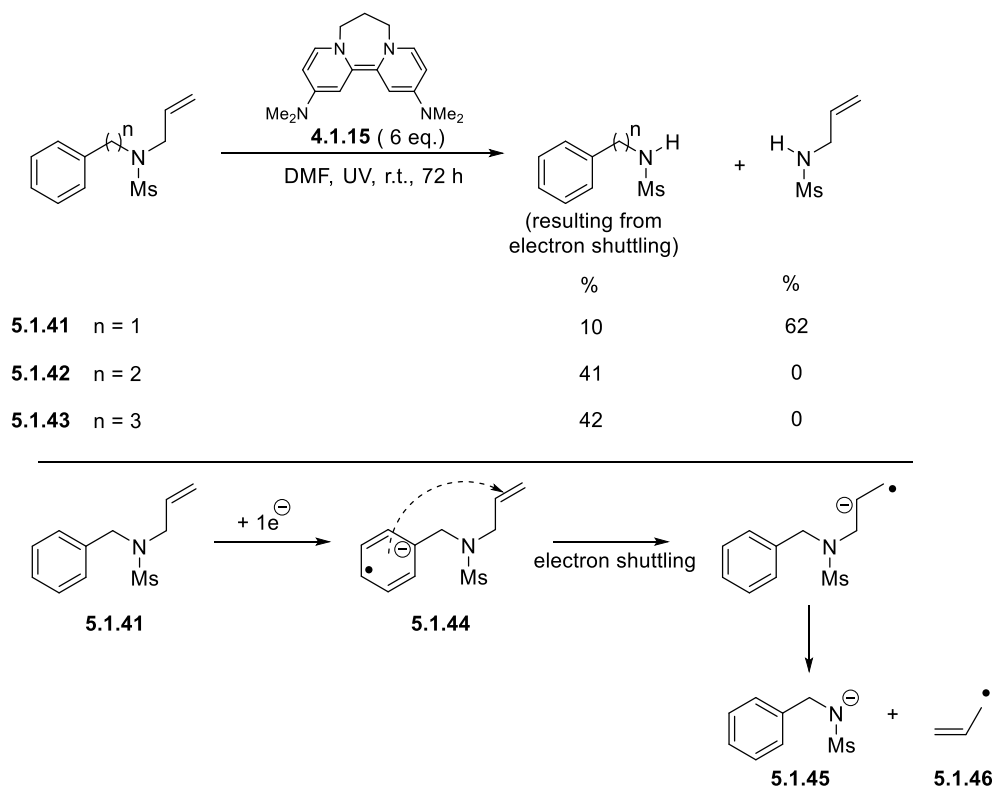
Conclusion and Future work.

Cinnamyl-based and propargylic-type esters have been discovered to undergo reductive bond cleavage when tested with photoactivated **4.1.15**. It is proposed that the bond cleavage occurs when the radical anion of the substrate was formed. The initial electron transfer proceeds from the photoactivated donor to the aromatic moiety (LUMO) of these substrates, followed by an intramolecular electron transfer onto the σ^* orbital of the C-O bond whereupon cleavage occurs. Experimental results strongly suggested that the cleavage favoured the formation of the oxyanion. Accordingly, the radical resided on the aromatic fragment which was prone to coupling with the radical cation of **4.1.15**. Based on experimental and computational investigations, it was shown that electron shuttling could account for the enhanced reactivity observed in the reduction of benzoate **5.1.28**.

Although the efficiencies for both processes (intramolecular transfer and electron shuttling) were low and at best moderate, it highlighted that simple molecules were capable of being used in this way upon reduction to their radical anions.

It has recently been discovered that electron hopping is an important biological processes which commonly occurs in polypeptides and DNA.¹⁵¹

There are limited examples of intramolecular electron shuttling proceeding from reduction by photoactivated **4.1.15**; three examples **5.1.41–5.1.43** were provided by Steven O’Sullivan’s work with allyl methanesulfonamides (Scheme 5.1.19).¹⁴¹ In this project, we have observed this effect on a benzoate-based substrate for the first time. This could be explored further in future work.



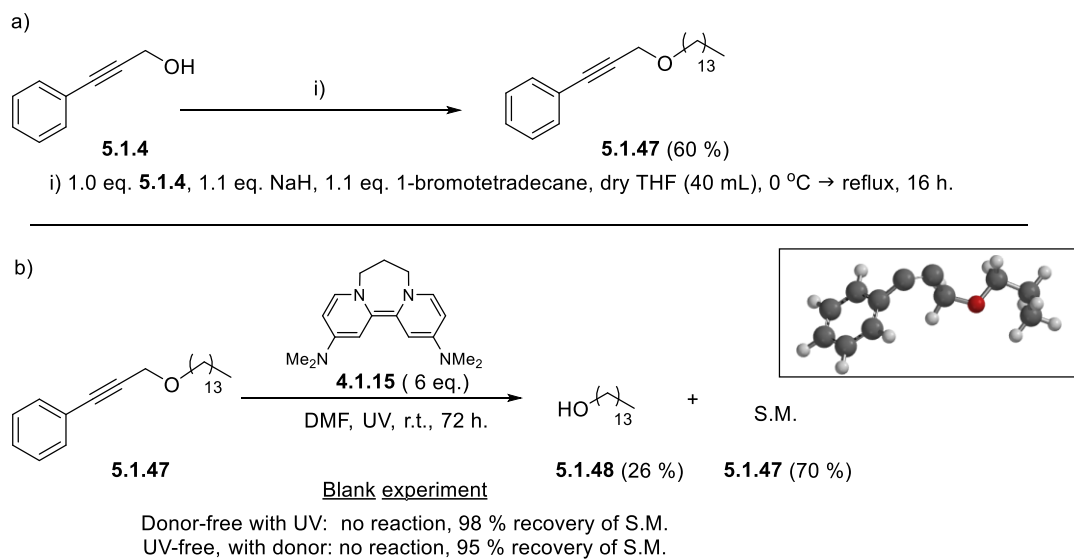
Scheme 5.1.19. Through-space electron transfer was previously observed by Steven O’Sullivan when studying the reduction of methanesulfonamides.¹⁴¹

Previously, when Eswararao Doni had successfully reduced benzylic ethers with photoactivated **4.1.15**, it was realised that the C-O bond reduction proceeded *via* double electron transfer from the super-electron donor. Therefore, benzylic ethers were necessarily more challenging to reduce than their ester analogues.¹³⁹

As an extension of this concept, propargylic ether **5.1.47** was synthesised using the Williamson ether methodology and then tested for reduction with photoactivated **4.1.15** (Scheme 5.1.20). Not surprisingly, there was a significant drop in the efficiency of the reduction of ether **5.1.47** compared to ester **5.1.5**.

In this instance, the starting material was isolated in good yield which might indicate that back electron transfer to the radical cation **4.1.15a** from the radical anion of **5.1.47** was the dominant process.

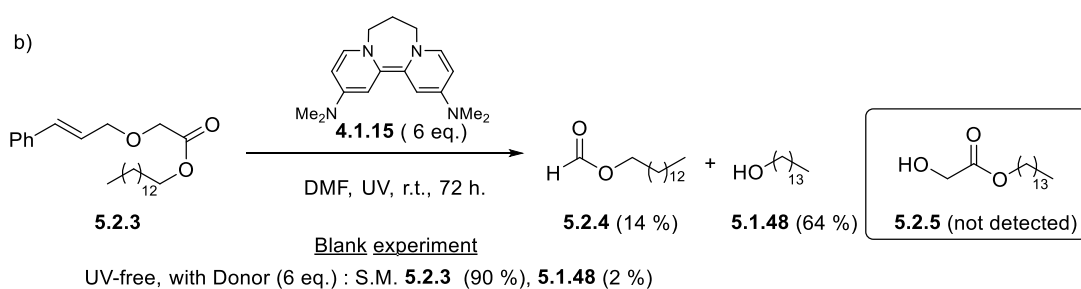
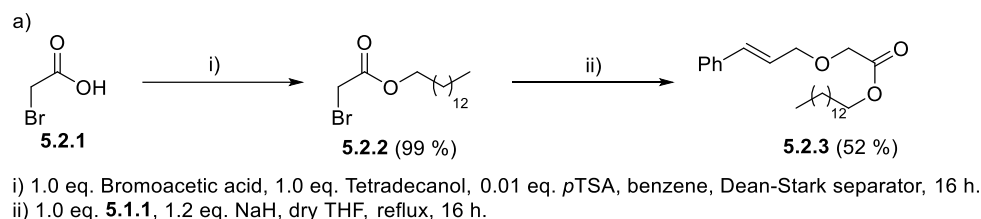
Computationally, slight perturbations in the bonds of the radical anion generated from **5.1.47** were observed but no spontaneous C-O bond cleavage was predicted (Scheme 5.1.20 b) i.e. there is an energetic barrier for the cleavage. Further studies on ethers can be conducted to determine the mechanism.



Scheme 5.1.20. a) Propargylic ether 5.1.47 was synthesised following the Williamson ether methodology. b) When tested for reduction with photoactivated 4.1.15, C-O bond cleavage ensued in low yields. Inset: Computational investigation on the radical anion generated from 5.1.47 showed DFT changes in bond angles but no spontaneous C-O bond cleavage was observed. (Spartan 2010 version, DFT, B3LYP, 6-31G(d,p) in DMF was employed).

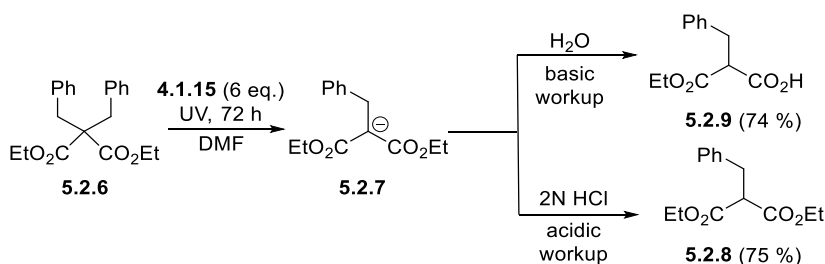
5.2 C-O & C-C bond cleavages from esters and amides with aromatic auxiliaries

In the preceding section, C-O bond cleavage of esters and ethers with extended conjugation was disclosed. In an attempt to expand the substrate scope of C-O bond reduction of ethers, substrate **5.2.3** was synthesised (Scheme 5.2.1).



Scheme 5.2.1. a) Two-step synthesis of ester-based substrate **5.2.3** was designed and conducted. b) When tested for reduction, formate ester **5.2.4** and alcohol **5.1.48** were isolated.

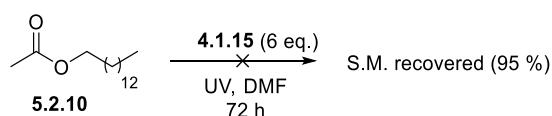
Surprisingly, when **5.2.3** was tested for the expected C-O bond reduction with photoactivated **4.1.15**, the expected alcohol **5.2.5** was not observed. Instead, formate ester **5.2.4** and tetradecanol **5.1.48** had formed. Previously, when attempting the reduction of malonate ester **5.2.6**, it was discovered by Eswararao Doni that hydrolysis of ester **5.2.8** was suppressed when an acidic workup procedure using 2N HCl was employed (Scheme 5.2.2).¹⁵²



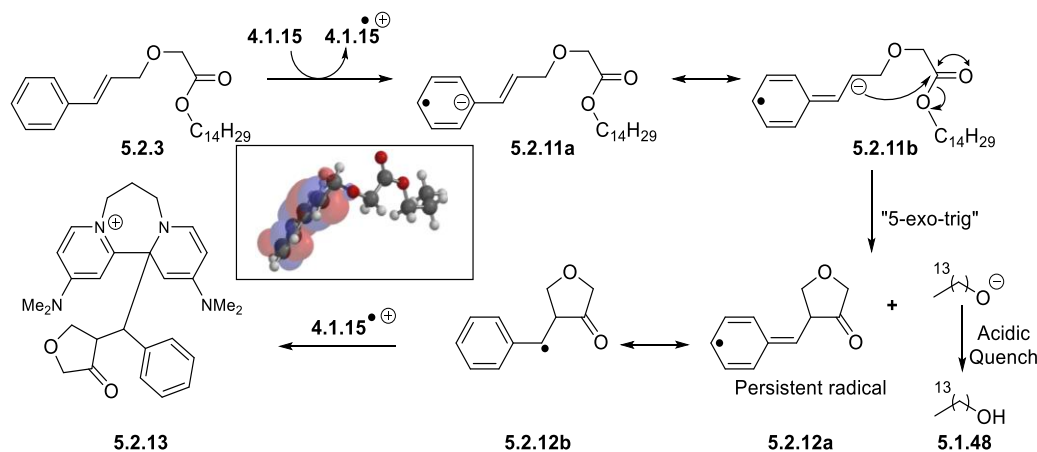
Scheme 5.2.2. Doni discovered that the employment of acidic workup conditions could suppress the hydrolysis of diethyl malonate **5.2.8**.¹⁵²

Hence, a similar acidic workup procedure was adopted for most experiments, unless otherwise stated. This was employed after the attempted reduction of **5.2.3** which had

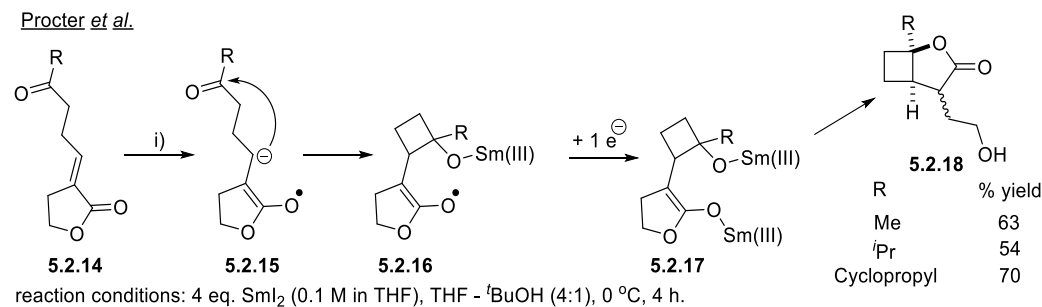
led to a substantial amount of tetradecanol being isolated (64 %). Furthermore, the blank experiment (no photoexcitation of **4.1.15**) led to only trace amounts of tetradecanol. These evidences gave confidence that hydrolysis of the substrate **5.2.3** could not account for the observed reactivity leading to **5.1.48**. Further evidence that the tetradecanol formation indeed resulted from reduction by photoactivated **4.1.15** (and not hydrolysis) was provided by an experiment conducted previously by Steven O'Sullivan¹⁵³ involving **5.2.10** (Scheme 5.2.3). Crucially, the lack of reactivity with **5.2.10** strongly suggested that the aromatic fragment was crucial for the reduction of **5.2.3**.¹⁵⁴



Scheme 5.2.3. a) Previous experiments conducted by Steven O'Sullivan¹⁵³ involving ester **5.2.10** showed no reactivity with **4.1.15**.



Procter *et al.*



Scheme 5.2.4. a) A possible mechanism for the formation of tetradecanol upon reduction of **5.2.3**. b) Nucleophilic reactivity of radical anion **5.2.15** was reported recently by Procter *et al.*¹⁵⁵ Inset: The LUMO of **5.2.3** was predicted to reside on the aromatic fragment (DFT, B3LYP, 6-31G(d,p) in ethanol was employed).

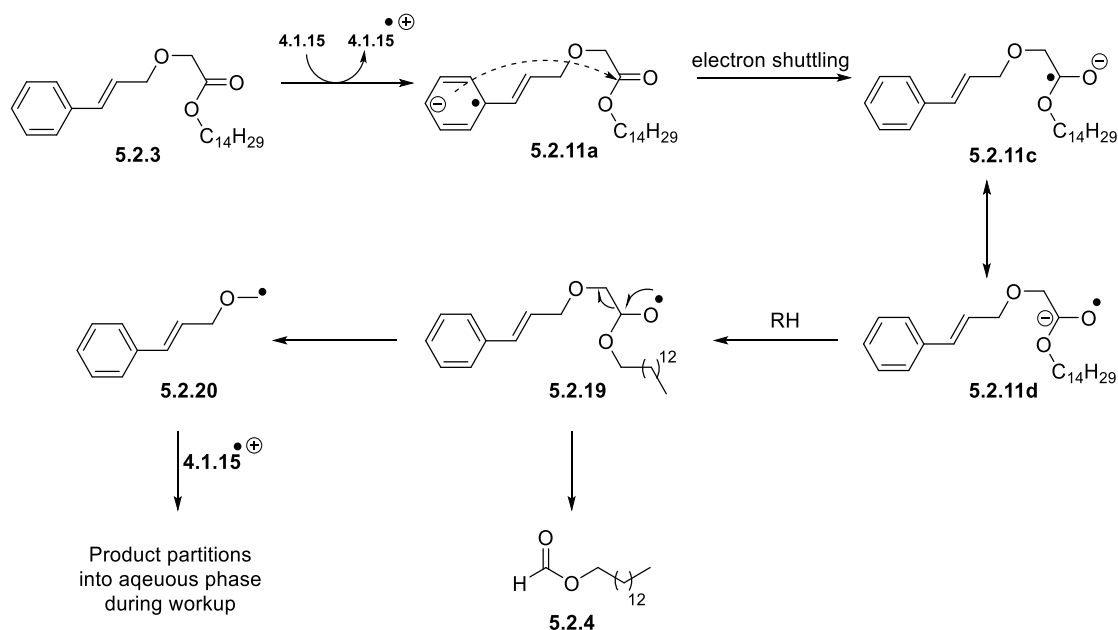
It is thought that the observed reactivity involves the initial generation of the benzene radical anion **5.2.11** (Scheme 5.2.4 a). This would agree with computational

investigations which predict that the LUMO of **5.2.3** resides on the cinnamyl fragment (Scheme 5.2.4 inset).

The extended conjugation in the cinnamyl fragment could allow for the resonance form **5.2.11b** to conduct a favourable 5-*exo*-trig cyclisation leading to the expulsion of tetradecyl alkoxide. As discussed previously, the radical fragment is thought to couple with the donor's radical cation resulting in **5.2.13** which would partition into the aqueous layer upon workup.

Nucleophilic reactivity of radical anions has recently been reported by Procter *et al.*¹⁵⁵⁻¹⁵⁷; by employing SmI₂ with HMPA and ^tBuOH as additives, radical anion **5.2.15** can be generated from lactone **5.2.14**. The nucleophilic radical anion proceeds to attack the ketone terminus of the substrate which, upon further reduction and cyclisation, results in the bicyclic product **5.2.18** (Scheme 5.2.4 b). In a similar case, it is possible that radical anion **5.2.11** is also operating as a nucleophile with the cyclisation and alkoxide expulsion driving the reaction forward.

A second competing mechanism is thought to lead to the production of formate ester **5.2.4** (Scheme 5.2.5).

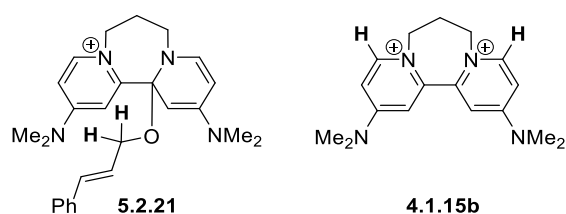


Scheme 5.2.5. The proposed mechanism for the formation of formate ester **5.2.4** involved electron shuttling from the LUMO to the ester moiety.

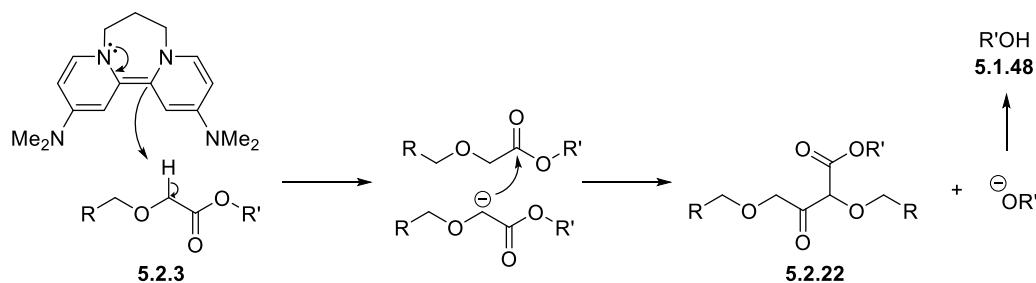
This mechanism involves the intramolecular electron shuttling from the aromatic fragment to the ester (it was already evidenced that non-aromatic esters could not be reduced by photoactivated **4.1.15**). The resulting ketyl radical anion **5.2.11d** was then protonated, followed by a homolytic bond cleavage to yield **5.2.4**.

Proton source(s) could be present in the reaction. Work carried out by previous students had strongly indicated that the dication salt **4.1.15b** was a potential source of proton(s). It could also be possible for the donor-derived product **5.2.21** to be another proton source in the reaction (Figure 5.2.6).

Figure 5.2.6. Possible sources of proton (in bold) available during the reaction.



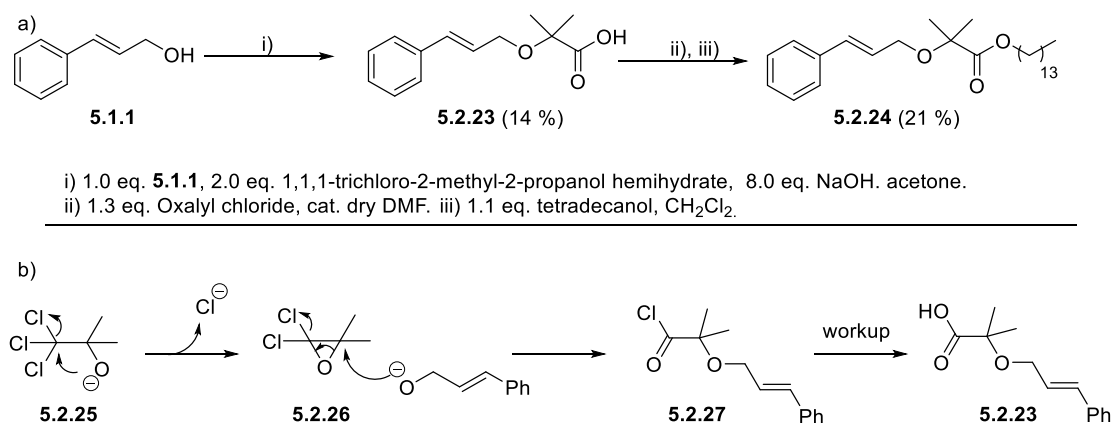
Essentially, the substrate **5.2.3** is an α -alkoxy ester and it was possible that this functional group could be deprotonated under the reaction conditions employed. If so, the resulting anion could attack a second substrate molecule, leading to the formation of tetradecanol **5.1.48** (Scheme 5.2.7).



Scheme 5.2.7. Possible deprotonation of 5.2.3 could also lead to the formation of tetradecanol.

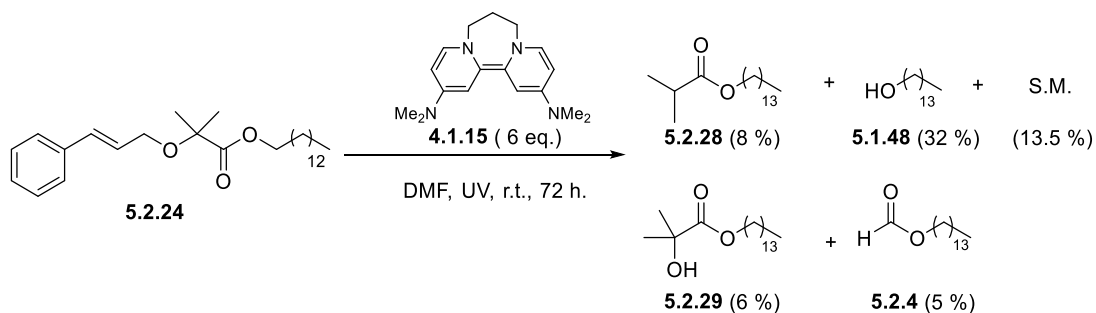
However, the blank reaction involving **5.2.3** and non-photoactivated **4.1.15** (Scheme 5.2.1) showed no reactivity and so it was highly unlikely that deprotonation should account for any significant production of tetradecanol. Nevertheless, firm evidence for this would be desirable and so ester **5.2.24** was designed and synthesised (Scheme 5.2.8 a).

The installation of the geminal-dimethyl fragment was conducted using 1,1,1-trichloro-2-methyl-2-propanol hemihydrate. Under the basic conditions employed, the oxyanion **5.2.25** would be generated, which would rapidly cyclise to give epoxide **5.2.26**.¹⁵⁸ The addition of cinnamyl alcohol at this stage would lead to selective ring-opening to yield the acyl chloride **5.2.27** which would be conveniently isolated upon workup as its carboxylic acid **5.2.23** (Scheme 5.2.8 b).



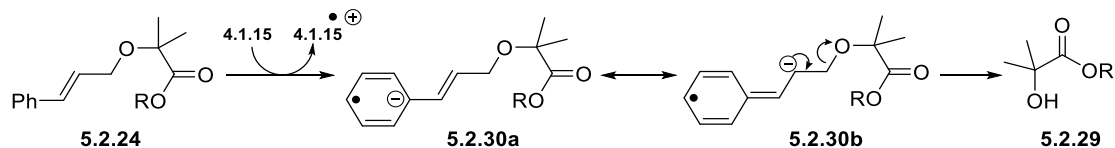
Scheme 5.2.8. a) Ester **5.2.24** was obtained from a 2-step synthesis starting from cinnamyl alcohol. b) The proposed mechanism for the synthesis of **5.2.23** using 1,1,1-trichloro-2-methyl-2-propanol hemihydrate.

When ester **5.2.24** was subjected to reduction conditions with photoactivated **4.1.15**, tetradecanol was obtained in considerable amount (32 %), thus indicating that deprotonation of the starting material was not responsible for the observed reactivity. Furthermore, formate ester **5.2.4** (5 %), ester **5.2.28** (8 %), alcohol **5.2.29** (6 %) and the starting material (13.5 %) were also isolated and characterised (Scheme 5.2.9).

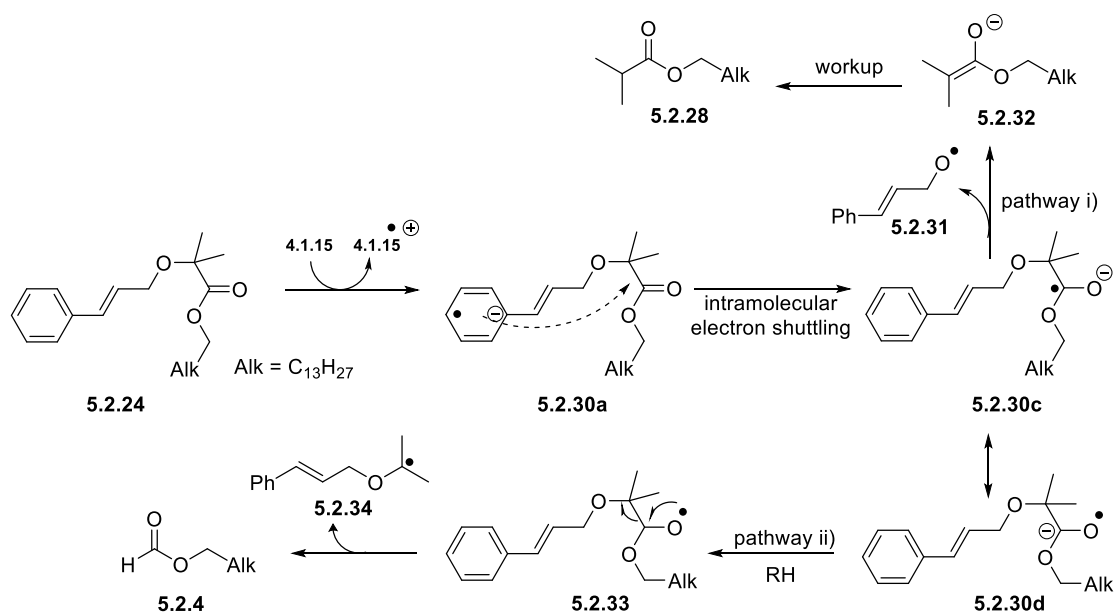


Scheme 5.2.9. The reduction of **5.2.24** with photoactivated **4.1.15** led to the isolation of five different compounds.

An account for the formation of these products is now attempted. Firstly, product **5.2.29** is thought to result from electron transfer from the cinnamyl fragment to the C-O bond (Scheme 5.2.10). This mechanism would be similar to that previously discussed in Chapter 5.1.



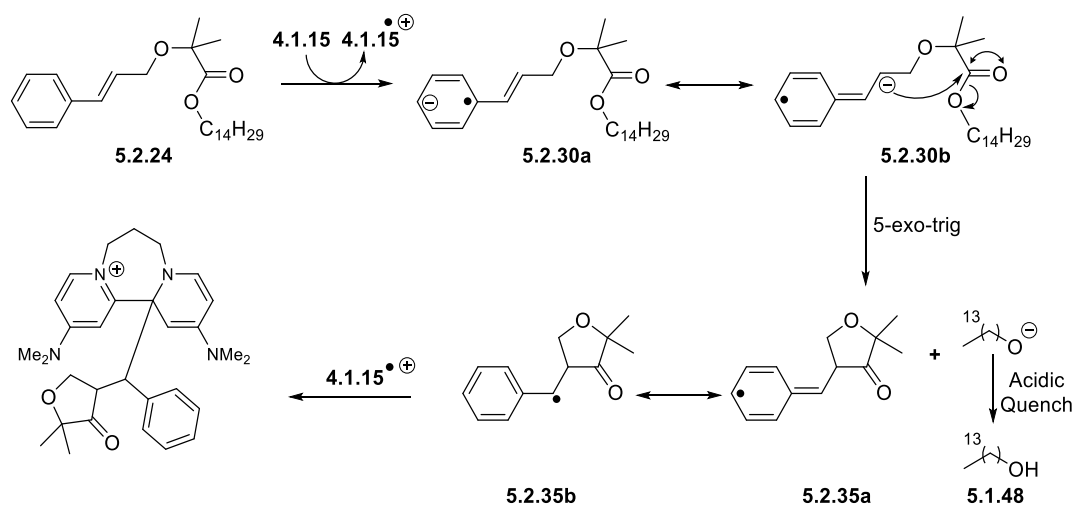
Scheme 5.2.10. Electron transfer from the cinnamyl moiety to the C-O bond led to the formation of **5.2.29**.



Scheme 5.2.11. Electron shuttling between the aromatic fragment and the carbonyl group of the ester could lead to products **5.2.4** and **5.2.28**.

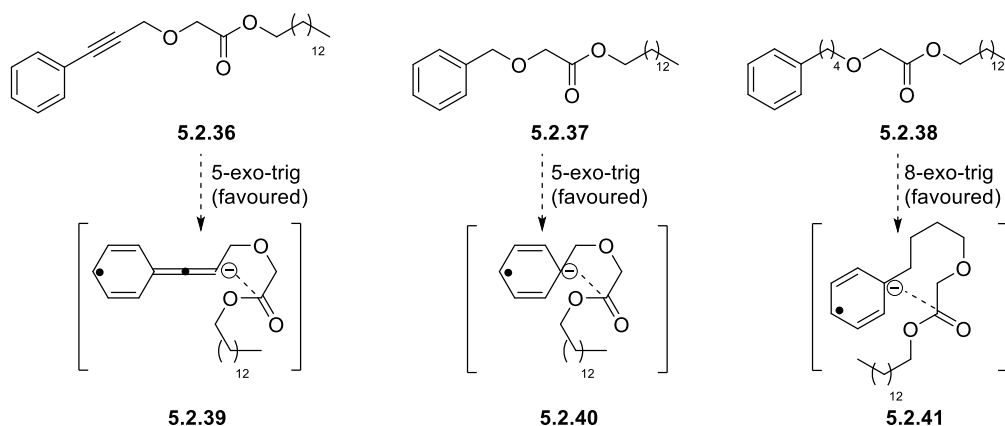
Alternatively, products **5.2.4** and **5.2.28** could have resulted from the shuttling of the electron from the LUMO (aromatic fragment) to the ester moiety (Scheme 5.2.11). The resulting ketyl radical anion **5.2.30c** can proceed with fragmentation to yield the thermodynamically stable enolate **5.2.32** and the radical **5.2.31** (Scheme 5.2.11, pathway i). The formation of **5.2.4** has been previously disclosed (See Scheme 5.2.5). Products derived from the radical fragments **5.2.31** and **5.2.34** were not detected upon workup and this, as with previous cases, was attributed to radical trapping with **4.1.15a**.

Similar to the reduction of **5.2.3** by photoactivated **4.1.15**, tetradecanol formation was thought to proceed from the nucleophilic attack of the radical anion **5.2.30b** onto the ester fragment (Scheme 5.2.12).



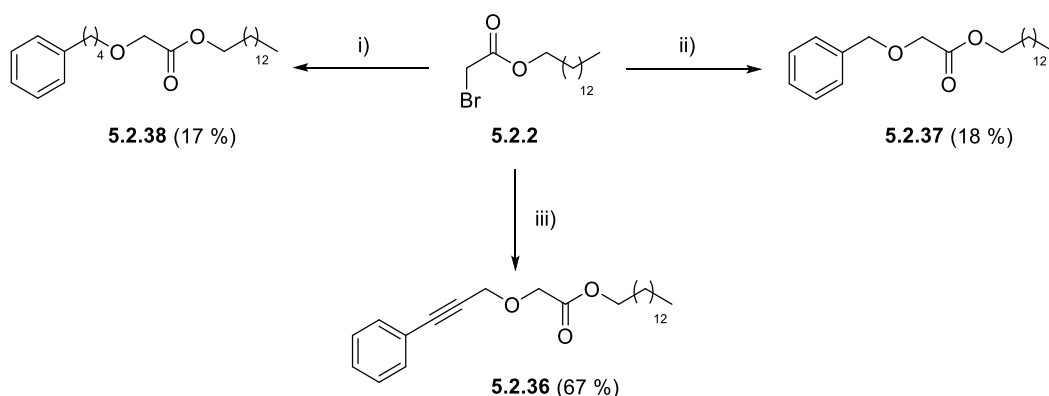
Scheme 5.2.12. Tetradecanol formation resulted from nucleophilic attack of the radical anion **5.2.30b** onto the ester fragment.

With convincing evidence that tetradecanol formation was a result of reduction by photoactivated **4.1.15**, attention was turned to extending the substrate scope. As long as the required intermediate cyclisation step could be accessed by the radical anion, the formation of the tetradecanol should proceed. To this end, substrates **5.2.36**–**5.2.38** were designed and synthesised (Scheme 5.2.13).



Scheme 5.2.13. Radical anions from substrates **5.2.36**–**5.2.38** should undergo cyclisation.

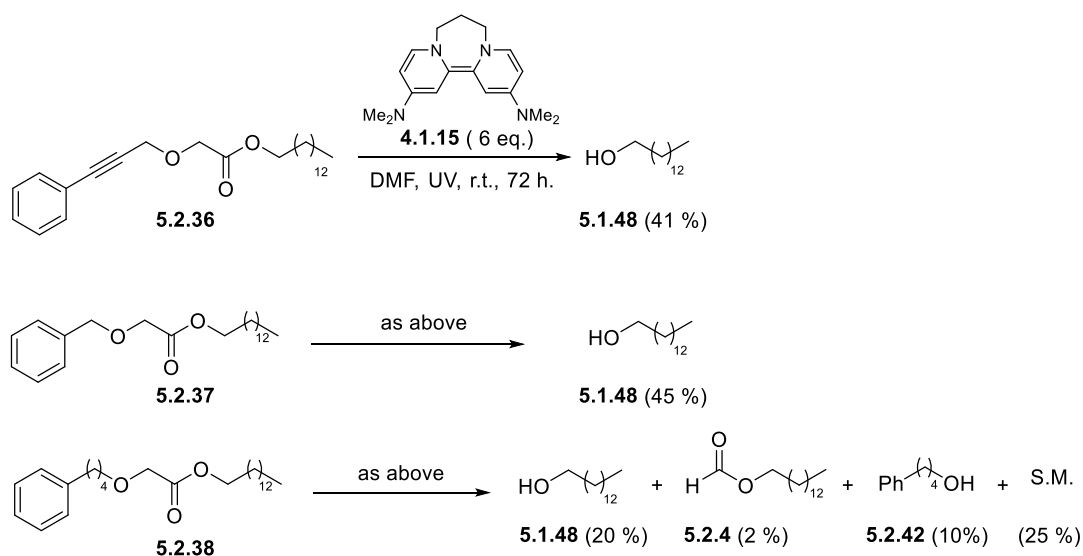
The synthesis of the three substrates all utilised intermediate **5.2.2** which was previously synthesised on a large scale when preparing **5.2.3** (Scheme 5.2.14).



- i) 1.0 eq. 4-phenyl-1-butanol, 1.1 eq. NaH, 1.1 eq. **5.2.2**, dry THF (10 mL), reflux, 16 h.
 ii) 1.0 eq. Benzyl alcohol, 1.2 eq. NaH, 1.0 eq. **5.2.2**, dry THF (10 mL), reflux, 16 h.
 iii) 1.0 eq. 3-phenyl-2-propyn-1-ol, 1.1 eq. NaH, 1.1 eq. **5.2.2**, dry THF (10 mL), reflux, 16 h.

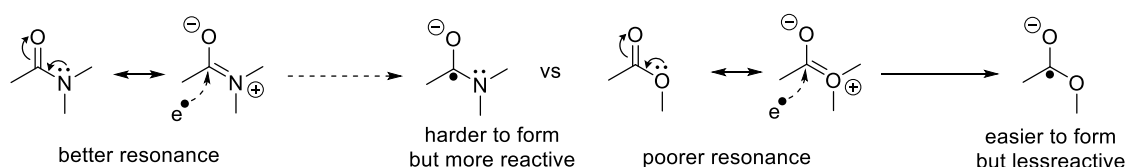
Scheme 5.2.14. Synthesis of esters 5.2.36-5.2.38 from precursor 5.2.2.

When these substrates were tested for reduction with photoactivated **4.1.15**, tetradecanol **5.1.48** was successfully isolated in every case (Scheme 5.2.15) confirming that the cyclisation was possible on the grounds of stereoelectronic effects. Compared to **5.2.36** and **5.2.37**, the reduction of **5.2.38** led to a smaller yield of tetradecanol (20 %), with unreacted starting material (25 %) and formate ester **5.2.4** (2 %) also present. This could indicate that kinetically, the cyclisation *via* 8-exo-trig was difficult to achieve, leading to less reactivity.



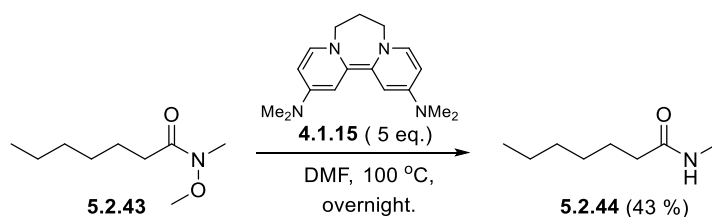
Scheme 5.2.15. The reduction of ester-based substrates 5.2.36-5.2.38 proceeded with photoactivated 4.1.15.

Since the amide functional group should experience stronger resonance than the corresponding ester, it should follow that SET onto the former would be more challenging (Scheme 5.2.16). However, if the amide radical anion could be generated it would be expected to be more reactive.



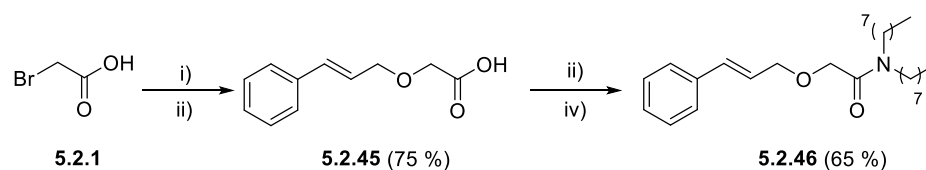
Scheme 5.2.16. Amides would be more difficult to reduce than esters but the resulting radical anions would be more reactive.

On a previous account, the C-O bond reduction of activated Weinreb amides using thermally activated **4.1.15** had been explored.¹⁵⁴ Even the non-aromatic Weinreb amide, **5.2.43** could be reduced to the corresponding carboxamide **5.2.44** under harsh reaction conditions (Scheme 5.2.17).



Scheme 5.2.17. Non-aromatic Weinreb amide **5.2.43** could be reduced by **4.1.15** with heating.¹⁵⁴

On this occasion, it would be interesting to see if non-activated amides (i.e., not Weinreb amides) could also be reduced by photoactivated **4.1.15** via the electron shuttling mechanism which has been observed previously with esters **5.2.3**, **5.2.24** and **5.2.36-5.2.38**. To this end, amide **5.2.46** was synthesised (Scheme 5.2.18). By keeping all other functional groups in the molecule constant, the experimental results from amide **5.2.46** would allow for direct comparisons with the results from its related ester **5.2.3** (Schemes 5.2.18 and 5.2.19).

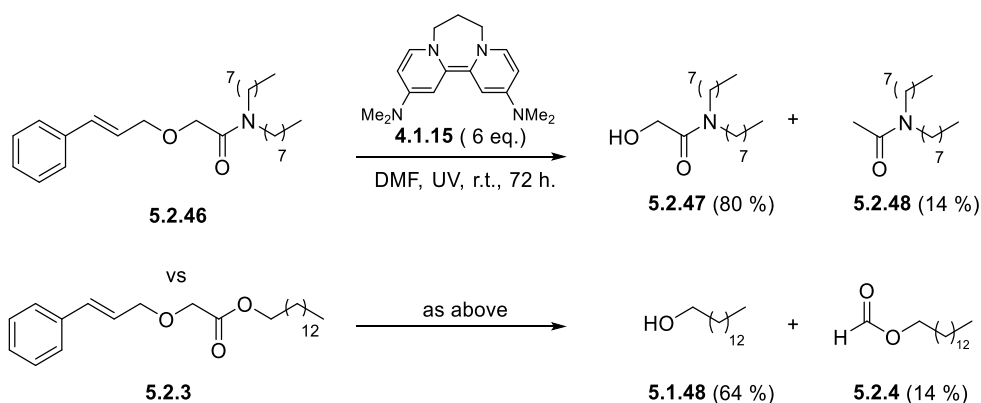


- i) 1.0 eq. **5.2.1**, 2.0 eq. NaH, dry THF (50 ml), 0 °C.
- ii) 1.0 eq. cinnamyl alcohol, dry THF (30 ml), reflux, 16 h.
- iii) 1.0 eq. **5.2.45**, 1.1 eq. oxalyl chloride, cat. dry DMF, dry CH₂Cl₂ (30 mL), 0 °C.
- iv) 1.1 eq. pyr. 1.2 eq. N,N-dioctylamine, r.t., 16 h.

Scheme 5.2.18. Synthesis of amide **5.2.42** starting from commercially available starting materials.

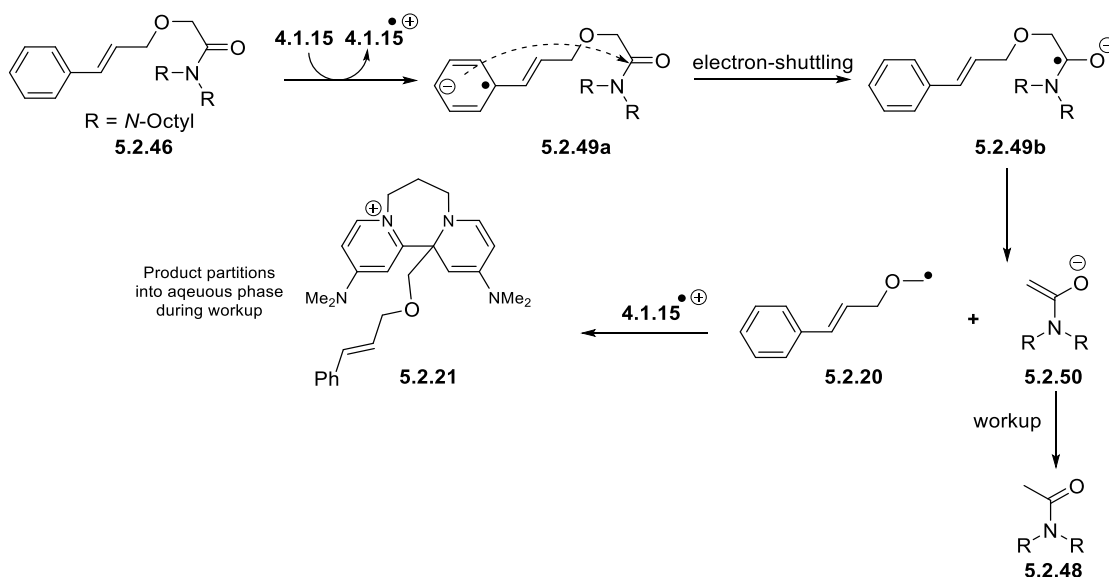
The attempted reduction of amide **5.2.46** by photoactivated **4.1.15** led to products **5.2.47** and **5.2.48** (Scheme 5.2.19) with an overall excellent mass recovery. Alcohol **5.2.47** was the major product (80 %); this was a result of the through-bond electron transfer from the cinnamyl to the σ^* orbital of the C-O bond. In retrospect, it was not

surprising that this was the preferred mode of cleavage since SET onto the carbonyl group of the amide would be challenging (see previous discussion, Scheme 5.2.16).



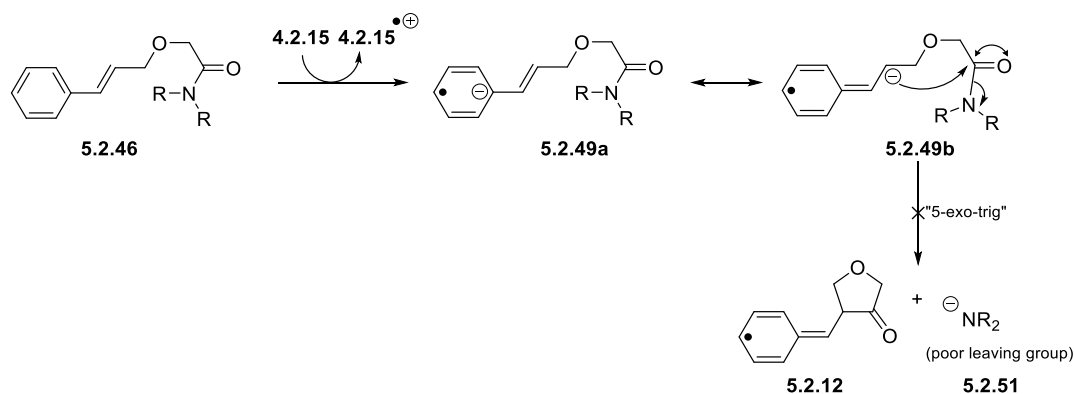
Scheme 5.2.19. Reductive C-O bond cleavages were observed with amide **5.2.46**. The results can be compared to ester **5.2.3**.

Nevertheless, electron shuttling onto the amide fragment was still possible as evidenced by the formation of amide **5.2.48** (Scheme 5.2.20).



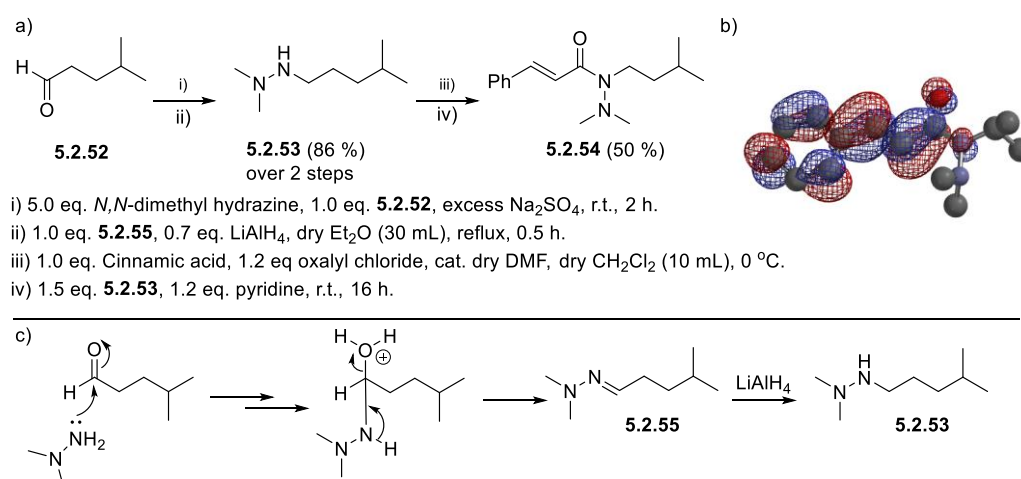
Scheme 5.2.20. The formation of amide **5.2.48** was a result of electron shuttling.

It is noteworthy that no amine product was formed *via* the intermediary cyclisation route; this had been previously reported with the ester substrates **5.2.3**, **5.2.24** and **5.2.36-5.2.38** to account for the formation of tetradecanol **5.1.43**. In the present case with amide **5.2.46**, the hypothetical formation of the aminyl anion **5.2.51** would be highly disfavoured since it is a poor leaving group (Scheme 5.2.21).



Scheme 5.2.21. Amine formation was not detected, presumably due to the poor leaving group ability of the aminyl anion.

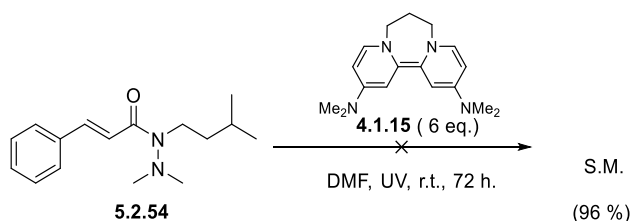
Aware that amine expulsion from the parent amide was not possible under the conditions employed, it was decided to investigate if this resistance could be offset by the breaking of a weaker N-N bond present in hydrazine-based **5.2.54** (Scheme 5.2.22 a).



Scheme 5.2.22. a) Synthesis route for hydrazine **5.2.54**. b) SOMO of **5.2.54**. DFT, B3LYP, 6-31G(d,p) in DMF was employed; calculation set at -1 charge and multiplicity of 2. c) Mechanism for hydrazine formation.

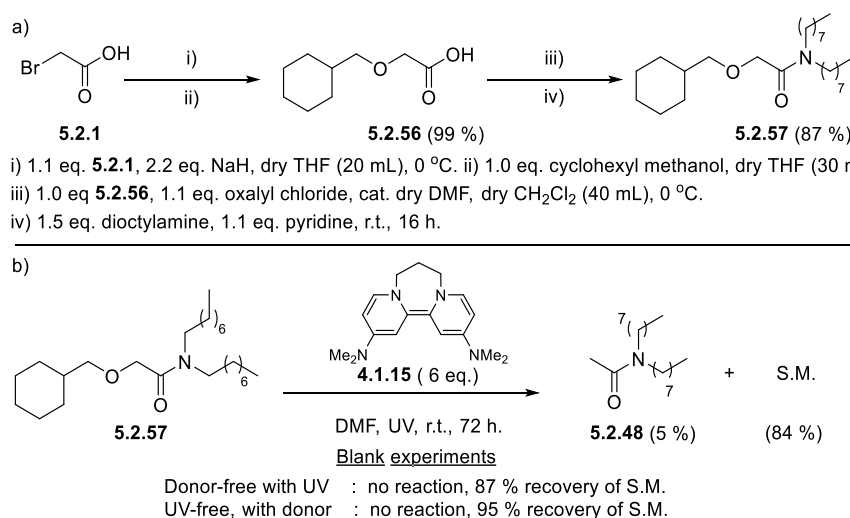
Computational investigations had indicated that the SOMO of the radical anion would not extend onto the envisaged amine leaving group (Scheme 5.2.22 b). If successful, this would be the first instance of N-N bond cleavage employing a metal-free, super-electron donor. The substrate was successfully synthesised over two steps, with the first step consisting of imine formation followed by its *in situ* reduction using LiAlH₄ (Scheme 5.2.22 c). However, no reactivity was observed when **5.2.54** was subjected to reductive conditions with photoactivated **4.1.15** (Scheme 5.2.23).

The calculated LUMO energy level for this hydrazine-type substrate (2.2 eV) was similar to that of amide **5.2.46**. Yet, in the latter, reductive cleavage had proceeded efficiently. Therefore, it was likely that the difficulty in N-N bond cleavage did not lie in the difficulty in generating the radical anion, but rather, could be due to the poor leaving group ability of the amide anion.



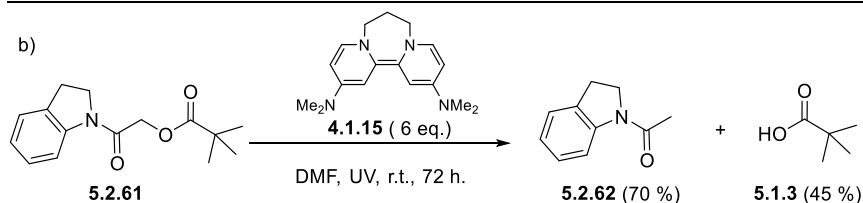
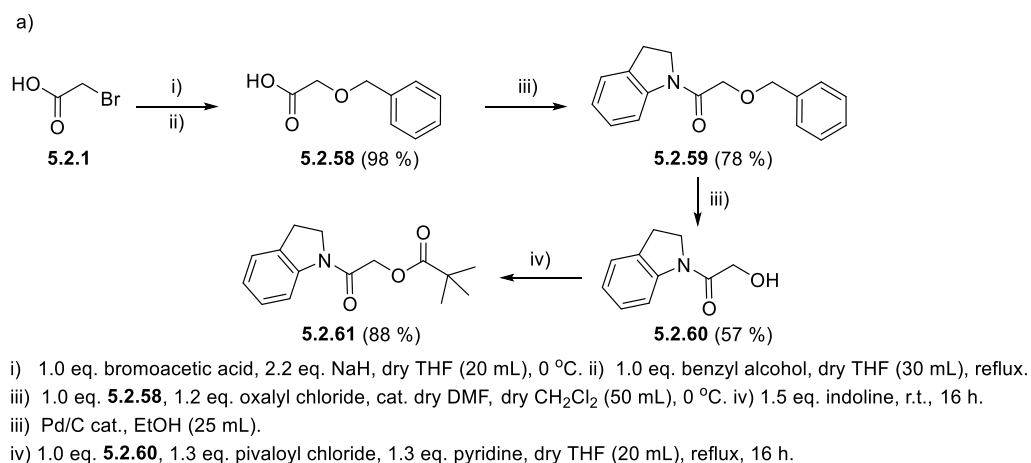
Scheme 5.2.23. No reactivity was seen when the reduction of **5.2.54** was attempted using photoactivated **4.1.15**.

Interestingly, when the non-aromatic amide **5.2.57** was synthesised (Scheme 5.2.24 a) and subjected to reduction with photoactivated **4.1.15**, C-O bond cleavage leading to **5.2.48** was still observed albeit in very low yield, thereby indicating that unactivated alkoxyamides could also undergo reduction (Scheme 5.2.24 b).

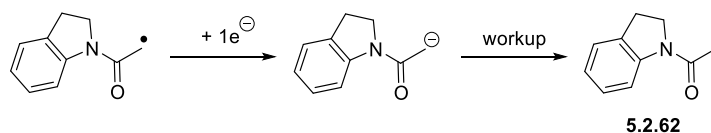


Scheme 5.2.24. Synthesis and attempted reduction of non-aromatic amide **5.2.57**.

Since aromatic amides possess lower LUMO levels than aliphatic analogues, the former should be more susceptible to reduction by the photoactivated **4.1.15**. Therefore, the use of the indoline fragment, as an auxiliary, to increase the efficiency in reductive bond cleavage was explored. To this end, **5.2.61** was synthesised using a four-step procedure and then tested for reduction with photoactivated **4.1.15** (Scheme 5.2.25).



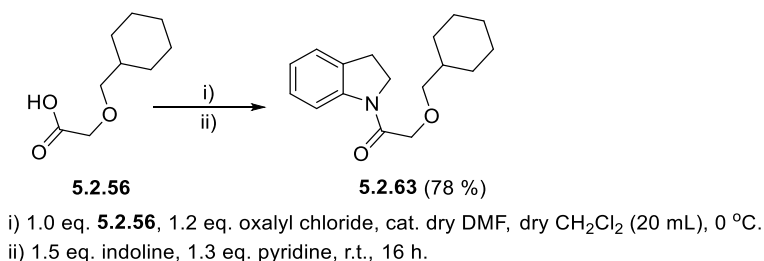
5.2.62 is derived from its parent radical formed after C-O bond cleavage



Scheme 5.2.25. a) Synthesis of indoline-based substrate **5.2.61**. b) Reductive C-O bond cleavage was observed when **5.2.61** was tested with photoactivated **4.1.15**.

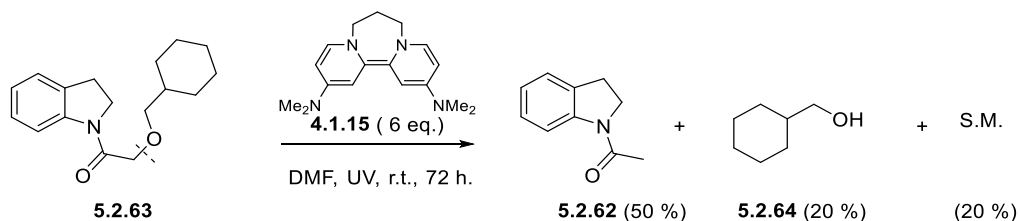
It was pleasing to observe reductive C-O bond cleavage from **5.2.61** with the successful isolation of fragments **5.2.62** and **5.1.3**. In the case of **5.2.62**, this fragment is thought to derive from the enyl radical present after the C-O bond cleavage. Under the reductive conditions employed, the enyl radical is readily reduced further to its enolate which is then protonated upon workup (Scheme 5.2.25 b).

Following this success, ether **5.2.63** was synthesised (Scheme 5.2.26) to allow direct comparison with the reaction profiles of **5.2.57** and **5.2.61** (Scheme 5.2.27).

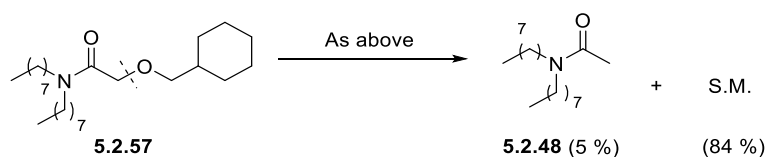


Scheme 5.2.26. Synthesis of indole-based **5.2.63**. The synthesis of intermediate **5.2.56** was shown previously (Scheme 5.2.24).

In the event, the photoreduction proceeded more efficiently than the non-aromatic analogue **5.2.57**; less starting material was recovered and the amide fragment **5.2.62** was isolated in moderate yield (50 %), (Scheme 5.2.27). This reaffirmed that the installation of an aromatic amide could enhance reductive cleavages.



previously



Scheme 5.2.27. Aromatic amide **5.2.63** showed increased reactivity compared to the non-aromatic analogue **5.2.57**.

Meanwhile SET from photoactivated **4.1.15** to amides was being extensively studied by Steven O'Sullivan and his results were later reported.¹⁴¹ As such, it was decided to digress from amide-based substrates and explore other possible novel reductions with photoactivated SED **4.2.15**.

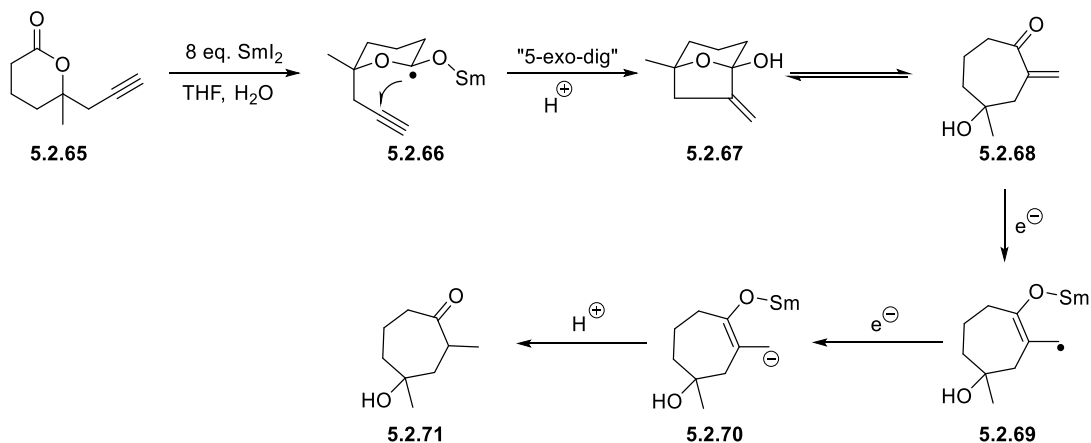
This led to the discovery of the reduction of phenolate esters which is disclosed in the next section.

Conclusion

In the previous section, the intramolecular electron shuttling effect was observed with benzoate **5.1.28**. In this section, this less well-explored reaction was studied further and was found to be present with ester **5.2.3** and to a lesser extent with **5.2.24** (formate ester **5.2.4** was evidence for these novel C-C bond cleavages).

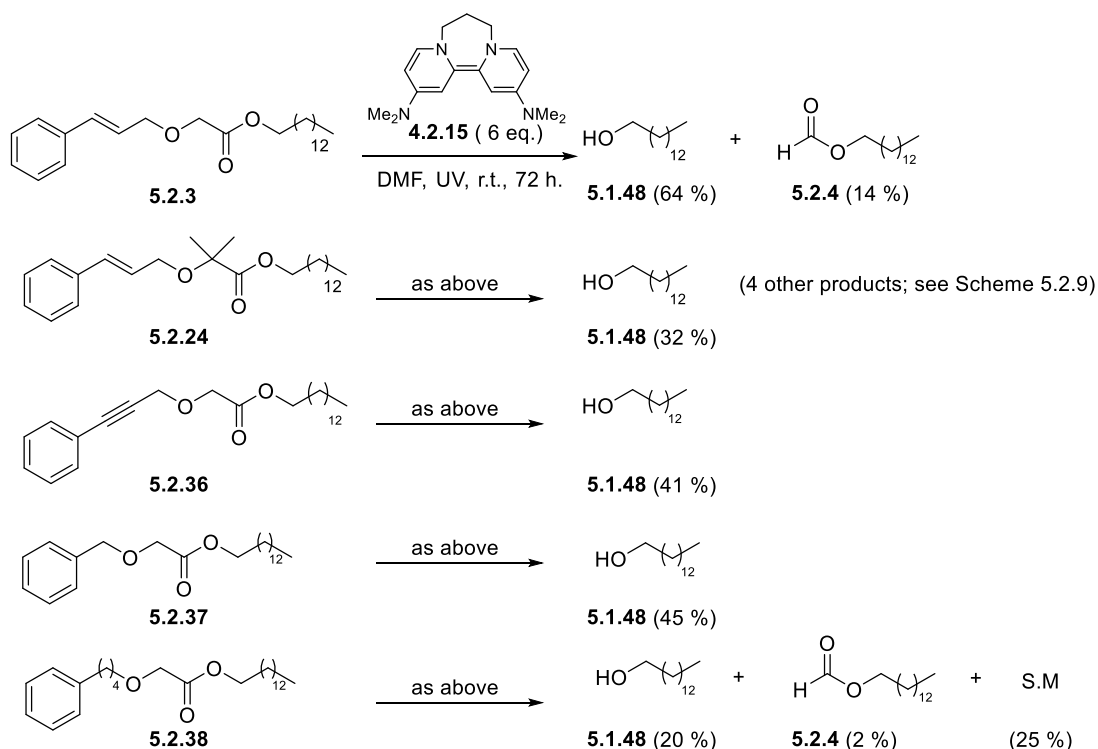
The electron shuttling between the LUMO (cinnamyl fragment) and the distal ester, creates the ketyl radical anion; this process is thought to be more challenging with amides. Yet, amide **5.2.46** could still be transiently reduced to its radical anion *via* electron shuttling; further reactivity ensues from this state which restores the amide fragment. The overall resistance of amides towards reduction and their ability to momentarily receive electron(s) renders this functionality a useful auxiliary for electron reception and transfer. This was briefly explored, with success, in the use of indoline-based substrates e.g. **5.2.61** and **5.2.63**.

Recently, Procter *et al.*¹⁵⁹ were successful in employing SmI₂ to reduce esters to their radical anions e.g. **5.2.65** (Scheme 5.2.28). The resulting species **5.2.66** was then used to induce intramolecular cyclisation *via* radical attack on the proximal alkyne. It would be interesting to explore the possibility of using photoactivated **4.1.15** in such cyclisations beginning with the transient reduction of esters.



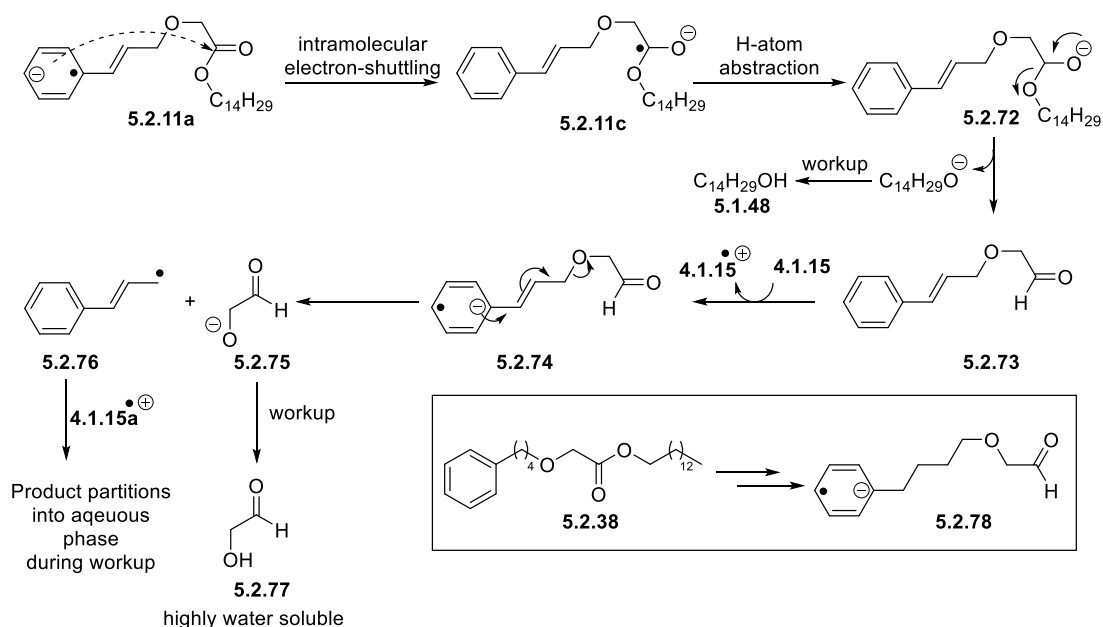
Scheme 5.2.28. SmI₂ was successfully employed in the reduction of esters which was followed by cyclisation and ring expansion. A specific example is shown here.

It has been established that the tetradecanol formation from reduction of ester substrates indeed resulted from activity by photoactivated **4.1.15** (Scheme 5.2.29).



Scheme 5.2.29. A list of ester-based substrates that were synthesised and successfully underwent cyclisation *via* the proposed ring closure at the radical anion stage.

Alternative mechanisms were also considered for the formation of **5.1.48**. Using **5.2.11a** as an example, the reaction proceeds with the initial electron shuttling from the cinnamyl moiety (LUMO) to the ester.

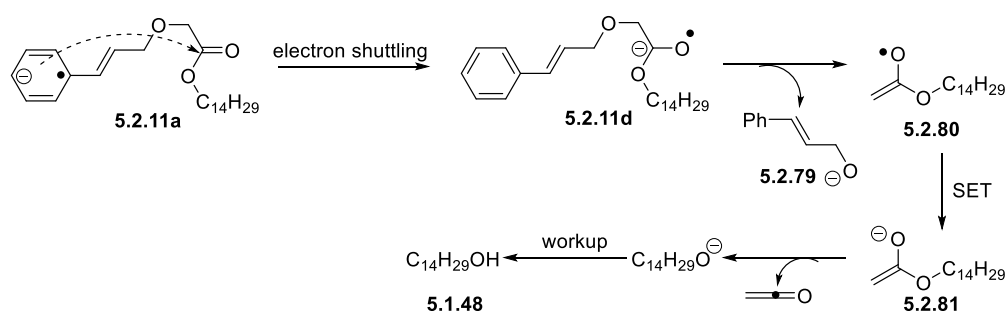


Scheme 5.2.30. An alternative mechanism could explain the formation of tetradecanol **5.1.48**. This mechanism would not apply to **5.2.38**.

A hydrogen abstraction by **5.2.11c** would result in the oxyanion **5.2.72** which could then collapse with the expulsion of the alkoxide anion thereafter isolated as tetradecanol **5.1.48** upon quenching and workup. The corresponding aldehyde **5.2.74** still retains the arene fragment and is therefore susceptible to a second SET from the photoactivated **4.1.15**. Building upon earlier experimental results from **5.1.2**, it is certainly feasible that **5.2.74** proceeds with C-O bond cleavage. This time, the resulting cleavage results in the aryl radical fragment **5.2.76** which is subsequently trapped by the radical cation **4.1.15a**. The oxyanion **5.2.75** is converted to glycolaldehyde which is water-soluble and partitions into the aqueous phase upon workup.

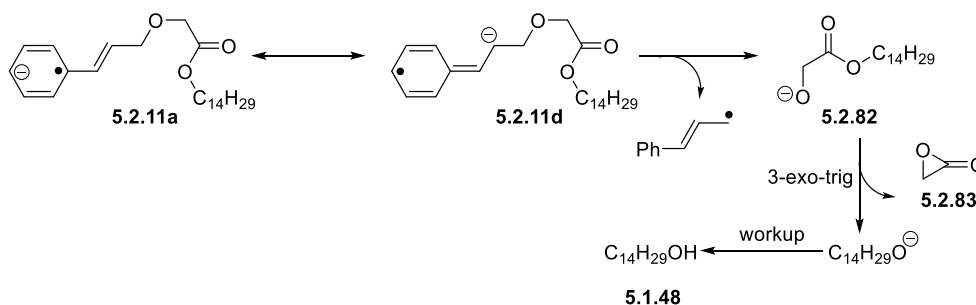
Although this mechanism might explain the formation of tetradecanol **5.1.48**, it would not apply to **5.2.38** (i.e., the C-O bond is not conjugated to the arene unit) in which the postulated second SET event resulting in C-O bond cleavage could not have occurred (Scheme 5.2.30 inset). The ring-closure mechanism might still be a better proposal.

Tetradecanol formation could also be due to the C-O bond cleavage of **5.2.11a** as shown in Scheme 5.2.31. Here, the stabilised radical **5.2.80** could be further reduced to its anion **5.2.81** which collapses to yield the corresponding ketene and alkoxy anion; the latter can then be isolated as tetradecanol **5.1.48** upon workup. Ketene formation from pyrolysis of simple esters have previously been reported.¹⁶⁰⁻¹⁶¹ Possibly, the highly reducing environment in the present case also promotes such a fragmentation. More experiments need to be conducted to determine if such is the case.



Scheme 5.2.31. Tetradecanol **5.1.48** could also result from the collapse of **5.2.81**.

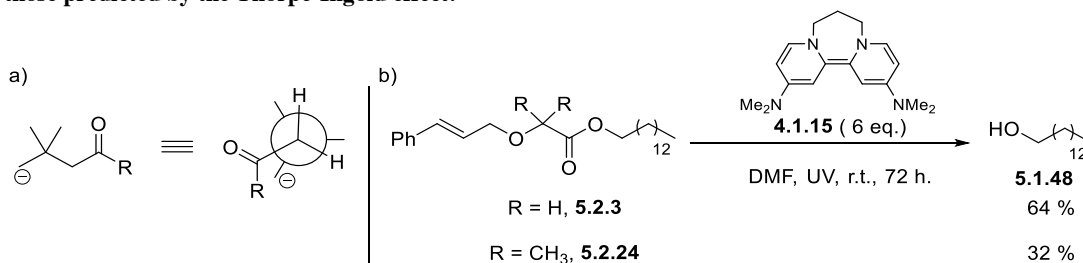
The synthesis of α lactones from esters¹⁶² or acid chlorides¹⁶³ is a well-established process. This suggests that there is a third possibility in which tetradecanol **5.1.48** forms from the 3-exo-trig cyclisation of **5.2.82** (Scheme 5.2.32). This alkoxy anion derives from the reductive C-O bond reductive cleavage of **5.2.11**; analogous to the mechanism previously proposed for ester **5.1.5** (see Scheme 5.1.7).



Scheme 5.2.32. A third mechanism can be proposed for the formation of **5.1.48**.

In any case, it is still unclear as to why the yield of tetradecanol from the reduction of **5.2.24** was lower than that obtained from **5.2.3** since the Thorpe-Ingold effect would predict the opposite of what was observed experimentally (Figure 5.2.31).

Figure 5.2.31. a) The Thorpe-Ingold effect predicts faster intramolecular cyclisations when the geminal-dimethyl fragment is present next to the reacting carbon. b) The experimental results were contrary to those predicted by the Thorpe-Ingold effect.



The Thorpe-Ingold effect is widely accepted to be a kinetically-driven process¹⁶⁴⁻¹⁶⁶ in which the installation of the geminal-dimethyl fragment adjacent to the reacting carbon is found to accelerate the rate of intramolecular cyclisation between the nucleophilic carbon and an electrophilic site of the molecule.

The prevalence of the gauche conformations due to the geminal-dimethyl fragment is thought to bring the reacting groups into closer proximity and in so doing speeds up cyclisation (Figure 5.2.31 a).

Although the Thorpe-Ingold effect has been commonly applied in organic synthesis,^{164,167-172} there are no reports (to the best of our knowledge) on its effect on ring closures of radical anions. Time constraints towards the end of this section of work meant that further probing of the mechanism was not possible.

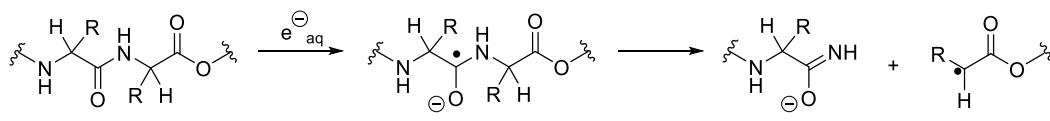
Electron shuttling and hopping are found in many biological systems including photosynthesis and respiration.¹⁷³ In many cases, it has been found that the enzymes capable of such electron transfer processes do so through an interplay between their cofactor(s) and strategically positioned amino acid residues, particularly tyrosine and tryptophan, which have relatively low oxidation potentials (Table 5.2.32). This can proceed as multiple sequential electron hops between the side-chains of the amino acids present in the protein, thereby allowing long range electron transfer to proceed efficiently.^{151,174-176}

Table 5.2.32. Measured oxidation potentials for the amino acids which are thought to be involved in electron hopping in proteins.¹⁷⁷⁻¹⁸⁰

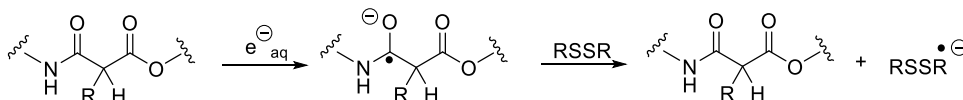
Amino acid-derived radical	E^{ox}
Glycine	1.22 V (pH 10.5)
Cysteine	1.33 V
Tyrosine	0.93 V
Tryptophan	1.01 V, 1.05 V

Redox activity is not limited to the side-chain substituents of amino acids; studies have also shown that the amide functionality in the protein backbone is also capable of such behaviour upon generation of its radical anion¹⁸¹ which can lead to protein damage (Scheme 5.2.33 a)¹⁸¹⁻¹⁸³ or electron transfer to other molecules e.g. disulfides (Scheme 5.2.33 b).¹⁸⁴

Peptide damage



Electron transfer



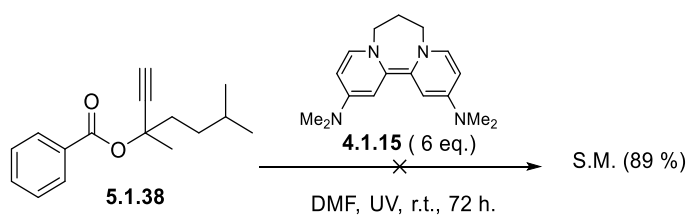
Scheme 5.2.33. a) Peptide damage has been observed upon reduction of the amide moiety present in proteins.¹⁸¹⁻¹⁸³ **b) Alternatively, electron transfer by amides in proteins has been observed.**¹⁸⁴ The authors utilised gamma radiation of deaerated aqueous solutions to obtain solvated electrons.

What has been showcased in this project was that small molecules could be used to study the electron-shuttling mechanism which proceeded with both the ester and amide-based substrates. In future, this might allow researchers to conduct preliminary tests on simpler, easy to synthesise amide-based substrates for electron transfer activity before testing more elaborate systems such as enzymes that involve more variables for electron transfer.

5.3 C-O bond cleavage of phenolic esters.

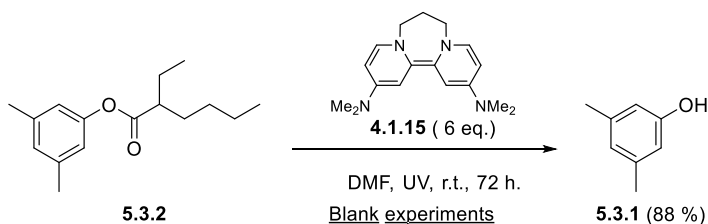
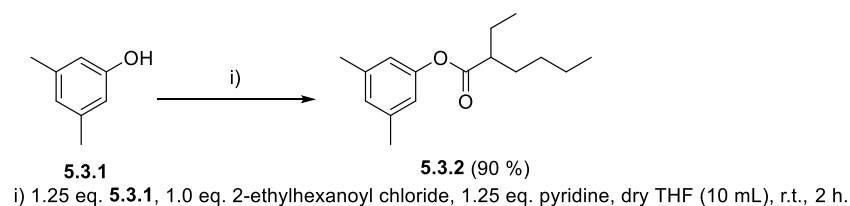
The previous section has shown that aliphatic esters were resistant to reduction by photoactivated **4.1.15**, but reactivity could be tuned-in by attaching a proximal aromatic ring.

This section explores the possibility of reductive cleavage on aromatic esters i.e. phenolates. It was previously determined that benzoate **5.1.38** was resistant to reductive cleavage with photoactivated **4.1.15** (Scheme 5.3.1) and so it was decided to test for the reduction of phenolic esters.



Scheme 5.3.1. Benzoate **5.1.38** was resistant to reductive cleavage by photoactivated **4.1.15**.

The study began with the synthesis of **5.3.2** which was conducted *via* esterification (Scheme 5.3.2 a).



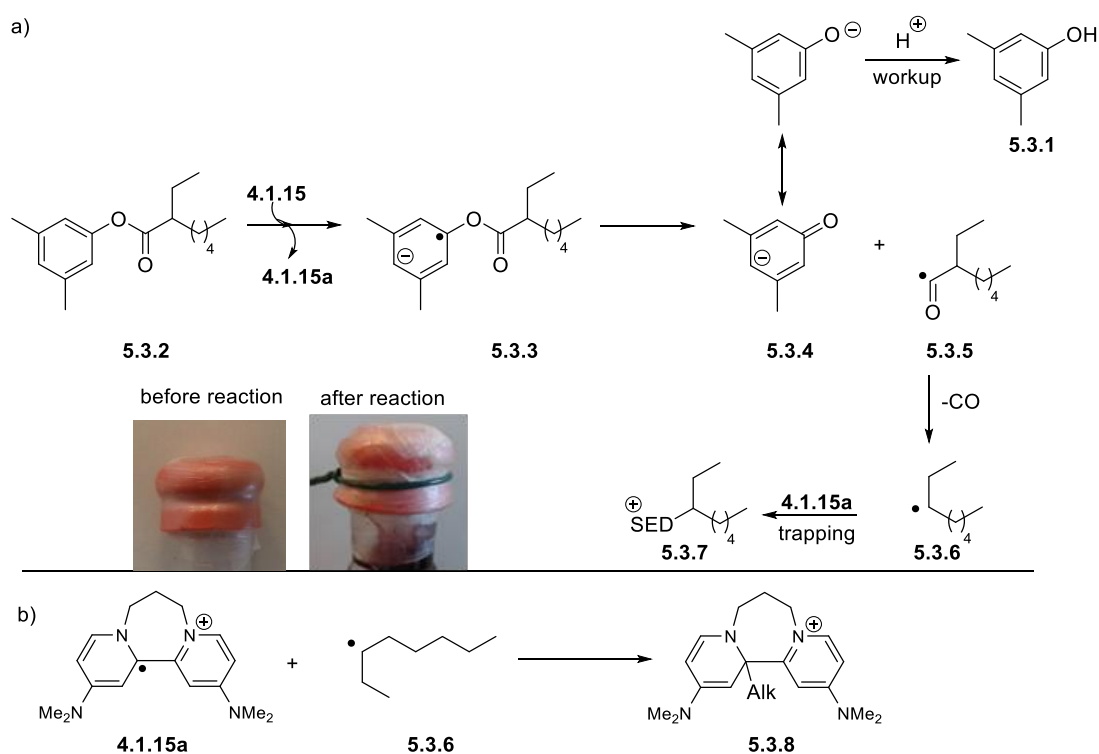
Blank experiments
Donor (6eq.), non UV reaction: **5.3.1** (10 %), S.M. (90 %)
Donor-free, UV active reaction: no reaction, quantitative recovery of S.M. (95 %)

Scheme 5.3.2. a) Synthesis of phenolic ester **5.3.2**. b) Reductive cleavage was observed when **5.3.2** was reacted with photoactivated **4.1.15**.

In contrast to benzoate **5.1.38**, phenolic ester **5.3.2** showed extensive reactivity with photoactivated **4.1.15** resulting in the isolation of 3,5-dimethylphenol **5.3.1** in good yield (88 %). To confirm that the observed reactivity was due to reduction of the substrate by photoactivated **4.1.15**, blank experiments were conducted in parallel. In the first instance, the reaction was conducted without UV exposure which led to

good recovery of the starting material and a small amount of **5.3.1** (10 %). A second blank experiment, which involved UV exposure of the substrate in the absence of **4.1.15**, led to good recovery of the starting material. These results confirmed that photoactivation of the super-electron donor was responsible for the high conversion of the substrate.

Upon generation and bond cleavage of the radical anion, it was postulated that the anion remained on the aromatic fragment with the radical migrating to the carbonyl fragment (Scheme 5.3.3 a). The subsequent irreversible formation of gaseous carbon monoxide might serve as a good driving force for the overall reaction.

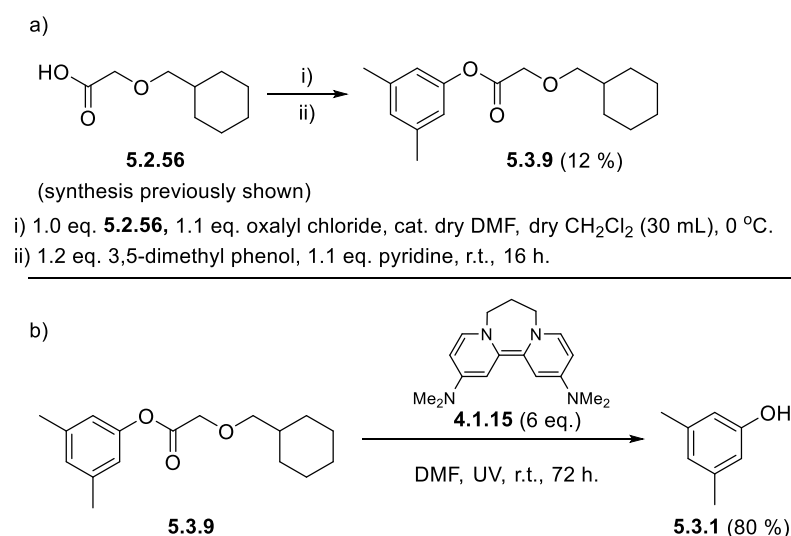


Scheme 5.3.3. a) Proposed mechanism for the observed C-O bond cleavage of **5.3.2** under reductive conditions with photoactivated **4.1.15**. The photographs depict the swelling of the subaseal after the photoactivated reduction of the phenolic esters. b) Radical trapping of **5.3.6** by **4.1.15a**.

Experimentally, a pressure build-up on the subaseal was experienced in all the photoactivated donor reactions attempted in this study (a later experiment involving **5.3.35** was the only exception); this swelling of the subaseal was not observed with photoactivated donor reactions of other projects. Furthermore, a forceful repulsion of an empty syringe was experienced whenever a needle was pierced into the sealed reaction vessel after the stipulated reaction time. These were clues that a gas had

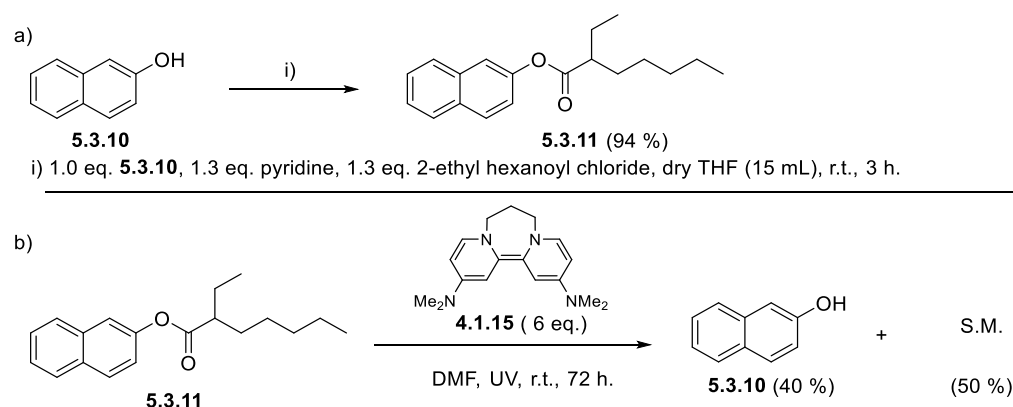
been generated during these reactions. Following the bond cleavage and decarbonylation steps, the derived alkyl radical **5.3.6** likely proceeded to couple with **4.1.15a** which would then partition into the aqueous phase upon workup (Scheme 5.3.3 b).

Phenolic ester **5.3.9**, conveniently synthesised from **5.2.56** was also tested for reduction with photoactivated **4.1.15**. As with the previous test substrate (i.e. **5.3.2**), a good reaction profile was observed with **5.3.1** being isolated in 80 % yield (Scheme 5.3.4).



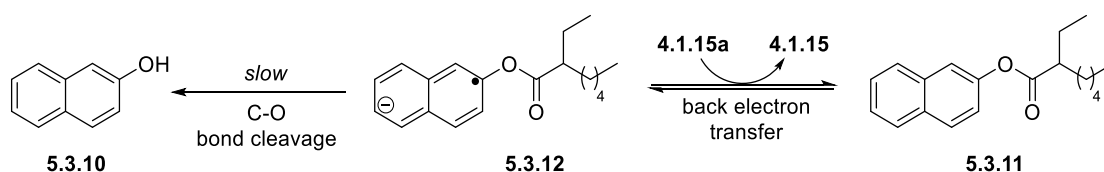
Scheme 5.3.4. a) Synthesis of phenolic ester **5.3.9**. The synthesis of **5.2.56** was shown previously. b) Reduction of **5.3.9** proceeded with photoactivated **4.1.15** with **5.3.1** being isolated in good yield.

The naphthyl-based substrate **5.3.11** was also synthesised (Scheme 5.3.5 a) in order to investigate the effect of electron delocalisation (in the aromatic system) on the reductive C-O bond cleavage (Scheme 5.3.5 b).



Scheme 5.3.5. a) Synthesis of naphthyl-based phenolic ester **5.3.11**. b) C-O bond cleavage was observed when tested for reduction with photoactivated **4.1.15**.

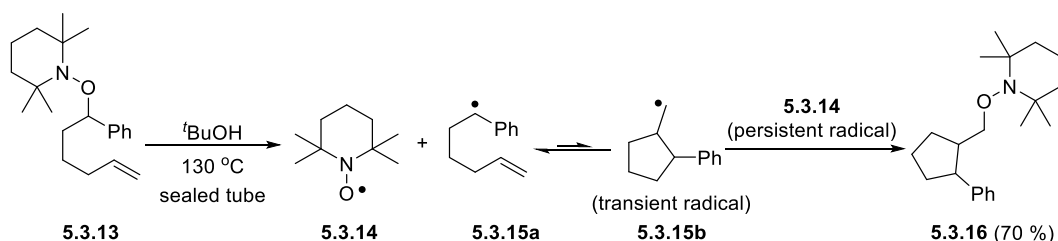
Compared to the previous experiment with phenolic **5.3.2**, the reactivity of the naphthyl-based substrate **5.3.11** was significantly lowered. In this instance, 2-naphthol **5.3.10** was isolated in moderate yield (40 %) along with the starting material (50 %). It was highly likely that the extensive conjugation present in the naphthyl moiety had increased the stability of the radical anion. In so doing, the bond cleavage would be slow and back electron transfer to the super-electron donor would be the more favourable process (Scheme 5.3.6). Another possibility was that the naphthyl chromophore was competing with **4.1.15** for photoexcitation.



Scheme 5.3.6. Back electron transfer could be competing with reductive C-O bond cleavage.

It was also possible that the radical anion **5.3.12**, generated upon SET from photoactivated **4.1.15**, remained unreactive and was then retrieved as starting material upon workup.

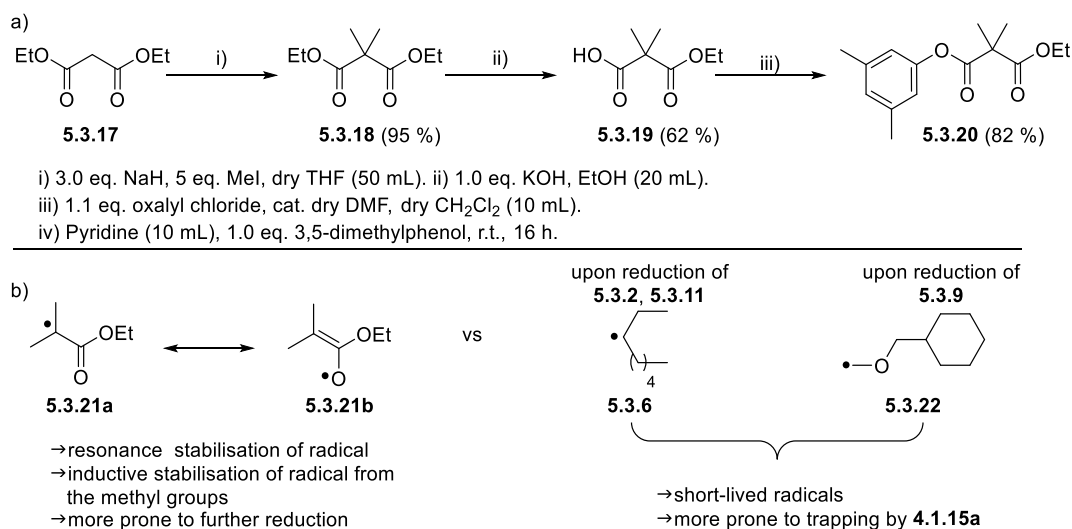
In all the preceding cases, only the aromatic fragments could be successfully retrieved after the reductive bond cleavages. Fischer¹⁸⁵ and Studer¹⁸⁶ have shown that the coupling between persistent (stabilised) and transient radicals is a very favourable reaction (Scheme 5.3.7, a cyclisation example is shown). This reaction, commonly known as the “persistent radical” effect, is reported for both inter and intramolecular radical couplings.¹⁸⁷ Based on this concept, it is highly likely that the short-lived alkyl radicals, generated after the reductive bond cleavage were being trapped by the highly-stable, long-lived donor radical cation.



Scheme 5.3.7. The persistent radical effect describes the tendency for coupling between radicals.¹⁸⁵

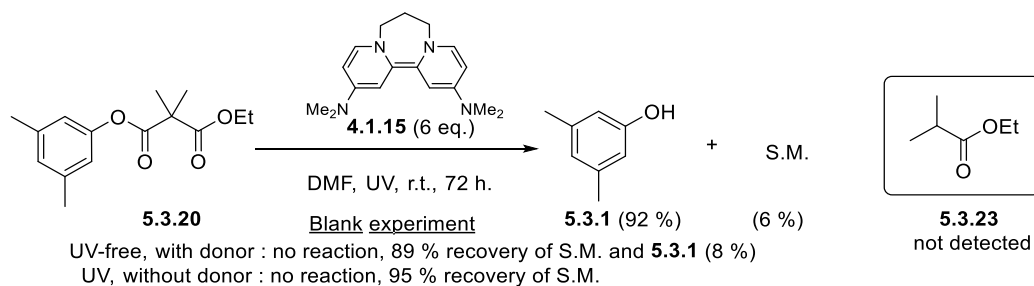
One strategy to evade or decrease radical trapping during the reaction would be to afford an initial radical after bond cleavage that would be easily converted to its

anion in the highly reducing medium. The resulting anion should then be retrievable upon protonation. The isolation of the fragment derived from the radical would be useful in confirming the proposed mechanism which involved decarbonylation of the substrate. To this end, substrate **5.3.20** was synthesised; in which the anticipated alkyl radical **5.3.21**, formed after reductive cleavage should be more prone to further reduction compared to **5.3.6** and **5.3.22** (Scheme 5.3.8 b).



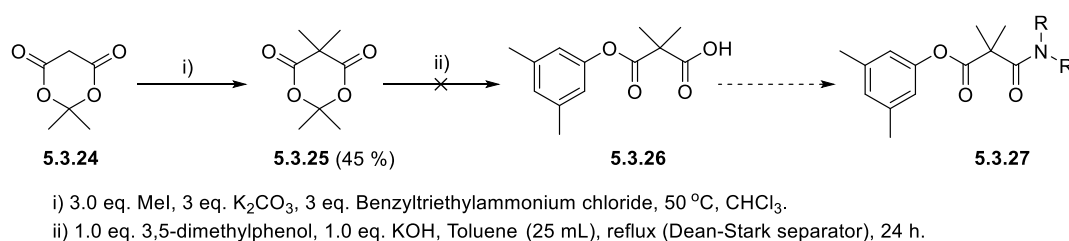
Scheme 5.3.8. a) Synthesis of malonate **5.3.20** conducted using diethylmalonate. b) The alkyl fragment **5.3.21** resulting from the reductive cleavage of **5.3.20** should experience both resonance and inductive stabilisation.

Installing the *gem*-dimethyl group in **5.3.20** was to prevent any deprotonation of any acidic protons which could stall the desired reduction. Furthermore, the presence of the *gem*-dimethyl group should result in a tertiary alkyl radical **5.3.21** that experiences both inductive (from the methyl groups) and resonance (adjacent carbonyl group) stabilising effects (Scheme 5.3.8 b).

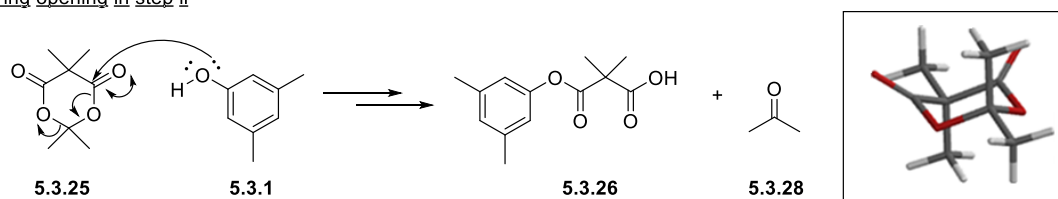


Scheme 5.3.9. C-O bond reduction of **5.3.20** was achieved in quantitative yield with photoactivated **4.1.15**, albeit the alkyl fragment **5.3.23** could not be detected after workup.

However, when **5.3.20** was subjected to reduction with photoactivated **4.1.15**, only the phenol fragment **5.3.1** could be isolated (Scheme 5.3.9). The lack of reactivity in the blank experiment (a repeat of the experiment but without UV exposure) reaffirmed that the formation of **5.3.1** was a result of reductive activity of the photoactivated **4.1.15** and not hydrolysis (Scheme 5.3.9). Isolation of the alkyl fragment **5.3.23** was unsuccessful, which was thought to be due to volatility issues (reported¹⁸⁸ boiling point of ethyl isobutyrate: 23 °C at 27 mbar). To circumvent this, candidate **5.3.27** was designed; with its synthesis starting from commercially available Meldrum's acid **5.3.24** (Scheme 5.3.10).



ring opening in step ii

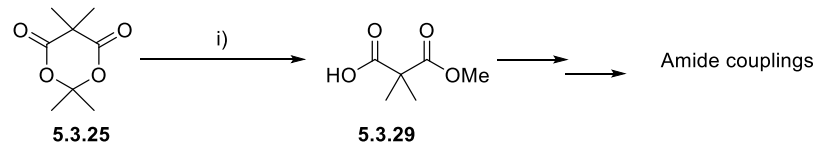


Scheme 5.3.10. Attempted synthesis of amide **5.3.27** starting with **5.3.25**. Ring opening of **5.3.25** was required in step ii. Inset: Molecular modelling depicted **5.3.25** in a stable conformation with methyl groups hindering nucleophilic attack.

Attempts were made to install the *gem*-dimethyl group at an early stage; this proceeded in moderate yield but the subsequent ring opening of **5.3.25** with 3,5-dimethylphenol was unsuccessful (Scheme 5.3.10 inset). In retrospect, it was realised that the *gem*-dimethyl groups would extensively impede nucleophilic attack on **5.3.25** since the required approach (following the Bürgi-Dunitz angle¹⁸⁹ ($105^\circ \pm 5^\circ$)) for the nucleophile would be hindered from both faces of the ring. This became obvious with computer modelling (Scheme 5.3.10). Under the reaction conditions employed,¹⁹⁰ the alkylated Meldrum's acid **5.3.25** would probably decompose before any meaningful reaction took place.

There is only one report, by Li *et al.*¹⁹¹ in which **5.3.25** was ring-opened by a small nucleophile before subsequent amidation reactions (Scheme 5.3.11). This testifies to the difficulty in the required reaction involving **5.3.1** as the nucleophile.

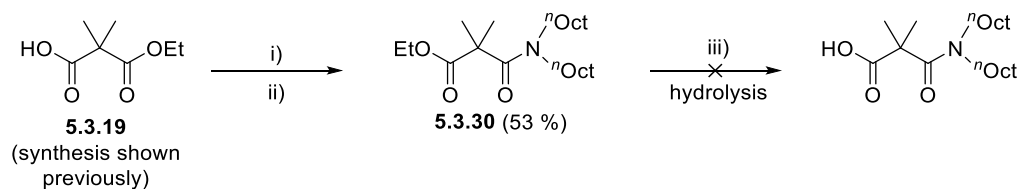
Li *et al.*



reaction conditions: i) 4 eq. KOH, MeOH/THF (1:5, 50 mL), r.t., 24 h.

Scheme 5.3.11. Only one report by Li *et al.* could be located which described the successful ring-opening of **5.3.25**.¹⁹¹

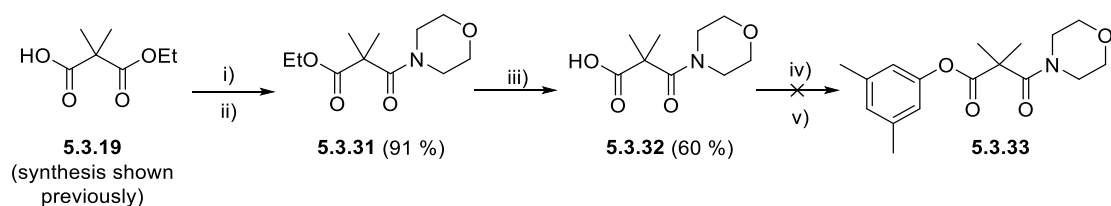
It was therefore decided to revert to using the non-cyclic precursor **5.3.19** (Scheme 5.3.12). This provided the intermediate **5.3.30** which would then require hydrolysis to obtain the carboxylic acid.



reaction conditions: i) 1.3 eq. oxalyl chloride, cat. dry DMF, dry CH₂Cl₂ (20 mL), 0 °C.
 ii) 1.3 eq. dioctylamine, r.t., 16 h.
 iii) 4 eq. NaOH, EtOH, reflux, 24 h. (2nd attempt, 5 days).
 Subsequently, other solvents including DMF & THF were tested.

Scheme 5.3.12. Synthesis of amide **5.3.30** from the non-cyclic precursor **5.3.19**.

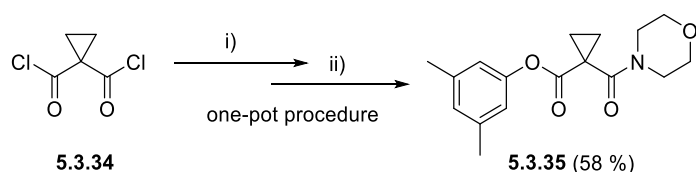
However, **5.3.30** was found to be resistant to hydrolysis even with prolonged heating (Scheme 5.3.12). It was suspected that the resistance was due to the poor solubility of the amide in a range of solvents. To this end, the amide was redesigned with the installation of a morpholine moiety (Scheme 5.3.15).



i) 1.3 eq. oxalyl chloride, cat. dry DMF, dry CH₂Cl₂ (20 mL), 0 °C.
 ii) 1.1 eq. pyr., 1.3 eq. morpholine, r.t., 16 h.
 iii) 3.0 eq. NaOH, EtOH (20 mL), reflux, 16 h.
 iv) 1.3 eq. oxalyl chloride, cat. DMF, dry CH₂Cl₂ (30 mL).
 v) 2.1 eq. pyr., 1.3 eq. 3,5-dimethylphenol, r.t., 16 h.

Scheme 5.3.15. Attempted synthesis of amide **5.3.36** containing the morpholine fragment.

In the event, the intermediate **5.3.31** was formed in high yield and the subsequent hydrolysis proceeded moderately to yield the corresponding acid **5.2.32**. Regrettably, the final installation of 3,5-dimethylphenol proved challenging and there was insufficient material for further attempts. At this stage, the synthesis of the required substrate was proving arduous and it was decided to attempt a one-pot synthesis of **5.3.35** from commercially available **5.3.34** in order to reduce the number of steps in the synthesis. This involved the sequential amide formation followed by the addition of 3,5-dimethylphenol (Scheme 5.3.16). Gratifyingly, the one-pot experiment afforded the desired product **5.3.35** in moderate yield (58 %).

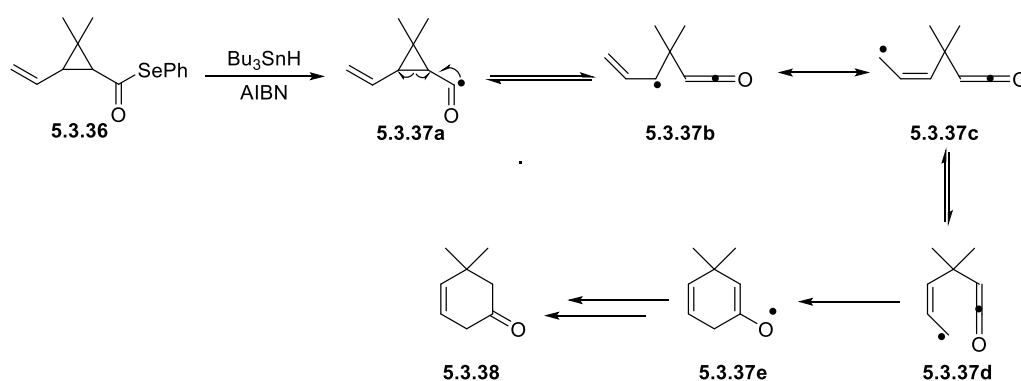


i) 1.0 eq. **5.3.34**, 1.1 eq. 3,5-dimethylphenol, 1.0 eq. Hunig's base, dry CH_2Cl_2 (10 mL), 0°C , 2h.

ii) 1.0 eq. morpholine, 1.0 eq. Hunig's base, dry CH_2Cl_2 (15 mL), $0^\circ\text{C} \rightarrow \text{r.t.}$, 16 h.

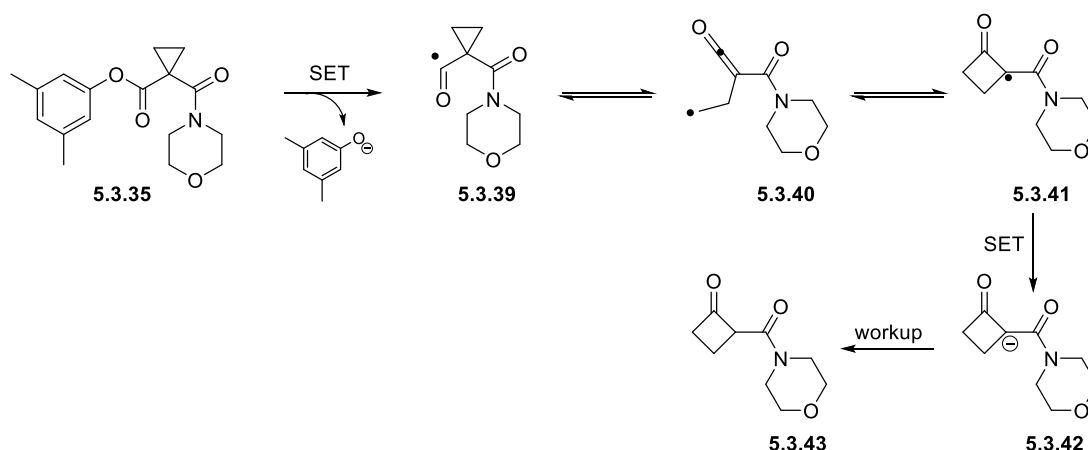
Scheme 5.3.16. The one-pot procedure to obtain amide **5.3.35** was successful.

Installing the cyclopropyl moiety was deliberate as this might alter the fate of the radical fragment formed after the C-O bond reduction of **5.3.35**. In a recent study, Pattenden *et al.*¹⁹² revealed that it was possible to generate ketene alkyl radicals from their precursory cyclopropyl acyl radicals (Scheme 5.3.17). Instead of decarbonylation, the cyclopropane adjacent to the ketyl radical collapsed to yield the allylic radical **xxx** which proceeded with cyclisation to form **xxx**. Pattenden *et al.* was able to exploit this reactivity to access cyclic ketones.



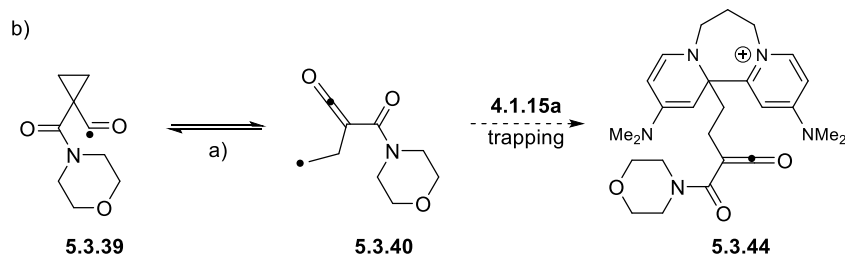
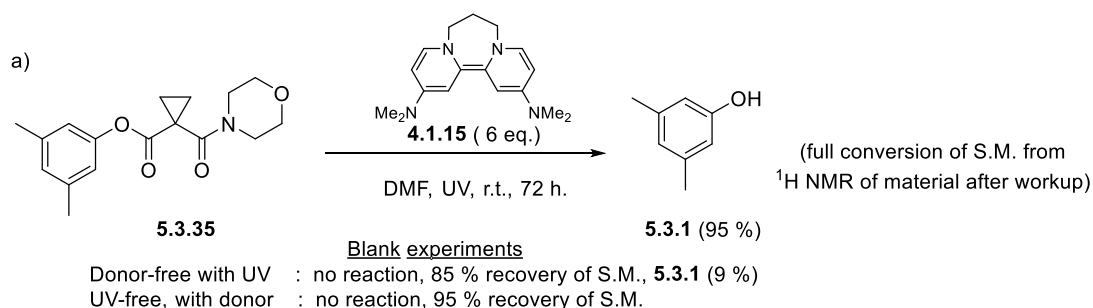
Scheme 5.3.17. Pattenden *et al.* have shown that cyclopropyl acyl radicals have the propensity to collapse into ketene alkyl radicals.¹⁹²

In a similar fashion, it was postulated that the radical fragment **5.3.39**, formed after the reduction of substrate **5.3.35**, could collapse to yield **5.3.40** which would then cyclise to yield **5.3.41** (Scheme 5.3.18). Under the reductive environment employed, this highly stabilised radical should be easily converted to its anion **5.3.43** thereby evading trapping with radical cation **4.1.15b**. If successful, this reaction will not only be diagnostic of the proposed reduction mechanism but might also afford a novel method of accessing cyclobutanones.



Scheme 5.3.18. Proposed mechanism for the formation of **5.3.43** after the C-O bond cleavage of **5.3.35**.

In the event, substrate **5.3.35** was successfully reduced when subjected to the standard photoactivation conditions with **4.1.15**. (Scheme 5.3.19 a).

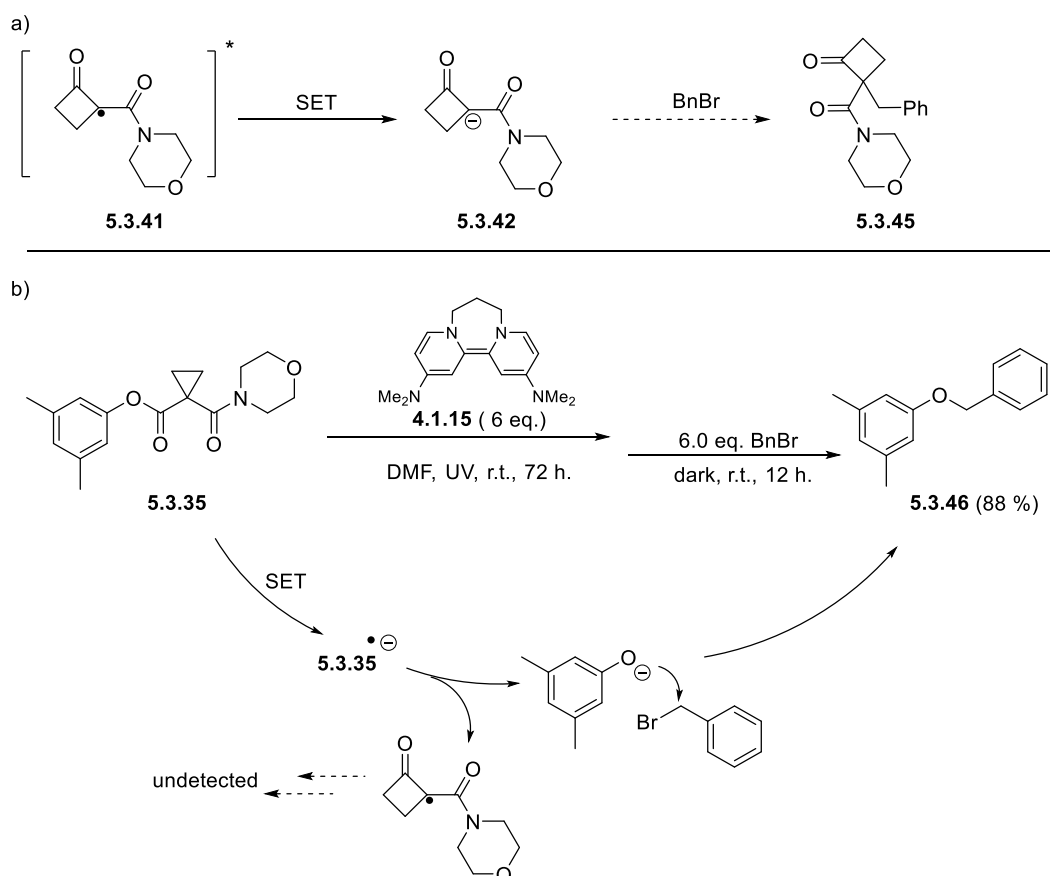


Scheme 5.3.19. a) Photoactivated **4.1.15** was successfully employed in the reductive bond cleavage of **5.3.35**. b) Possible trapping of **5.3.40** by the radical cation of **4.1.15**.

Interestingly, there was no significant swelling of the subaseal for this experiment (which had been observed with previous substrates). This could indicate that the evolution of CO was not prevalent. Blank experiments were also conducted in parallel to confirm that photoactivated **4.1.15** was required for the observed reactivity (Scheme 5.3.19 a). However, the postulated morpholinyl fragment i.e. **5.3.43** could not be detected; it might be that trapping of radical **5.3.40** by **4.1.15a** was out-competing with its cyclisation (Scheme 5.3.19 b).

Alternatively, it was possible that the proposed anion **5.3.42** had formed but the protonated form **5.3.43** was lost upon workup due to volatility issues. If this was the case, then it might be possible to derivatise the morpholinyl fragment by adding a trapping reagent after the reduction step (*via* S_N2, Scheme 5.3.20 a).

To this end, the reduction experiment of **5.3.35** was repeated and, after 72 h exposure to UV, the reaction vessel was placed in a dark fume cupboard whereupon benzyl bromide (6.0 eq.) was added. The reaction was allowed to stir overnight (12 h) before quenching, workup and purification (Scheme 5.3.20 b).



Scheme 5.3.20. a) If the radical fragment could be reduced to its anion 5.3.42, then trapping with benzyl bromide could allow for easier isolation and characterisation after workup and purification. b) Result of the trapping experiment attempted after the reduction of 5.3.35.

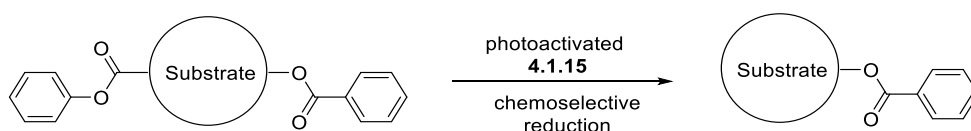
In the event, the only product isolated from the attempted trapping experiment was 5.3.46. This indicated that the phenolate anion was formed during the reaction (Scheme 5.3.20 b). The morpholinyl fragment remained undetected which could be due to volatility issues of 5.3.42 if it had failed to react with benzyl bromide to yield 5.3.45.

Further work is required to test the proposed mechanisms – decarbonylation of phenolic esters and cyclobutanone formation in the case of 5.3.35.

Conclusions and Future Work

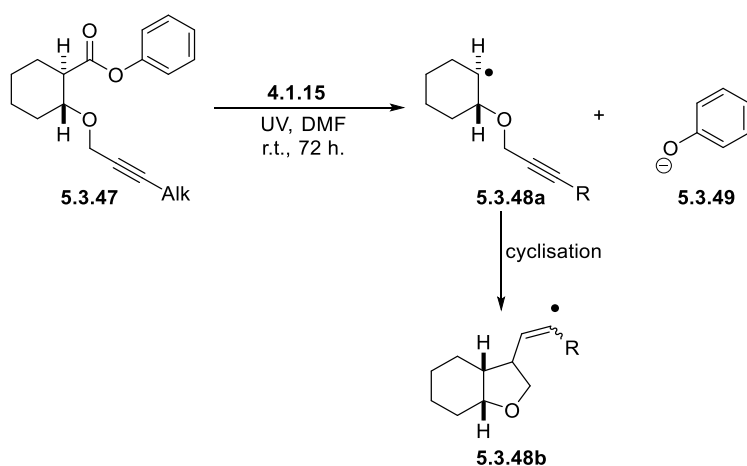
The generation of a gas e.g., carbon monoxide, is often a powerful driving force for organic reactions. Presently, a novel decarbonylation methodology has been discovered which could be conducted efficiently under benign and metal-free reaction conditions.

The ArO-C bond cleavage of phenolic esters proceeded efficiently with all the candidates tested, resulting in the isolation of the phenolic fragment in good yields. In contrast, the reduction of benzoates was not achievable with photoactivated **4.1.15** but this result suggests that the super-electron donor has the potential for chemoselective reduction of compounds which possess both benzoate and phenolic esters if radical trapping by the donor radical cation **4.1.15a** can be arrested (Scheme 5.3.21). To the best of our knowledge, there are no existing reports of metal-free reductive cleavage of phenolic esters.



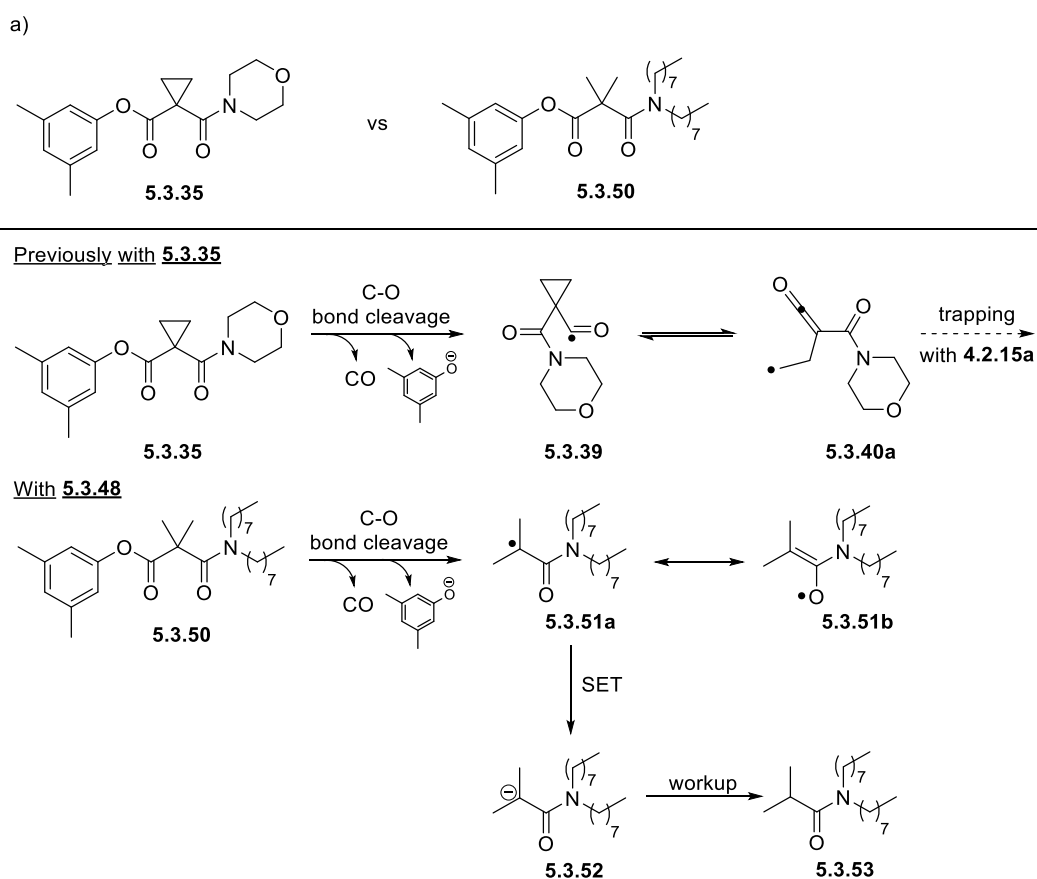
Scheme 5.3.21 Chemoselective reduction would be possible with substrates bearing both phenolate and benzoate fragments.

Another application of this chemistry involves intramolecular cyclisation of the resulting radical fragment (Scheme 5.3.22), e.g. substrate **5.3.47**, akin to the reactivity of toluates which was reported by Marko *et al.*⁵¹



Scheme 5.3.22. Reduction of phenolates by photoactivated **4.1.15** could be applied to substrates that are setup for further cyclisation.

Validation of the proposed mechanism for this novel C-O bond reduction could be provided by the detection and/or isolation of the resulting radical fragment. Having realised that the one-pot synthesis of the mixed amide and ester substrate **5.3.35** was possible, then the synthesis of **5.3.50** should be straightforward by employing the one-pot methodology. In contrast to **5.3.35**, the non-cyclopropyl analogue **5.3.50** cannot undergo ring-opening to yield the ketene alkyl radical (Scheme 5.3.23). The fate of the alkyl radical **5.3.51** could potentially assist in confirming the proposed reductive mechanism.



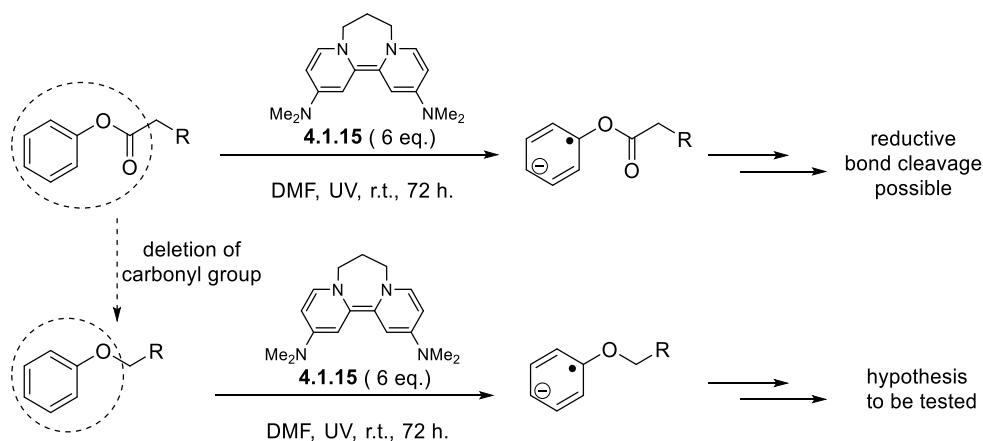
Scheme 5.3.23 a) Substrate **5.3.50** could be synthesised using a one-pot methodology and then tested for reduction with photoactivated **4.1.15**. b) The proposed radical **5.3.51**, resulting from reductive cleavage and decarbonylation of **5.3.50**, could undergo further SET to yield **5.3.52**, which could then be protonated upon workup with possible isolation of **5.3.53**.

During the course of this project, attempts were made to detect the production of carbon monoxide during the reaction using instruments owned by Dr Liggat's team within the department. Detection of carbon monoxide would have greatly assisted this project in confirming the proposed reductive cleavage mechanism. Unfortunately, this equipment had repeatedly malfunctioned and it was not available for further tests.

Certainly, the use of these instruments would allow for easier confirmation of carbon monoxide evolution during these reductive C-O bond cleavages. This would provide evidence for the proposed mechanism. It would be an area of research worth revisiting in the future.

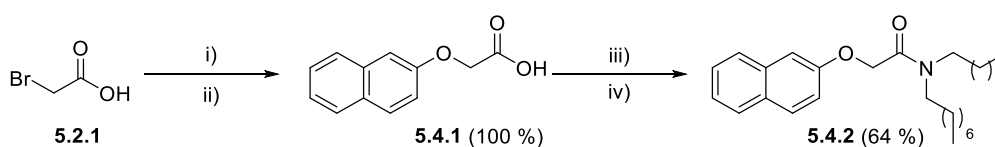
5.4 C-O bond cleavage of aryl ethers

Having established that i) the reductive bond cleavage of benzoates could not be achieved by photoactivated **4.1.15** and that ii) the C-O bond cleavage of phenolic esters proceeded well under the same reaction conditions, another exciting area of research which has not been attempted before concerns the reductive cleavage of C-O bonds of alkyl aryl ethers. Essentially, such substrates can be perceived as a simple yet significant functional modification of the phenolic esters (Scheme 5.4.1).



Scheme 5.4.1. Aromatic ethers have not been explored for reductive C-O bond cleavage with **4.1.15**.

Preliminary studies involved the synthesis and testing of naphthyl-based substrate **5.4.2** (Scheme 5.4.2). The amide fragment was strategically chosen since earlier experiments had already indicated that this functional group would not undergo reductive bond cleavage and so would allow easier interpretation of experimental results. The synthesis of **5.4.2** proceeded in good yields over two steps.

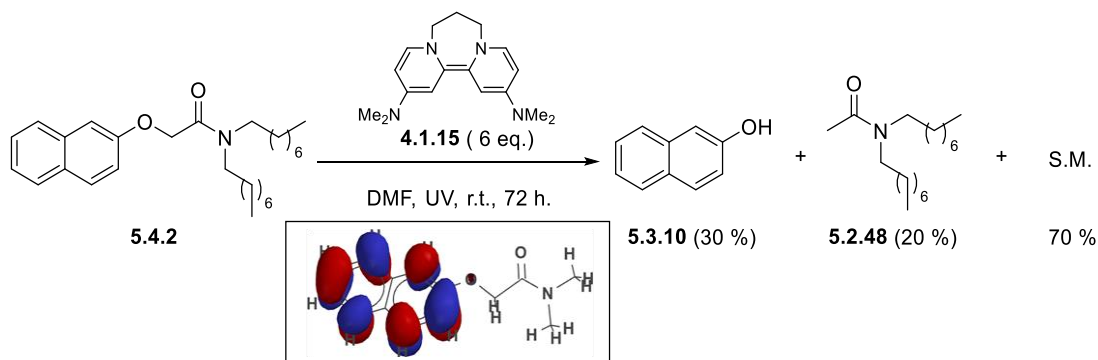


- 1.0 eq. 2-naphthol, 2.1 eq. NaH, dry THF (35 mL), 0 °C.
- 1.2 eq. **5.2.1**, dry THF (20 mL) reflux, 10 h.
- 1.1 eq. **5.4.1**, 1.2 eq. oxalyl chloride, cat. dry DMF, dry CH₂Cl₂ (5 mL), 0 °C.
- 1.5 eq. *N,N*-dioctylamine, 1.2 eq. pyridine, dry CH₂Cl₂ (30 mL), r.t., 16 h.

Scheme 5.4.2. The synthesis of **5.4.2** proceeded in good yields.

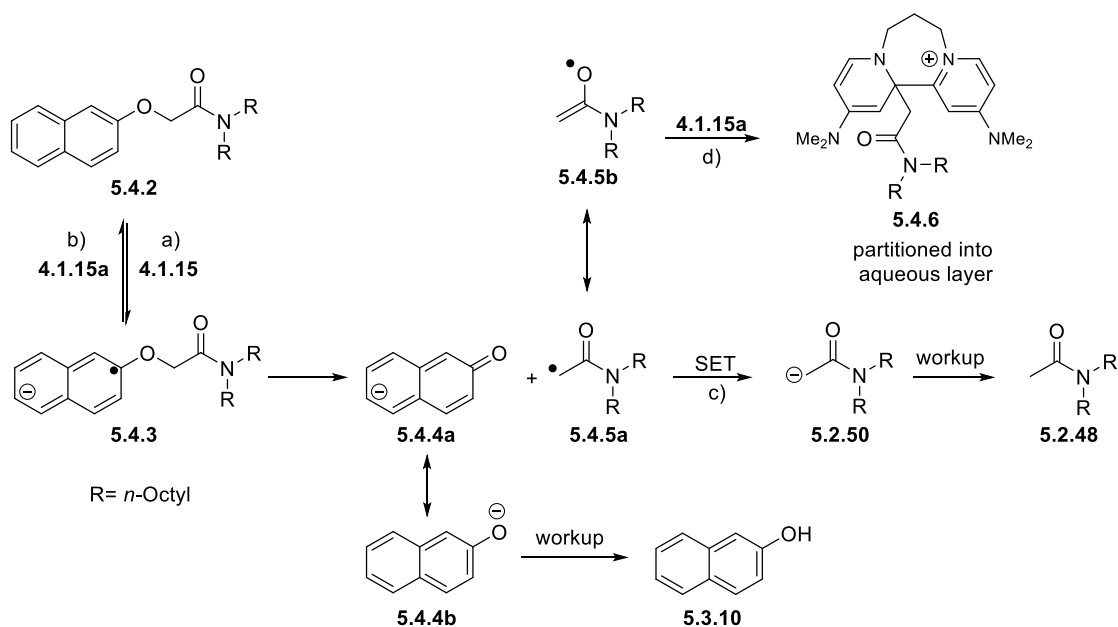
When tested for reductive cleavage with photoactivated **4.1.15**, the result unambiguously revealed that the ArO-C bond cleavage had ensued with the two resulting fragments **5.3.10** and **5.2.48** isolated in low yields (Scheme 5.4.3). The

starting material was also recovered in good yield and overall, the mass recovery was excellent.



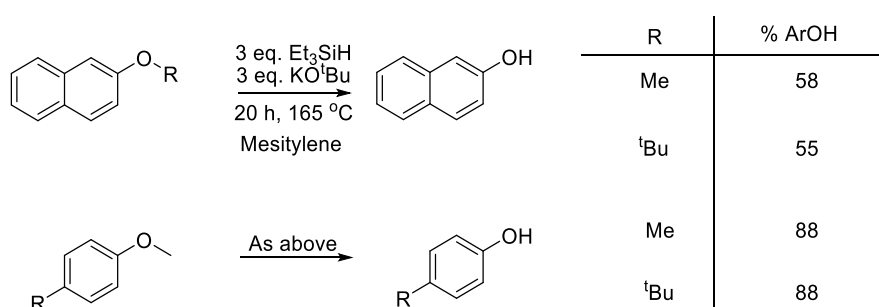
Scheme 5.4.3. Reductive C-O bond cleavage was achieved with substrate **5.4.2** using photoactivated **4.1.15**. Inset: Predicted SOMO of the radical anion of **5.4.2**; (Spartan 2010 version, DFT, B3LYP, 6-31G(d,p) in DMF was employed with calculation set at -1 charge and multiplicity of 2.

In theory, both fragments should have been recovered in equal yield (30%). In the event, the amide **5.2.48** was retrieved in lower yield than 2-naphthol **5.3.10** thus suggesting that the parent amidyl radical **5.4.5**, formed immediately after bond cleavage, could have been trapped by the donor radical cation (Scheme 5.4.4, pathway d) in competition with a second SET to yield **5.2.50** (Scheme 5.4.4, pathway c).



Scheme 5.4.4. Proposed mechanistic pathways involved in the reduction of **5.4.2**.

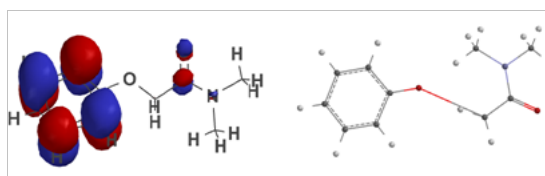
It was evident from the amount of starting material recovered (70 %) that the C-O bond cleavage of **5.4.2** was challenging. Based on computational investigations (Scheme 5.4.3, inset), it was predicted that the radical anion would not spontaneously undergo bond rupture. It was most likely that the extended resonance in the naphthyl ring would greatly stabilise the unpaired electron in the radical anion **5.4.3** rendering it less prone to fragmentation. Re-oxidation of **5.4.3** to the neutral starting material could also be the preferred pathway (Scheme 5.4.4 pathway b). A similar process was also proposed by Grubbs *et al.*⁴¹ in which they reported on the diminished reactivity of naphthyl-based substrates compared to phenol-based molecules (Scheme 5.4.5).



Scheme 5.4.5. Grubbs *et al.* observed diminished reductive cleavage when naphthyl-based substrates were tested.⁴¹

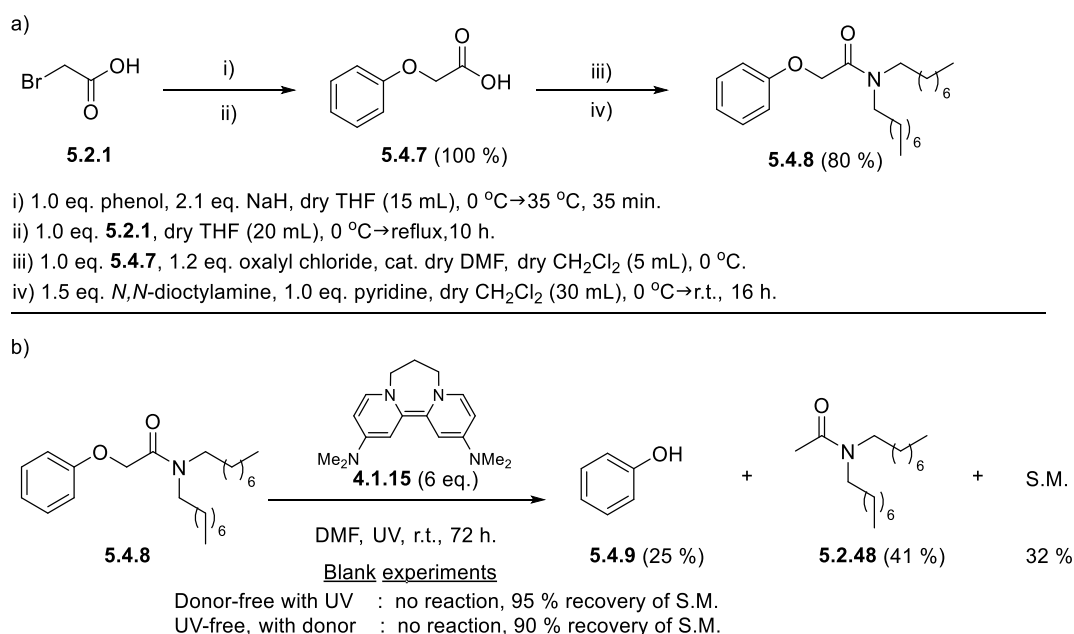
To improve this novel ArO-C bond reduction, the phenol analogue was synthesised and tested for reduction with photoactivated **4.1.15**. In this instance, computational calculations suggested spontaneous cleavage of the radical anion (Figure 5.4.6).

Figure 5.4.6. Left: The Predicted LUMO of the phenol analogue of **5.4.2**. Right: Energy minimisation of the corresponding radical anion was attempted; the calculation failed with spontaneous C-O bond cleavage. Note that the elongated line does not represent a bond. (Spartan 2010 version, DFT, B3LYP, 6-31G(d,p) in DMF was employed with calculation set at -1 charge and multiplicity of 2).



To test the computational calculations experimentally, substrate **5.4.8** was synthesised following a two-step procedure (Scheme 5.4.7 a). When tested for reduction with photoactivated **4.1.15**, it was pleasing to observe an improved reaction profile by comparing the yields of the amide fragment **5.2.48** and that of the

starting material recovered (Scheme 5.4.7 b). The blank experiments (Scheme 5.4.7 b) reaffirmed that the observed reactivity required photoactivation of the donor.

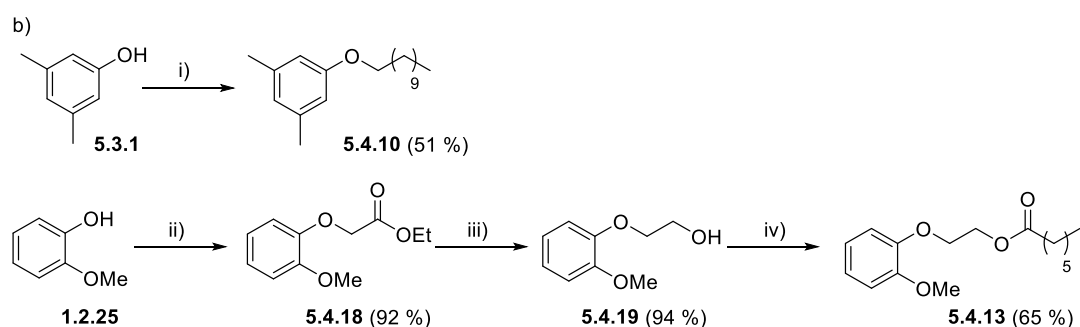
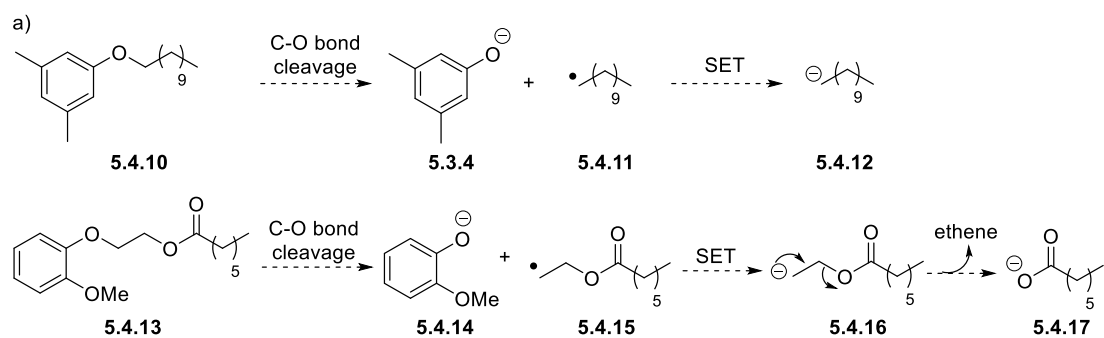


Scheme 5.4.7. a) The synthesis of phenol-based substrate 5.4.8 proceeded in good yields. b) Reductive C-O bond cleavage of 5.4.8 was more efficient compared to naphthyl-based analogue 5.4.2 as reflected in the yields of 5.2.48 and the starting material.

The proposed mechanism for the observed cleavage at the radical anion stage would be similar to that of the naphthyl-based substrate **5.4.2** (Scheme 5.4.4). In the present case, the overall mass recovery was lower (73 %) than that of the naphthyl analogue. This was not surprising since the amidyl radical **5.4.5** could be trapped by **4.1.15a** in which case the resulting salt **5.4.6** would not be easily retrieved during workup (Scheme 5.4.4).

In order to probe the reduction parameters of this newly-discovered C-O bond cleavage, substrates **5.4.10** and **5.4.13** were synthesised (Scheme 5.4.8). ArO-C bond cleavage on **5.4.10** would result in the formation alkyl radical **5.4.11** which might be further reduced to its anion **5.4.12**, or more likely, trapped by **4.1.15a**.

In a similar fashion, the reduction of substrate **5.4.13** could ultimately lead to anion **5.4.16** which would proceed to eliminate ethene (Scheme 5.4.8 a) leading to the formation of heptanoic acid **5.4.17**. In the latter case, characterisation by ¹H and ¹³C NMR would be more definitive. The synthesis of both substrates proceeded in good yields overall (Scheme 5.4.8 b).

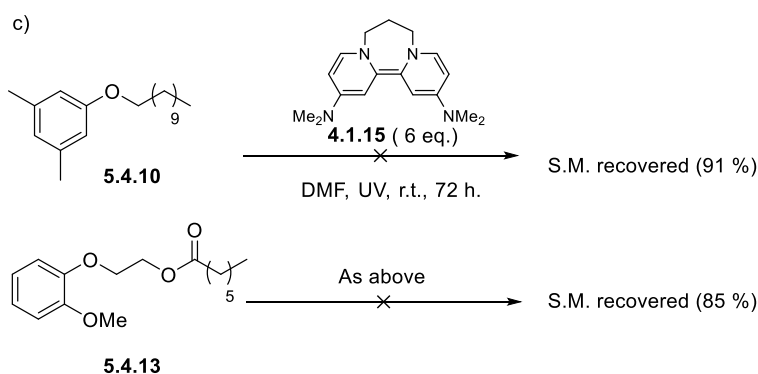


i) 1.0 eq. **5.3.1**, 1.1 eq. K_2CO_3 , 1.0 eq. 1-bromoundecane, acetone (30 mL), reflux, 16 h.

ii) 1.0 eq. **1.2.25**, 2.4 eq. K_2CO_3 , 2.4 eq. ethyl 2-bromoacetate, 80 °C, 16 h.

iii) 1.0 eq. **5.4.18**, 0.8 eq. LiAlH_4 , dry THF (20 mL), 0 °C \rightarrow r.t., 2 h.

iv) 1.0 eq. **5.4.19**, 1.3 eq. pyridine, 1.2 eq. heptanoyl chloride, dry THF (15 mL), reflux, 16 h.

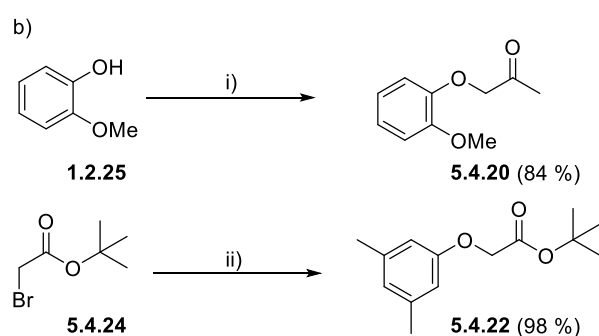
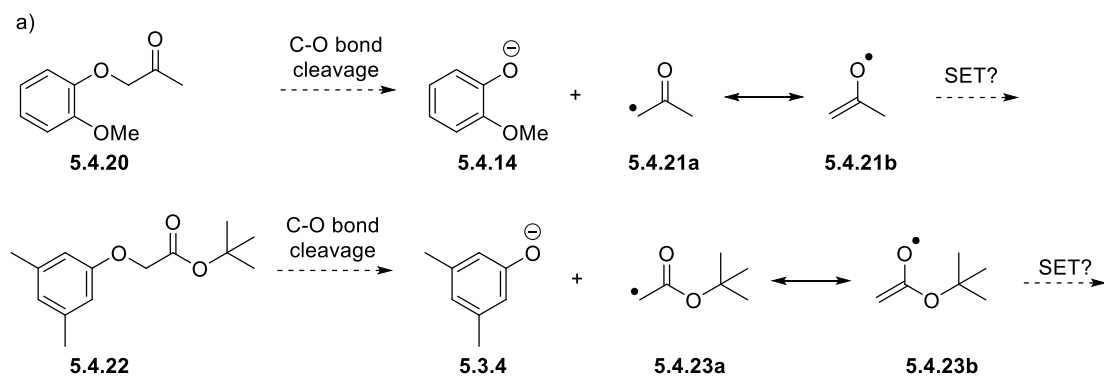


Scheme 5.4.8. a) Substrates **5.4.10** and **5.4.13** were planned with a view to testing the reductive capability of photoactivated **4.1.15** on aryl ethers. b) Synthesis routes for substrates both substrates. c) No reduction was observed for both **5.4.10** and **5.4.13**.

However, when tested for reduction with photoactivated **4.1.15**, both substrates showed no reactivity (Scheme 5.4.8 c) and this indicated that some form of stabilisation of the departing fragment was required for the desired ArO-C bond cleavage.

With this in mind, substrates **5.4.20** and **5.4.22** were designed and synthesised (Scheme 5.4.9 b). In the case of **5.4.20**, the departing radical upon reductive bond cleavage would be stabilised as an enolyl fragment **5.4.21**. With **5.4.22**, the

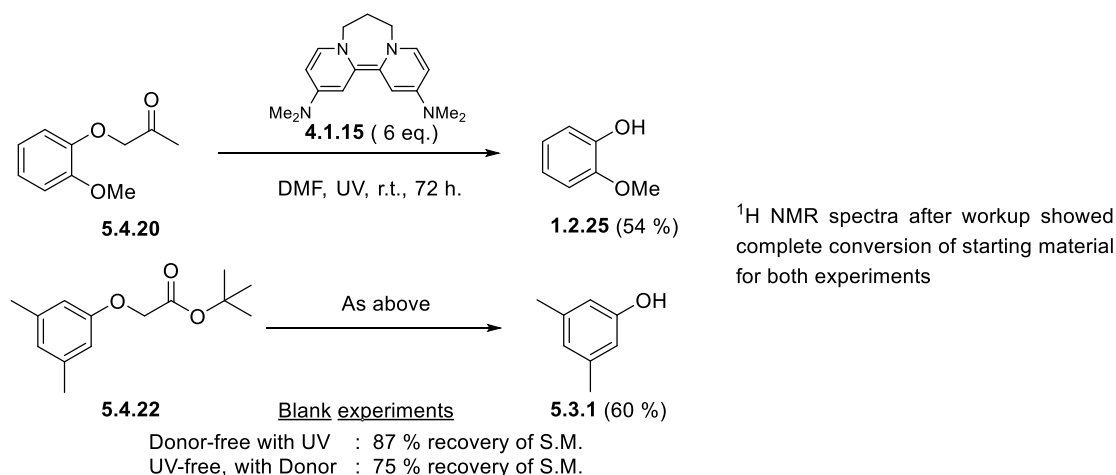
postulated radical **5.4.23** upon C-O bond cleavage would also be stabilised by the ester moiety (Scheme 5.4.9 a).



- i) 1.0 eq. **5.4.17**, 1.5 eq. K_2CO_3 , 1.5 eq. acetyl chloride, acetone (15 mL), reflux, 15 h.
 ii) 2.0 eq. **5.4.24**, 1.2 eq. K_2CO_3 , 1.0 eq. 3,5-dimethylphenol, DMF (10 mL), 80 °C, 20 h.

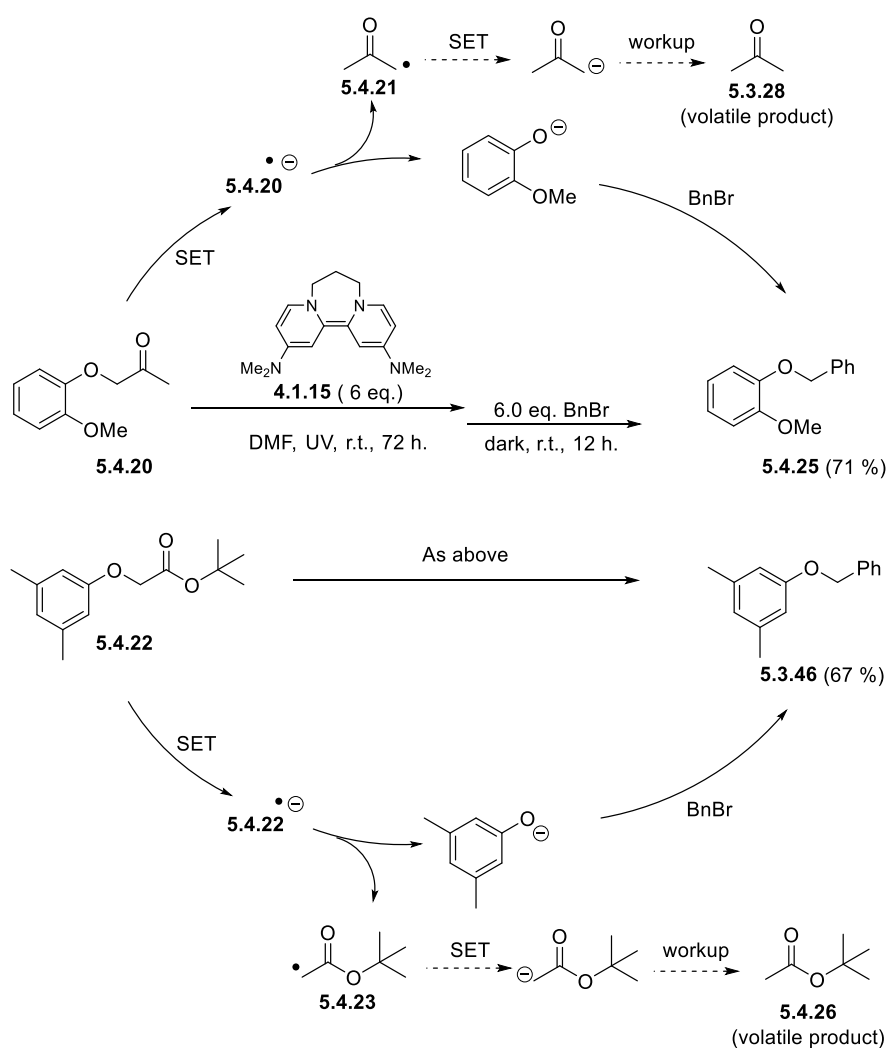
Scheme 5.4.9. a) Substrates 5.4.20 and 5.4.22 both possessed activated leaving groups which might promote C-O bond reduction b) The syntheses of substrates 5.4.20 and 5.4.22 proceeded in good yields.

When tested for reduction with photoactivated **4.1.15**, the phenolic products were isolated in moderate yields in both cases (Scheme 5.4.10).



Scheme 5.4.10. The novel ArO-C bond cleavage was observed for both substrates when tested with photoactivated 4.1.15.

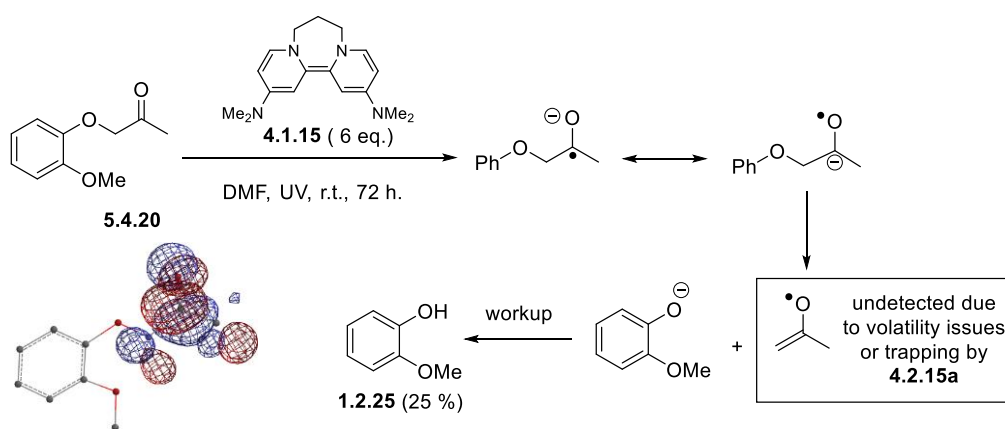
Moreover, ^1H NMR and TLC analyses after the workup procedures confirmed that the test substrates were fully consumed. The two blank reactions conducted with **5.4.22** led only to the recoveries of starting material which confirmed that the photoactivated **4.1.15** was responsible for the observed reactivity. This aroused suspicion that the moderate yields of **5.3.1** and **1.2.25** were due to potential volatility issues. To determine if this was the case, the experiments were repeated with the subsequent addition of excess benzyl bromide. The addition of benzyl bromide after the standardised reaction time for photoactivation of the super-electron donor would ensure that the reagent was not interfering with the C-O bond reduction in any way (Scheme 5.4.11).



Scheme 5.4.11. The experiments involving test substrates **5.4.20** and **5.4.22** were repeated with subsequent trappings with benzyl bromide. These led to the improved yields of the phenolic-derived fragments.

In the event, improvements in the yields of the phenolic products were observed as evidenced by the isolation of **5.3.46** and **5.4.25** in moderate yields. The corresponding non-phenolic fragments resulting from the reductive bond cleavages i.e. **5.3.28** and **5.4.26**, remained undetected in these repeats. It is most likely that these fragments could not be retrieved after workup due to volatility issues.

In the case of ketone-containing **5.4.20**, computational investigations reveal that the LUMO lies on the ketone and not on the aromatic fragment (as seen in the previous substrates). This being the case, it was most likely that the observed C-O bond reduction proceeded *via* SET onto the carbonyl moiety, generating the ketyl radical anion which then collapses to yield the observed products (Scheme 5.4.12).

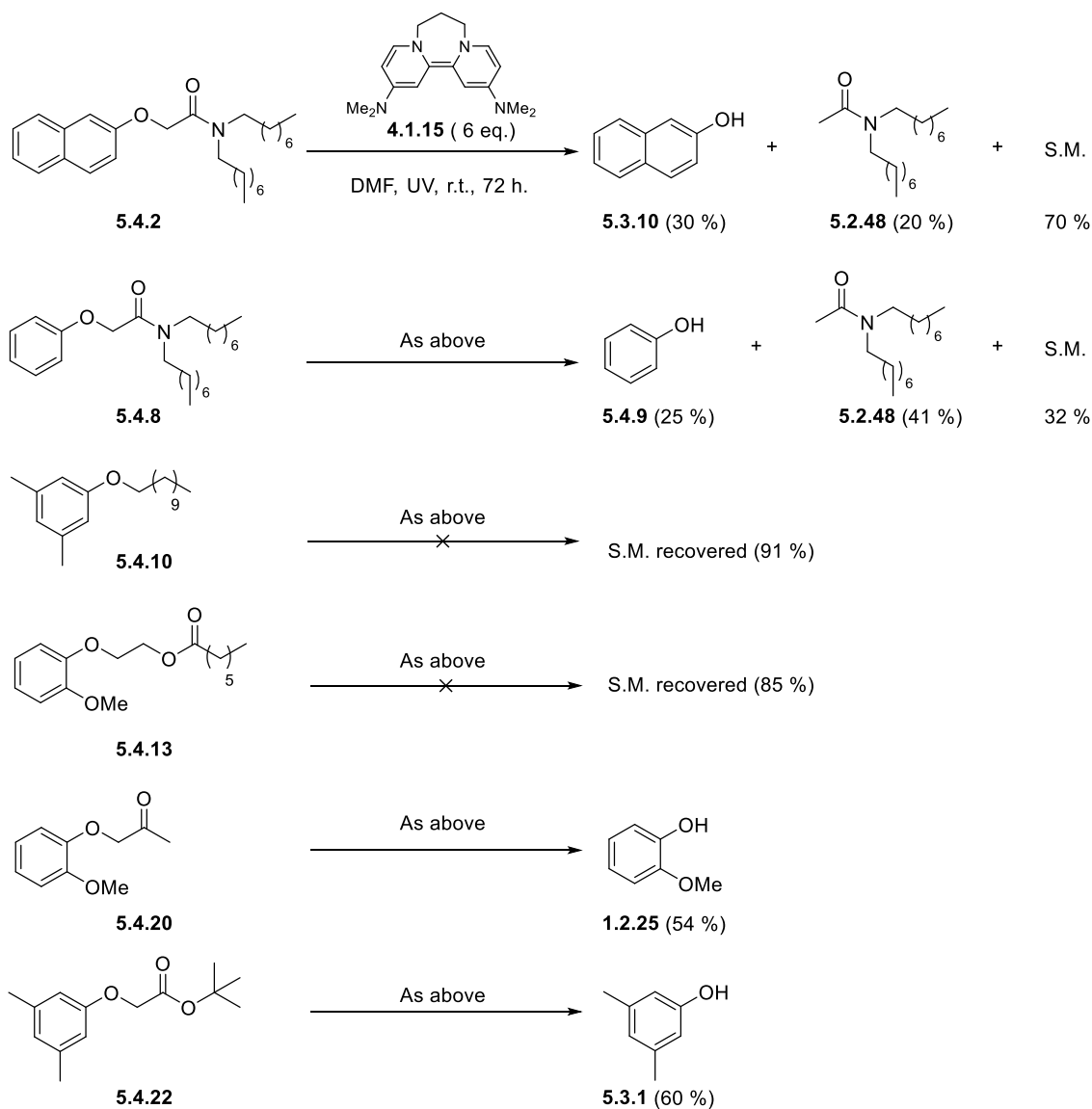


Scheme 5.4.12. An alternative mechanism involving the generation of the ketyl radical anion could lead to the observed C-O bond cleavage. Inset: LUMO of **5.4.20** was predicted to reside on the ketone. (Spartan 2010 version, DFT, B3LYP, 6-31G(d,p) in DMF was employed).

Overall, it has been shown through experiments with **5.4.2**, **5.4.8**, **5.4.20** and **5.4.22** that these carbonyl-containing functional groups were essential in activating the substrates towards reductive C-O bond cleavage.

Conclusions and Future Work

This section has disclosed yet another novel reductive cleavage afforded by the photoactivated **4.1.15**, namely the reductive bond cleavage of alkyl aryl ethers. It was discovered that the reduction required a degree of activation in the substrate as simple alkyl aryl ethers remained unreactive when tested (e.g. **5.4.10** and **5.4.13**). With amides **5.4.2** and **5.4.8**, chemoselectivity was achieved in which the amide functionality remained intact and C-O bond cleavage was the only reaction observed.



Scheme 5.4.13. Simple aryl-alkyl ethers (e.g. **5.4.10** and **5.4.13**) could not be reduced. In contrast, ethers **5.4.2**, **5.4.8**, **5.4.20** and **5.4.22** which contained activated leaving groups showed reactivity with photoactivated **4.1.15**.

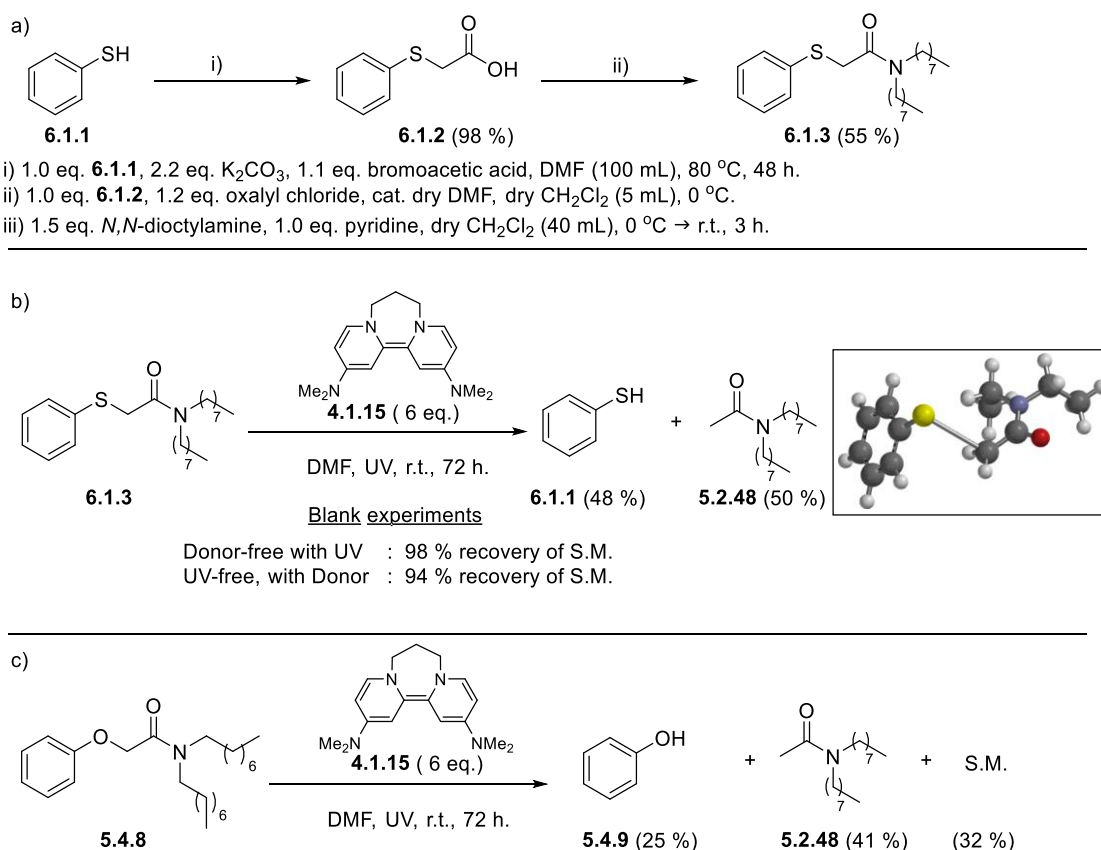
Activation of the substrates was not limited to the use of amides; it has been shown using **5.4.20** and **5.4.22** that esters and ketones can also be used. In these cases, the reaction profiles were better but the non-phenolic fragments could not be detected due to volatility issues. This novel reductive cleavage can certainly be explored in the future with the exciting possibility of applying it towards lignin degradation. The Introduction has already highlighted the extensive research efforts in this area in which aromatic ethers are employed as model substrates. Perhaps a combination of the flow-technique with UV exposure would improve the reduction profile of the model substrates employed in this project; this was certainly the case for Stephenson *et al.* in their lignin degradation studies.³⁶

Chapter 6 Results and Discussion - C-S bond cleavages

6.1 C-S bond cleavage of aromatic sulfur compounds

6.1.1 Aromatic sulfides

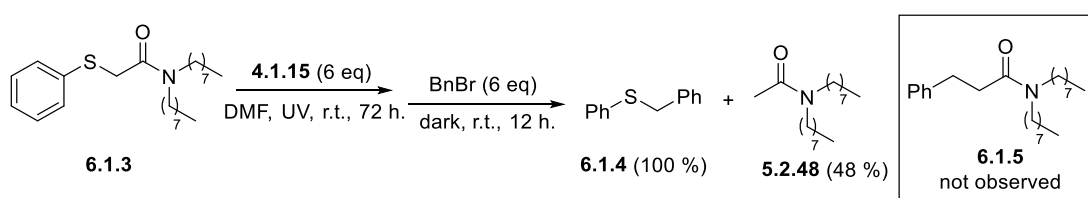
The motivation for this part of the project stemmed from the previous successes with photoreductive ArC-O bond cleavages. It has been shown in Chapter 5.4 that sufficiently activated aryl ethers would undergo cleavage with moderate to good yields. A good starting point for this project involved sulfide **6.1.3** since any reactivity could be directly compared to the reduction of ether **5.4.8** achieved previously (Scheme 6.1.1 c). The synthesis was straightforward and the required sulfide was obtained in moderate yield (Scheme 6.1.1 a).



Scheme 6.1.1. a) Synthesis of sulfide **6.1.3**. b) Sulfide **6.1.3** was reduced by photoactivated **4.1.15**. Inset: spontaneous C-S bond cleavage of the radical anion of **6.1.3** was predicted by computational calculations. (Spartan 2010 version, DFT, B3LYP, 6-31G(d,p) in DMF was employed with calculation set at -1 charge and multiplicity of 2. c) The reduction of aryl ether **5.4.8** could be directly compared to that of sulfide **6.1.3**.

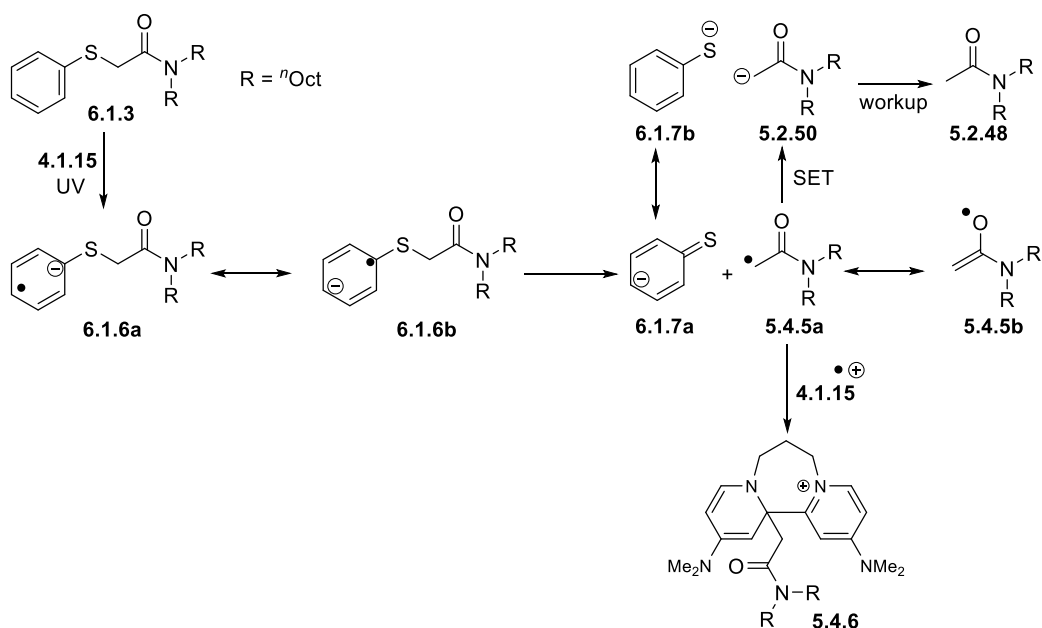
In the first instance, the attempted reduction of **6.1.3** clearly indicated that C-S bond reduction had occurred when photoactivated **4.1.15** was employed. This was confirmed when blank reactions were conducted. In the first instance, the reaction was performed without UV exposure which provided quantitative recovery of the starting material. In the separate experiment, a solution of the substrate **6.1.3** was photoexcited. This also provided good recovery of the starting material indicating that the C-S bond cleavage was solely due to the photoexcitation of the super-electron donor.

A cursory glance may have led to the conclusion that the sulfide displayed a similar reaction profile to the ether analogue **5.4.8** (based on the recovered yields of amide **5.2.48**). However, there was a striking contrast in that full conversion of sulfide **6.1.3** was observed by ^1H NMR and TLC after the reduction was attempted. It was suspected that the low yield of thiophenol was due to volatility issues. As such, the experiment was repeated and benzyl bromide was added after the stipulated time for UV exposure. This would prevent any interference that benzyl bromide might have on the reduction. In the event, it was pleasing to obtain **6.1.4** in quantitative yield (Scheme 6.1.2) which indicated that the ArC-S bond cleavage had proceeded very efficiently. The observed reactivity of sulfide reductions was further supported by computational calculations which suggested a spontaneous C-S bond cleavage of the sulfide radical anion (Scheme 6.1.1 b).



Scheme 6.1.2. The reduction of **6.1.3** with photoactivated **4.1.15** was repeated with the subsequent addition of benzyl bromide.

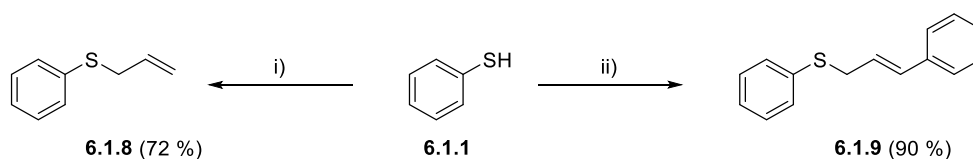
It is proposed that the mechanism (Scheme 6.1.3) for the observed C-S bond cleavage was similar to that of the previously reported aryl ethers. Bearing in mind that the amide fragment in **6.1.3** constitutes a good leaving group with stabilisation afforded by resonance, the radical **5.4.5** could compete for further reduction to its anion **5.2.50** as opposed to coupling with the radical cation **4.1.15a**. Upon workup, the protonated form **5.2.48** can be successfully purified and isolated in good yield.



Scheme 6.1.3. The isolated yield of amide **5.2.48** indicated that its radical precursor **5.4.5** was just as prone to trapping to form **5.4.6** as undergoing a second SET to generate anion **5.2.50**.

The successful trapping experiment also disclosed that the amide anion **5.2.50** does not readily react with benzyl bromide to yield the postulated product **6.1.5** (Scheme 6.1.2). Importantly, this strongly indicates that the morpholinyl anion **5.3.42** was not sufficiently nucleophilic to be trapped by benzyl bromide (See Chapter 5.3, Scheme 5.3.20).

Encouraged by this initial success, substrate modifications were made to test the scope of this novel reactivity of photoactivated **4.1.15**. These included the design and synthesis of **6.1.8** and **6.1.9**. Both products were obtained in good yields (Scheme 6.1.4).



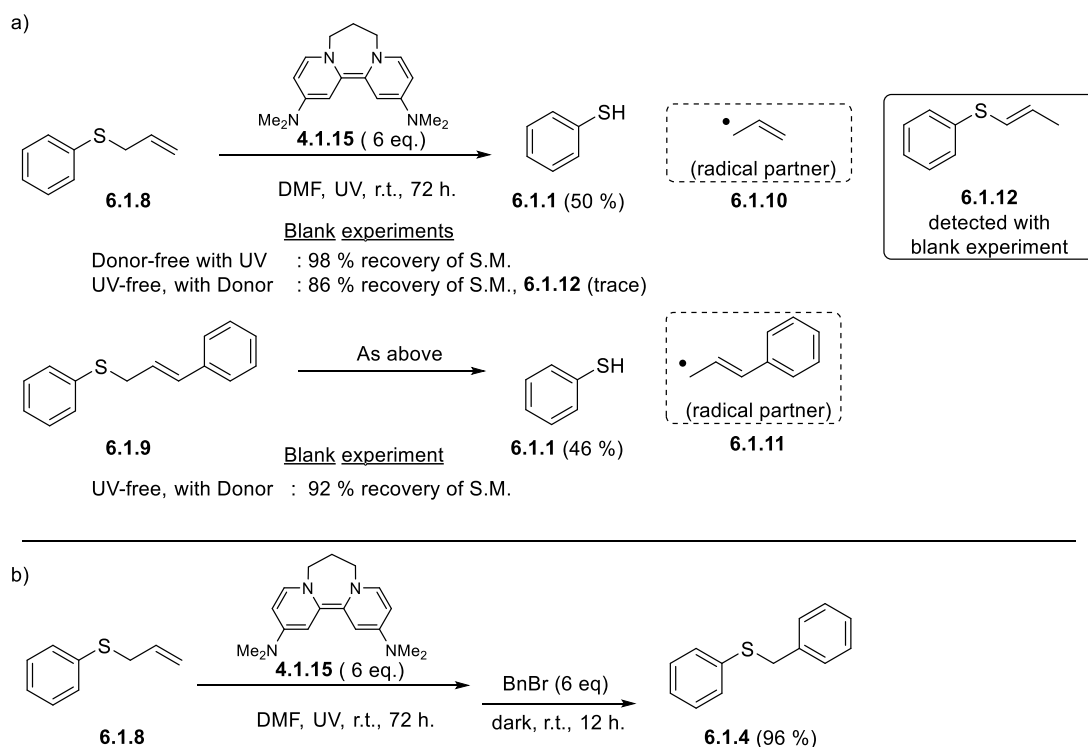
i) 1.0 eq. **6.1.1**, 1.3 eq. allyl bromide, 1.0 eq. K_2CO_3 , DMF (50 mL), 16 h.

ii) 1.0 eq. **6.1.1**, 1.1 eq. cinnamyl bromide, 1.1 eq. K_2CO_3 , DMF (40 mL), 90 °C, 16 h.

Scheme 6.1.4. Synthesis of sulfides **6.1.8** and **6.1.9** to test the reductive capability of photoactivated **4.1.15**.

When tested for reduction with photoactivated **4.1.15**, both these substrates underwent C-S bond cleavages as evident from the formation of thiophenol **6.1.1**

(Scheme 6.1.5). In both cases, the radical partners **6.1.10** and **6.1.11** could not be isolated. The volatility of the alkene derived from allylic radical **6.1.10** would have rendered it irretrievable upon workup. A trace of trans-2-methylstyrene derived from radical **6.1.11** was detected in the ^1H NMR of the crude product but the attempted purification of the material failed to isolate the cinnamyl fragment.



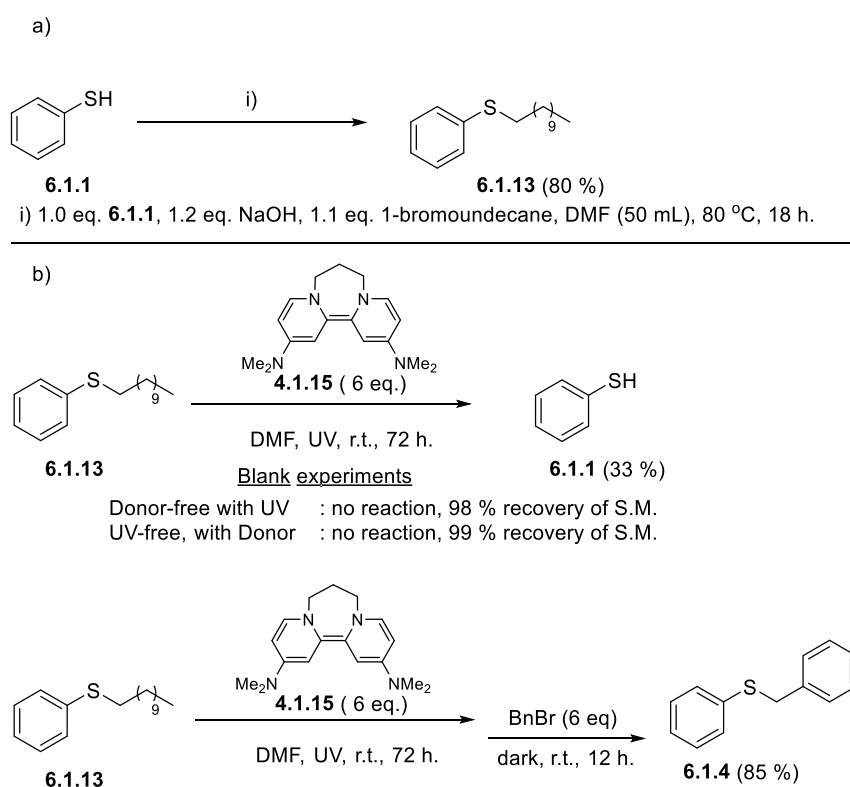
Scheme 6.1.5. The reductive C-S bond cleavages of sulfides **6.1.8** and **6.1.9** required photoactivation of **4.1.15**.

Corresponding blank experiments (Scheme 6.1.5) were also performed in parallel to confirm that the observed reactivity required photoactivation of **4.1.15**. A trace of **6.1.12** was detected from the ^1H NMR of the crude material in the case of substrate **6.1.8** with non-photoactivated **4.1.15**; presumably a result of hydrogen abstraction and subsequent isomerisation of the starting material. Nevertheless, both blank experiments with **6.1.8**, one consisting of UV exposure of just the substrate and the other consisting of non-photoactivated **4.1.15** with the substrate, confirmed that the observed C-S bond cleavage required the photo-excitation of the super-electron donor.

Similar to the amide **6.1.3**, the reaction profiles for both **6.1.8** and **6.1.9** showed good conversion of the starting material based on ^1H NMR analyses of the crude products.

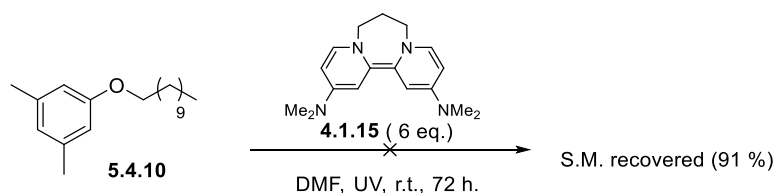
Intuitively, **6.1.9** would have similar or better reactivity than **6.1.8** based on the stability of the resulting radical (Scheme 6.1.5). As such, repeating the reduction experiment on **6.1.8** with the subsequent addition of benzyl bromide was attempted first (Scheme 6.1.5 b). Since this resulted in the high yield of **6.1.4** (96 %), it was decided that a similar trapping experiment using **6.1.8** was unnecessary; it has already been convincingly shown that aryl thioethers have profound reactivity with photoactivated **4.1.15**.

Based on the astounding reactivity observed so far with aromatic sulfides, it was further postulated that aryl thioethers with no activated leaving group might also experience ArS-C bond cleavage. Therefore, sulfide **6.1.13** was synthesised and tested for reduction with **4.1.15** (Scheme 6.1.6).



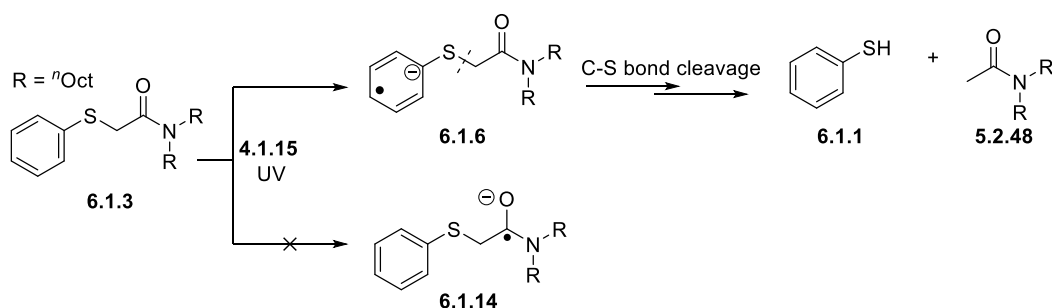
Scheme 6.1.6. a) Synthesis of sulfide **6.1.13**. b) Sulfide **6.1.13** which does not possess an activated leaving group was discovered to undergo C-S bond cleavage with photoactivated **4.1.15** in good yield.

The experimental results were impressive, revealing that even the formation of non-stabilised primary alkyl radical was not a barrier for reductive cleavage; this stands in stark contrast with aryl ether **5.4.10** which previously showed no reactivity with photoactivated **4.1.15** (Scheme 6.1.7).



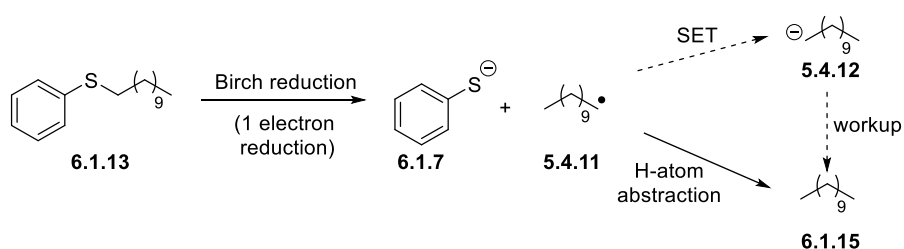
Scheme 6.1.7. The result from sulfide **6.1.13** was in contrast with the aryl ether analogue **5.4.10** which showed no reactivity with photoactivated **4.1.15**.

Additionally, the successful reduction of **6.1.13** confirmed that the observed C-S bond cleavage was due to SET from the super-electron donor onto the aromatic ring. This should also apply to the previous sulfide substrates, particularly amide-containing **6.1.3** in which the bond cleavage is thought to proceed from **6.1.6** and not **6.1.14** (Scheme 6.1.8).



Scheme 6.1.8. The C-S bond cleavage of **6.1.3** is thought to proceed from the radical anion **6.1.6** and not **6.1.14**.

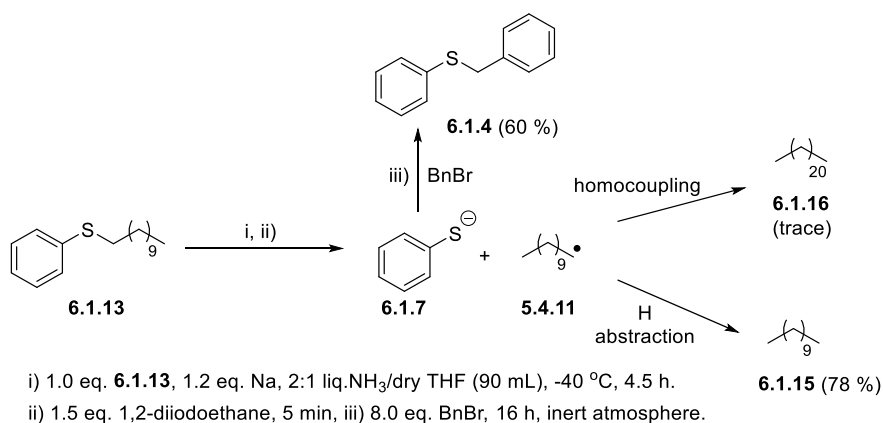
To further confirm that the observed C-S bond cleavage proceeded at the radical anion stage and led to the formation of the thiophenolate anion and the alkyl radical, it was decided to attempt the reduction of **6.1.13** under Birch conditions (Scheme 6.1.9).



Scheme 6.1.9. The results from the Birch reduction of **6.1.13** would disclose key details on the reduction mechanism particularly the presence of thiophenolate anion **6.1.7** and alkyl radical **5.4.11** after the bond cleavage.

By employing sodium (one electron donor), the radical anion generated from the substrate should proceed with bond cleavage as seen previously with SED **4.1.15**.

Unlike the reduction with photoactivated **4.1.15**, the alkyl radical **5.4.11** in this instance, would have no trapping partner and so should proceed with hydrogen abstraction (Scheme 6.1.10). The alternative pathway which predicts further reduction of the radical **5.4.11** to its anion **5.4.12** cannot be discounted at this stage. Although (to the best of our knowledge) this transformation has not been reported under Birch conditions, electrochemical studies by Grimshaw suggest that such a transformation should proceed at mild reduction potentials (e.g. $\text{CH}_3(\text{CH}_2)_{10}\text{CH}_2^\bullet$; $E_{1/2}(\text{DMF}) = -2.12 \text{ V vs. SCE}$)¹⁹³. In either case, the isolation of **6.1.15** must necessarily result from its radical precursor **5.4.11**.



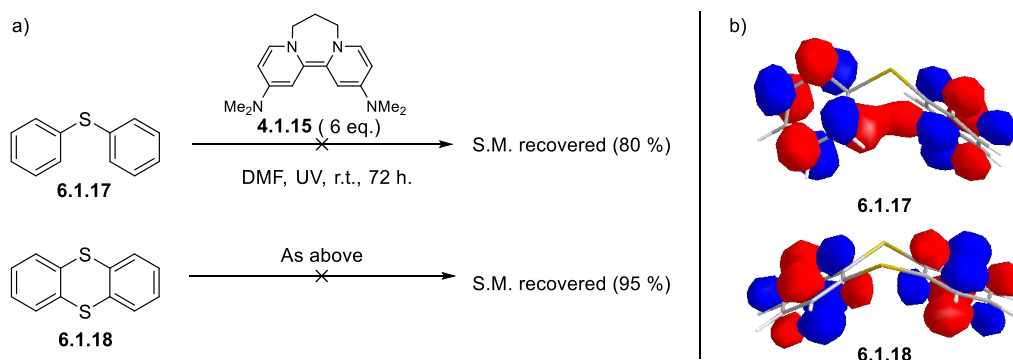
Scheme 6.1.10. The Birch reduction on **6.1.13** yielded the alkyl fragment **6.1.15**, sulfide **6.1.4** (upon trapping with benzyl bromide), and a trace of **6.1.16**.

In the event, the attempted Birch reduction on **6.1.13** yielded products **6.1.4**; **6.1.15** and **6.1.16** in trace amount which was detected by GCMS (Scheme 6.1.10). The trace of **6.1.16** necessarily resulted from the homocoupling of **5.4.11**, again, proving the existence of the alkyl radical upon C-S bond cleavage. Objectively, the results of the Birch reduction on **6.1.13** has provided evidence for the electron transfer-based reduction mechanism proposed earlier for the bond cleavages of the sulfides tested.

In the case of the reduction of **6.1.13** with photoactivated **4.1.15**, one electron is transferred onto the sulfide substrate leading to C-S bond cleavage (confirmed experimentally by the successful Birch reduction). The bond cleavage leads to thiophenolate **6.1.7** (not the thiophenyl radical) and radical **5.4.11** (not the alkyl anion). It was not possible to detect **5.4.11** when the reduction was conducted using photoactivated **4.1.15** due to its trapping with radical cation **4.1.15a**. Nevertheless, its

existence was proven by the isolation of **6.1.15** and the detection of **6.1.16** (trace amounts) when the reduction was attempted under Birch conditions.

Phenyl radicals are less stable than primary alkyl radicals; to determine if C-S bond cleavage afforded by photoactivated **4.1.15** was possible with these challenging systems, commercially available products **6.1.17** and **6.1.18** were tested (Scheme 6.1.11 a).

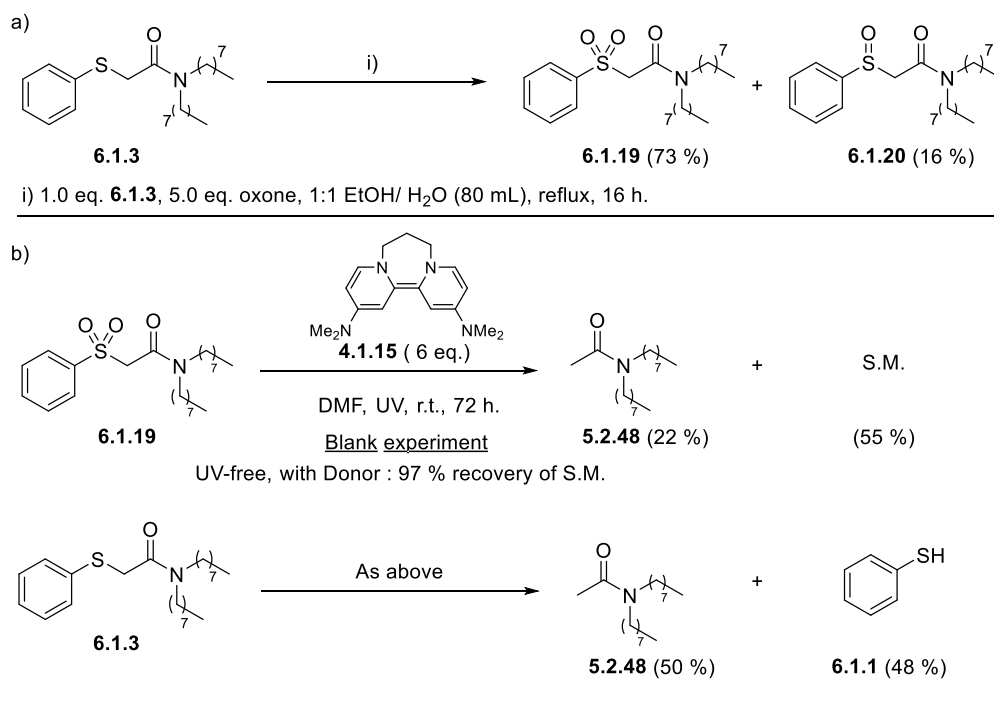


Scheme 6.1.11. a) Reductions of sulfides **6.1.17 and **6.1.18** using photoactivated **4.1.15** were attempted. b) Predicted SOMO of the radical anions of both substrates. (Spartan 2010 version, DFT, B3LYP, 6-31G(d,p) in DMF was employed with calculation set at -1 charge and multiplicity of 2.**

However, no reactivity was observed in both cases. This could be due to the extensive delocalisation of the SOMO of the radical anions (Scheme 6.1.11 b), which resulted in the formation of highly stabilised radical anions that have little inclination towards C-S bond cleavage. It was also possible that both these substrates were efficiently competing for photoexcitation with the super-electron donor, resulting in none of the desired reactivity.

6.1.2 C-S bond cleavage of aromatic sulfoxides and sulfones

Aromatic sulfoxides and sulfones provide further extensions for the newly discovered reductive chemistry afforded by **4.1.15** with aromatic sulfides. By treating **6.1.3** with oxone, the corresponding sulfone **6.1.19** and sulfoxide **6.1.20** were obtained (Scheme 6.1.12 a).

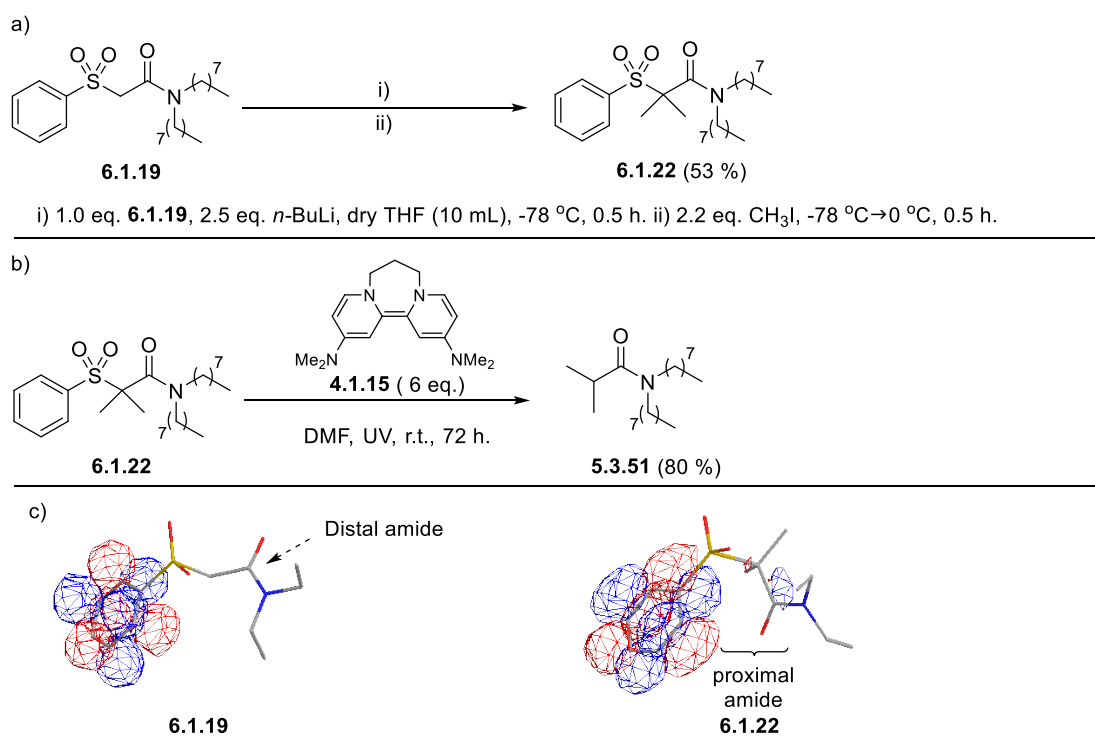


Scheme 6.1.12. a) Sulfone **6.1.19** and sulfoxide **6.1.20** were obtained from the oxidation of sulfide **6.1.3**. b) Sulfone **6.1.19** underwent reductive cleavage with photoactivated **4.1.15** to a smaller extent than its parent sulfide **6.1.3**. c) Deprotonation of **6.1.19** could have effectively prevented further reduction by photoactivated **4.1.15**.

When tested for reduction using photoactivated **4.1.15**, sulfone **6.1.19** showed diminished reactivity compared to its parent sulfide **6.1.3**. (Scheme 6.1.12 b). This was showcased by the recovery of starting material (55 %) in the present case whereas the aryl thioether analogue **6.1.3** showed full conversion. The blank experiment, in which the reaction of **6.1.19** was repeated without UV exposure, confirmed that the observed reduction required photoactivated **4.1.15**. This did not

necessarily indicate that sulfones were more challenging substrates for reduction. It was possible that the radical anion formed upon reduction of **6.1.19** was too stabilised to undergo spontaneous C-S bond cleavage, in which case the radical anion would re-oxidise upon workup to yield unreacted starting material.

Alternatively, the sulfone **6.1.19** could have been deprotonated by the super-electron donor at the onset thereby impeding further reduction (Scheme 6.1.12 c). To verify if deprotonation of the sulfone was competing with reductive bond cleavage, substrate **6.1.22** was synthesised by methylating **6.1.19** under basic conditions (Scheme 6.1.13 a) When subjected to reduction conditions with photoactivated **4.1.15**, the amide fragment **5.3.51** was isolated in good yield (Scheme 6.1.13 b). This result indicated that deprotonation of **6.1.19** was likely competing with its reductive cleavage.

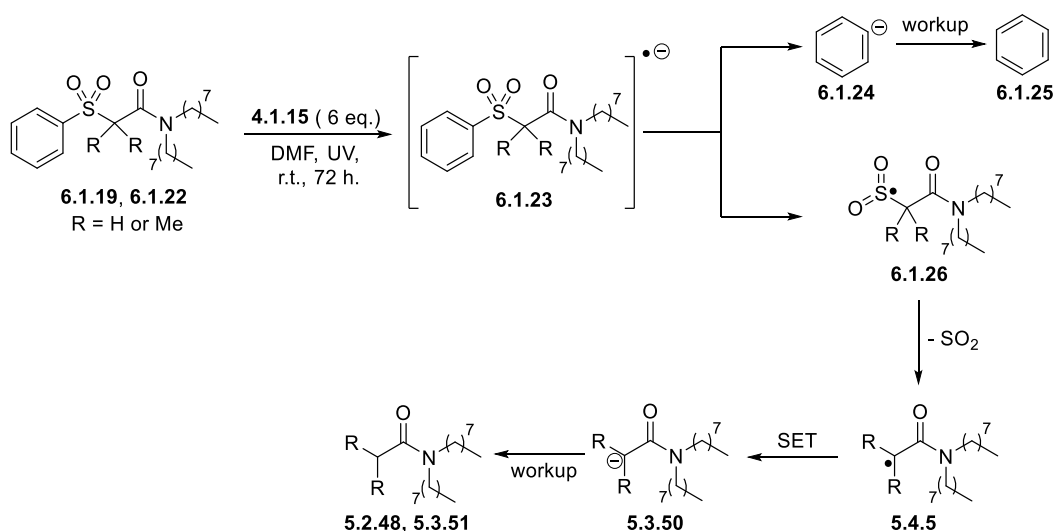


Scheme 6.1.13 a) The *gem*-dimethyl groups on **6.1.22** would prevent possible deprotonation under the reduction conditions employed with **4.1.15**. b) Sulfone **6.1.22** underwent reductive cleavage smoothly to yield the amide fragment **6.1.23** c) Computational investigations indicated that the LUMO of **6.1.22** extended onto the amide fragment in contrast to that of **6.1.19**. (Spartan 2010 version, DFT, B3LYP, 6-31G(d,p) in DMF was employed. Calculations were done from optimised geometries of energy-minimised ground states of the sulfones.

Furthermore, the marked increase in reductive bond cleavage of **6.1.22** could be related to its preferred conformation. Computational investigations revealed that the installation of the methyl groups had altered the stable conformation of the molecule

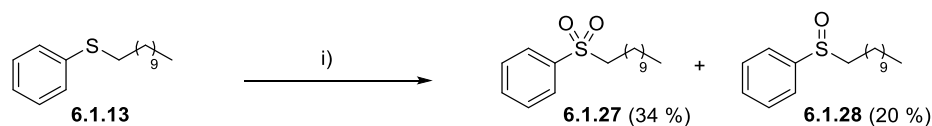
such that the amide fragment is now brought into close proximity to the benzene ring. This close proximity could also be responsible for further delocalisation of the LUMO onto the amide fragment, in turn making it easier for reductive C-S bond cleavage (Scheme 6.1.13 c).

Using sulfone **6.1.19** as an example, it is possible that the observed reduction proceeded *via* the cleavage of the radical anion **6.1.23** (Scheme 6.1.14) to yield the aryl anion **6.1.24** and the sulfonyl radical **6.1.26**. The radical fragment then proceeds with desulfonylation resulting in the generation of the stabilised amidyl radical **5.4.5** which, as seen with previous cases, undergoes further SET leading to anion **5.3.50**. Upon quenching and workup, the amide can be successfully isolated while benzene remains undetected due to its high volatility.



Scheme 6.1.14. Proposed reduction mechanism for sulfones **6.1.19** and **6.1.22** with photoactivated **4.1.15**.

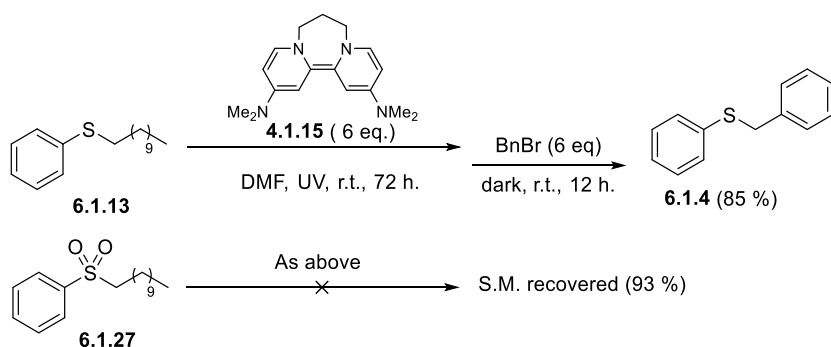
Encouraged by the successful C-S bond reductions of sulfones **6.1.19** and **6.1.22**, it was decided to attempt the reduction with sulfone **6.1.27** which was obtained from the oxidation of the parent sulfide **6.1.13** (Scheme 6.1.15).



i) 1.0 eq. **6.1.13**, 5.0 eq. oxone, 1:1 EtOH/ H₂O (80 mL), reflux, 16 h.

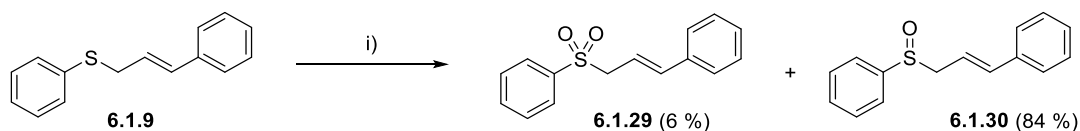
Scheme 6.1.15. Sulfone **6.1.27** and sulfoxide **6.1.28** were obtained by the oxidation of the parent sulfide **6.1.13**.

Previously, it was discovered that phenyl(undecyl)sulfane **6.1.13** could be reduced efficiently with photoexcited **4.1.15** despite the lack of an activated leaving group (Scheme 6.1.16) and so testing sulfone **6.1.27** for reduction would allow for direct comparison. In the event, no reactivity was observed which could be the result of the increased stability of the radical anion by the inductive effect of the sulfone moiety. It could also be possible that deprotonation of **6.1.27** by the super-electron donor had effectively prevented its reduction.



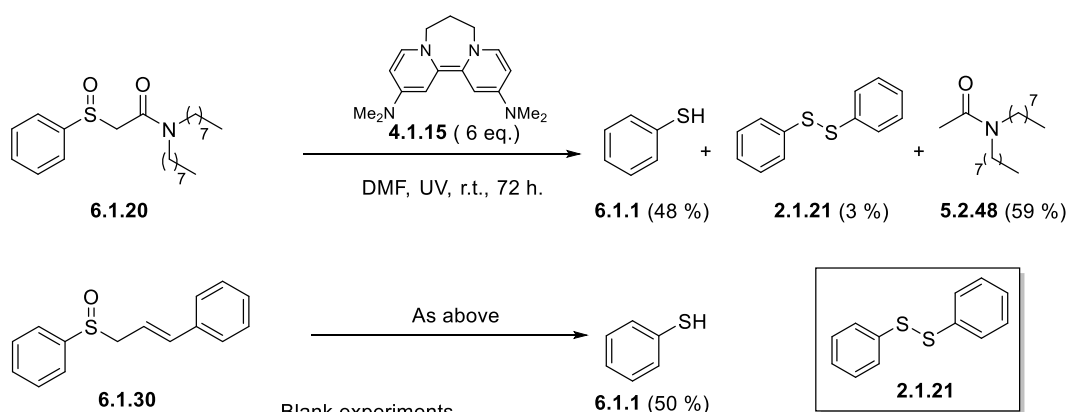
Scheme 6.1.16. Sulfone **6.1.27** could not be reduced by photoactivated **4.1.15**; this was in contrast with sulfide **6.1.13** which was efficiently reduced under similar reaction conditions.

The reduction of sulfoxides was also investigated using substrates **6.1.20** and **6.1.30**. The amide-containing sulfoxide **6.1.20** was previously synthesised (Scheme 6.1.12) and **6.1.30** was obtained from the oxidation of sulfide **6.1.9** (Scheme 6.1.17).



i) 1.0 eq. **6.1.9**, 5.0 eq. oxone, 1:1 CH₃CN/H₂O (50 mL), r.t., 18 h.

Scheme 6.1.17. The synthesis of the required sulfoxide **6.1.30** via oxidation of the parent sulfide **6.1.9**.



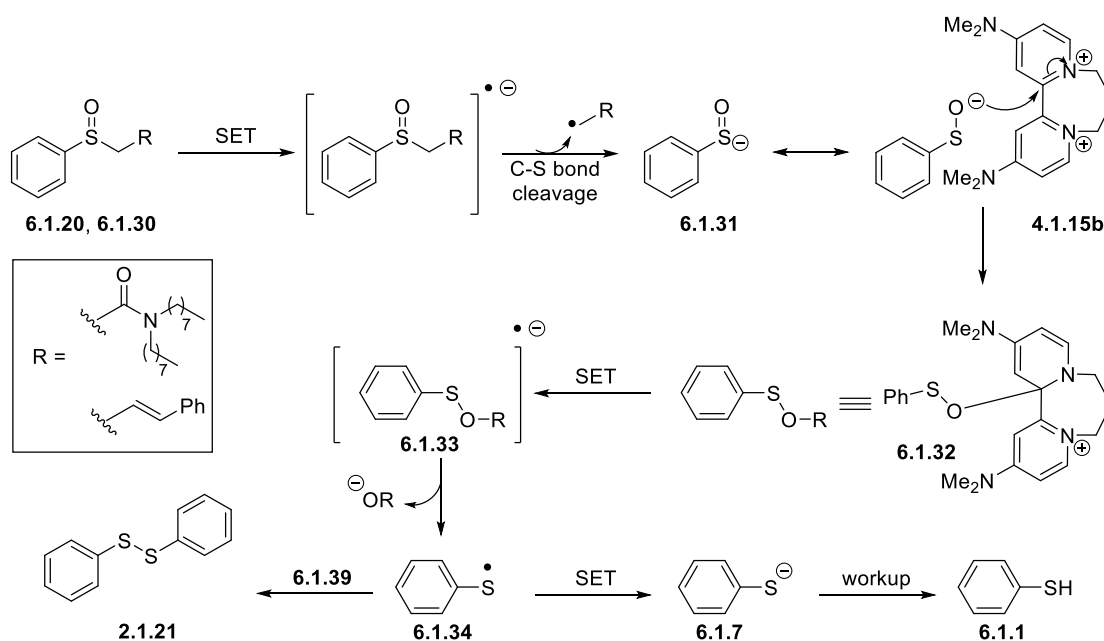
Donor free, with UV: no products were detected. Workup and solvent removal resulted in a highly insoluble gum

UV-free, with Donor: 1st attempt: **6.1.1** (51 %)

: 2nd attempt: **6.1.1** (40 %), **2.1.21** (trace)

Scheme 6.1.18. The reductive cleavage of **6.1.20** and **6.1.30** were observed when tested with photoactivated **4.1.15**.

When these substrates were tested against photoactivated **4.1.15**, it was pleasing to observe reductive C-S bond cleavage in both instances (Scheme 6.1.18). It is noteworthy that the blank experiments (substrate and **4.1.15** were reacted together without UV exposure) attempted with **6.1.30** also revealed C-S bond cleavage, indicating that the reduction of this substrate did not require photoactivation of **4.1.15**.



Scheme 6.1.19. The proposed mechanism for the formation of thiophenol **6.1.1**.

Interestingly, thiophenol **6.1.1**, and not sulfenic acid, was isolated after the reduction. It is thought that this could have resulted from the nucleophilic attack by the sulfenic anion **6.1.31** onto an electrophile e.g. the dication **4.1.15b**. The resulting species **6.1.32** could be further reduced at the thiophenol portion (ArS reduction is highly feasible as shown in this project) which then fragments to ultimately yield thiophenol. (Scheme 6.1.19). Presently, trapping experiments have not been attempted to determine the extent of the C-S bond cleavage of the sulfoxides. Nevertheless, the preliminary results, particularly from **6.1.20**, compare well with the reduction of its parent sulfide **6.1.3** which indicates that these substrates show a similar extent of reactivity.

Also of interest was the detection of 1,2-diphenyldisulfane **2.1.21** after the reduction of both sulfoxides. This product could have resulted from the dimerisation

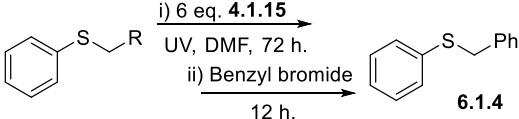
thiophenylic radicals generated from the C-S bond cleavage (Scheme 6.1.19). However, it is also known that thiophenol is liable to dimerisation when exposed to oxygen and this process could have occurred upon workup.¹⁹⁴ As such, the disulfane **2.1.21** was not necessarily related to the reaction profile of the sulfoxides tested. In this regard, firmer conclusions should only be drawn upon further repeats of the experiments.

Conclusions and Future work

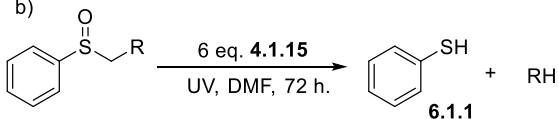
The chemistry of super-electron donor **4.1.15** has been successfully applied in a novel way in the reduction of aromatic sulfides, sulfoxides and sulfones (Table 6.1.20).

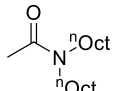
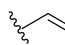
Table 6.1.20. Summary of the results obtained from successful C-S bond cleavages of sulfides, sulfoxides and sulfones.

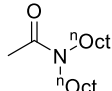
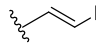
a)



b)

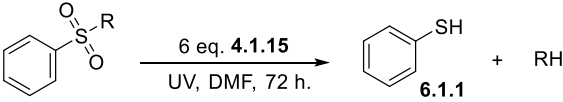


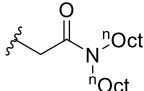
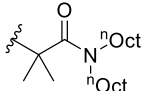
Compound	R	% 6.1.4
6.1.3		100
6.1.8		96
6.1.13	<i>n</i> undecyl	85

Compound	R	% 6.1.1	RH
6.1.20		48	50
*6.1.30		~ 50	0

* UV activation of **4.1.15** not required.

c)



Compound	R	% 6.1.1	% RH
6.1.19		0	23
6.1.22		0	80

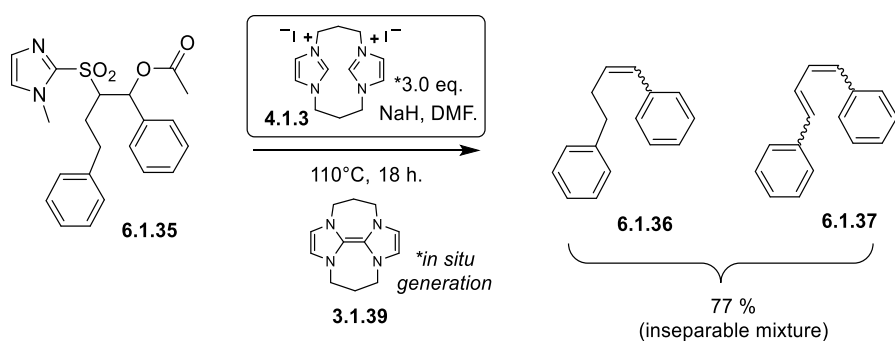
¹ S.M. recovered (55 %)

On the whole, alkyl aryl sulfides were found to outperform their ether analogues. The sulfur atom possesses more diffuse p-orbitals than oxygen and this may allow for an easier SET onto the aryl-sulfur region. This may account for the increased reactivity observed with the aromatic sulfides.

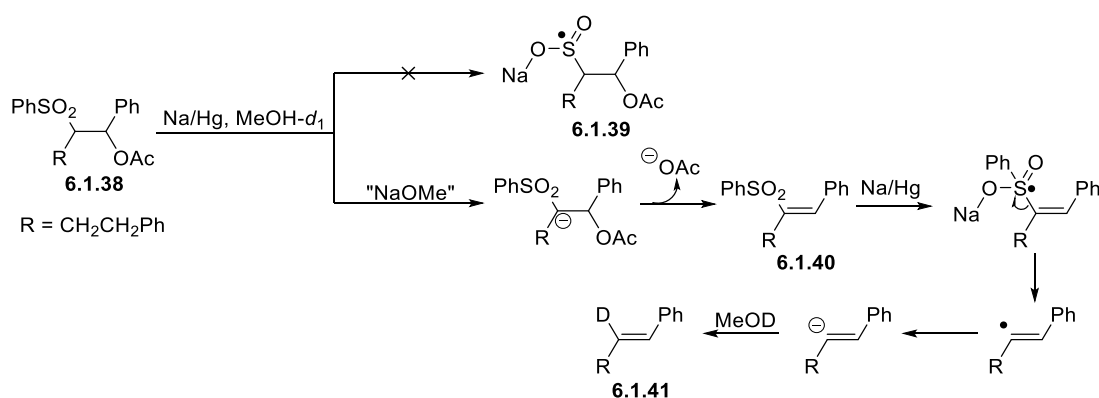
One very useful application of this chemistry would be a metal-free approach towards Julia-Lythgoe olefination.¹⁹⁵⁻¹⁹⁷ This reaction utilises alkali metals (usually sodium) to reduce an aromatic sulfone. A subsequent elimination of a leaving group

in the substrate leads to the installation of the alkene (see Scheme 6.1.21 for an example).

Recently, Schoenebeck (previous group member) had initiated work on metal-free Julia olefination using donor **3.1.39** under thermal conditions. The reduction was successfully applied to imidazole-based sulfone **6.1.35** (Scheme 6.1.21), yielding an inseparable mixture of alkenes **6.1.36** and **6.1.37**. When the imidazole auxiliary was replaced with an arene, no reactivity was observed indicating that the thermally activated super-electron donor **3.1.39** was not sufficiently powerful in transferring electron(s) to the substrate. However, it has now been shown in this project that phenyl-based sulfone reduction (e.g. **6.1.19** and **6.1.22**) using photoexcited **4.1.15** was possible and so it would be interesting to revisit this chemistry.



Scheme 6.1.21. Metal-free Julia olefination was previously conducted using SED **3.1.39** with thermal activation.

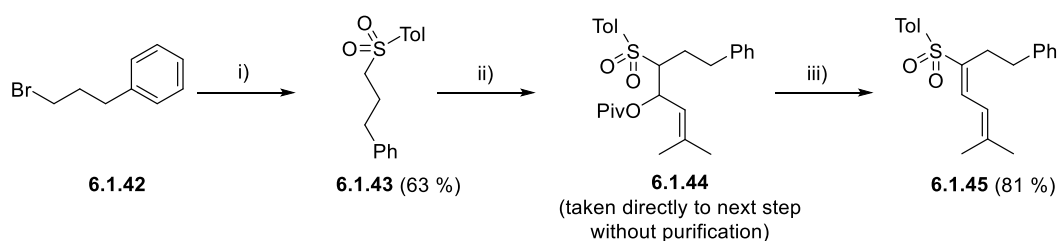


Scheme 6.1.22. The Julia-Lythgoe olefination conducted by Keck *et al.* was found to proceed via **6.1.40** suggesting that the reduction step did not begin from **6.1.38**.¹⁹⁸

In a separate account,¹⁹⁸ Keck *et al.* were studying the mechanism of the Julia-Lythgoe olefination using acetoxy sulfone **6.1.38** (Scheme 6.1.22). When the reduction of this substrate was monitored, it was discovered that phenyl sulfone

6.1.40 was formed as an intermediate (this was confirmed by quenching the reaction prematurely and **6.1.40** was isolated in 55 % yield).

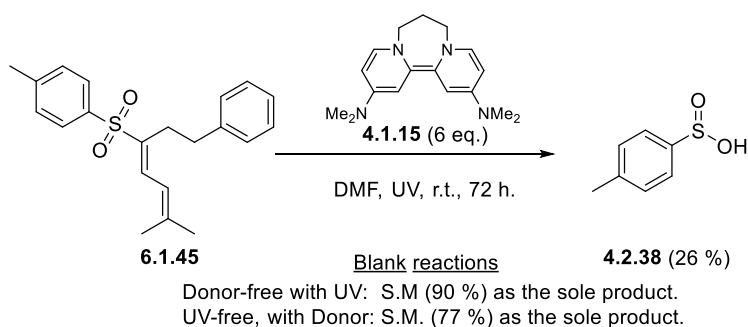
Furthermore, deuterium incorporation leading to alkene **6.1.41** was extensive when the reduction was carried out in the presence of MeOD. This suggested that the initial reaction during the reduction was not the immediate reduction of the sulfone moiety but the deprotonation-elimination process by NaOMe which was generated *in situ* (Scheme 6.1.22). This mechanism would suggest that the aromatic sulfone **6.1.40**, and not the acetoxy **6.1.38**, was the required precursor for successful alkene formation. This being the case, it was decided that sulfone **6.1.45** would be a suitable candidate to test the reduction mechanism proposed by Keck *et al.* The synthesis of **6.1.45** required three steps (Scheme 6.1.23) following closely the procedure described by Keck and co-workers.¹⁹⁸



- i) 1.0 eq. **6.1.42**, 1.0 eq. sodium-*p*-toluenesulfinate, 2:1 DMF/H₂O (40 mL), 80 °C, 16 h.
 ii) 1.0 eq. **6.1.43**, 1.2 eq. *n*-BuLi, dry THF (10 mL), -78 °C → r.t.,
 1.1 eq. 3-methyl-2-butenal, 1.1 eq. pivaloyl chloride, 16 h.
 iii) 1.0 eq. **6.1.44**, 10 eq. DBU, dry THF (10 mL), r.t., 16 h.

Scheme 6.1.23. Synthesis of sulfone 6.1.45.

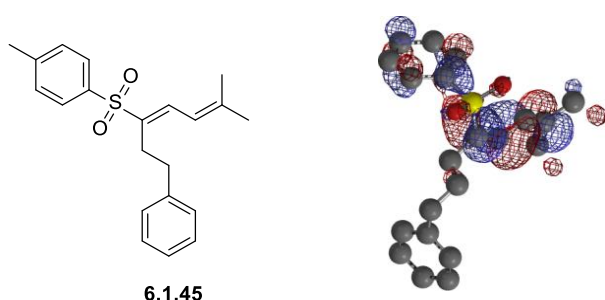
When sulfone **6.1.45** was tested for reduction with **4.1.15**, toluenesulfinic acid **4.2.38** was successfully isolated in 26 % yield (Scheme 6.1.24).



Scheme 6.1.24. The reduction of 6.1.45 was attempted with photoactivated 4.1.15. Blank experiments were also performed to determine if photoactivation of 4.1.15 was required for reactivity.

Blank reactions conducted in parallel strongly indicated that photoactivation of SED **4.1.15** was responsible for the formation of **4.2.38**. Further investigations will be required to understand why the mass recovery was so poor.

Computational investigations had revealed that the SOMO of the radical anion from **6.1.45** was extensively delocalised over the sulfone and diene fragments (Scheme 6.1.25). This may have led to unforeseen side reactions of the radical anion of **6.1.45**. Perhaps for future work, a better starting point for such work would be to establish the reductive capability of photoactivated **4.1.15** with the imidazole-based sulfone **6.1.35**. The result from such an experiment would also allow better comparisons with super-electron donor **3.1.39** before expanding further into more challenging sulfones.

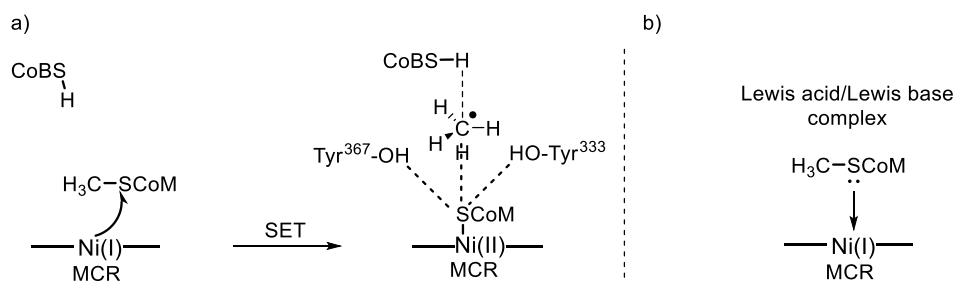


Scheme 6.1.25. The SOMO of the radical anion of **6.1.45** was found to be highly delocalised which may have suppressed C-S bond cleavage (Spartan 2010 version, DFT, B3LYP, 6-31G(d,p) in DMF was employed).

6.2 C-S Bond cleavage of non aromatic sulfides

In the introduction (Chapter 2.3), the biological importance of dialkyl sulfide reduction was highlighted in which demethylation of MeCoM by MCR played an important role in methanogenesis. One of the plausible mechanisms involved single electron transfer from the Ni(I) centre present in MCR, to MeCoM, resulting in its homolysis and the generation of a methyl radical (Scheme 6.2.1 a).

The strong affinity for sulfur could promote Lewis acid/Lewis base coordination between the sulfur of MeCoM and the nickel of F₄₃₀ (Scheme 6.2.1 b). It is possible that the resulting complex facilitates electron transfer onto the σ^* orbital of the methyl-sulfur bond leading to its cleavage.

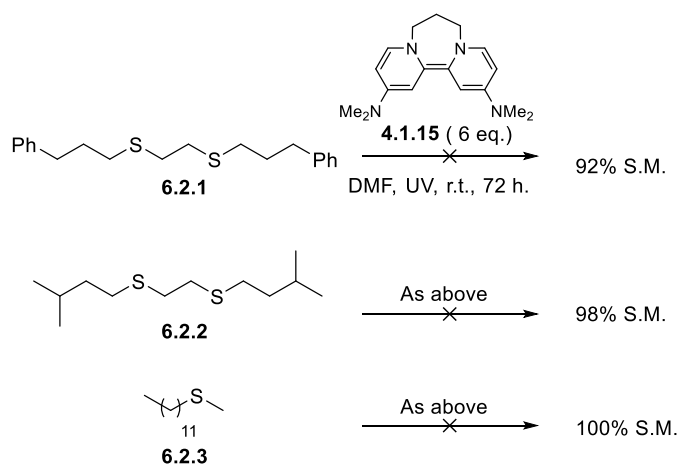


Scheme 6.2.1. a) The radical-mediated mechanism is thought to begin with the single electron transfer from Ni(I) to MeCoM. b) Initial formation of a Lewis acid/Lewis base complex could facilitate the subsequent SET process.

The idea that complexation between the electron donor and the substrate would facilitate the electron transfer process was observed in the reduction of aromatic sulfides by photoactivated **4.1.15** (Section 6.1.1). Essentially, π - π stacking between the aryl moiety of the substrate and the highly conjugated SED brings the substrate and reductant in close proximity. Thus, SET onto the arene is facilitated and the unpaired electron could then be transferred to the σ^* orbital of the ArS-C bond leading to bond cleavage of the radical anion.

The successful reductions of aromatic sulfides using photoactivated **4.1.15** inspired further probing into more challenging substrates, namely alkyl sulfides. At this stage, a preliminary study by a previous group member, Steven O'Sullivan, on alkyl sulfides **6.2.1-6.2.3** had shown that **4.1.15** was too weak to reduce such compounds, owing to the higher (therefore inaccessible to the super-electron donor) LUMO levels

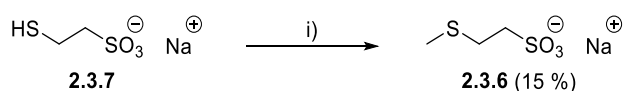
of alkyl sulfides and possibly due to the lack of initial complexation between the donor and the substrates (Scheme 6.2.2).



Scheme 6.2.2. Alkyl sulfides could not be reduced by photoactivated **4.1.15** as shown previously by Steven O'Sullivan.

This being the case, attention was now focused on testing for C-S reductive bond cleavage of dialkyl sulfides using sodium as a stronger one-electron donor. In particular, MeCoM would be the ideal candidate as it was thought that the experimental results would contribute extensively to our understanding of MCR activity.

The synthesis of methyl coenzyme M **2.3.6** was straightforward following the procedure described by Thauer *et al.*⁷⁷ with the pure product obtained after repeated recrystallisations (Scheme 6.2.3).



i) 1.0 eq. **2.3.7**, 1.0 eq. NaOEt, 1.1 eq. MeI, MeOH (25 mL), reflux, 16 h.

Scheme 6.2.3. A modest yield of **2.3.6** was obtained upon repeated recrystallisations to achieve high purity of the product.

If the Birch reduction on **2.3.6** was successful, the product(s) would be water-soluble and the conventional workup followed by column chromatography could not be applied in order to isolate these compounds. In the first attempt, a workup was conducted and the freeze-dry technique was employed to remove water and other volatile substances. However, this technique proved to be very time-consuming and another strategy was devised (See Experimental, 1st attempt at Birch reduction on **2.3.6**).

The second strategy involved analyzing the crude material by ^1H NMR data immediately after the duration of reaction. In this case, the mass of the crude material was recorded and it was then dissolved in 2 mL D_2O (measured using a 5 ml syringe). 18-Crown-6 ether was selected as an internal standard and a set amount (3 mg) was dissolved in the solution. The yield of the reduced product(s) could then be determined by its ratio with reference from the internal standard. This was also attempted but it was quickly realized that the crown ether was not a reliable standard; the ^1H NMR signal for this compound consisted of a very broad peak (at 3.61 ppm) overlapped by a small shoulder, which could be due to complexation of the crown ether with the metal ion. Several attempts were made to try and reduce the broadness of the peak by varying the concentration of the ether but without success. A better standard is still being sought.

Finally, it was decided in this early stage of the project, to determine the product distribution of the crude material based on the integration values of the protons in the ^1H NMR spectrum. Since coenzyme M **2.3.7** and ethane sulfonate **6.2.4** were commercially available compounds, their ^1H NMR spectra could be recorded and conveniently used to determine if these two compounds had formed during the Birch reduction of MeCoM. Although it was expected that MeSH and CH_4 (possible products of C-S bond cleavages of MeCoM) would not be detected due to volatility issues, integration of the assigned peaks in the ^1H NMR spectrum of the crude material would provide an estimate on the product distribution of **2.3.7** and **6.2.4**. This could be used to determine the extent of the two possible C-S bond cleavages.

Table 6.2.4. Quantitative C-S bond cleavage was observed in all attempts at Birch reduction with 2.3.6.

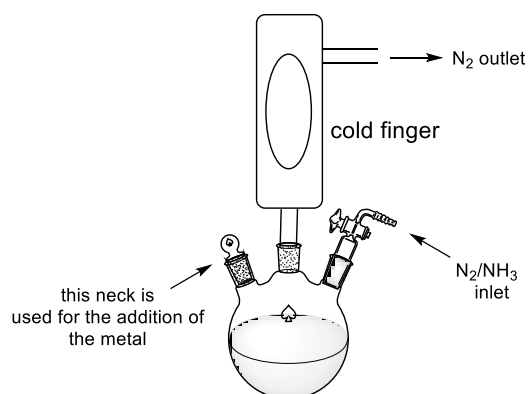
$\text{Me-S-CH}_2\text{-CH}_2\text{-SO}_3^- \text{Na}^+$ 2.3.6	$\xrightarrow[\text{liq. NH}_3, 8\text{h}]{6 \text{ eq. Na}}$	$\text{HS-CH}_2\text{-CH}_2\text{-SO}_3^-$ 2.3.7	$+$	$\text{CH}_3\text{-SO}_3^-$ 6.2.4	$+$	MeS^- 6.2.5	$+$	S.M. 2.3.6
	1st Attempt	0.9		0.1		not detected		0
	2nd Attempt	0.6		0.4		not detected		0
	3rd Attempt	0		> 0.9		not detected		0

Product ratios in the table were calculated from the ^1H NMR spectra of the crude products.

In the first attempt, **2.3.6** was observed to have cleaved quantitatively and with selectivity to yield mainly coenzyme M **2.3.7** under Birch conditions using sodium. However, repeats revealed that the selectivity was surprisingly irreproducible (Table 6.2.4).

Admittedly, although every care had been taken to replicate the reaction conditions, slight variations would be inevitable (A standard equipment setup is shown in Figure 6.2.5). Variations in reaction conditions included i) the actual volume of liq. NH_3 dispensed during the reaction and ii) the surface area of the metal being introduced into the reaction. The required amount of metal was measured out in the glovebox and then transferred out using a capped vial. The sample was then further cut up just before quick successive additions to the reaction mixture. Due to the small scale of the reaction it was difficult to cut out a constant surface area of each slice. These slight variations could have profound impact on the experimental results which are discussed later in the section.

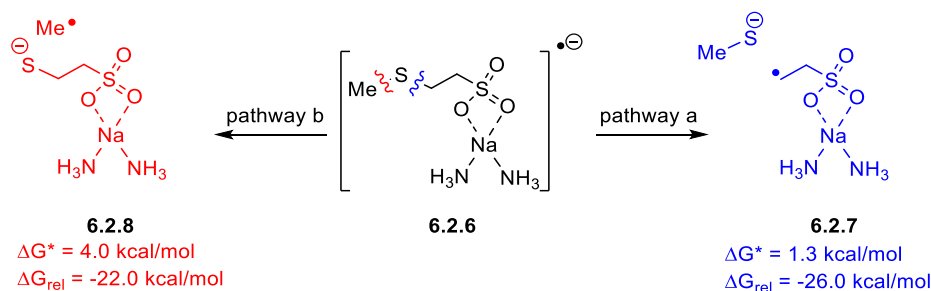
Figure 6.2.5. A typical experimental setup for the Birch reduction.



Although the experimental results for **2.3.6** were irreproducible, it was certainly clear that the Birch reduction could be employed for its quantitative reduction. In every case the starting material was fully consumed although the selectivity in cleavage was poor. Extensive calculations using a higher level of theory were also being conducted by another group member (Greg Anderson) on the radical anion of **2.3.6**. By submitting **6.2.6**² to both possible C-S bond cleavages (Scheme 6.2.6), it was discovered that desulfurisation i.e. de-thiomethylation had a significantly lower

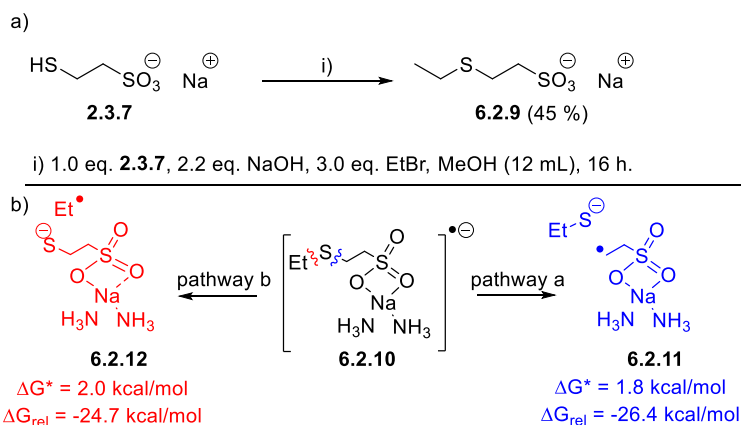
² (sodium was treated in a tetrahedral environment following Hoffmann's proposal.¹⁹⁴ This should also allow for comparative studies with $\text{Li}(\text{NH}_3)_4$ when lithium was used in later Birch reductions)

energy barrier (pathway a, 1.3 kcal/mol) than the alternative demethylation (pathway b, 4.0 kcal/mol). Based on these energy profiles, desulfurisation (pathway a) to yield **6.2.7** should have been the preferred pathway and it is unclear why this preference was not observed experimentally. It could have been that an energy barrier of 4.0 kcal/mol for demethylation was still easily accessible under the reaction conditions employed.



Scheme 6.2.6. Further computational investigations revealed that desulfurisation (pathway a) had a slightly higher energy barrier than demethylation (pathway b) although the free energies of the products from either bond cleavage was very similar. (Calculations were conducted by Greg Anderson using M06/6-311G with CPCM chosen as the solvation model and ethanol as the solvent). Ethanol ($\epsilon = 24.3$) was chosen as it was closest to NH_3 ($\epsilon = 16.5$) in the Gaussian software used. ΔG^* denotes the activation energy required for the bond cleavage and $\Delta G(\text{rel})$ refers to the free energy of the products relative to the starting radical anion.

Parallel reactions were also being conducted with ethyl coenzyme M **6.2.9**. This substrate was synthesised using conditions that were modified from those employed previously for the synthesis of MeCoM (Scheme 6.2.7 a).



Scheme 6.2.7. a) Synthesis of ethyl coenzyme M **6.2.9**. b) Computational calculations predicted that radical anion **6.2.10** should not have considerable preference for either C-S bond cleavage. (Calculations were conducted by Greg Anderson using M06/6-311G with CPCM chosen as the solvation model and ethanol as the solvent) ΔG^* denotes the activation energy required for the bond cleavage and $\Delta G(\text{rel})$ refers to the free energy of the products relative to the starting radical anion.

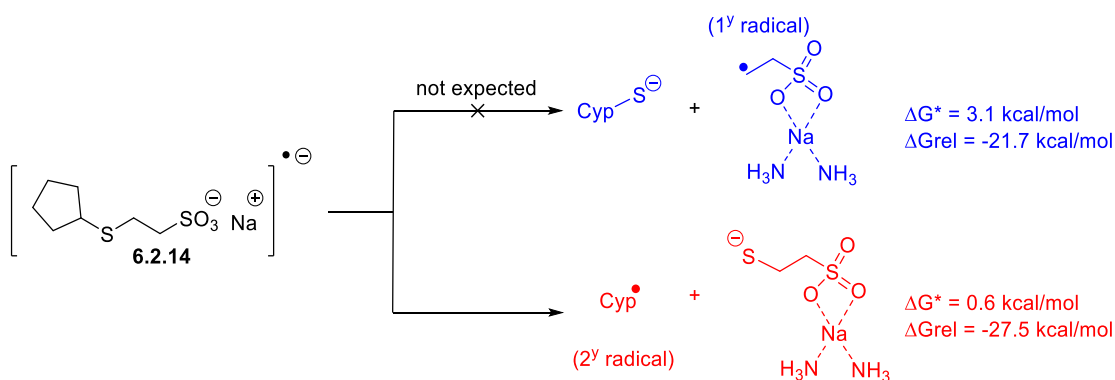
In the present case, the computational investigations predicted that the free energies of the products (ΔG_{rel}) resulting from either pathway were very similar (Scheme 6.2.7 b). In contrast with MeCoM, there was now no significant difference in the energy barriers for the two pathways. These computational calculations were closely reflected by the experimental results (Table 6.2.8). In both experiments, both types of C-S bond cleavages were observed to proceed in nearly equal yields.

Table 6.2.8. The experimental results for the Birch reduction of 6.2.9. In both cases, quantitative but not selective C-S bond cleavages were observed.

	$\xrightarrow[\text{liq. NH}_3, 8\text{h.}]{6 \text{ eq. Na}}$		+		+	
6.2.9		2.3.7		6.2.4		6.2.13
	1st Attempt	0.6		0.4		not detected
	2nd Attempt	0.5		0.5		not detected

Product ratios in the table were calculated from the ^1H NMR spectra of the crude products.

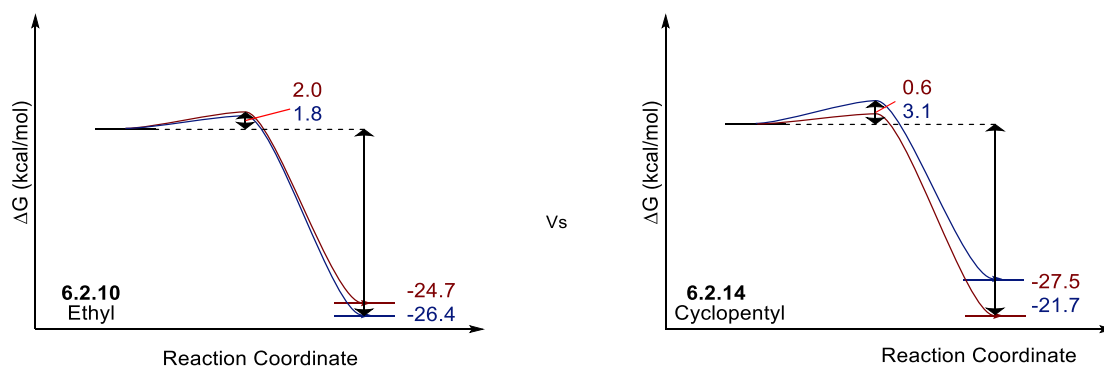
A possible strategy which might promote regioselectivity in the C-S bond cleavage would involve stabilisation of the resulting radical fragment. By designing cyclopentyl-based coenzyme M, the envisaged secondary carbon radical formed upon C-S bond cleavage, should experience more stabilization compared to the previous cases with methyl and ethyl analogues. This was also supported by computational calculations (Scheme 6.2.9) which predicted that the preferred pathway (giving rise to more energetically stable products) was almost barrierless ($\Delta G^* = 0.6$ kcal/mol).



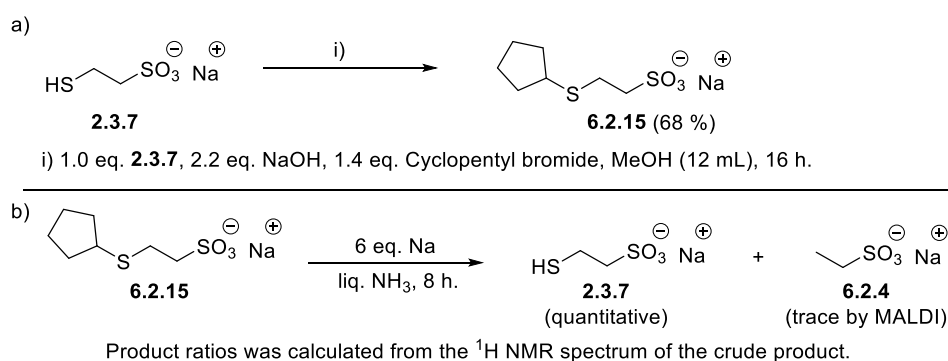
Scheme 6.2.9. Computational calculations predicted that there would be a preference for dealkylation over desulfurisation. (Calculations were conducted by Greg Anderson using M06/6-311G with CPCM chosen as the solvation model and ethanol as the solvent). Ethanol ($\epsilon = 24.3$) was chosen as it was closest to NH_3 ($\epsilon = 16.5$) in the Gaussian software used. A graphical presentation of these values is shown in Figure 6.2.10. ΔG^* denotes the activation energy required for the bond cleavage and ΔG_{rel} refers to the free energy of the products relative to the starting radical anion.

The very modest energy barrier in the present case, unlike the ethyl and methyl-based substrates, could be crucial for regioselectivity in the bond cleavage (Figure 6.2.10).

Figure 6.2.10. Compared to ethyl co-enzyme M, the cyclopentyl-based substrate had a significant energy difference in the products resulting from the two possible reductive C-S bond cleavages, with the red path almost barrierless. (Calculations were conducted by Greg Anderson using M06/6-311G with CPCM chosen as the solvation model and ethanol as the solvent). Ethanol ($\epsilon = 24.3$) was chosen as it was closest to NH_3 ($\epsilon = 16.5$) in the Gaussian software used.

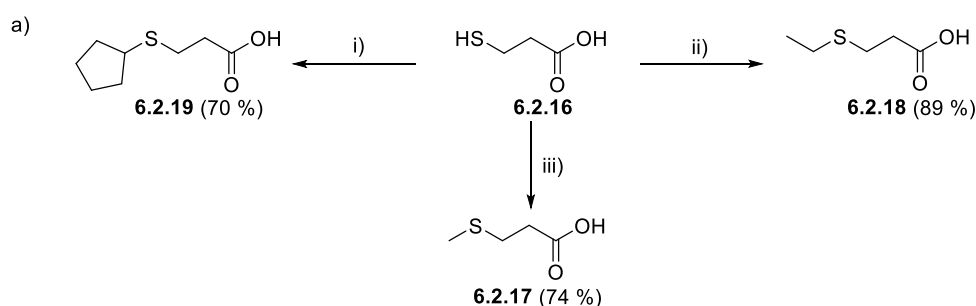


The synthesis of **6.2.15** followed that of **6.2.10** (Scheme 6.2.11 a) and the substrate was then subjected to Birch reduction with sodium (Scheme 6.2.11 b). This time, the C-S reductive cleavage proceeded quantitatively to yield coenzyme M. This experimental result agreed well with the aforementioned hypothesis which postulated that the stabilisation of the resulting radical could enhance regioselectivity in the bond cleavage fragment of the parent radical anion. Due to time constraints the experiment could not be repeated but admittedly, this would be crucial in confirming the observed regioselectivity in the reduction.

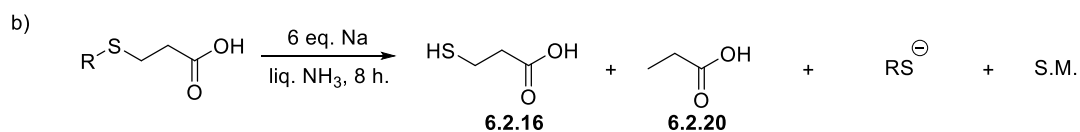


Scheme 6.2.11. a) The synthesis of **6.2.15** proceeded smoothly. b) Regioselective C-S bond cleavage, resulting in the formation of the 2° radical, was observed under Birch reduction with sodium.

All of the published reports on the mechanisms for enzymatic demethylation of MCR focus primarily on the sulfide end of the substrate. Located at the opposite end of the substrate, the sulfonate fragment is believed to be important only for the anchoring of the molecule (see Chapter 2.3). The possibility that the sulfonate group electronically assists substrate reactivity has not been explored. To determine if the sulfonate group functions more than just an anchor in the reductase, carboxylic acid analogues **6.2.17-6.2.19** were synthesised to be studied in the Birch conditions. (Scheme 6.2.12 a).



- i) 1.0 eq. **6.2.16**, 1.3 eq. Cyclopentyl bromide, 2N NaOH/MeOH (8.0 mL), 18 h.
 ii) 1.0 eq. **6.2.16**, 1.3 eq. EtBr, 2N NaOH/MeOH (8.0 mL), 18 h.
 iii) 1.0 eq. **6.2.16**, 1.3 eq. MeI, 2N NaOH/MeOH (8.0 mL), 18 h.



R = Me, 6.2.17	90 %	trace	not detected	0 %
R = Et, 6.2.18	0 %	0 %	0 %	88 %
R = cyclopentyl, 6.2.19	0 %	0 %	0 %	95 %

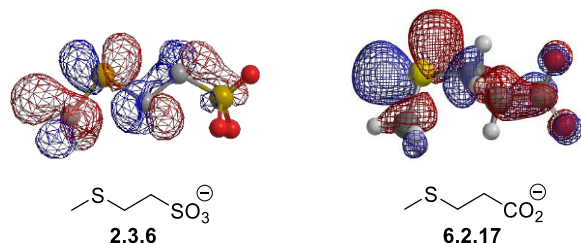
% yield = yield after purification

Scheme 6.2.12. a) Carboxylic acids **6.2.17-6.2.19** were conveniently synthesised from commercially available compounds. b) Birch reductions using sodium were attempted on all three carboxylates; only **6.2.17** showed reactivity.

When these carboxylic acids were tested for reduction with sodium in liquid ammonia, it was discovered that only the methyl analogue **6.2.17** underwent quantitative dealkylation. Both the ethyl and cyclopentyl analogues remained unreactive and were successfully recovered in good yields. When **6.2.17** was investigated computationally, it was discovered that the LUMO was delocalised over the molecule, similar to the sulfonate case **2.3.6** (Figure 6.2.13). This strongly

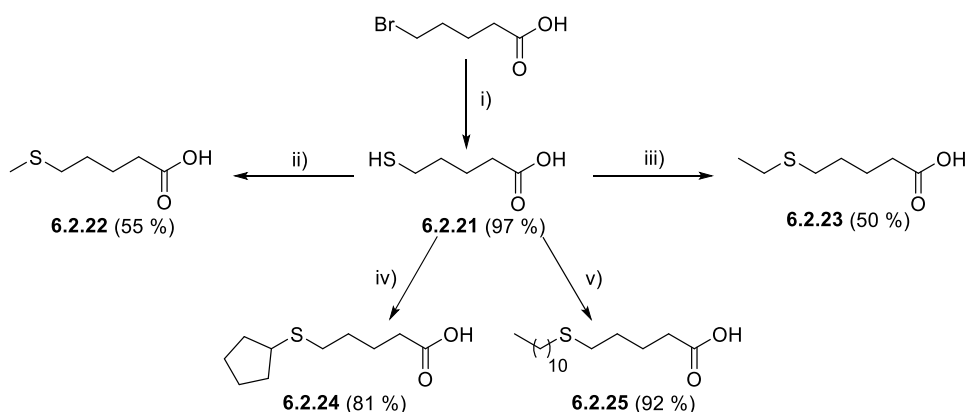
suggested that the difference in reactivity was due to the nature of the anionic terminus. This might include the degree of coordination with the reductive species and the lowering of the LUMO energy levels of the substrate.

Figure 6.2.13. The LUMO of **6.2.17** was predicted to be extensively delocalised, similar to that of the sulfonate **2.3.6**. (DFT, B3LYP, 6-31G(d,p) in ethanol was employed). Ethanol ($\epsilon = 24.3$) was chosen as it was closest to NH_3 ($\epsilon = 16.5$) in the Gaussian software used.



It was not fully understood why demethylation was the only observed reaction in this series of carboxylic acid-based substrates. If radical stability was the crucial factor (as previously proposed to account for the regioselectivity observed with sulfonate-based **6.2.15**), then the reduction in the present series should not have been restricted to **6.2.17**. Even more intriguing were the results from another set of valeric acid-based substrates.

By using 5-mercaptovaleric acid as the building block, a longer spacer group was installed between the sulfide and the carboxylate fragments (Scheme 6.2.14). As before, substrates **6.2.22-6.2.25** were conveniently synthesised from commercially available compounds.

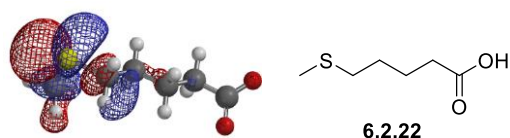


- i) 1st: 1.0 eq. 5-bromovaleric acid, 1.5 eq. thiourea, EtOH (35 mL), r.t. → reflux, 20 h.
 2nd: 7.5 M NaOH (25 mL), 90 °C, 19 h.
 ii) 1.0 eq. **6.2.21**, 1.3 eq. MeI, 2N NaOH/EtOH (8.0 mL), 0 °C, 12 h.
 iii) 1.0 eq. **6.2.21**, 2.0 eq. EtBr, 2N NaOH/EtOH (8.0 mL), 0 °C, 12 h.
 iv) 1.0 eq. **6.2.21**, 2.0 eq. Cyclopentyl bromide, 2N NaOH/EtOH (8.0 mL), 0 °C, 12 h.
 v) 1.0 eq. **6.2.21**, 4.0 eq. Undecyl bromide, 2N NaOH/EtOH (8.0 mL), 0 °C, 12 h.

Scheme 6.2.14. Synthesis of carboxylic acids **6.2.22-6.2.25** from 5-bromovaleric acid.

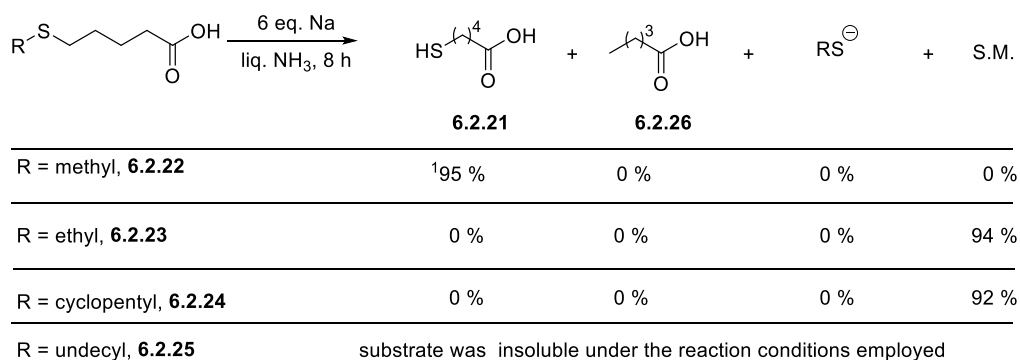
The idea of installing a longer alkyl chain was to determine if electron shuttling between the carboxylate and sulfide regions was responsible for C-S bond reduction which might have been present with **6.2.17**. Computational investigations predicted that the LUMO of **6.2.22** would not be extensively delocalised. Instead, it was localised on the sulfide fragment (Figure 6.2.15).

Figure 6.2.15. The LUMO of **6.2.22** was predicted to reside on the sulfide fragment. (DFT, B3LYP, 6-31G(d,p) in ethanol was employed). Ethanol ($\epsilon = 24.3$) was chosen as it was closest to NH_3 ($\epsilon = 16.5$) in the Gaussian software used.



When the Birch reduction was conducted on these candidates, it was discovered that the ethyl and cyclopentyl derivatives **6.2.23** and **6.6.24** remained unreactive and only the methyl substrate proceeded with almost quantitative and specific Me-S bond cleavage (Table 6.2.16). The undecyl derivative **6.2.25** was highly insoluble in liquid NH_3 ; several attempts were made to solubilise the substrate with the use of cosolvents (e.g. THF, Et_2O) but with limited success.

Table 6.2.16. a) Results from the attempted Birch reductions on valeric acid-based substrates 6.2.22-6.2.25. Only 6.2.22 was successfully reduced.



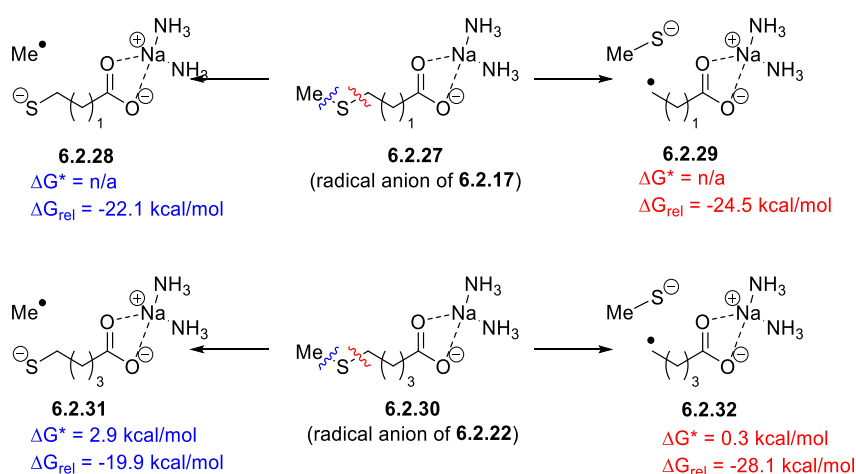
¹Experiment was repeated and yielded the same result % yield = yield after purification

The results from the two series of carboxylic acids (valeric and propanoic acid-based substrates) suggested that there was some unique reactivity available only to methyl sulfides. Interestingly, a closer examination of **6.2.27** and **6.2.30** (radical anions of **6.2.17** and **6.2.22**) using computational methods suggested that i) C-S bond cleavages for both substrates were energetically feasible (Figure 6.2.17).

This was reflected in the low energy barriers for **6.2.30**. In the case of **6.2.27**, the computational method used could not optimise the transition states leading to the bond cleavages. ii) for **6.2.27**, the similar ΔG_{rel} values for both bond cleavages possibly indicated poor selectivity in the C-S bond cleavage and iii) for **6.2.30**, desulfurisation should be the preferred process (Figure 6.2.17).

However, it was clear that the computational calculations attempted did not agree well with the experimental results with regards to selectivity in the C-S bond cleavage. It should be noted that the computational method could only calculate the energy profiles for the C-S bond cleavages starting from the radical anion state; how this species was generated (directly onto the sulfide region, or electron shuttling from the carboxylate) would not have been predicted by the calculations. Furthermore, the calculations did not consider the conformation(s) of the radical anion which could be significant as described in the Curtin-Hammett principle.¹⁹⁹

Figure 6.2.17. Computational investigations on the feasibility of C-S bond cleavages proceeding from 6.2.27 and 6.2.30 (radical anions of methyl-based substrates 6.2.17 and 6.2.22). (Calculations were by Greg Anderson conducted using M06/6-311G with CPCM chosen as the solvation model and ethanol as the solvent). $\Delta G^* = \text{n/a}$ indicates that the computational method employed could not obtain an optimised transition state.



This being the case, it was still not known if the reductive species generated under the Birch conditions was interacting directly with the sulfide portion of the methyl-based substrates, or, coordination with the carboxylate region (the LUMO) with subsequent electron shuttling was responsible for the observed bond reductions.

Thus far, the Birch reductions attempted on the sulfonates and carboxylic acid derivatives have not shown any clear trend in reactivity and the bond cleavage

mechanism remained ambiguous. A possible way forward would be to further increase the tether length between the carboxylate and the sulfide terminals to discourage electron-shuttling. However, this strategy was not pursued since there were concerns about solubility of the substrate in liquid ammonia (solubility problems were already encountered with undecyl-based **6.2.25**, the undecyl-based sulfide). Moreover, the parameters for electron-shuttling were unknown and so, preparing longer chain carboxylates might not be as useful as envisaged. Instead, attention was focused on the metal species being used. Besides sodium, lithium is commonly used in the Birch reduction. Lithium bears a smaller atomic radius and is also a more powerful reducing agent as reflected by its reduction potential ($E_0 = -3.03$ V vs. SHE for lithium. $E_0 = -2.71$ V vs. SHE for sodium). These two properties may influence both the reactivity and regioselectivity of the C-S bond reductions previously observed with sodium.

Lithium was first tested on the sulfonate series with results shown in Table 6.2.18.

Table 6.2.18. The Birch reductions on sulfonate-based substrates were reattempted using lithium. The results could be compared to those obtained from the reductions involving sodium.

$\text{R-S-CH}_2\text{-CH}_2\text{-SO}_3^- \text{Na}^+ \xrightarrow[\text{liq. NH}_3, 8\text{h}]{6 \text{ eq. Metal}} \text{HS-CH}_2\text{-CH}_2\text{-SO}_3^- + \text{CH}_2\text{-SO}_3^- + \text{RS}^- + \text{S.M.}$		2.3.7	6.2.4		
With Na					
R = methyl, 2.3.6	1st Attempt	0.9	0.1	not detected	0
	2nd Attempt	0.6	0.4	not detected	0
	3rd Attempt	0	> 0.9	not detected	0
R = ethyl, 6.2.9	1st Attempt	0.6	0.4	0.2	0
	2nd Attempt	0.5	0.5	not detected	0
R = cyclopentyl, 6.2.15		quantitative	trace (MALDI)	not detected	not detected
With Li					
R = methyl, 2.3.6	1st Attempt	> 0.9	trace (MALDI)	not detected	0
	2nd Attempt	> 0.9	trace (MALDI)	not detected	0
R = ethyl, 6.2.9	1st Attempt	0.6	0.4	not detected	0
R = cyclopentyl, 6.2.15	1st Attempt	> 0.9	0	0	0

Product ratios in the table are calculated from the ^1H NMR spectrum of the crude product

It was realised from the experimental results that lithium certainly improved regioselectivity with methyl coenzyme M **2.3.6** and this was reaffirmed by a repeated attempt. The observed reactivity for the ethyl **6.2.9** and cyclopentyl **6.2.15** sulfonates paralleled that of the experiments using sodium metal (Table 6.2.18).

Following these new findings which revealed that regioselectivity was significantly enhanced by the use of lithium for the sulfonate-based substrates, it was decided to proceed with lithium-based reductions on the propanoic and valeric acid-based substrates (the syntheses of these compounds have been shown previously).

For the propanoic acid-based series (Table 6.2.19), the observed reactivity for the methyl-containing substrate **6.2.17** was relatively similar to that observed with the sodium-based reduction. In stark contrast, lithium-based reduction was observed quantitatively with the ethyl analogue **6.2.18** which had previously remained unreactive when sodium was employed. Impressively, the cyclopentyl analogue **6.2.19** was also discovered to be moderately reactive when lithium was used.

Table 6.2.19. The Birch reductions on propanoic acid-based substrates were reattempted using lithium. The results could be compared to those obtained from the reductions involving sodium.

$\text{R-S-CH}_2\text{-CH}_2\text{-C(=O)OH} \xrightarrow[\text{liq. NH}_3]{6 \text{ eq. Metal}}$		$\text{HS-CH}_2\text{-CH}_2\text{-C(=O)OH}$	$+ \text{CH}_3\text{-CH}_2\text{-C(=O)OH}$	$+ \text{RSH}$	$+ \text{S.M.}$
		6.2.16	6.2.20		
With Na					
R = methyl, 6.2.17		93 %	trace	0 %	0 %
<hr/>					
R = ethyl, 6.2.18		0 %	0 %	0 %	88 %
<hr/>					
R = cyclopentyl, 6.2.19		0 %	0 %	0 %	95 %
With Li					
R = methyl, 6.2.17	1st attempt	93 %	0 %	0 %	0 %
	2nd attempt	74 %	0 %	0 %	0 %
<hr/>					
R = ethyl, 6.2.18		48 %	50 %	*50 %	0 %
<hr/>					
R = cyclopentyl, 6.2.19		23 %	0 %	0 %	72 %

*Yield was based on integration of the ^1H NMR of the crude material; ethanethiol was not isolated presumably due to its volatility.

This enhanced reactivity with lithium was also seen with the valeric acid-based series in which the ethyl analogue **6.2.23** underwent C-S bond reduction with lithium

(Table 6.2.20). A slight trace (< 1 %) of the dealkylated thiol product resulting from the reduction of the cyclopentyl analogue **6.2.24** was also be detected by GCMS (CI). These experimental results were most likely due to the increased reducing power of lithium compared to sodium.

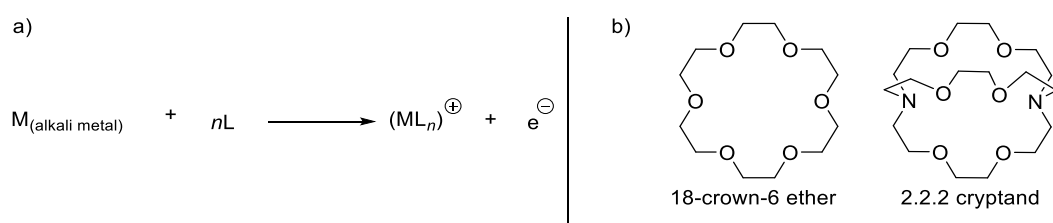
Table 6.2.20. The Birch reductions on valeric acid-substrates were reattempted using lithium.

$\text{R-S-CH}_2\text{CH}_2\text{CH}_2\text{CH}_2\text{C(=O)OH} \xrightarrow[\text{liq. NH}_3]{6 \text{ eq. Metal}}$	$\text{HS-CH}_2\text{CH}_2\text{CH}_2\text{CH}_2\text{C(=O)OH}$	$+$	$\text{CH}_2\text{CH}_2\text{CH}_2\text{C(=O)OH}$	$+$	RSH	$+$	S.M.
	6.2.21		6.2.26				
With Na							
R = methyl, 6.2.22	95 %		0 %		0 %		0 %
R = ethyl, 6.2.23	0 %		0 %		0 %		94 %
R = cyclopentyl, 6.2.24	trace (GCMS)		0 %		0 %		92 %
With Li							
R = methyl, 6.2.22	93 %		0 %		0 %		0 %
R = ethyl, 6.2.23	45 %		18 %		0 %		36 %
R = cyclopentyl, 6.2.24	trace (GCMS)		0 %		0 %		94 %

Conclusions and future work

The simplest and most powerful reductant that can be harnessed is the electron which would be highly attractive in terms of atom economy. Using the electron as a reagent is not a new concept, for example, the Birch reduction²⁰⁰ has been extensively used for a wide range of reductive transformations in organic synthesis. However, to exploit this chemistry would necessarily require a better understanding of the actual reduction mechanism. There is still ambiguity regarding the actual reductive species generated during the Birch reduction. In fact, recent studies suggest that the reductive capability of metal-ammonia mixtures is not simply due to “solvated electrons that give the solution its distinctive blue colour” previously proposed by Sir Humphry Davy²⁰¹ and Kraus.²⁰² The crucial questions would be i) where are the electrons located during the reaction? and ii) what is the environment of the electron-containing sites?

On a macroscopic level, clues are provided from the extensive studies on electrides. Electrides are usually crystalline solids which can be generated (under cryogenic, oxygen- and moisture-free conditions) by encapsulating the alkali metal ions with stable (i.e., non-reducible) ligands, usually cryptands or crown ethers (Scheme 6.2.21). The encapsulation also creates cavities within the crystalline framework where the electrons are thought to reside.

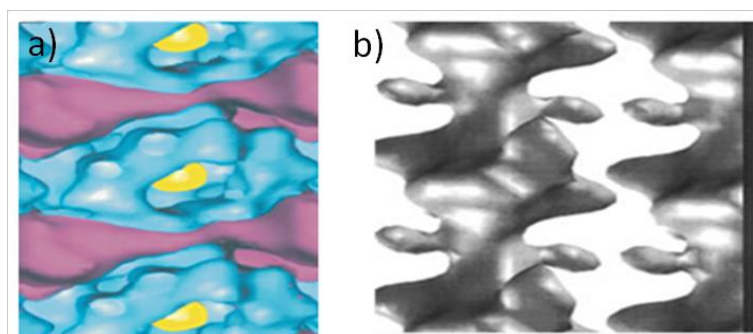


Scheme 6.2.21. a) Encapsulation of the metal cation by appropriate ligands can generate electrides. b) Suitable ligands include crown ethers and cryptands, an example of each is shown.

Extensive close packing of the complexes in an orderly fashion would mean that the electron-containing cavities can be connected by channels. The result is that the electrons can now be relayed through these channels, although this is heavily dependent on the size of the channels and the polarity of the ligands employed.

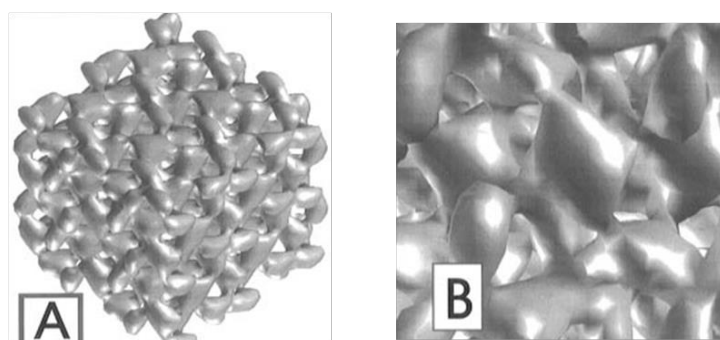
Using $\text{Cs}(\text{15-crown-5})_2^+ e^-$ to illustrate this, Figure 6.2.22 a) depicts the cavities in mauve;²⁰³ these cavities are 4.0 Å in diameter and 8.89 Å apart. In Figure 6.2.22 b) the same electride is depicted²⁰⁴ with emphasis on the extensive 2D network of channels present. Here, the channels were measured to be 1.5 Å wide.

Figure 6.2.22. a) The electron channels are depicted in mauve. In blue are the cryptands (18-crown-6-ether in this case) encapsulating the metal ion in yellow (Cs^+).²⁰³ b) This depiction shows how the channels allow electrons to delocalise resulting in spin pair.³ Reproduced with permission from the American Chemical Society.²⁰⁴



It is possible to extend the channels into three dimensions which would allow electrons to be highly delocalised. A classic example would be $\text{Li}(\text{ND}_3)_4$ (Figure 6.2.23) which is thought to be closely similar to $\text{Li}(\text{NH}_3)_4$. Each cavity (Figure 6.2.23 b) is 2.6 Å in diameter and connected to four other cavities through short channels 1.6 Å long with narrow diameters of 1.4 Å. The extensive network of cavities and the narrow diameters which suppress electron pairing are thought to be responsible for the metallic nature of this electride.²⁰⁴⁻²⁰⁶

Figure 6.2.23. a) The electron tunnels present in $\text{Li}(\text{ND}_3)_4$ extend into a 3D network. b) Closeup view of the channels. Reproduced with permission from the American Chemical Society.²⁰⁴.



³ The authors had generated the isosurfaces depicted in Figures 6.2.22 and 6.2.23 using AVS and EXPLORER programmes on Silicon Graphics computers (see J.L. Dye, M. J. Wagner, G. Overney, R.H. Huang, R.H. Nagy, T.F. Tomanek, *J. Am. Chem. Soc.*, **1996**, *118*, 7329-7336).

Extensive research in the field of electrides has been conducted by Dye,²⁰³ Singh,²⁰⁷ and Matsuishi.²⁰⁸ Crucially, the study of electrides has helped in understanding why these species can vary significantly in their magnetic, optical and electronic properties, which are highly dependent on the availability of unpaired electrons. Clearly, the nature of the cavities, channels and their extent of networks will influence the extent of electron pairing.

On a micro scale, like that of the Birch reduction, extensive experimental and computational investigations have been attempted on the poorly-understood $\text{Li}(\text{NH}_3)_4$ system. The difficulty in understanding this system is partly due to the complex array of metallic species that could form during the reaction. To add to this complication, the different metallic species are also in dynamic equilibrium, which is affected by both the concentration of the metal²⁰⁹ and the temperature.²¹⁰

Essentially, the reductive nature of $\text{Li}(\text{NH}_3)_4$ in the blue solution can only be achieved at very low concentrations of metal ($\leq 10^{-4}$ MPM⁴). At higher concentrations, spin pairing of both the solvated electrons, indicated as $e^-(\text{NH}_3)_n$, and ion pairs, $\text{Li}(\text{NH}_3)_4^+ \cdot e^-(\text{NH}_3)_n$ increases, resulting in stable coupled radicals which are not reducing. Increasing the concentration further results in the oligomerisation of discrete $\text{Li}(\text{NH}_3)_4$ molecules which promotes spin pairing of the electrons and the formation of a metallic band.^{209,211}

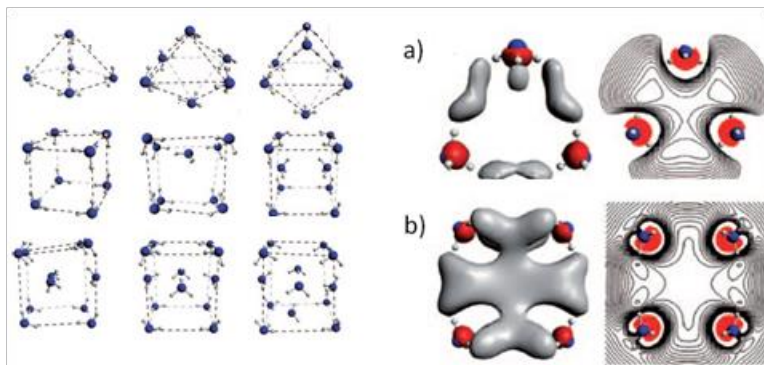
Bearing in mind that 90 % of electrons are already spin paired at 0.5 MPM,²⁰⁹ and that this concentration would still appear blue during the reaction, it would be experimentally very challenging to achieve $\leq 10^{-4}$ MPM in order to obtain electrons in their “active” form.

When the unpaired solvated electron $e^-(\text{NH}_3)_n$ is successfully generated during the reaction, computational investigations predict that this can exist in three forms,²⁰⁹ all of which are in dynamic equilibrium with each other. The ammonia-based cavity for the electron can vary largely in size ($5 \leq n \leq 14$, where n is the number of NH_3 molecules) depending on the availability of the solvent (Figure 6.2.24). Furthermore,

⁴ MPM = mol % metal i.e. $[\text{moles of metal}]/[\text{moles of metal} + \text{moles of solvent}] \times 100$.

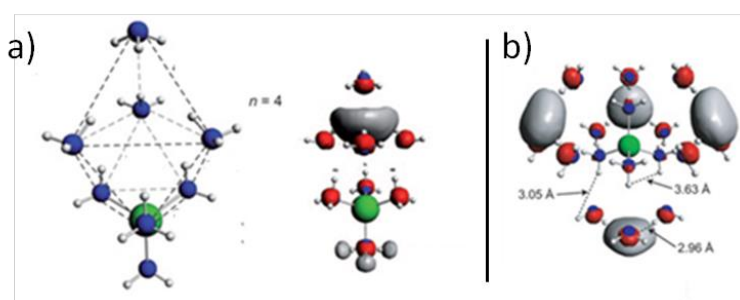
it has been discovered that the solvated electron preferentially resides at the perimeter of the cavity.²¹²

Figure 6.2.24. Left: The cavity size for the electron can vary greatly in size depending on the availability of the solvent. Right: a) For three NH₃ molecules, computational calculations reveal that the electron density is greatest at the periphery of the cavity. b) The same prediction is true for four NH₃ and for all the higher orders too.⁵ Reproduced with permission from the John Wiley and Sons.²⁰⁹



Increasing the concentration of lithium results in more $e^-(NH_3)_n$ units existing as ion pairs $Li(NH_3)_4^+ \cdot e^-(NH_3)_n$, formed *via* strong electrostatic attractions between the two charged species (Figure 6.2.25 a). Even in the formation of $Li(NH_3)_4^+ \cdot e^-(NH_3)_n$, computational calculations on the net spin polarisation still predicts that the unpaired electron preferentially resides in the ammonia cavity, although the electron density (depicted in grey) is not restricted to the periphery as was previously seen with $e^-(NH_3)_n$ (Figure 6.2.24).

Figure 6.2.25. a) The formation of the ion pair $Li(NH_3)_4^+ \cdot e^-(NH_3)_4$ upon increase of lithium concentration was very favourable. The electron in this complex still resides in the NH₃ cavity (shown in grey). b) With increased availability of NH₃ molecules, a second solvation shell on $Li(NH_3)_4^+$ provides an alternative method of generating an ion pair, $Li(NH_3)_4^+ \cdot e^-(4NH_3)_3$. Reproduced with permission from the John Wiley and Sons.²⁰⁹



⁵ The cartoons depicted in Figures 6.2.31 and 6.2.32, the authors conducted their computational calculations using the Amsterdam Density Functional Package with the application of the revised Perdew-Burke-Ernzerhof (revPBE) non-hybrid gradient density functional, along with Vosko-Wilk_Nusain (VNN) local spin density approximation (see E. Zurek, P. Edwards, R. Hoffmann, *Angew. Chem. Int. Ed.* **2009**, *48*, 8198-8232).

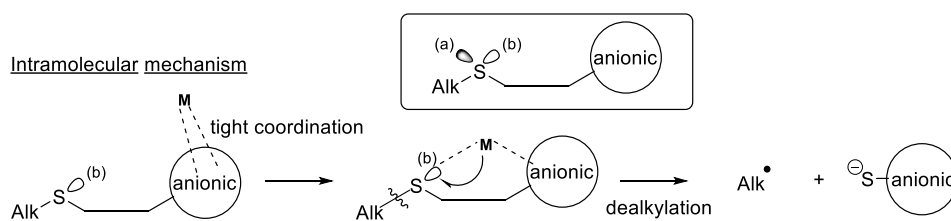
The unpaired electron can exist in a third another environment²⁰⁹ which can be abbreviated as $\text{Li}(\text{NH}_3)_4^+ \cdot e^- 4(\text{NH}_3)_3$ (Figure 6.2.25 b). In this instance, four units of $(\text{NH}_3)_3$ are introduced as a second solvent shell around $\text{Li}(\text{NH}_3)_4^+$. As seen previously with $\text{Li}(\text{NH}_3)_4^+ \cdot e^- (\text{NH}_3)_n$, the valence electron is still predicted to be residing in the NH_3 cavities, away from the $\text{Li}(\text{NH}_3)_4^+$ clusters. Although not explicitly mentioned in the review by Hoffmann *et al.*, it should be obvious that this species, which requires extensive stabilisation by ammonia molecules, will be prevalent at lower concentrations of lithium, possibly in equilibrium with $e^- (\text{NH}_3)_n$. The three different forms of the solvated electron $e^- (\text{NH}_3)_n$, $\text{Li}(\text{NH}_3)_4^+ \cdot e^- (\text{NH}_3)_n$ and $\text{Li}(\text{NH}_3)_4^+ \cdot e^- 4(\text{NH}_3)_3$ can be considered to be the reactive reductants present in the Birch reduction (it should be noted that there might still be other reactive forms present during the reaction yet to be discovered). It is possible that these different species will display different modes of reduction.

To the best of our knowledge, the $\text{Na}(\text{NH}_3)_n$ model has not been investigated to the same extent as $\text{Li}(\text{NH}_3)_4$. However, based on the increase in atomic size, it has been proposed²¹³ and shown from experimental and ab initio calculations by Ellis *et al.* that the sodium atom can readily accommodate up to six ammonia ligands (i.e. an octahedral environment) in its primary solvation shell.²¹⁴ This does not necessarily mean that $\text{Na}(\text{NH}_3)_4$ is not present during the experiment since studies have indicated that this species is relatively stable.²¹⁵ Since the atomic size of sodium can heavily influence the extent of its solvation, it follows that the envisaged reductive species $\text{Na}(\text{NH}_3)_n^+ \cdot e^- (\text{NH}_3)_n$ and $\text{Na}(\text{NH}_3)_n^+ \cdot e^- 4(\text{NH}_3)_3$ would be larger and more sterically demanding than in the case of lithium. Overall, studies towards understanding the Birch reduction have showcased the complexity of this reaction.

Hypothesis for the observed C-S bond reductions

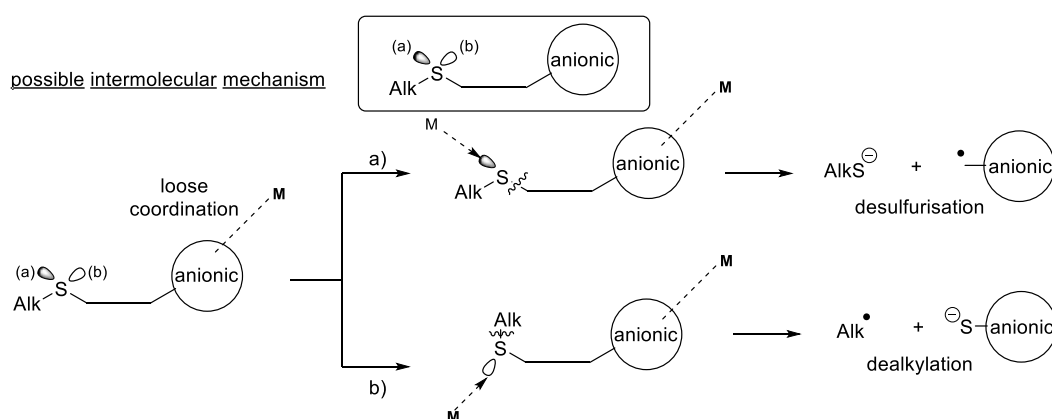
Possible explanations are now provided to account for the observed reactivity of the sulfonate and carboxylic acid-based substrates. It must be stressed that the following hypotheses are purely theoretical attempts at making sense of the observed C-S reductive cleavages. Further experiments would necessarily involve testing these ideas.

During the reactions, two possible reduction mechanisms are thought to occur; the “intermolecular” and “intramolecular” modes of C-S bond cleavages. In the proposed “intramolecular mechanism”, the metal-based reductive species **M** is thought to coordinate well with the anionic terminus of the substrate (Scheme 6.2.26). It follows that the extent of coordination would depend on both the nature of the anionic terminus and the size of **M**. Thus, a tighter interaction will promote the electron shuttling from the coordinated **M** onto the sulfide terminus. Although there are two C-S σ^* orbitals, it would presently, be much easier for occupancy of $\sigma^*(b)$, resulting exclusively in dealkylation of the substrate (Scheme 6.2.26).



Scheme 6.2.26. The proposed intramolecular mechanism gives rise to dealkylation of the sulfide.

If the reductive species **M** is unable to coordinate effectively with the anionic terminus, then the intramolecular mechanism is diminished and the alternative “intermolecular” mechanism is thought to compete. In this instance, the “intermolecular mechanism” involves a second entity of **M** to directly attack the sulfide terminus. Since the reduction is no longer influenced by coordination with the substrate, both $\sigma^*(a)$ and $\sigma^*(b)$ orbitals of the C-S bonds can be attacked and would therefore lead to a mixture of dealkylated and desulfurised products (Scheme 6.2.27).



Scheme 6.2.27. The proposed intermolecular mechanism involves a second reductive species. Both C-S bond cleavages can result from this mechanism.

The three series of substrates are now revisited and plausible explanations are given to account for the observed reactivity based on the proposed mechanisms.

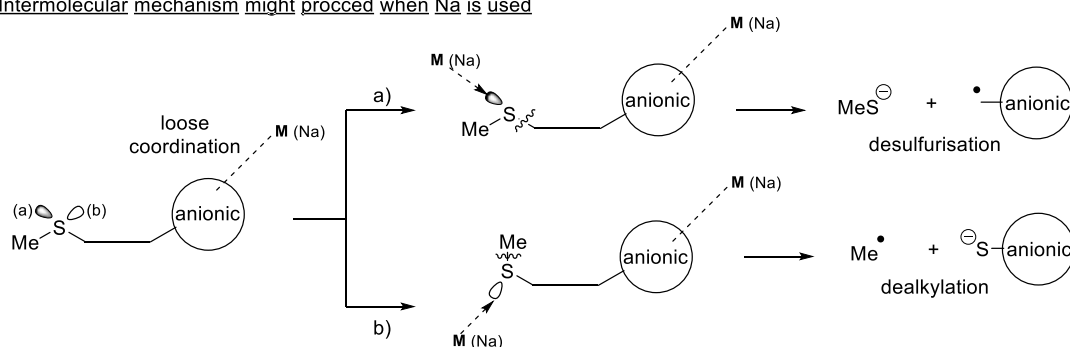
1. Sulfonate-based substrates

- Methyl coenzyme M **2.3.6**.

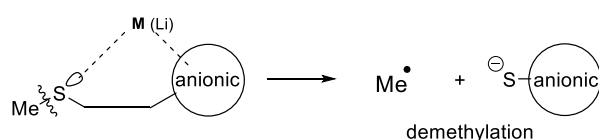
When sodium was utilised in the Birch reduction, it is possible that the reductive species **M** generated *in situ* was loosely coordinated to the sulfonate terminus. As such, the intramolecular mechanism is not active and the alternative intermolecular mechanism dominates. Within this mechanism, both C-S bond cleavages could proceed to yield a mixture of coenzyme M sodium salt **2.3.7** and ethanesulfonate **6.2.4** (Figure 6.2.28). Previously, computational calculations had shown that both bond cleavages were energetically accessible under the reaction conditions employed and so should be expected in the event.

Figure 6.2.28. The intermolecular mechanism is thought to give rise to product mixture when sodium was used while the intramolecular mechanism in the case of lithium resulted in preferential demethylation.

Intermolecular mechanism might proceed when Na is used



Intramolecular mechanism might have been operating in the case of Li

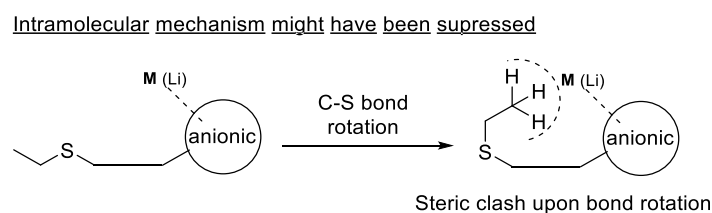


The use of lithium led to a distinctively different result. Lithium would necessarily generate a smaller reductive species **M** compared to sodium. It is possible that this allowed tighter interactions between the sulfonate terminus and **M**, which sets up the system for the intramolecular mechanism. Demethylation becomes the preferred process leading to the observed enhancement in regioselectivity of the C-S bond cleavage (Figure 6.2.28).

- Ethyl coenzyme M **6.2.9**

When sodium was utilised, a mixture of products was obtained. As with the methyl coenzyme M substrate, the size of the sodium-based reductant is thought to discourage tight coordination with the sulfonate terminus. Possibly, this suppresses the intramolecular mechanism and the intermolecular mechanism is thought to dominate. This gives rise to the product mixtures observed in both experiments attempted. Computational investigations had already revealed that the two reduction pathways were energetically very similar and so these calculations agree well with the proposed intramolecular mechanism. Although the lithium-based reductant should still be able to coordinate well with the sulfonate terminus, it is thought that the slight increase in the steric demands resulting from the ethyl fragment offsets the intramolecular mechanism (Figure 6.2.29).

Figure 6.2.29. It is thought that steric clash between lithium and the ethyl terminus might have suppressed the intramolecular mechanism.



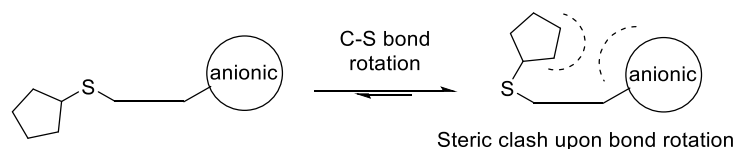
Nevertheless, the intermolecular mechanism, which is less affected by steric clash, is thought to be active, leading to both types of C-S bond cleavages to yield the observed product mixture.

- Cyclopentyl coenzyme M **6.2.15**

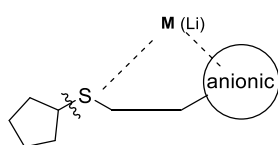
As with previous cases, it is thought that the sodium-based reductant generated *in situ* would preferentially reduce the substrate *via* the intermolecular mechanism. In this case, there is a marked difference in the energy profiles for the two possible C-S bond cleavages (Figure 6.2.10), with dealkylation being thermodynamically more accessible. This being the case, the intermolecular mechanism is thought to be predisposed towards dealkylation resulting in little desulfurisation.

With the lithium-based reductant, the intramolecular mechanism is thought to dominate. Unlike the ethyl analogue **6.2.9**, the marked increase in steric bulk here is

thought to make the rotation of cyclopentyl fragment unfavourable (i.e., the alkyl fragment folds over the substrate, Scheme 6.2.30). This allows the reductant to coordinate tightly to the sulfonate terminus thereby promoting the intramolecular mechanism and resulting in exclusive dealkylation. Further computational investigations are required to determine the actual energy barriers towards bond rotation of the cyclopentyl group.



Intramolecular mechanism is active, dealkylation ensues



Scheme 6.2.30. The cyclopentyl fragment is thought to suppress the “folding” of the molecule. This allows the intramolecular mechanism to proceed efficiently when lithium is employed.

2. Propanoic acid-based substrates

In general, the carboxylic acid-based substrates showed less reactivity compared to the sulfonate-based substrates. Possibly, this was due to the greater degree of influence which the sulfonate has, by inductive effects, on the energy level of the σ^* orbital of the sulfide bonds.

- **Methyl-based substrate 6.2.17**

By modifying the anionic fragment from sulfonate to carboxylate, changes in coordination with the metal-based reductive species should be expected. In the present case, it is suggested that the carboxylate is sterically and electronically more compatible than the sulfonate in coordinating with the reductant. This being the case, both the reductive species generated from sodium and lithium are thought to proceed with the intramolecular mechanism resulting in the preferred demethylation of **6.2.17**.

The slight trace of propanoic acid **6.2.20** observed with the sodium-based reduction (Table 6.2.19) could indicate that the intermolecular mechanism was faintly possible.

This can be attributed to a slight incompatibility in the interactions at the anionic terminus due to the larger size of sodium, and could also explain why **6.2.20** was not observed when lithium was used.

- Ethyl-based substrate **6.2.18**

Reactivity was observed only when lithium was employed; highly indicative of its stronger reducing capability compared to sodium. The product mixture showed that both C-S bonds could be reduced to equal extents with lithium.

It is thought that a similar situation to **6.2.9** (ethyl coenzyme M) is encountered here, in which the ethyl terminus folds over into the molecule thereby diminishing the extent of the intramolecular mechanism. The alternative intermolecular mechanism is thought to compete, resulting in the observed product mixture (Figure 6.2.29).

- Cyclopentyl-based substrate

Again, reduction was only observed when lithium was employed. Here, the extent of reduction was mediocre. Selective dealkylation is thought to proceed from the intramolecular mechanism. This is similar to that proposed for cyclopentyl coenzyme M **6.2.15** (Scheme 6.2.30).

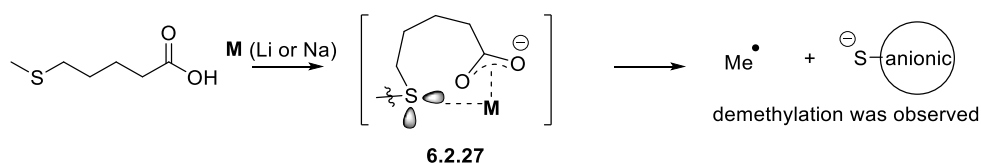
3. Valeric acid-based substrates

This series of substrates showed very similar experimental results to the previous propanoic acid-based substrates.

- Methyl-based substrate **6.2.22**

Since the substrates in this series experience more conformational flexibility due to the increase in alkyl chain length, it is possible that these molecules are able to adopt stable conformations similar to **6.2.27** (Scheme 6.2.31). The cyclic conformation should still allow the intramolecular mechanism to proceed leading to the observed demethylation.

Intramolecular mechanism can still proceed



Scheme 6.2.31. The cyclic conformation **6.2.27** is thought to bring the anionic terminus and the sulfide into close proximity which might allow the intramolecular mechanism to proceed.

- Ethyl-based substrate **6.2.23**

As with the ethyl analogue **6.2.18** in the propanoic acid series, reactivity was only observed with the more powerful lithium albeit the reduction proceeded to a lesser extent.

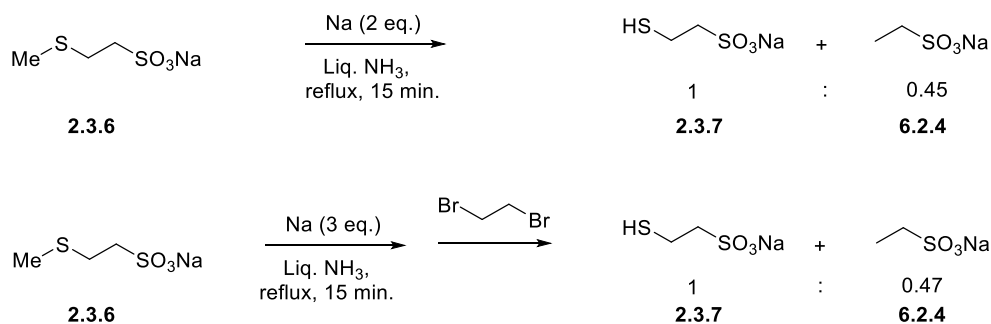
Although the cyclic conformation **6.2.27** could still be adopted, it is thought that the ethyl fragment renders this less favourable due to greater steric demands. Possibly, this suppresses the intramolecular mechanism and the alternative intermolecular mechanism proceeds, leading to both the desulfurised and dealkylated products.

- Cyclopentyl-based substrate **6.2.24**

No appreciable reduction was observed possibly due to the higher energy levels of the σ^* orbital of the sulfide bonds which are inaccessible to the metal-based reductant. This could have resulted from the increased tether length between the electron withdrawing carboxylate and the sulfide which diminishes the inductive effects the carboxylate terminus has on the σ^* orbital energy level of the sulfide where the LUMO is located (see previous example with **6.2.22**, Figure 6.2.15).

The great potential which this current project has towards i) understanding methanogenesis and ii) throwing light on Birch reduction using sodium and lithium - both of which are still not well understood, has inspired Eswararao Doni to pursue this project further. Following the proposal by Hoffmann *et al.*²⁰⁹ that dynamic equilibrium of the reductive species is present in such systems, and that the equilibrium is affected by temperature and the concentration of the metal, Eswararao Doni has repeated the Birch reduction of sulfonate-based sulfides with several modifications to the reaction conditions. His attempts have shown that the product

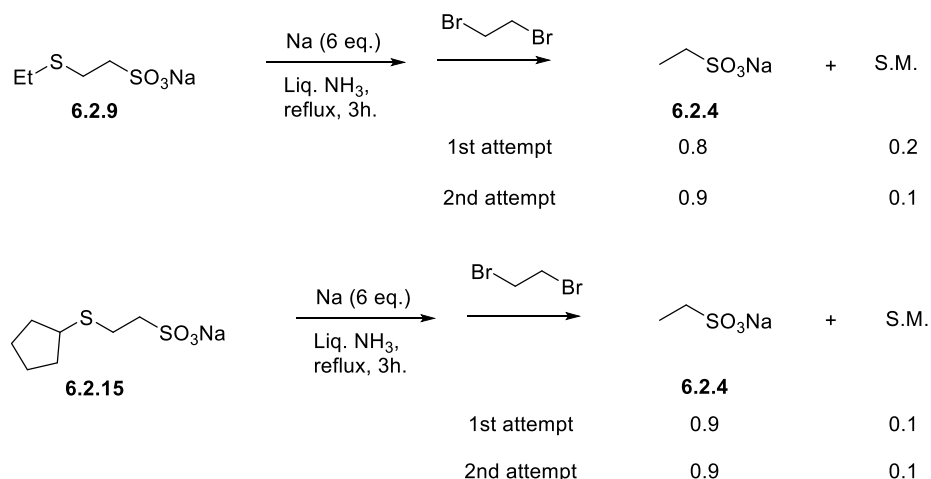
distribution of **2.3.7** and **6.2.4** was reproducible (Scheme 6.2.32) when a short reaction time was set (15 minutes) and with a decrease in metal loading (2 or 3 eq.).



Product ratios in the table are calculated from the ¹H NMR spectrum of the crude product.

Scheme 6.2.32. Experiments on methyl coenzyme M, conducted by Doni with shorter time and less metal, yielded reproducible results.

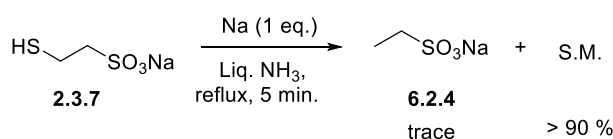
Additionally, Eswararao Doni has attempted Birch reductions using sodium on ethyl CoM **6.2.9** and cyclopentyl CoM **6.2.15** (Scheme 6.2.33). These experiments revealed that shortening the overall reaction time by enforced quenching of sodium using 1,2-dibromopropane (as opposed to 1 h maintained reflux and then stirring at room temperature for 7 h) led to good yields of ethane sulfonate sodium salt **6.2.4**. This is in stark contrast with the earlier method which had yielded mixtures for the ethyl substrate and quantitative dealkylation for the cyclopentyl-substrate. Crucially, these results suggest that the reduction profile can be significantly altered by reaction times.



Product ratios are calculated from the ¹H NMR spectrum of the crude product.

Scheme 6.2.33. Birch reductions on 6.2.9 and 6.2.15 using large excess of metal but with shorter time gave ethylsulfonate as the only reduced product.

Most interestingly, when Doni subjected coenzyme M **2.3.7** to Birch reduction using sodium, an unambiguous trace of ethane sulfonate **6.2.4** was detected by ^1H NMR. It is noteworthy that this desulfurisation proceeded in under 5 minutes (Scheme 6.2.34).



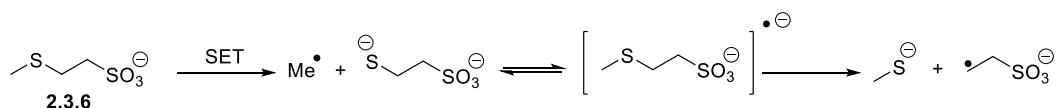
Scheme 6.2.34. Coenzyme M **2.3.7** was also susceptible to C-S bond cleavage.

If this result was extrapolated time-wise, it is possible that a significant amount of ethane sulfonate detected at the end of these reactions was actually derived from coenzyme M and not a direct result from the reduction of the substrate. Accordingly, it follows that the Birch reduction attempted with large excess of sodium (6 eq.) and with an extended period of time could have actually yielded more coenzyme M than what was detected.

There was also an indication that the method used to generate the reductive species could also influence the outcome. The work conducted by the author all involved generating a clear solution of the substrate in liq. NH_3 before addition of the metal. This was the only method to ensure that the substrate had dissolved prior to reduction.

Having confirmed that the substrates being tested were all soluble in liquid NH_3 , Eswararao Doni is presently attempting to generate the reductive species before addition of the substrate.

It also cannot be discounted at this stage that the methyl radical could recombine with its sulfur anion counterpart. The resulting radical anion could disproportionate again to yield the other set of reduced products (Scheme 6.2.35). This mechanism has yet to be tested experimentally.



Scheme 6.2.35. There is the possibility for the recombination of the methyl radical with the thiol anolate

Overall, this project has showcased unprecedented results which indicate that demethylation in MCR can proceed *via* the proposed radical mechanism. Using alkali metals, C-S bond cleavages of methyl coenzyme M can be effected in good

yields. This meant that the reduction is not limited to the nickel porphyrin although the key to regioselectivity in the bond cleavage may lie in the enzyme's conformation. Nevertheless, this is the first instance when demethylation of methyl coenzyme M without the use of enzymes has been successfully conducted in the laboratory.

The Birch reduction mechanism is still not fully understood although it has been widely used for its ability to reduce a wide range of compounds. For example, the reduction is conveniently employed by research groups to demethylate methionine in order to access homocysteine-based compounds used in enzymatic studies²¹⁶ or drug discovery.²¹⁷

The interesting results from this project, along with ongoing work, showcase the complex nature of the Birch reduction. Several factors have been determined to affect the reduction profile of aliphatic sulfides. These have been discussed at length and include, but are not limited to, the concentration of the metal, the temperature and the method used to generate the reductive species. Perhaps the experimental results in this project provide further evidence to support the proposed idea that different reductive species exist during the Birch reaction, and that these different species are capable of different modes of reduction.

The proposed intramolecular and intermolecular mechanisms used to explain the different C-S bond cleavages afforded by the Birch reductions need to be validated. There might also be different reductive species responsible for the observed C-S bond cleavages. This would most likely require more extensive computational investigations in the future.

Chapter 7 Experimental

7.1 General information

All reagents were bought from commercial suppliers and used without further purification unless stated otherwise. All the reactions were performed in oven-dried or flame-dried apparatus and preparation of the substrates was carried out under argon atmosphere using dry solvents. Diethyl ether, tetrahydrofuran, dichloromethane and hexane were dried with a Pure-Solv 400 solvent purification system by Innovative Technology Inc., U.S.A. Organic extracts were, in general, dried over anhydrous sodium sulfate (Na_2SO_4). A Büchi rotary evaporator was used to concentrate the reaction mixtures. Thin layer chromatography (TLC) was performed using aluminium-backed sheets of silica gel and visualised under a UV lamp (254 nm). The plates were developed using vanillin or KMnO_4 solution. Column chromatography was performed to purify compounds by using silica gel 60 (200-400 mesh).

A glovebox (Innovative Technology Inc., U.S.A.) was used for the workup of the super-electron donor **4.1.15** preparation reaction. Solvents used in the glovebox were degassed for at least 30 min, then purged with argon prior to being sealed and transferred to the glovebox port. The port was evacuated and then purged with nitrogen at least ten times before transfer into the glovebox. To weigh out the super electron donor (SED) into the reaction flask, the same procedure as above was followed. All UV reactions were carried out by using two focused UV lamps with filters ($\lambda = 365$ nm, each 100 watts) bought from Ultra-Violet products (UVP) company. During the reaction, the two UV lamps were placed opposite to each other, around the reaction flask, at room temperature.

Proton (^1H) NMR spectra were recorded at 400.13 and 500.16 MHz on Bruker AV3, AV400 and AV500 spectrometers, respectively. Carbon (^{13}C) NMR spectra were similarly recorded at 100.61 and 125.75 MHz on Bruker AV3 and AV500 spectrometers, respectively. The NMR experiments were carried out in deuteriochloroform (CDCl_3), d_6 -dimethylsulfoxide ($\text{DMSO-}d_6$) and d_6 -benzene (C_6D_6). The chemical shifts are quoted in parts per million (ppm) by taking

tetramethylsilane as a reference ($\delta = 0$) but calibrated on the residual non-deuterated solvent signal. Signal multiplicities are abbreviated as: s, singlet; d, doublet; t, triplet; q, quartet; m, multiplet; bs, broad singlet; coupling constants (J) are given in Hertz (Hz).

Infra-Red spectra were recorded on a Shimadzu IRAffinity-1 FTIR spectrophotometer with a Pike Technologies MIRacleTM Single Reflection Horizontal ATR Accessory with a ZnSe crystal.

Melting points were determined on a Gallenkamp Griffin SG94/05/530 Melting point apparatus and were unammended.

High resolution mass spectra were recorded at the EPSRC National Mass Spectrometry Service Centre, Swansea on a LTQ Orbitrap XL using Atmospheric Pressure Chemical Ionisation (APCI) or High Resolution Nano-Electrospray (HNESP) and masses observed were accurate to within 5 ppm.

Low resolution mass spectral analyses were carried out on a Thermofinnigan LCQ DUO LDU 00377 Mass Spectrometer operating electrospray ionisation (ESI). GC(EI) was carried out using Thermofinnigan PolarisQ Ion Trap Spectrometer with an Agilent DB5-MS 30 m x 0.25 mm column with 0.25 μ m packing. The carrier gas was helium at 1 mL/min. Chemical ionization GC(CI) was carried out using Agilent Technologies 7890A GC system, 5975C Inert XL EI/CI MSD with Triple Axis Detector with an Agilent DB5-MS 30 m x 0.25 mm column with 0.25 μ m packing. The carrier gas was helium at 1 mL/min and the reagent gas was methane.

Computational predictions were conducted using Spartan 2010 software jointly developed by Q-Chem Inc. and Wavefunction. Density Functional Theory was the commonly-used method unless otherwise stated. B3LYP and 6-31G(d,p) were usually used as the level of theory unless otherwise stated.

7.2 General procedures

1. UV irradiation experiment with 4.1.15

The experiment was set up in a glovebox. An oven-dried 10 mL round-bottomed flask was charged with a solution of **4.2.15** in degassed, anhydrous DMF (5 mL). The substrate was weighed out in a vial, dissolved in degassed, anhydrous DMF (2 ml) and then transferred to the donor solution. The reaction flask was then clamped between two focused UV lamps (365 nm, each 100 W) and stirred for the stated time.

2. Blank reaction with 4.1.15 without UV exposure

Samples were prepared following the standard protocol devised for UV-activated SED reactions. Both the UV-free blank reaction and the original reaction under UV conditions were carried out for the same amount of stipulated time. The reactions were then quenched and worked-up following the general acidic workup procedure. As standard practice, a small sample of the crude material was analysed by ^1H NMR and then purified by column chromatography using silica gel to yield the stated products or recovery of the starting material.

3. Blank reaction without 4.1.15 with UV exposure

Samples were prepared in the glovebox and dissolved in degassed, anhydrous DMF (7 mL). Both the SED-free blank reaction and the original reaction under UV conditions were carried out for the same duration of stipulated time. The reactions were then quenched and worked-up following the general acidic workup procedure. As standard practice, a small sample of the crude material was analysed by ^1H NMR with the main crude product taken onto purification by column chromatography using silica gel to yield the stated products or recovery of the starting material.

4. General acidic work up

After the reaction, the mixture was carefully quenched with a few drops of 2N HCl. Then, the reaction mixture was poured into a 50 mL separating funnel containing 2N HCl (15 mL) and organic solvent-usually Et_2O (20 mL, unless otherwise stated). The aqueous layer was extracted thrice (3 x 20 mL) and the organic extracts were

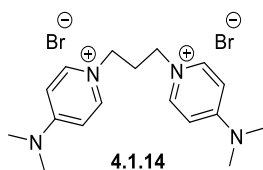
combined, washed with brine, dried over anhydrous Na₂SO₄ and filtered. The solvent was then removed under reduced pressure to obtain the crude material

5. Esterification or amidation using oxalyl chloride

All glassware used in the reaction was dried in the oven overnight. A round-bottomed flask was charged with the carboxylic acid, dissolved or diluted with dry CH₂Cl₂, sealed and left under a steady stream of argon. The reaction was cooled to 0 °C using an ice bath whereupon oxalyl chloride was added slowly. A few drops of dry DMF was added slowly, during which efferverscence was observed. When the efferverscence ceased, the reaction was stirred for 10 min (unless otherwise stated) at 0 °C whereupon the amine or alcohol was added as a solution in CH₂Cl₂. Pyridine was then added and the reaction was left to warm to room temperature.

7.3 Experimental for Chapter 5.1

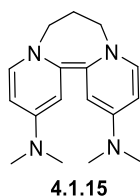
Synthesis of 1,3-bis(*N,N*-dimethyl-4-aminopyridinium)propane dibromide 4.1.14



N,N-Dimethyl-4-aminopyridine (5.33 g, 43.6 mmol) was added to an oven-dried round-bottomed flask and then dissolved in acetonitrile (60 mL). The resulting suspension was stirred at room temperature for 5 min and 1,3-dibromopropane (2.0 ml, 19.8 mmol) was added in one portion. The reaction mixture was heated under reflux for 18 h during which a colourless solution was formed. The solution was cooled to room temperature and Et₂O (40 mL) was added and a white solid formed. The white solid was filtered under vacuum and then dried under reduced pressure at 100 °C for 18 h to give the desired compound 1,3-bis(*N,N*-dimethyl-4-aminopyridinium)propane dibromide **4.1.14** (8.80 g, 99%).¹³⁹ [Found: (ESI⁺) (M-Br)⁺ 365.1338 and 367.1317. [M]⁺ 315.9460. C₁₇H₂₆BrN₄ (M-Br) requires 365.1336 and 367.1315); M.pt. 199-203 °C (lit. 199-203 °C)¹³⁹; ν_{\max} (KBr disc)/cm⁻¹ 3443, 3381, 3027, 2725, 2466, 1653, 1539, 1451, 1175, 1073, 1037, 946, 817, 766; δ_{H} (400 MHz, DMSO-d₆) 2.35 (2H, quintet, *J* 8.0), 3.19 (12H, s), 4.26 (4H, t, *J* 8.0), 7.05 (4H,

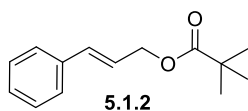
d, J 8.0), 8.32 (4H, d, J 8.0); δ_C (125 MHz, DMSO- d_6) 31.2, 40.0, 53.7, 108.0, 142.0, 155.8; The compound data was consistent with the reported analytical data.¹³⁹

Synthesis of *N,N,N',N'*-Tetramethyl-7,8-dihydro-6H-dipyrido[1,2-a;2',1'-c][1,4]diazepine-2,12-diamine **4.1.15**



A mixture of 1,3-bis(*N,N'*-dimethyl-4-aminopyridinium)propane dibromide **4.1.14** (5 g, 11.2 mmol) and NaH (60% dispersed in mineral oil, 1.8 g, 44.8 mmol) was placed under argon in a Schlenk flask equipped with a dry-ice cooler. The mixture was washed with dry hexane (3 x 50 mL) and then dried under reduced pressure for 1 h before backfilling with argon. Ammonia gas was then condensed (150 mL) onto the stirring suspension and the reaction left under reflux for 4 h, after which the ammonia was allowed to evaporate overnight. The Schlenk flask was then transferred to a glovebox and the desired solid was extracted with generous amounts of diethyl ether. The solvent was removed under reduced pressure to afford *N,N,N',N'*-Tetramethyl-7,8-dihydro-6H-dipyrido[1,2-a;2',1'-c][1,4]diazepine-2,12-diamine **4.1.15** as a purple-black, moisture-sensitive and oxygen-sensitive powder (2.51g, 80 %). δ_H (500 MHz, C_6D_6) 0.96 (2H, quintet, J 8.0), 2.46 (12H, s), 3.01 (4H, t, J 8.0), 4.92 (2H, d, J 8.0), 5.16 (2H, bs), 5.62 (2H, d, J 8.0); δ_C (125 MHz, C_6D_6) 24.5, 40.8, 52.6, 95.8, 96.2, 116.0, 138.7, 143.7. The compound data were consistent with the reported analytical data.²¹⁸

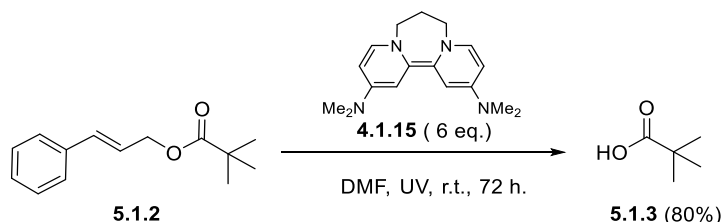
Synthesis of cinnamyl pivalate **5.1.2**



Cinnamyl alcohol (300 mg, 2.24 mmol) was dissolved in anhydrous CH_2Cl_2 (50 mL) in an oven-dried 100 mL round-bottomed flask. The resulting solution was then

cooled to 0 °C and NaH (60% dispersion in mineral oil, 110.0 mg, 2.70 mmol) was added under argon. The suspension was stirred at 0 °C for 0.5 h and then warmed to room temperature. Pivaloyl chloride (0.28 mL, 3.40 mmol) and pyridine (0.30 mL, 3.40 mmol) were then added to the reaction mixture. The reaction was stirred for 72 h, quenched with H₂O (40 mL) and then extracted with CH₂Cl₂ (3 x 30 mL). The organic extracts were combined, washed with brine (50 mL), dried over Na₂SO₄, filtered and then concentrated under reduced pressure to yield a yellow oil. The product was then purified by column chromatography on silica gel (5 % EtOAc/Hexane) to afford cinnamyl pivalate **5.1.2** as a colourless oil (390.8 mg, 80 %). ν_{\max} (neat/cm⁻¹) 2872, 2340, 1724, 1479, 1396, 1278, 1141, 1029, 962, 742, 690; δ_{H} (400 MHz, CDCl₃) 1.25 (9H, s), 4.73 (2H, d, *J* 6.3), 6.30 (1H, dt, *J* 16.2, 1.5), 6.65 (1H, m), 7.28 (1H, m), 7.34 (2H, t, *J* 7.5), 7.40 (2H, d, *J* 7.5); δ_{C} (125 MHz, CDCl₃) 27.2, 38.8, 64.9, 123.6, 126.6, 128.0, 128.6, 133.6, 136.4, 178.4; (GCMS EI) 218 (M⁺, 10 %), 117.5 (60), 95.3 (100), 57.4 (70).²¹⁹The compound data were consistent with reported data.²²⁰

Reduction of cinnamyl pivalate **5.1.2** with **4.1.15**

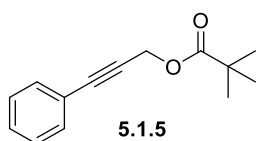


The general procedure for UV-activated reductions was applied to the substrate (100 mg, 0.45 mmol) using SED **4.1.15** (785 mg, 3.0 mmol) for 72 h at room temperature. The reaction mixture was then subjected to the general acidic workup procedure and the resulting crude material was purified by column chromatography to afford pivalic acid **5.1.3** as a white solid (37 mg, 80 %). 33-35 °C; (lit.: 34 °C)²²¹; [Found: (HNESP⁺)(M)⁺ 102.0675. C₅H₁₀O₂ (M) requires 102.0675]; ν_{\max} (neat) /cm⁻¹ 3400, 2965, 1718, 1400, 1322, 78; δ_{H} (400 MHz, CDCl₃) δ 1.24 (9H, s, (CH₃)₃); δ_{C} (125 MHz, CDCl₃) 27.1, 38.7, 185.6. The spectral data were consistent with the literature data.²²¹

The UV-activated reduction of **5.1.2** was repeated with pivalic acid obtained as a white solid (39 mg, 84 %).

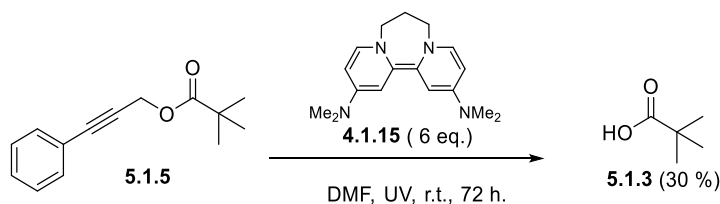
Blank reactions: i) SED-free, UV-active and ii) SED (6 eq.), UV-free experiments were performed following the general procedure. For the first blank reaction, the starting material **5.1.2** was recovered (96 mg, 96 %). For the second blank reaction, the starting material **5.1.2** was recovered (90 mg, 90 %). The spectral data for the starting material **5.1.2** were previously reported.

Synthesis of 3-phenylprop-2-yn-1-yl pivalate **5.1.5**



A solution of 3-phenyl-2-propyn-1-ol **5.1.4** (0.90 ml, 7.3 mmol) in CH₂Cl₂ (30 mL), pivaloyl chloride (1.0 mL, 8.1 mmol), and pyridine (0.7 mL, 8.1 mmol) were used to carry out the esterification following the general procedure. The product was purified by column chromatography on silica gel (25 % CH₂Cl₂/hexane) to afford 3-phenylprop-2-yn-1-yl pivalate **5.1.5** as a colourless oil (1.25 g, 80 %). [Found [M+NH₄]⁺ 234.1490, C₁₄H₂₀NO₂ (M+NH₄)⁺ requires 234.1389]; ν_{\max} (neat/cm⁻¹) 3057, 2936, 1732, 1479, 1276, 1070, 1031, 756, 690, 651; δ_{H} (500 MHz, CDCl₃) 1.26 (9H, s), 4.90 (2H, s), 7.31-7.33 (3H, m), 7.45-7.47 (2H, m); δ_{C} (125 MHz, CDCl₃) 26.6, 38.3, 52.3, 82.8, 85.6, 121.8, 127.8, 128.2, 131.4, 177.3.

Reduction of 3-phenylprop-2-yn-1-yl pivalate **5.1.5** with **4.1.15**



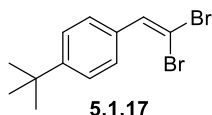
The general procedure for UV-activated reductions was applied to the substrate (108 mg, 0.50 mmol) using SED **4.1.15** (853 mg, 3.0 mmol) for 72 h at room temperature. The reaction mixture was then subjected to the general acidic workup procedure and the resulting crude material was purified by column chromatography (30 %

EtOAc/hexane) to afford pivalic acid **5.1.3** as a white solid (15.3 mg, 30 %) with spectral data previously reported.

The UV-activated reduction of **5.1.5** was repeated with pivalic acid **5.1.3** obtained as a white solid (15.0 mg, 30 %) with spectral data previously reported.

Blank reaction: SED (6 eq.), UV-free was performed following the general procedure and the starting material **5.1.5** was recovered (97 mg, 90 %) with a trace of pivalic acid **5.1.3** as a white solid (< 2 mg, ~3 %) The spectral data for both compounds were previously reported.

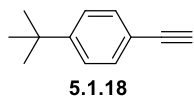
Synthesis of 1-*tert*-butyl-4-(2,2-dibromovinyl)benzene **5.1.17**



Tetrabromomethane (4.80 g, 14.5 mmol) was dissolved in CH₂Cl₂ (10 mL) in an oven-dried round-bottomed flask charged with argon. A solution of triphenylphosphine (6.35 g, 24.2 mmol) in CH₂Cl₂ (20 mL) was then added dropwise to the tetrabromomethane solution at 0 °C. The solution gradually turned from colourless to bright orange. The solution was left to stir at 0 °C for 10 min. A solution of 4-*tert*-butylbenzaldehyde (1.62 mL, 9.70 mmol) in CH₂Cl₂ (10 mL) was then added dropwise to the reaction mixture and then gradually warmed to room temperature, when it was left to stir for 48 h. The reaction mixture was then partitioned between CH₂Cl₂ (80 mL) and H₂O (100 mL). The aqueous fraction was extracted further with CH₂Cl₂ (3 x 40 mL). The organic fractions were combined, washed with 2N NaOH (3 x 50 mL), brine (50 mL) dried over anhydrous Na₂SO₄, filtered and then concentrated under reduced pressure to yield a yellow oil. The product was then purified using silica gel column chromatography (100 % hexane) to give 4-*tert*-butyl (2,2-dibromovinyl)benzene **5.1.17** as a yellow oil (2.76 g, 95 %). [Found [M]⁺ 315.9460 and 317.9438. C₁₂H₁₄Br₂ (M)⁺ requires 315.9457 and 317.9435]; ν_{\max} (neat/cm⁻¹) 2960, 2902, 2866, 1510, 1463, 1406, 1363, 1269, 1109, 875, 781, 667; δ_{H} (500 MHz, CDCl₃) 1.33 (9H, s), 7.40 (2H, d, *J* 8.5), 7.46 (1H, s),

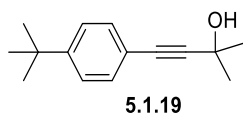
7.50 (2H, d, J 8.4); δ_{C} (125 MHz, CDCl_3) 31.2, 34.8, 88.5, 125.3, 128.2, 132.4, 136.7, 151.8.

Synthesis of *tert*-butyl-4-ethynylbenzene **5.1.18**



4-*tert*-butyl (2,2-dibromovinyl)benzene **5.1.17** (112.0 mg, 0.35 mmol) was dissolved in anhydrous THF (10 mL) and cooled to $-78\text{ }^{\circ}\text{C}$. Freshly titrated $n\text{-BuLi}$ (0.48 mL, 2.22 M in hexanes) was then added dropwise and the mixture was stirred at $-78\text{ }^{\circ}\text{C}$ for 2 h after which it was warmed to $0\text{ }^{\circ}\text{C}$ and quenched dropwise with H_2O (5 mL). The mixture was then warmed to room temperature whereupon the reaction mixture was extracted with Et_2O (3 x 10 mL). The organic fractions were combined, washed with brine (20 mL), dried over Na_2SO_4 and filtered and the solvent was removed under reduced pressure to afford *tert*-butyl-4-ethynylbenzene **5.1.18** as a colourless oil (33.5 mg, 65 %). m/z (EI) 143.07 ($[\text{M}-\text{CH}_3]^+$, 100 %), 158.02 ($[\text{M}+\text{H}]^+$, 20); ν_{max} ($\text{neat}/\text{cm}^{-1}$) 3298, 2960, 2927, 2870, 2150, 1606, 1502, 1462, 1363, 1269, 1201, 1105, 1016, 833, 739, 632. 603; δ_{H} (500 MHz, CDCl_3) 1.32 (9H, s), 3.03 (1H, s), 7.35 (2H, d, J 8.5), 7.43 (2H, J 8.5); δ_{C} (125 MHz, CDCl_3) 31.2, 34.8, 76.4, 83.8, 119.1, 124.9, 131.9, 152.1. The compound data were consistent with the reported data.²²²

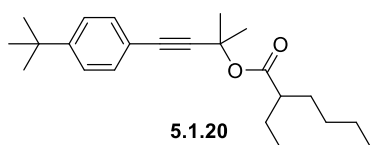
Synthesis of 4-(4-*tert*-butylphenyl)-2-methylbut-3-yn-2-ol **5.1.19**



A solution of *tert*-butyl-4-ethynyl benzene **5.1.18** (20.0 mg, 0.13 mmol) in anhydrous THF (10 mL) was cooled to $-78\text{ }^{\circ}\text{C}$ and $n\text{-BuLi}$ (0.70 mL, 2.33 M in hexanes) was added dropwise using a micro syringe. The reaction was then allowed to warm to $-10\text{ }^{\circ}\text{C}$ during which the solution turned from colourless to yellow. The reaction mixture was left at $-10\text{ }^{\circ}\text{C}$ for 10 min and then cooled to $-78\text{ }^{\circ}\text{C}$. In a separate still, acetone was freshly distilled over K_2CO_3 and then delivered to the reaction mixture dropwise (0.46 mL, 0.63 mmol). The yellow solution gradually turned orange. The reaction mixture was left to stir at room temperature for 16 h and then quenched with

saturated NH_4Cl solution (30 mL). The quenched mixture was then extracted with Et_2O (4 x 10 mL). The organic fractions were combined, washed with brine (2 x 20 mL) dried over anhydrous Na_2SO_4 , filtered and then concentrated under reduced pressure to yield a yellow oil. The product was then purified by column chromatography on silica gel (10 % EtOAc /hexane) to afford 4-(4-*tert*-butylphenyl-2-methylbut-3-yn-2-yl) 2-ethylhexanoate **5.1.19** as a colourless oil (20.0 mg, 70 %). [Found: $[\text{M}]^+$ 216.1511. $\text{C}_{15}\text{H}_{20}\text{O}$ (M^+) requires 216.1509]; $\nu_{\text{max}}(\text{neat}/\text{cm}^{-1})$ 3344, 2962, 2868, 2231, 1656, 1508, 1462 1363, 1269, 1109, 875, 781, 667; δ_{H} (400 MHz, CDCl_3) 1.31 (9H, s), 1.62 (6H, s), 7.33 (4H, m); δ_{C} (125 MHz, CDCl_3) 31.2, 31.6, 34.7, 65.7, 82.2, 93.1, 119.7, 125.2, 131.3, 151.5.

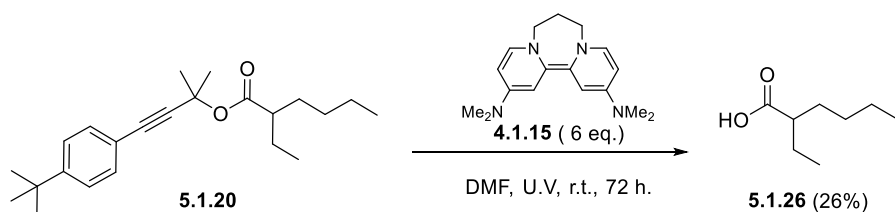
Synthesis of 4-(4-*tert*-butyl)phenyl-2-methylbut-3yn-2-yl 2-ethylhexanoate **5.1.20**



A solution of 4-(4-*tert*-butylphenyl-2-methylbut-3-yn-2-yl) **5.1.19** (120.0 mg, 0.56 mmol) was dissolved in anhydrous CH_2Cl_2 (15 mL) and NaH (60 % dispersion in mineral oil, 34.0 mg, 0.84 mmol) was added in one portion. The reaction mixture was then left to stir at room temperature for 0.5 h. In a separate 50 mL oven-dried round-bottomed flask, 2-ethylhexanoyl chloride (0.12 mL, 0.62 mmol) was dissolved in pyridine (0.2 mL) and then cannulated into the reaction mixture. *N,N*-dimethyl-4-aminopyridine (75.6 mg, 0.62 mmol) was then added in one portion to the reaction. The reaction mixture was left to stir at room temperature for 4 h. TLC profile revealed mainly starting materials so another portion of 2-ethylhexanoyl chloride (0.12 mL, 0.62 mmol), pyridine (2 mL), *N,N*-dimethyl-4-aminopyridine (75.6 mg, 0.62 mmol) were added. The reaction mixture was left to stir for 16 h after which it was quenched with H_2O (50 mL) and extracted with EtOAc (4 x 30 mL). The organic layers were combined, washed with brine (20 mL), dried over Na_2SO_4 , filtered and then concentrated under reduced pressure to yield a green oil. The crude was azeotroped with toluene (4 x 20 mL) and then purified by column chromatography on silica gel (3 % EtOAc /hexane) to afford 4-(4-*tert*-butyl)phenyl-2-methylbut-3yn-2-yl 2-ethylhexanoate **5.1.20** as a colourless oil (101.0 mg, 50 %).

[Found: $[M+NH_4]^+$ 360.2897. $C_{23}H_{38}NO_2$ ($M+NH_4$) $^+$ requires 360.2897]; ν_{max} (neat/ cm^{-1}) 2960, 2933, 2231, 1739, 1506, 1462, 1361, 1178, 1114, 833; δ_H (400 MHz, $CDCl_3$) 0.89-0.94 (6H, m), 1.44 (13H, bs), 1.51-1.53 (4H, m), 1.64 (6H, s), 2.22-2.24 (1H, m), 7.32 (4H, m); δ_C (125 MHz, $CDCl_3$) 11.3, 13.4, 22.1, 25.2, 28.7, 29.0, 30.7, 31.4, 34.2, 47.3, 71.7, 83.4, 89.3, 119.4, 124.6, 130.9, 150.9, 174.1.

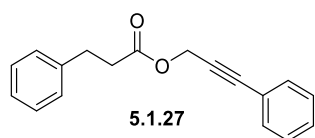
Reduction of 4-^tbutyl-phenyl-2-methylbut-3-yn-2-yl 2-ethylhexanoate **5.1.20** with **4.1.15**



The general procedure for UV-activated reductions was applied to the substrate (85 mg, 0.25 mmol) using **4.1.15** (427 mg, 1.5 mmol) for 72 h at room temperature. The reaction mixture was then subjected to the general acidic workup procedure and the resulting crude material was purified by column chromatography to afford 2-ethylhexanoic acid **5.1.26** as a colourless oil (9.3 mg, 26 %); δ_H (400 MHz, $CDCl_3$) 0.90 (3H, m), 0.95 (3H, t, J 7.5), 1.31 (4H, bs), 1.50-1.51 (2H, m), 1.64-1.65 (2H, m), 2.26-2.32 (1H, m); δ_C (125 MHz, $CDCl_3$) 11.3, 13.9, 22.1, 25.1, 29.5, 31.4, 47.1, 183.1. The compound data were consistent with the reported data.²²³

The UV-activated reduction of **5.1.20** was repeated with 2-ethylhexanoic acid **5.1.26** obtained as a colourless oil (9.8 mg, 27 %).

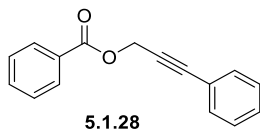
Synthesis of 3-phenylprop-2-yn-1 3-phenylpropanoate **5.1.27**



Hydrocinnamic acid (1.66 mmol, 250 mg) was dissolved in anhydrous CH_2Cl_2 (20 mL). Oxalyl chloride (2.16 mmol, 0.20 mL) was then added to the reaction mixture and then cooled to 0 °C whereupon 2 drops of anhydrous DMF were added. Initial vigorous effervescence was observed and the reaction mixture was left to stir at 0 °C

for 1 h, during which the bubbling ceased. Solvent was then removed from the reaction mixture under reduced pressure to afford the corresponding acid chloride which was then immediately used for esterification following the general procedure with 3-phenyl-2-propyn-1-ol (0.23 mL, 1.83 mmol) in CH₂Cl₂ (15 mL), and pyridine (0.15 mL, 1.83 mmol.). The reaction mixture was left to stir for 16 h after which it was quenched with H₂O (50 mL) and extracted with EtOAc (4 x 30 mL). The organic layers were combined, washed with brine (20 mL), dried over Na₂SO₄, filtered and then concentrated under reduced pressure. The crude product was purified by column chromatography on silica gel (30 % CH₂Cl₂/hexane) to afford 3-phenylprop-2-yn-1 3-phenylpropanoate **5.1.27** as a yellow oil (348 mg, 80 %). [Found [M+NH₄]⁺ 282.1491. C₁₈H₂₀NO₂ (M+NH₄)⁺ requires 282.1489]; ν_{\max} (neat/cm⁻¹) 3061, 3028, 2933, 2235, 1737, 1599, 1489, 1377, 1141, 952, 754; δ_{H} (500 MHz, CDCl₃) 2.73 (2H, t, *J* 7.7), 3.01 (2H, t, *J* 7.4), 4.93 (2H, s), 7.21-7.36 (8H, m), 7.46-7.48 (2H, m); δ_{C} (125 MHz, CDCl₃) 30.9, 35.7, 52.8, 82.9, 86.5, 111.1, 126.3, 128.3, 128.4, 128.5, 128.8, 131.9, 140.3, 172.2. The compound data were consistent with the reported data.²²⁴

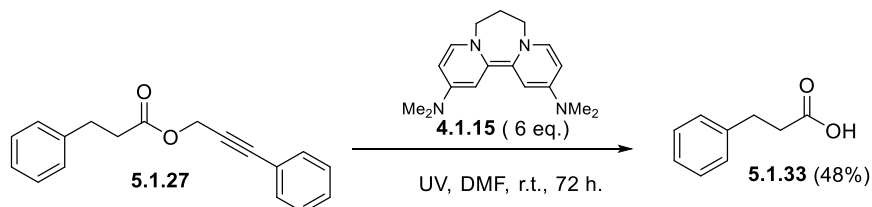
Synthesis of 3-phenylpropyn-benzoate **5.1.28**



A solution of 3-phenyl-2-propyn-1-ol (0.14 mL, 1.14 mmol) in CH₂Cl₂ (15 mL), benzoyl chloride (0.16 mL, 1.36 mmol), and pyridine (0.10 mL, 1.25 mmol) were used to carry out the esterification following the general procedure. The reaction mixture was left to stir for 16 h after which it was quenched with H₂O (50 mL) and extracted with EtOAc (4 x 30 mL). The organic layers were combined, washed with brine (20 mL), dried over Na₂SO₄, filtered and then concentrated under reduced pressure. The crude product was purified by column chromatography on silica gel (30 % CH₂Cl₂/hexane) to afford 3-phenylpropyn-benzoate **5.1.28** as a colourless oil (188 mg, 70 %). ν_{\max} (neat/cm⁻¹) 3034, 2939, 2229, 1720, 1489, 1261, 1093, 1026, 756, 688; δ_{H} (500 MHz, CDCl₃) 5.17 (2H, s, CH₂), 7.32-7.34 (3H, m, ArH), 7.45-7.49 (4H, m, ArH), 7.57-7.61 (1H, m, ArH), 8.11 (2H, d, *J* 7.2, ArH); δ_{C} (125 MHz,

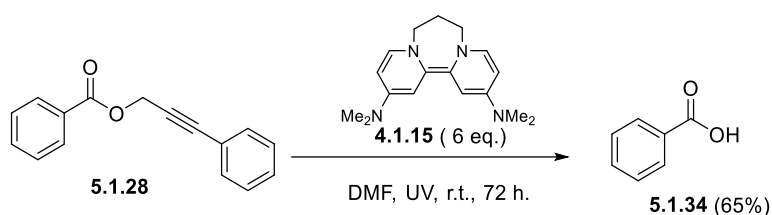
CDCl₃) 52.8, 82.5, 86.1, 121.7, 127.8, 127.9, 128.2, 129.1, 129.3, 131.3, 132.7, 165.4; GCMS (CI, CH₄) 258.0 ([M+Na]⁺, 100%); The compound data were consistent with the reported data.²²⁵

Reduction of 3-phenylprop-2-yn-1 3-phenylpropanoate **5.1.27** with **4.1.15**



The general procedure for UV-activated reductions was applied to the substrate (100 mg, 0.38 mmol) using SED **4.1.15** (648 mg, 2.3 mmol) for 72 h at room temperature. The reaction mixture was then subjected to the general acidic workup procedure and the resulting crude material was purified by column chromatography to afford hydrocinnamic acid **5.1.33** as a yellow oil (28.2 mg, 48 %). ν_{\max} (neat/cm⁻¹) 3028, 2953, 2933, 2860, 2779, 2358, 1693, 1408, 1301, 1219, 929, 700 (no OH stretch was observed); δ_{H} (500 MHz, CDCl₃) 2.70 (2H, t, *J* 7.8), 2.98 (2H, t, *J* 7.8), 7.21-7.32 (5H, m); δ_{C} (125 MHz, CDCl₃) 30.6, 35.5, 126.4, 128.3, 128.6, 140.2, 178.5; *m/z* (ESI) 149.0 ([M-H]⁻, 100 %); The compound data were consistent with the reported data.²²⁶

Reduction of 3-phenylpropyn-benzoate **5.1.28** with **4.1.15**

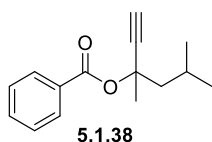


The general procedure for UV-activated reductions was applied to the substrate (117 mg, 0.50 mmol) using SED **4.1.15** (853 mg, 3.0 mmol) for 72 h at room temperature. The reaction mixture was then subjected to the general acidic workup procedure and the resulting crude material was purified by column chromatography to afford benzoic acid **5.1.34** as a white solid (39.5 mg, 65 %). M.pt. 120-121 °C (lit. 121-122 °C)²²⁷; ν_{\max} (powder/cm⁻¹) 3070, 2956, 2893, 2848, 2555, 2341, 1682, 1600, 1583,

1452, 1421, 1323, 1288, 1180, 1128, 1072, 1026, 931, 804, 667, 551 (no OH stretch was observed); δ_{H} (500 MHz, CDCl_3) 7.50 (2H, t, J 7.5), 7.63 (1H, t, J 7.5), 8.12 (2H, d, J 7.8); δ_{C} (125 MHz, CDCl_3) 128.5, 129.2, 130.2, 133.7, 170.6; m/z (ESI) 121.00 ($[\text{M}-\text{H}]^-$, 100 %), 76.87 ($[\text{M}-\text{CO}_2]^-$, 10). The compound data were consistent with the reported data.²²⁷

Blank reactions: i) SED-free, UV-active and ii) SED (6 eq.), UV-free experiments were performed following the general procedure. For the first blank reaction, the starting material **5.1.38** was recovered (112 mg, 96 %). For the second blank reaction, the starting material **5.1.38** was recovered (113 mg, 95 %) The spectral data for the starting material **5.3.22** was previously reported.

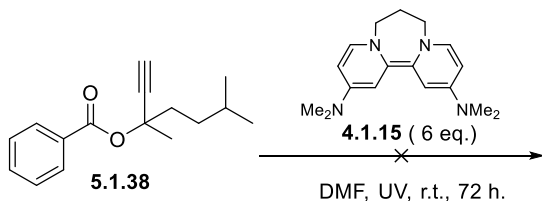
Synthesis of 3,5-dimethylhex-1-yn-3-yl benzoate **5.1.38**



A suspension of NaH (60 %, 485 mg, 12.0 mmol) in dry THF (10 mL) was treated dropwise with a 15 mL solution of 3,6-dimethylhept-1-yn-3-ol (1.0 g, 8 mmol) in dry THF at 0 °C. The resulting slurry was warmed to room temperature whereupon benzoyl chloride (1.24 g, 8.8 mmol) was added. 4-DMAP (1.0 g, 8.8 mmol) was added to the reaction mixture and then left to stir at room temperature for 16 h. The reaction was then cooled to 0 °C and then quenched with H_2O . The quenched mixture was then partitioned between CH_2Cl_2 (40 mL) and H_2O (80 mL). The organic phase was collected and the aqueous layer was extracted further with CH_2Cl_2 (2 x 30 mL). The organic extracts were combined, washed with brine and dried over Na_2SO_4 . The suspension was filtered and the solvent was removed under reduced pressure. The resulting crude was purified by column chromatography (3 % EtOAc/hexane) to afford 3,6-dimethylhept-1-yn-3-yl benzoate **5.1.38** as a colourless oil (780 mg, 40 %). [Found: (HNESP⁺) $[\text{M}+\text{H}]^+$ 231.1383. $\text{C}_{15}\text{H}_{19}\text{O}_2$ requires 231.1380]; ν_{max} (neat/ cm^{-1}) 3302, 2954, 2250, 1720, 1450, 1263, 1095, 707; δ_{H} (500 MHz, CDCl_3) 1.00-1.09 (6H, m, 2 x CHCH_3), 1.87 (3H, s, CCH_3), 1.92 (1H, m, CH_2CH), 2.02-2.12 (2H, m, $(\text{C})\text{CH}_2$) 2.62 (1H, s, CH), 7.43 (2H, t, J 7.6, ArH), 7.55 (1H, t, J 7.6, ArH), 8.01 (2H,

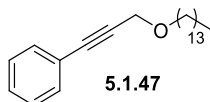
d, J 7.6, ArH); δ_C (125 MHz, $CDCl_3$) 23.4, 23.6, 24.4, 26.8, 49.3, 73.2, 75.1, 83.6, 127.8, 129.0, 130.5, 132.3, 164.3.

Attempted reduction of 3,4-dimethylhex-1-yn-3-yl benzoate **5.1.38** with **4.1.15**



The general procedure for UV-activated reductions was applied to the substrate (114 mg, 0.5 mmol) using SED **4.1.15** (853 mg, 3.0 mmol) for 72 h at room temperature. The reaction mixture was then removed from the UV setup and then subjected to the general acidic workup procedure. 1H NMR analysis of the crude showed only starting material as the sole product. The crude was then purified by column chromatography (2 % EtOAc/hexane) to yield the starting material **5.1.38** (82 mg, 89 %). The spectral data were as previously reported.

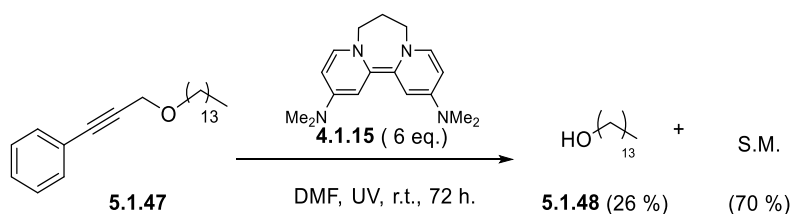
Synthesis of (3-(tetradecyloxy)prop-1-yn-1-yl)benzene **5.1.47**



Sodium hydride (60 % in mineral oil, 10.0 mmol) was washed with anhydrous hexane, dried and then suspended in anhydrous THF (20 mL) in an oven-dried round-bottomed flask. The suspension was then cooled to 0 °C whereupon a solution of 3-phenyl-2-propyn-1-ol **5.1.4** (0.93 mL, 7.57 mmol) in anhydrous THF (20 mL) was added dropwise. The resulting brown suspension was stirred at room temperature for 0.5 h whereupon 1-bromotetradecane (2.31 g, 8.33 mmol) was added in one portion. The reaction mixture was refluxed at 80 °C for 16 h. After this time, the reaction mixture was cooled to room temperature, filtered and the reaction flask was rinsed with Et_2O (3 x 20 mL). Solvent was removed from the orange filtrate under reduced pressure to yield an orange oil which was then partitioned between Et_2O (50 mL) and H_2O (30 mL). The organic layer was washed with more H_2O (2 x 20 mL), brine (30 mL), dried over anhydrous Na_2SO_4 , filtered and solvent removed

under reduced pressure to give an orange oil. The resulting product was purified by column chromatography on silica gel (5 % EtOAc/hexane) to afford (3-(tetradecyloxy)prop-1-yn-1-yl)benzene **5.1.47** as a colourless oil (1.50 g, 60 %). [Found $[M+NH_4]^+$ 346.3102. $C_{23}H_{40}NO$ ($M+NH_4$)⁺ requires 346.3104]; ν_{max} (neat/cm⁻¹) 2922, 2852, 2200, 1599, 1489, 1465, 1442, 1354, 1255, 1099, 1028, 1001, 912, 754, 721, 690; δ_H (500 MHz, CDCl₃) 0.90 (3H, t, *J* 6.9), 1.26-1.39 (22H, m), 1.64 (2H, quintet, *J* 6.8), 3.58 (2H, t, *J* 6.8), 4.37 (2H, s), 7.30-7.32 (3H, m, *ArH*), 7.44-7.47 (2H, m, *ArH*); δ_C (125 MHz, CDCl₃) 13.6, 22.2, 25.6, 28.8, 28.9, 29.0, 29.1, 29.2, 31.4, 58.3, 69.9, 85.0, 85.4, 122.3, 127.7, 127.8, 131.3.

Reduction of 3-(tetradecyloxy)prop-1-yn-1-yl)benzene **5.1.47** with **4.1.15**



The general procedure for UV-activated reductions was applied to the substrate (150 mg, 0.5 mmol) using SED **4.1.15** (853 mg, 3.0 mmol) for 72 h at room temperature. The reaction mixture was then subjected to the general acidic workup procedure. The crude product was then purified by column chromatography on silica gel (5 % EtOAc/hexane) to afford the starting material **5.1.47** as a colourless oil (105 mg, 70 %) and tetradecanol **5.1.48** as a white solid (23 mg, 26 %). M.pt. 37-38 °C (lit.²²⁸ 38 °C); δ_H (500 MHz, CDCl₃) 0.88-0.90 (3H, m, *CH*₃), 1.20 (20H, m, 10 x *CH*₂), 1.60-1.67 (4H, m, *OCH*₂*CH*₂), 3.65 (2H, t, *J* 7.5, *OCH*₂); δ_C (125 MHz, CDCl₃) 13.6, 22.2, 25.2, 28.8, 28.9, 29.1, 29.2, 29.3, 31.4, 32.3, 62.6. The compound data were consistent with the reported data.²²⁹

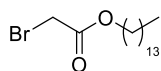
(3-(tetradecyloxy)prop-1-yn-1-yl)benzene **5.1.47**: The data were as previously reported.

Blank reactions: i) SED-free, UV-active and ii) SED (6 eq.), UV-free experiments were performed following the general procedure. For the first blank reaction, the starting material **5.1.47** was recovered (87 mg, 98 %). For the second blank reaction,

the starting material **5.1.47** was recovered (84 mg, 95 %). The spectral data for the starting material **5.1.47** were previously reported.

7.4 Experimental for Chapter 5.2

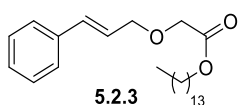
Synthesis of tetradecyl-2-bromoacetate 5.2.2



5.2.2

A mixture of tetradecanol (10.7 g, 50 mmol), bromoacetic acid (6.9 g, 50 mmol) and *p*-toluenesulfonic acid (100 mg, 0.5 mmol) were dissolved in benzene (200 mL). The resulting solution was warmed to reflux and water was constantly removed by attaching a Dean-Stark apparatus. The reaction mixture was cooled to room temperature after 16 h and the solvent was removed under reduced pressure. The crude material was partitioned between Et₂O (50 mL) and sat. NaHCO₃ (100 mL). The organic phase was collected and the aqueous layer was extracted further with Et₂O (2 x 40 mL). washed with brine (150 mL) and dried over Na₂SO₄. The suspension was filtered and the solvent was removed under reduced pressure to afford tetradecyl-2-bromoacetate **5.2.2** as a colourless oil (16.7 g, 99 %). [Found: (HNESP⁺) [M+NH₄]⁺ 352.1852 and 354.1829. C₁₆H₃₅NO₂Br requires (M+NH₄)⁺ 352.1846 and 354.1829]; ν_{\max} (neat)/cm⁻¹ 2920, 2850, 1735, 1465, 1276, 1161, 1109, 719; δ_{H} (500 MHz, CDCl₃) 0.90 (3H, t, *J* 6.8, CH₂CH₃), 1.28 (22H, m, 11 x CH₂), 1.67 (2H, quintet, *J* 6.8, C(O)OCH₂CH₂), 3.85 (2H, s, C(O)CH₂Br), 4.19 (2H, t, *J* 6.8, C(O)OCH₂CH₂); δ_{C} (125 MHz, CDCl₃) 13.6, 22.1, 25.2, 25.4, 27.9, 28.6, 28.8, 28.9, 29.0, 29.1, 31.4, 65.9, 166.8.

Synthesis of tetradecyl-2-(cinnamyloxy)acetate 5.2.3

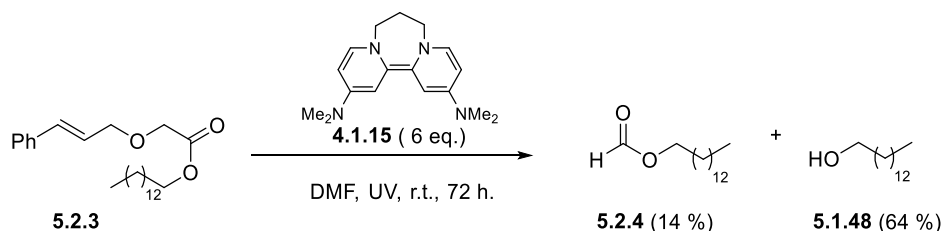


5.2.3

A solution of cinnamyl alcohol (800 mg, 6.0 mmol) in dry THF (10 mL) was added dropwise to a suspension of NaH (170 mg, 7.1 mmol) in dry THF (15 mL) at 0 °C. The reaction mixture was stirred at 0 °C for 0.5 h (during which the effervescence ceased) and then warmed to room temperature whereupon a solution of tetradecyl-2-bromoacetate (2.0 g, 6.0 mmol) in dry THF (10 mL) was added. The reaction

mixture was refluxed for 16 h, cooled to room temperature, quenched carefully with 2N HCl (10 mL) and then partitioned between Et₂O (30 mL) and 2N HCl (20 mL). The organic phase was collected and the aqueous layer was extracted further with Et₂O (2 x 20 mL). washed with brine (80 mL) and dried over Na₂SO₄. The suspension was filtered and the solvent was removed under reduced pressure. The crude was purified by column chromatography (15 % EtOAc/hexane) on silica gel to afford tetradecyl-2-(cinnamyloxy)acetate **5.2.3** as a pale yellow solid (1.2 g, 52 %). [Found:(APCI⁺) [M+NH₄]⁺ 406.3315. C₂₅H₄₀NO₃ requires (M+NH₄)⁺ 406.3316]; ν_{\max} (neat)/cm⁻¹ 3053, 2916, 2848, 2366, 1749, 1450, 1201, 1139, 966, 721, 692; δ_{H} (500 MHz, CDCl₃); 0.90 (3H, t, *J* 6.8, CH₃), 1.26-1.43 (22H, m, 11 x CH₂), 1.64 (2H, quintet, *J* 6.8, C(O)OCH₂CH₂), 4.13 (2H,s, C(O)CH₂O), 4.18 (2H, t, *J* 6.8, C(O)OCH₂CH₂), 4.28 (2H, dd, *J* 6.3, 1.3, ArCH=CHCH₂), 6.30 (1H, dt, *J* 16.0, 6.3, ArCH=CH), 6.61 (1H, d, *J* 16.0 Hz, ArCH=CH), 7.25-7.41 (5H, m, ArH); δ_{C} (125 MHz, CDCl₃) 14.1, 22.6, 25.8, 28.5, 29.2, 29.3, 29.4, 29.5, 29.6, 31.9, 65.0, 67.1, 72.0, 124.9, 126.5, 126.6, 128.7, 133.6, 136.4, 170.5.

Reduction of tetradecyl-2-(cinnamyloxy)acetate **5.2.3** with **4.1.15**



The general procedure for UV-activated reductions was applied to the substrate (140 mg, 0.5 mmol) using SED **4.1.15** (853 mg, 3.0 mmol) for 72 h at room temperature. The reaction mixture was then subjected to the general acidic workup procedure and the resulting crude material was purified by column chromatography (10 % EtOAc/hexane) to afford tetradecyl formate **5.2.4** (35 mg, 14 %) and tetradecanol **5.1.48** (57 mg, 64 %). ¹H NMR spectrum analysis of the crude material after workup had revealed complete conversion of the starting material.

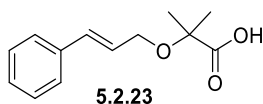
Tetradecyl formate **5.2.4**; colourless oil; [Found: (HNESP⁺) [M+H]⁺ 243.2315. C₁₅H₃₁O₂ (M+H)⁺ requires 243.2319]; ν_{\max} (neat)/cm⁻¹ 2923, 2853, 1729, 1466, 1378,

1165, 731; δ_{H} (500 MHz, CDCl_3) 0.90 (3H, t, J 7.0, CH_3), 1.28-1.35 (22H, m, 11 x CH_2), 1.66 (2H, quintet, J 7.0, $\text{COOCH}_2\text{CH}_2$), 4.18 (2H, t, J 7.0, COOCH_2), 8.08 (1H, s, CHO); δ_{C} (125 MHz, CDCl_3) 14.1, 22.7, 25.8, 28.5, 29.1, 29.3, 29.4, 29.5, 29.6, 31.9, 64.1, 161.2.

Tetradecanol **5.1.48**: The data were as previously reported.

Blank reaction: SED (6 eq.), UV-free experiment was performed following the general procedure. The starting material **5.2.3** was recovered as a pale yellow solid (84 mg, 90 %) along with tetradecanol **5.1.48** as a white solid (1.5 mg, 2 %). The spectral data for both compounds were as previously reported.

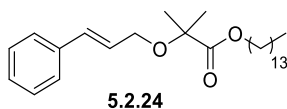
Synthesis of 2-(cinnamyloxy)-2-methylpropanoic acid **5.2.23**



The synthesis was conducted following the procedure reported by Murphy *et al.*²³⁰ Finely crushed 1,1,1-trichloro-2-methyl-2-propanol hemihydrate (5.6 g, 30 mmol) was dissolved in acetone (20 mL) whereupon finely crushed NaOH (4.8 g, 120 mmol) was added to the reaction 0 °C. The reaction was stirred for at 0 °C for 0.5 h, warmed to room temperature, whereupon a solution of cinnamyl alcohol (2.1 g, 15 mmol) in acetone (5 mL) was added. The reaction mixture was stirred at room temperature for 16 h after which the solvent was removed under reduced pressure. The crude material was partitioned between Et_2O (50 mL) and 2N HCl (80 mL). The organic phase was collected and the aqueous layer was extracted further with Et_2O (2 x 40 mL). washed with brine (100 mL) and dried over Na_2SO_4 . The suspension was filtered and the solvent was removed under reduced pressure. The crude was purified by column chromatography (40 % EtOAc /hexane) on silica gel to afford 2-(cinnamyloxy)-2-methylpropanoic acid **5.2.23** as a yellow viscous oil (14 %, 460 mg). ν_{max} (neat)/ cm^{-1} 3024 (br), 2981, 2933, 2868, 2625, 1708, 1697, 1631, 1601, 1452, 1386, 1288, 1200, 1118, 964, 735, 690; δ_{H} (400 MHz, CDCl_3) 1.57 (6H, s, 2 x CH_3), 4.20 (2H, dd, J 6.0, 1.5, OCH_2CH), 6.34 (1H, dt, J 16.0, 6.0, $\text{ArCH}=\text{CH}$), 6.65 (1H, d, J 16.0, $\text{ArCH}=\text{CH}$), 7.27 (1H, d, J 7.0, ArH), 7.30 (2H, t, J 7.0, 2 x ArH),

7.42 (1H, d, J 7.0, ArH); δ_C (125 MHz, CDCl₃) 23.7, 65.1, 77.3, 125.0, 126.1, 127.3, 128.0, 132.1, 136.0, 178.5; m/z (ESI) 218.80 ([M-H]⁻, 100 %). The material was used immediately in the next step of esterification.

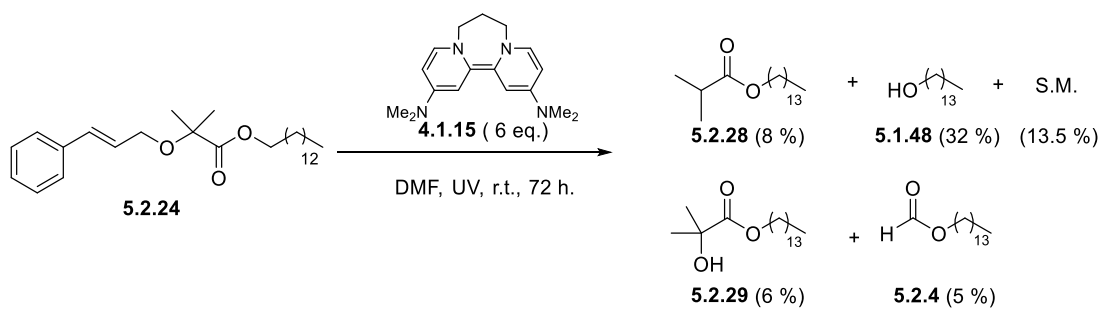
Synthesis of tetradecyl 2-(cinnamyloxy)-2-methylpropanoate **5.2.24**



The general procedure for the *in situ* generation of acyl chloride followed by esterification was employed.

Reagents: 2-(cinnamyloxy)-2-methylpropanoic acid **5.2.23** (400 mg, 1.8 mmol), oxalyl chloride (0.21 mL 2.4 mmol) and tetradecanol (429 mg, 2.0 mmol). The reaction mixture was stirred for 12 h and then partitioned between 2N HCl (20 mL) and CH₂Cl₂ (15 mL). The organic phase was collected and the aqueous layer was extracted further with CH₂Cl₂ (2 x 15 mL). The organic collections were combined, washed with brine (50 mL), dried over Na₂SO₄, filtered and solvent removed under reduced pressure. The crude was purified by column chromatography (5 % EtOAc/hexane) on silica gel to afford tetradecyl 2-(cinnamyloxy)-2-methylpropanoate **5.2.24** as a colourless oil (160 mg, 21 %). [Found: [M+NH₄]⁺ 434.3625. C₂₇H₄₈NO₃ (M+NH₄)⁺ requires 434.3629]; ν_{\max} (neat)/cm⁻¹ 3059, 2922, 2852, 1730, 1496, 1465, 1277, 1139, 1055, 963, 733, 690; δ_H (400 MHz, CDCl₃) 0.90 (3H, m, CH₂CH₃), 1.28 (22H, bs, 11 x CH₂), 1.51 (6H, s, 2 x CH₃), 1.70 (2H, quintet, J 6.5, C(O)OCH₂CH₂), 4.13-4.18 (4H, m, C(O)OCH₂ and OCH₂CH=CH), 6.33 (1H, dt, J 16.0, 6.5, ArCH=CH), 6.62 (1H, d, J 16.0, ArCH=CH), 7.24-7.40 (3H, m, ArH), 7.41 (2H, d, J 7.5, ArH); δ_C (125 MHz, CDCl₃) 13.6, 22.1, 22.2, 24.3, 25.5, 18.1, 28.7, 28.8, 29.0, 29.1, 29.2, 31.5, 64.7, 65.4, 77.3, 125.8, 126.0, 127.0, 127.9, 131.5, 136.4, 174.3.

Reduction of tetradecyl 2-(cinnamyloxy)-2-methylpropanoate **5.2.24** with **4.1.15**

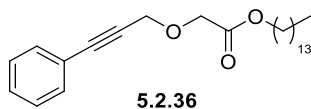


The general procedure for UV-activated reductions was applied to substrate **5.2.24** (155 mg, 0.4 mmol) using SED **4.1.15** (630 mg, 2.4 mmol) for 72 h at room temperature. The reaction mixture was then subjected to the general acidic workup procedure and the resulting crude material was purified by column chromatography (2-5 % EtOAc/hexane) to afford tetradecanol **5.1.48** (27.5 mg, 32 %), the starting material **5.2.24** (21 mg, 13.5 %), tetradecyl isobutyrate **5.2.28** (9 mg, 8 %), tetradecyl- 2-hydroxy-2-methyl propanoate **5.2.29** (7 mg, 6 %) and tetradecyl formate **5.2.4** (5 mg, 5 %) The spectral data for tetradecanol **5.1.48**, tetradecyl formate **5.2.4** and the starting material **5.2.24** were as previously reported.

Tetradecyl isobutyrate **5.2.28**: colourless oil; [Found: $[\text{M}+\text{H}]^+$ 285.2786, $\text{C}_{18}\text{H}_{37}\text{O}_2$ ($\text{M}+\text{H})^+$ requires 285.2788; ν_{max} (neat/ cm^{-1}) 2922, 2852, 1735, 1467, 1255, 1188, 1170, 1097; δ_{H} (400 MHz, CDCl_3) 0.91 (3H, t, J 7.0, CH_2CH_3), 1.18 (6H, d, J 7.0, 2 x CH_3), 1.28-1.30 (22H, m, 11 x CH_2), 1.64 (2H, quintet, J 7.0, $\text{C}(\text{O})\text{OCH}_2\text{CH}_2$), 2.56 (1H, septet, J 7.0, $\text{CH}(\text{C})(\text{CH}_3)_2$), 4.08 (2H, t, J 7.0, $\text{C}(\text{O})\text{OCH}_2$); δ_{C} (125 MHz, CDCl_3) 14.1, 19.0, 22.7, 25.1, 25.9, 28.6, 29.2, 29.3, 29.5, 29.6, 29.7, 31.9, 34.0, 64.4, 177.3.

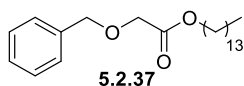
Tetradecyl- 2-hydroxy-2-methylpropanoate **5.2.29**; colourless oil; [Found: $[\text{M}+\text{H}]^+$ 301.2740, $\text{C}_{18}\text{H}_{37}\text{O}_3$ ($\text{M}+\text{H})^+$ requires 301.2737]; ν_{max} (neat/ cm^{-1}) 3537, 2922, 2852, 1726, 1465, 1377, 1359, 1263, 1179, 1147, 975, 767, 719; δ_{H} (400 MHz, CDCl_3) 0.91 (3H, t, J 7.0, CH_2CH_3), 1.28-1.30 (22H, m, 11 x CH_2), 1.45 (6H, s, 2 x CH_3), 1.68 (2H, quintet, J 7.0, $\text{C}(\text{O})\text{OCH}_2\text{CH}_2$), 3.12 (1H, s, OH), 4.19 (2H, t, J 7.0, $\text{C}(\text{O})\text{OCH}_2$), δ_{C} (125 MHz, CDCl_3) 13.6, 22.2, 25.3, 26.7, 28.0, 28.7, 28.8, 28.9, 29.0, 29.1, 29.2, 31.3, 65.5, 71.5, 177.1.

Synthesis of tetradecyl 2-((3-phenylprop-2-yn-1-yl)oxy)acetate **5.2.36**



A solution of 3-phenyl-2-propyn-1-ol (500 mg, 3.8 mmol) in dry THF (10 mL) was added dropwise to a suspension of NaH (100 mg, 4.2 mmol) in dry THF (15 mL) at 0 °C. The reaction mixture was stirred at 0 °C for 0.5 h (during which the effervescence ceased) and then warmed to room temperature, whereupon a solution of tetradecyl 2-bromoacetate **5.2.2** (1.4 g, 4.2 mmol) in dry THF (10 mL) was added. The reaction mixture was refluxed for 16 h, cooled to room temperature, quenched carefully with 2N HCl (10 mL) and then partitioned between Et₂O (50 mL) and 2N HCl (100 mL). The organic phase was collected and the aqueous layer was extracted further with Et₂O (2 x 40 mL), washed with brine (150 mL) and dried over Na₂SO₄. The suspension was filtered and the solvent was removed under reduced pressure. The crude was purified by column chromatography (40 % EtOAc/hexane) on silica gel to afford tetradecyl 2-((3-phenylprop-2-yn-1-yl)oxy)acetate **5.2.36** as a colourless oil (984 mg, 67 %). [Found:(HNESP⁺) [M+H]⁺ 387.2896. C₂₅H₃₉O₃ requires (M+H)⁺ 387.2894]; ν_{\max} (neat)/cm⁻¹ 2914, 2848, 2210, 1751, 1600, 1471, 1213, 1130, 759, 692; δ_{H} (500 MHz, CDCl₃); 0.90 (3H, t, *J* 6.8, CH₃), 1.28-1.40 (22H, m, 11 x CH₂), 1.68 (2H, quintet, *J* 6.8, C(O)OCH₂CH₂), 4.20 (2H, t, *J* 6.8, C(O)OCH₂CH₂), 4.21 (2H, s, C(O)CH₂CH₂C≡C), 4.56 (2H, s, C(O)CH₂OCH₂C≡C), 7.28-7.35 (3H, m, ArH), 7.46-7.48 (2H, m, ArH); δ_{C} (125 MHz, CDCl₃) 14.1, 22.7, 25.8, 28.5, 29.2, 29.3, 29.4, 29.5, 29.6, 31.9, 59.0, 65.1, 66.3, 84.8, 87.3, 122.3, 128.3, 128.6, 131.7, 170.1.

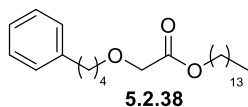
Synthesis of tetradecyl 2-(benzyloxy)acetate **5.2.37**



A solution of benzyl alcohol (800 mg, 6.0 mmol) in dry THF (10 mL) was added dropwise to a suspension of NaH (170 mg, 7.1 mmol) at 0 °C. The reaction mixture was stirred at 0 °C for 0.5 h (during which the effervescence ceased) and then warmed to room temperature, whereupon a solution of tetradecyl 2-bromoacetate

5.2.2 (2.0 g, 6.0 mmol) in dry THF (10 mL) was added. The reaction mixture was refluxed for 16 h, cooled to room temperature, quenched carefully with 2N HCl (10 mL) and then partitioned between Et₂O (30 mL) and 2N HCl (20 mL). The organic phase was collected and the aqueous layer was extracted further with Et₂O (2 x 20 mL). washed with brine (80 mL) and dried over Na₂SO₄. The suspension was filtered and the solvent was removed under reduced pressure. The crude was purified by column chromatography (15 % EtOAc/hexane) on silica gel to afford tetradecyl 2-(benzyloxy)acetate **5.2.37** as a white solid (380 mg, 18 %). M.pt. 25-26 °C; [Found:(APCI⁺) [M+NH₄]⁺ 380.3160. C₂₃H₄₂NO₃ requires (M+NH₄)⁺ 380.3159]; ν_{\max} (neat)/cm⁻¹ 2920, 2850, 1753, 1735, 1465, 1274, 1193, 1126, 734, 696; δ_{H} (500 MHz, CDCl₃); 0.90 (3H, t, *J* 7.0, CH₂CH₃), 1.28-1.34 (22H, m, 11 x CH₂), 1.64 (2H, quintet, *J* 7.0, C(O)OCH₂CH₂), 4.11 (2H, s, C(O)CH₂O), 4.18 (2H, t, *J* 7.0, C(O)OCH₂), 4.66 (2H, s, ArCH₂), 7.29-7.39 (5H, m, ArH); δ_{C} (125 MHz, CDCl₃) 14.1, 22.6, 25.8, 28.5, 29.2, 29.3, 29.5, 29.6, 29.7, 31.9, 65.0, 67.2, 73.3, 128.0, 128.1, 128.5, 137.1, 170.4.

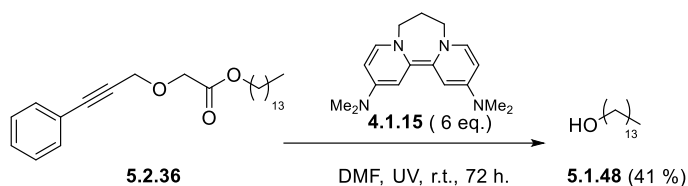
Synthesis of tetradecyl 2-(4-phenylbutoxy)acetate **5.2.38**



A solution of 4-phenyl-1-butanol (600 mg, 4.0 mmol) in dry THF (10 mL) was added dropwise to a suspension of NaH (100 mg, 4.2 mmol) at 0 °C. The reaction mixture was stirred at 0 °C for 0.5 h and then warmed to room temperature, whereupon a solution of tetradecyl 2-bromoacetate **5.2.2** (1.5 g, 4.4 mmol) in dry THF (10 mL) was added. The reaction mixture was refluxed for 16 h, cooled to room temperature, quenched carefully with 2N HCl (10 mL) and then partitioned between Et₂O (50 mL) and 2N HCl (100 mL). The organic phase was collected and the aqueous layer was extracted further with Et₂O (2 x 40 mL). washed with brine (150 mL) and dried over Na₂SO₄. The suspension was filtered and the solvent was removed under reduced pressure. The crude was purified by column chromatography (60 % CH₂Cl₂/hexane) on silica gel to afford tetradecyl 2-(4-phenylbutoxy)acetate **5.2.38** as a colourless oil (273 mg, 17 %). [Found: (APCI⁺) [M+NH₄]⁺ 422.3635. C₂₆H₄₈NO₃ requires (M+NH₄)⁺ 422.3629]; ν_{\max} (neat)/cm⁻¹ 2922, 1755, 1454, 1193,

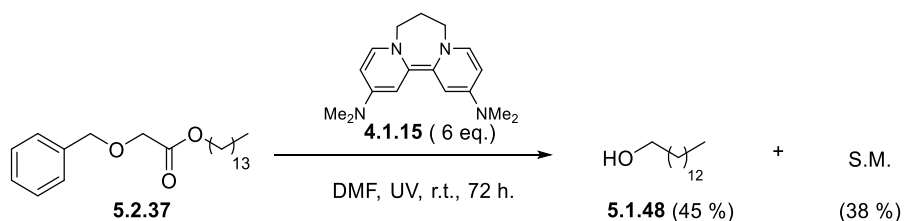
1134, 744, 698; δ_{H} (500 MHz, CDCl_3) 0.90 (3H, t, J 6.8 CH_2CH_3), 1.28-1.29 (24H, m, 12 x CH_2), 1.70-1.73 (4H, m, $\text{ArCH}_2\text{CH}_2\text{CH}_2$), 2.66 (2H, t, J 7.0, ArCH_2), 3.56 (2H, t, J 6.5, $\text{C(O)CH}_2\text{OCH}_2$), 4.07 (2H, s, $\text{C(O)CH}_2\text{O}$), 4.16 (2H, t, J 6.8, C(O)OCH_2), 7.19-7.31 (5H, m, ArH); δ_{C} (125 MHz, CDCl_3) 13.6, 22.1, 25.3, 25.5, 27.1, 27.3, 27.6, 28.0, 28.7, 28.8, 29.1, 31.4, 34.9, 35.1, 64.1, 64.4, 67.8, 71.2, 71.5, 125.2, 127.7, 127.9, 141.8, 170.1.

Reduction of tetradecyl 2-((3-phenylprop-2-yn-1-yl)oxy)acetate **5.2.36** with **4.1.15**



The general procedure for UV-activated reductions was applied to substrate **5.2.36** (155 mg, 0.4 mmol) using SED **4.1.15** (683 mg, 2.4 mmol) for 72 h at room temperature. The reaction mixture was then subjected to the general acidic workup procedure. The crude product was then purified by column chromatography on silica gel (5 % EtOAc/hexane) to afford tetradecanol **5.1.48** as a white solid (34 mg, 41 %) with data as previously reported. ^1H NMR spectrum analysis of the crude material after workup had revealed complete conversion of the starting material.

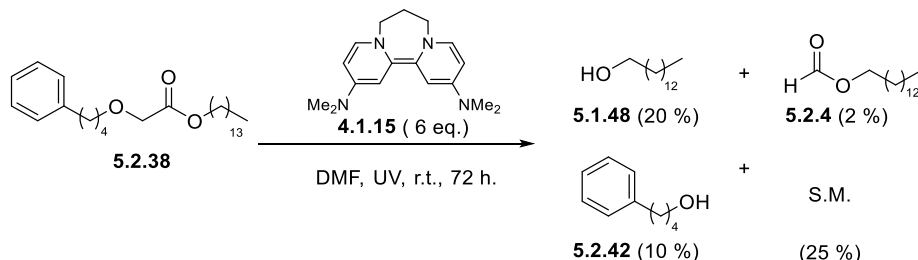
Reduction of afford tetradecyl 2-(benzyloxy)acetate **5.2.37** with **4.1.15**



The general procedure for UV-activated reductions was applied to substrate **5.2.37** (145 mg, 0.4 mmol) using SED **4.1.15** (683 mg, 2.4 mmol) for 72 h at room temperature. The reaction mixture was then subjected to the general acidic workup procedure and the resulting crude material was purified by column chromatography (5 % EtOAc/hexane) to afford tetradecanol **5.1.48** as a white solid (38 mg, 45 %) and

the starting material **5.2.37** as a white solid (55 mg, 38 %). The spectral data for both compounds were as previously reported.

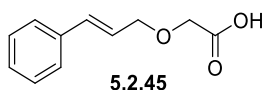
Reduction of tetradecyl 2-(4-phenylbutoxy)acetate **5.2.38** with SED **4.2.15**



The general procedure for UV-activated reductions was applied to substrate **5.2.38** (162 mg, 0.4 mmol) using SED **4.1.15** (683 mg, 2.4 mmol) for 72 h at room temperature. The reaction mixture was then subjected to the general acidic workup procedure and the resulting crude material was purified by column chromatography (2-5% EtOAc/hexane) to afford the starting material **5.2.38** (40.5 mg, 25 %), tetradecanol **5.1.48** (17.1 mg, 20 %), 4-(phenyl)butan-1-ol **5.2.42** (6.0 mg, 10 %) and tetradecyl formate **5.2.4** (2.0 mg, 2 %). The spectral data for the starting material **5.2.38**, tetradecanol **5.1.48** and tetradecyl formate **5.2.4** were as previously reported.

4-(phenyl)butan-1-ol **5.2.42**: colourless oil; δ_{H} (500 MHz, CDCl_3) 1.30 (1H, bs, OH), 1.64-1.73 (4H, m, 2 x CH_2), 2.67 (2H, t, J 7.4, ArCH_2), 3.67 (2H, J 6.4, CH_2OH), 7.20-7.32 (5H, m, ArH); δ_{C} (125 MHz, CDCl_3) 27.6, 32.3, 35.6, 62.8, 125.8, 128.3, 128.4, 142.3. The spectral data were consistent with the literature data.²³¹

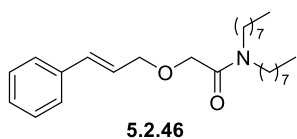
Synthesis of 2-(cinnamyloxy)acetic acid **5.2.45**



A solution of cinnamyl alcohol (15 g, 113 mmol) in dry THF (30 mL) was added portionwise to a suspension of NaH (5.5 g, 226 mmol) at 0 °C. The reaction mixture was stirred 0 °C for 1 h (during which effervescence ceased) and then warmed to room temperature whereupon a solution of bromoacetic acid (15 g, 110 mmol) in dry

THF (20 mL) was added. The reaction mixture was warmed to reflux for 16 h then cooled to room temperature, quenched carefully with 2N HCl (20 mL) and then partitioned between Et₂O (80 mL) and 2N HCl (150 mL). The organic phase was collected and the aqueous layer was extracted further with Et₂O (2 x 50 mL). washed with brine (150 ml) and dried over Na₂SO₄. The suspension was filtered and concentrated under reduced pressure. The crude was purified by column chromatography (35 % EtOAc/hexane) on silica gel to afford 2-(cinnamyloxy)acetic acid **5.2.45** as a pale yellow solid (15.6 g, 75 %). M.pt 61-62 °C (lit.²³² 59-61 °C); [Found: [M-H]⁻ 191.0710 , C₁₁H₁₁O₃ (M-H)⁻ requires 191.0714]; ν_{\max} (neat)/cm⁻¹ 3400-2617 (br), 1730, 1427, 1192, 1107, 1080, 972, 780, 694, 659; δ_{H} (400 MHz, CDCl₃) 4.21 (2H, s, OCH₂CO₂H), 4.30 (2H, dd, *J* 6.3, 1.4, OCH₂CH=CH), 6.30 (1H, dt, *J* 16.2, 6.3, OCH₂CH=CH), 6.65 (1H, d, *J* 16.2, ArCH=CH), 7.29-7.43 (5H, m, ArH); δ_{C} (125 MHz, CDCl₃) 66.0, 71.7, 123.7, 126.1, 127.5, 128.1, 133.7, 135.6, 174.1. The spectral data were consistent with the literature data.²³³

Synthesis of 2-(cinnamyloxy)-*N,N*-dioctylacetamide **5.2.46**

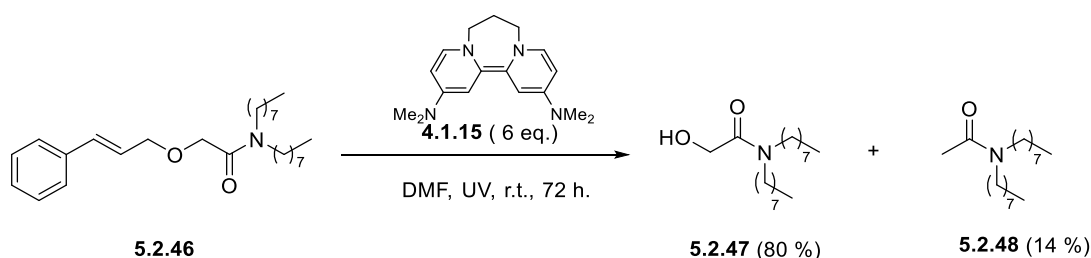


The general procedure for the *in situ* generation of acyl chloride followed by amide formation was employed.

Reagents: 2-(cinnamyloxy)acetic acid **5.2.45** (960 mg, 5.0 mmol), oxalyl chloride (0.48 mL, 5.5 mmol), pyridine (0.45 mL, 5.5 mmol), *N,N*-dioctylamine (1.45 g, 6.0 mmol), dry CH₂Cl₂ (30 mL). The reaction mixture was left to stir for 16 h after which it was quenched with H₂O (50 mL) and extracted with EtOAc (4 x 30 mL). The organic layers were combined, washed with brine (20 mL), dried over Na₂SO₄, filtered and then concentrated under reduced pressure. The crude product was purified by column chromatography (20 % EtOAc/hexane) and afforded 2-(cinnamyloxy)-*N,N*-dioctylacetamide **5.2.46** as a yellow oil (1.35 g, 65 %). [Found: (HNESP⁺) [M+H]⁺ 416.3521. C₂₇H₄₆NO₂ (M+H)⁺ requires 416.3523]; ν_{\max}

(neat)/cm⁻¹ 2922, 2852, 1643, 1454, 1114, 964, 690; δ_{H} (500 MHz, CDCl₃) 0.90 (6H, t, J 6.5, 2 x CH₃), 1.34 (20H, bs, 10 x CH₂), 1.56 (4H, bs, 2 x CH₂CH₂), 3.21 (2H, t, J 7.6, CH₂CH₂), 3.33 (2H, t, J 7.6, CH₂CH₂), 4.20 (2H, s, NC(O)CH₂O), 4.27 (2H, dd, J 6.2, 1.2, ArCH=CHCH₂O), 6.31 (1H, dt, J 16.1, 6.2, ArCH=CH), 6.63 (1H, d, J 16.0, ArCH=CH), 7.26-7.41 (5H, m, ArH); δ_{C} (125 MHz, CDCl₃) 13.5, 22.0, 22.1, 26.4, 26.5, 27.0, 28.5, 28.7, 28.8, 28.9, 29.0, 31.2, 31.3, 45.2, 46.6, 68.3, 71.2, 124.8, 126.0, 127.2, 128.0, 132.7, 136.0, 168.1.

Reduction of 2-(cinnamyloxy)-*N,N*-dioctylacetamide **5.2.46 with **4.1.15****



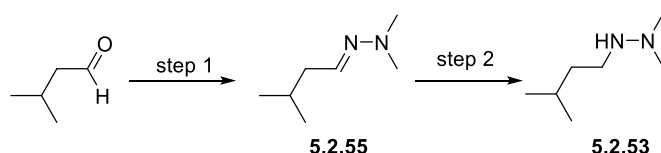
The general procedure for UV-activated reductions was applied to substrate **5.2.46** (208 mg, 0.5 mmol) using SED **4.1.15** (853 mg, 3.0 mmol) for 72 h at room temperature. The reaction mixture was then subjected to the general acidic workup procedure and the resulting crude material was purified by column chromatography (5-10 % EtOAc/hexane) to afford *N,N*-dioctyl-2-hydroxyacetamide **5.2.47** (120 mg, 80 %) and *N,N*-dioctylacetamide **5.2.48** (20 mg, 14 %).

N,N-dioctyl-2-hydroxyacetamide **5.2.47**: colourless oil; [Found: (HNESP⁺) [M+H]⁺ 300.2899. C₁₈H₃₇NO₂ requires (M+H)⁺ 300.2897]; ν_{max} (neat)/cm⁻¹ 3500-3410 (br), 2978, 1643, 1400, 1085, 721; δ_{H} (500 MHz, CDCl₃) 0.88-0.89 (6H, m, 2 x CH₃), 1.28-1.29 (20 H, m, 10 x CH₂), 1.52-1.54 (4H, m, NC(O)CH₂CH₂), 3.03-3.07 (2H, m, NC(O)CH₂), 3.34-3.38 (2H, m, NC(O)CH₂), 4.13 (2H, s, NC(O)CH₂OH); δ_{C} (125 MHz, CDCl₃) 13.5, 22.0, 22.1, 26.3, 26.4, 27.0, 28.0, 28.6, 28.7, 28.8, 28.9, 31.2, 31.3, 45.3, 45.6, 59.2, 170.5.

N,N-dioctylacetamide **5.2.48**: colourless oil; [Found: (HNESP⁺) [M+H]⁺ 284.2949. C₁₈H₃₈NO⁺ requires (M+H)⁺ 284.2949; ν_{max} (neat)/cm⁻¹ 2976, 2922, 2854, 1643, 1462, 1400, 1278, 1083, 964, 826, 721; δ_{H} (400 MHz, CDCl₃) 0.88-0.90 (6H, m,

CH_3), 1.29 (20H, bs, CH_2), 1.53-1.56 (4H, m, CH_2), 2.09 (3H, s, $NCOCH_3$), 3.22 (2H, t, J 7.8, NCH_2), 3.28 (2H, t, J 7.8, NCH_2); δ_C (100 MHz, $CDCl_3$) 13.6, 21.1, 22.1, 22.2, 26.4, 26.6, 27.3, 28.5, 28.7, 28.8, 28.9, 31.2, 31.33, 45.25, 48.3, 169.5.

Synthesis of 2-isopentyl-1,1-dimethylhydrazine 5.2.53



Step 1: Generation of hydrazone 5.2.55

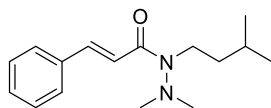
N,N-dimethylhydrazine (13.2 g, 220 mmol) was added portionwise to isovaleraldehyde (3.8 g, 44 mmol) at room temperature. The addition was controlled to ensure that the temperature of the reaction mixture did not exceed 50 °C. After complete addition, copious amounts of Na_2SO_4 were added, the reaction mixture warmed to reflux for 2 h and then cooled to room temperature. The reaction mixture was filtered and the filtrate was distilled to afford the intermediate hydrazone **5.2.55** as a colourless liquid (5.6 g, 85 %). δ_H (500 MHz, $DMSO-d_6$) 0.88 (6H, d, J 6.4, $N=CHCH_2CH(CH_3)_2$), 1.73 (1H, m, $N=CHCH_2CH$), 2.00 (2H, m, $N=CHCH_2$), 2.61 (6H, s, $N-NCH_3$), 6.57 (1H, m, $N=CH$); δ_C (125 MHz, $DMSO-d_6$) 15.6, 22.6, 27.2, 41.7, 43.4, 136.9. The spectral data were consistent with the literature data.²³⁴

Step 2: Reduction of hydrazone

The hydrazone **5.2.55** (3.8 g, 30 mmol) was diluted with dry Et_2O (10 mL) and then added dropwise to a suspension of $LiAlH_4$ (800 mg, 21 mmol) in dry Et_2O (30 mL). After complete addition the reaction mixture was warmed to reflux for 0.5 h and then cooled to room temperature. The reaction mixture quenched with H_2O which resulted in the formation of an emulsion. The emulsion was filtered under vacuum and the filtrate was distilled to afford 2-isopentyl-1,1-dimethylhydrazine **5.2.53** as a colourless liquid (3.4 g, 86 %). Boiling point: 129-130 °C; [Found: (APCI⁺) $[M+H]^+$ 131.1541. $C_7H_{19}N_2$ requires $(M+H)^+$ 131.1543]; ν_{max} (neat)/ cm^{-1} 3383-3200 (br), 2954, 2870, 1651, 1467, 1012, 665-648 (br); δ_H (500 MHz, $CDCl_3$) 1.34 (6H, d, J 6.7,

CHCH₃), 1.38-1.40 (2H, m, NHCH₂CH₂), 1.65 (1H, m, NCH₂CH₂CH), 2.00 (1H, bs, NH), 2.46 (6H, s, NCH₃), 2.78-2.80 (2H, m, NHCH₂); δ_C (125 MHz, CDCl₃) 22.1, 25.7, 36.9, 46.4, 47.2.

Synthesis of *N*-isopentyl-*N*'*N*'-dimethylcinnamoylhydrazide **5.2.54**

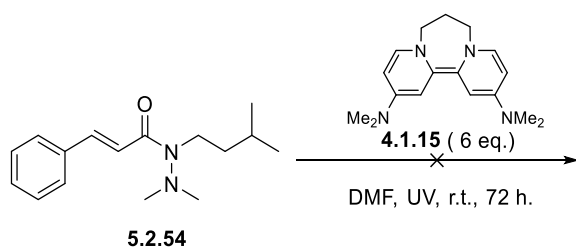


5.2.54

The general procedure for the *in situ* generation of acyl chloride followed by amide formation was employed.

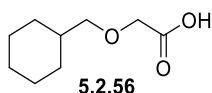
Reagents: 2-isopentyl-1,1-dimethylhydrazine **5.2.53** (586 mg, 4.5 mmol), oxalyl chloride (0.31 mL, 3.6 mmol), pyridine (0.27 mL, 3.6 mmol), cinnamic acid (445 mg, 3.0 mmol), dry CH₂Cl₂ (10 mL). The reaction mixture was left to stir for 16 h after which it was quenched with H₂O (50 mL) and extracted with EtOAc (4 x 30 mL). The organic layers were combined, washed with brine (20 mL), dried over Na₂SO₄, filtered and then concentrated under reduced pressure. The crude product was purified by column chromatography (15 % EtOAc/hexane) to afford *N*-isopentyl-*N*'*N*'-dimethylcinnamoylhydrazide **5.2.54** as a yellow solid (390 mg, 50 %). M.pt. 58-59 °C; [Found:(HNESP⁺) [M+H]⁺ 261.1961. C₁₆H₂₅N₂O requires (M+H)⁺ 261.1961]; ν_{max} (neat)/cm⁻¹ 2949, 1647, 1612, 1454, 1149, 995, 759, 700; δ_H (500 MHz, CDCl₃) 0.99 (6H, d, *J* 6.5, CH₂CHCH₃), 1.60-1.75 (3H, m, NCH₂CH₂ and NCH₂CH₂CH), 2.60 (6H, s, 2 x NCH₃), 3.43 (2H, m, NCH₂CH₂), 7.34-7.38 (3H, m, ArH), 7.48 (1H, d, *J* 16, NC(O)CH=CH), 7.59-7.60 (2H, m, ArH), 7.70 (1H, d, *J* 16.0, ArCH=CH); δ_C (125 MHz, CDCl₃) 21.9, 26.3, 37.1, 37.9, 43.8, 118.0, 127.3, 128.1, 128.6, 135.5, 140.8, 167.3.

Attempted reduction *N*-isopentyl-*N*'*N*'-dimethylcinnamoylhydrazide **5.2.45** with **4.1.15**



The general procedure for UV-activated reductions was applied to the substrate (130 mg, 0.5 mmol) using SED **4.1.15** (853 mg, 3.0 mmol) for 72 h at room temperature. The reaction mixture was then subjected to the general acidic workup procedure and the resulting crude material was purified by column chromatography (10 % EtOAc/hexane) to afford the starting material **5.2.54** as a yellow solid (125 mg, 96 %). The spectral data were as previously reported.

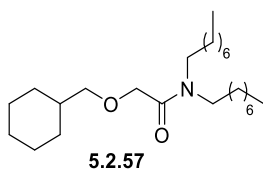
Synthesis of 2-(cyclohexylmethoxy)acetic acid **5.2.56**



A solution of cyclohexylmethanol (5.8 g, 50.0 mmol) in dry THF (30 mL) was added dropwise using a dropping funnel to a suspension of NaH (2.7 g, 110 mmol) at 0 °C. The reaction mixture was stirred 0 °C for 1 h and then warmed to room temperature, whereupon a solution of bromoacetic acid (7.7 g, 55 mmol) in dry THF (20 mL) was added. The reaction mixture was warmed to reflux for 16 h then cooled to room temperature, quenched carefully with 2N HCl (20 mL) and then partitioned between Et₂O (80 mL) and 2N HCl (150 mL). The organic phase was collected and the aqueous layer was extracted further with Et₂O (2 x 50 mL). washed with brine (150 mL) and dried over Na₂SO₄. The suspension was filtered and concentrated under reduced pressure to afford 2-(cyclohexylmethoxy)acetic acid **5.2.56** as a yellow oil (7.6 g, 99 %). [Found:(HNESP⁺) [M+NH₄]⁺ 190.1437. C₉H₂₀NO₃ requires (M+NH₄)⁺ 190.1438]; ν_{\max} (neat)/cm⁻¹ 3032 (br), 2926, 2850, 1714, 1435, 1255, 1136, 927, 856, 704; δ_{H} (500 MHz, DMSO-d₆) 0.88-0.91 (2H, m, CH₂CH₂), 1.18-1.32 (4H, m, 2 x CH₂) 1.49-1.51 (1H, m, OCH₂CH), 1.51-1.67 (4H, m, 2 x CH₂), 3.25 (2H, d, *J* 6.5, OCH₂CH), 3.25 (1H, bs, CO₂H), 3.94 (2H, s, OCH₂CO₂H); δ_{C} (125 MHz, DMSO-d₆)

25.7, 26.6, 29.8, 37.9, 68.1, 76.6, 172.2. The spectral data were consistent with the literature data.²³⁵

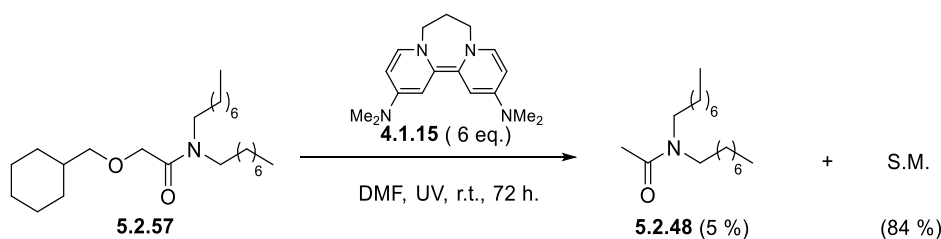
Synthesis of 2-(cyclohexylmethoxy)-*N,N*-dioctylacetamide **5.2.57**



The general procedure for the *in situ* generation of acyl chloride followed by amide formation was employed.

Reagents: 2-(cyclohexylmethoxy)acetic acid **5.2.56** (1.0 g, 6.0 mmol), oxalyl chloride (0.58 mL, 6.6 mmol), pyridine (0.53 mL, 6.6 mmol), dioctylamine (2.17 g, 9.0 mmol), dry CH₂Cl₂ (40 mL). The reaction mixture was left to stir for 16 h after which it was quenched with H₂O (50 mL) and extracted with EtOAc (4 x 30 mL). The organic layers were combined, washed with brine (20 mL), dried over Na₂SO₄, filtered and then concentrated under reduced pressure. The crude product was purified by column chromatography (10 % EtOAc/hexane) to afford 2-(cyclohexylmethoxy)-*N,N*-dioctylacetamide **5.2.57** (2.0 g, 87 %) as a colourless oil. [Found: (HNESP⁺) [M+H]⁺ 386.3833. C₂₅H₅₀NO (M+H)⁺ requires 396.3836]; ν_{\max} (neat)/cm⁻¹ 2922, 2852, 1647, 1450, 1377, 1118, 1097, 723; δ_{H} (500 MHz, CDCl₃) 0.88-0.89 (8H, m, 2 x CH₃ and CH₂CH₂), 1.26-1.28 (22H, m, 11 x CH₂CH₂), 1.77-1.77 (11H, m, OCH₂CH and 5 x CH₂CH₂), 3.22-3.31 (6H, m, 2 x NCH₂ and OCH₂CH), 4.10 (2H, s, NCOCH₂O); δ_{C} (125 MHz, CDCl₃) 22.1, 25.3, 26.0, 26.4, 26.5, 27.0, 28.4, 28.7, 28.8, 28.9, 29.0, 29.5, 31.2, 31.3, 37.6, 45.0, 46.5, 70.2, 168.4.

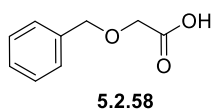
Reduction of 2-(cyclohexylmethoxy)-*N,N*-dioctylacetamide **5.2.57** with SED **4.1.15**



The general procedure for UV-activated reductions was applied to the substrate (198 mg, 0.5 mmol) using SED **4.1.15** (853 mg, 3.0 mmol) for 72 h at room temperature. The reaction mixture was then subjected to the general acidic workup procedure and the resulting crude material was purified by column chromatography (10 % EtOAc /hexane) to afford *N,N*-dioctylacetamide **5.2.48** as a colourless oil (7.1 mg, 5 %) and the starting material **5.2.57** (166 mg, 84 %). The spectral data for both compounds were previously reported.

Blank reactions: i) SED-free, UV-active and ii) SED (6 eq.), UV-free experiments were performed following the general procedure and the starting material **5.2.57** was recovered (174 mg, 87 %) and (190 mg, 95 %) respectively.

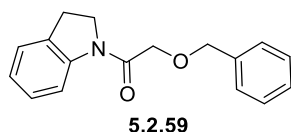
Synthesis of 2-(benzyloxy)acetic acid **5.2.58**



A solution of benzyl alcohol (3.2 g, 30 mmol) in dry THF (30 mL) was added dropwise to a suspension of NaH (1.6 g, 66 mmol) at 0 °C. The reaction mixture was stirred at 0 °C for 0.5 h and then warmed to room temperature, whereupon a solution of bromoacetic acid (4.2 g, 30 mmol) in dry THF (20 mL) was added. The reaction mixture was refluxed for 16 h, cooled to room temperature, quenched carefully with 2N HCl (10 mL) and then partitioned between Et₂O (50 mL) and 2N HCl (100 mL). The organic phase was collected and the aqueous layer was extracted further with Et₂O (2 x 50 mL). washed with brine (150 mL) and dried over Na₂SO₄. The suspension was filtered and the solvent was removed under reduced pressure. The crude was purified by column chromatography (30 % EtOAc/hexane) on silica gel to afford 2-(benzyloxy)acetic acid **5.2.58** as a pale yellow liquid (4.9 g, 98 %). δ_{H} (500 MHz, CDCl₃) 4.16 (2H, s, CH₂CO₂H), 4.67 (2H, s, ArCH₂O), 7.35-7.37 (5H, m,

ArH); δ_C (125 MHz, $CDCl_3$) 66.6, 73.5, 128.1, 128.3, 128.6, 136.5, 174.6. The spectral data were consistent with the literature data.²³⁶

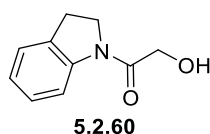
Synthesis of 2-(benzyloxy)-1-(indolin-yl)ethan-1-one **5.2.59**



The general procedure for the *in situ* generation of acyl chloride followed by amide formation was employed.

Reagents: 2-(benzyloxy)acetic acid **5.2.58** (1.0 g, 6.0 mmol), oxalyl chloride (0.64 mL, 7.0 mmol) and indoline (1.1 mL, 9.0 mmol) in dry CH_2Cl_2 (50 mL) Purification by column chromatography (30 % EtOAc/hexane) on silica gel afforded 2-(benzyloxy)-1-(indolin-yl)ethan-1-one **5.2.59** as a pale brown oil (1.25 g, 78 %). [Found: (HNESP⁺) [M+H]⁺ 268.1333. $C_{17}H_{18}NO_2$ requires (M+H)⁺ 268.1332]; ν_{max} (neat)/ cm^{-1} 3030, 2958, 1662, 1595, 1481, 1433, 1408, 1284, 1101, 920, 767; δ_H (500 MHz, $CDCl_3$) 3.20 (2H, t, J 8.0, ArCH₂CH₂NCO), 4.03 (2H, t, J 8.0, ArCH₂CH₂NCO), 4.25 (2H, s, NCOCH₂OCH₂), 4.73 (2H, s, ArCH₂O), 7.04-7.07 (1H, m, ArH), 7.20-7.43 (7H, m, ArH), 8.28 (1H, d, J 7.5, ArH); δ_C (125 MHz, $CDCl_3$) 27.8, 46.3, 69.4, 72.3, 116.6, 123.5, 124.0, 127.0, 127.4, 127.6, 128.0, 130.3, 136.8, 142.3, 166.8.

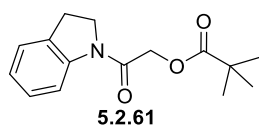
Synthesis of indolin-1-ylmethanol **5.2.60**



Palladium on carbon (200 mg, 0.2 mmol) was suspended in a solution of 2-(benzyloxy)-1-(indolin-yl)ethan-1-one **5.2.59** (1.0 g, 3.7 mmol) in EtOH (25 mL). The reaction mixture was evacuated and refilled with argon thrice after which H₂ was bubbled into the suspension for 5 min. The reaction mixture was left to stir vigorously for 16 h with a H₂-filled balloon attached to the flask. The suspension was then filtered under vacuum through a celite column and the solvent was removed from the filtrate under reduced pressure. The resulting crude material was then

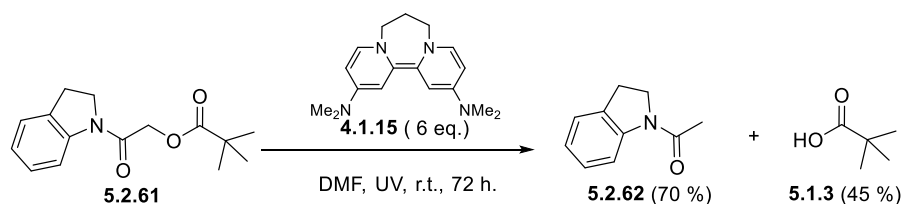
purified by column chromatography (50 % EtOAc/hexane) to afford indolin-1-ylmethanol **5.2.60** as a colourless oil (380 mg, 57 %). [Found: (HNESP⁺) [M+H]⁺ 178.0861, C₁₀H₁₂NO₂ (M+H)⁺ requires 178.0863]; ν_{\max} (neat)/cm⁻¹ 3423, 2897, 1651, 1485, 1427, 1365, 1251, 1095, 750; δ_{H} (500 MHz, CDCl₃) 3.25 (2H, t, *J* 8.3, ArCH₂CH₂NCO), 3.41 (1H, bs, OH), 3.90 (2H, t, *J* 8.3, ArCH₂CH₂NCO), 4.22 (2H, s, NCOCH₂OH), 7.06 (1H, t, *J* 7.6, ArH), 7.10-7.25 (2H, m, ArH), 8.21 (1H, d, *J* 7.8, ArH); δ_{C} (125 MHz, CDCl₃) 27.6, 44.9, 60.6, 116.2, 123.9, 124.2, 127.2, 130.3, 141.7, 169.1.

Synthesis of 2-pivaloyl-1-(indolin-1-yl)-ethane-1-one **5.2.61**



Indolin-1-ylmethanol **5.2.60** (370 mg, 2.1 mmol) was dissolved in dry THF (20 mL) whereupon pivaloyl chloride (0.22 mL, 2.7 mmol) and dry pyridine (0.25 mL, 2.7 mmol) were added in one portion. The reaction mixture was warmed to reflux for 16 h, cooled to room temperature and partitioned between Et₂O (30 mL) and 2N HCl (50 mL). The organic phase was collected and the aqueous layer was extracted further with Et₂O (2 x 15 mL). The organic extracts were combined, washed with brine, dried over Na₂SO₄, filtered and solvent removed under reduced pressure. The crude was purified by column chromatography (20 % EtOAc/hexane) on silica gel to afford 2-pivaloyl-1-(indolin-1-yl)-ethane-1-one **5.2.61** as a colourless viscous oil (410 mg, 88 %). [Found: (HNESP⁺) [M+H]⁺ 262.1437. C₁₅H₂₀NO₃ requires (M+H)⁺ 262.1438]; ν_{\max} (neat)/cm⁻¹ 2983, 2931, 1737, 1674, 1598, 1479, 1427, 1278, 1155, 906, 862, 767; δ_{H} (500 MHz, CDCl₃) 1.32 (9H, s, 3 x CH₃), 3.25-3.27 (2H, m, ArCH₂CH₂NCO), 4.05-4.07 (2H, m, ArCH₂CH₂NCO), 4.75 (2H, s, NCOCH₂OCO), 7.02-7.06 (1H, m, ArH), 7.18-7.21 (2H, m, ArH), 8.19-8.21 (1H, m, ArH); δ_{C} (125 MHz, CDCl₃) 27.2, 28.3, 38.8, 46.5, 61.9, 117.1, 124.1, 124.5, 127.6, 130.5, 142.5, 166.5, 178.1.

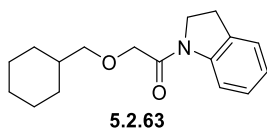
Reduction of 2-pivaloyl-1-(indolin-1-yl)-ethane-1-one **5.2.61** with **4.1.15**



The general procedure for UV-activated reductions was applied to the substrate (130 mg, 0.5 mmol) using SED **4.1.15** (853 mg, 3.0 mmol) for 72 h at room temperature. The reaction mixture was then subjected to the general acidic workup procedure. To separate the pivalic acid **5.1.3** from 1-(indolin-1-yl)ethan-1-one **5.2.62**, the organic collection was extracted with sat. NaHCO_3 (3 x 10 mL). The basic aqueous extracts were combined, re-acidified using 6N HCl and reextracted with CH_2Cl_2 (3 x 10 mL). Both sets of organic extracts were washed with brine, dried over Na_2SO_4 and filtered. The solvent was removed under reduced pressure and the products were purified on separate columns to yield 1-(indolin-1-yl)ethan-1-one **5.2.62** (20 % EtOAc/hexane) (55 mg, 70 %) and pivalic acid **5.1.3** (50% EtOAc/hexane) (23 mg, 45 %). The spectral data for pivalic acid **5.1.3** were as previously reported.

N-acetylintoline **5.2.62**: white solid; M.pt. 96-98 °C (lit.²³⁷ 97-99 °C); ν_{max} (neat)/ cm^{-1} 2960, 2914, 2850, 1739, 1651, 1600, 1479, 1460, 1400, 925, 883; δ_{H} (500 MHz, CDCl_3) 2.25 (3H, s, NCOCH_3), 3.23 (2H, t, J 8.5, $\text{NCOCH}_2\text{CH}_2$), 4.08 (2H, t, J 8.5, $\text{NCOCH}_2\text{CH}_2$), 7.01-7.03 (1H, m, ArH), 7.20-7.24 (2H, m, ArH), 8.22 (1H, d, J 8.0, ArH); δ_{C} (125 MHz, CDCl_3) 25.6, 27.2, 50.7, 118.5, 123.3, 126.1, 127.8, 133.4, 144.6, 169.8. The spectral data were consistent with the literature data.²³⁷

Synthesis of 2-(cyclohexylmethoxy)-1-(indolin-1-yl)ethan-1-one **5.2.63**

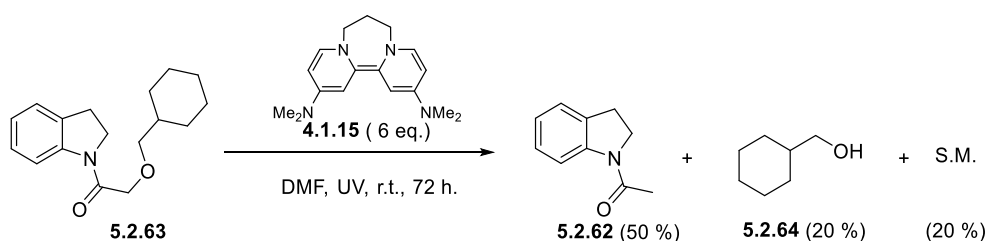


The general procedure for amidation using oxalyl chloride was employed.

Reagents: 2-(cyclohexylmethoxy)acetic acid **5.2.56** (260 mg, 1.5 mmol), oxalyl chloride (0.16 mL, 1.8 mmol), pyridine (0.15 mL, 2.0 mmol), indoline (268 mg, 2.25

mmol), dry CH₂Cl₂ (20 mL). Purification by column chromatography (30 % EtOAc/hexane) afforded 2-(cyclohexylmethoxy)-1-(indolin-1-yl)ethan-1-one **5.2.63** as a brown solid (320 mg, 78 %). M.pt. 67-69 °C; [Found: (HNESP⁺) [M+H]⁺ 274.1802. C₁₇H₂₄NO₂ requires (M+H)⁺ 274.1802]; ν_{\max} (neat)/cm⁻¹ 2916, 2846, 1672, 1599, 1483, 1425, 1338, 1136, 1022, 754; δ_{H} (500 MHz, CDCl₃) 0.89-1.27 (5H, m, cyclohexyl CH and 2 x CH₂), 1.67-1.80 (6H, m, cyclohexyl 3 x CH₂), 3.19 (2H, t, *J* 8.4, ArCH₂CH₂NCO), 4.08 (2H, t, *J* 8.4, ArCH₂CH₂NCO), 4.18 (2H, s, NC(O)CH₂O), 7.01 (1H, t, *J* 7.6, ArH), 7.18-7.20 (2H, m, ArH), 8.24 (1H, d, *J* 7.9, ArH); δ_{C} (125 MHz, CDCl₃) 25.8, 26.6, 28.4, 30.0, 38.1, 46.9, 71.7, 77.5, 117.1, 123.9, 124.5, 127.5, 130.9, 142.9, 167.7.

Reduction of 2-(cyclohexylmethoxy)-1-(indolin-1-yl)ethan-1-one **5.2.63** with **4.1.15**

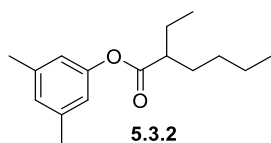


The general procedure for UV-activated reductions was applied to substrate **5.2.63** (137 mg, 0.5 mmol) using SED **4.1.15** (853 mg, 3.0 mmol) for 72 h at room temperature. The reaction mixture was then subjected to the general acidic workup procedure. The product was then purified by column chromatography on silica gel (2-15 % EtOAc/hexane) to afford *N*-acetylindoline **5.2.62** (39 mg, 50 %), the starting material **5.2.63** (55 mg, 20 %) and cyclohexylmethanol **5.2.64** (12 mg, 20 %). The spectral data for the starting material **5.2.63** and *N*-acetylindoline **5.2.62** were as previously reported.

Cyclohexylmethanol **5.2.64**: colourless oil; δ_{H} (500 MHz, CDCl₃) 0.80-0.96 (2H, m), 1.13-1.33 (3H, m), 1.51-1.54 (1H, m), 1.73-1.78 (5H, m), 2.40 (1H, bs, CH₂OH), 3.45 (2H, d, *J* 6.8, CH₂OH); δ_{C} (125 MHz, CDCl₃) 25.8, 26.4, 28.3, 41.2, 69.4; GCMS (EI) 97.2 (100 %), 83 (60). The spectral data were consistent with the literature data.^{233,234}

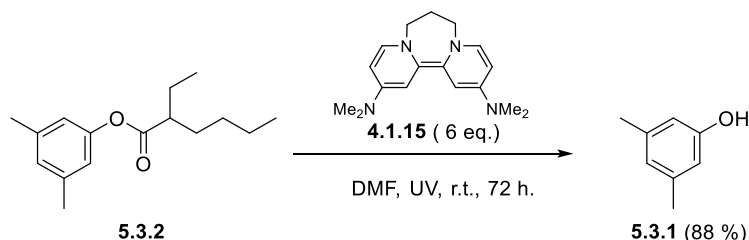
7.5 Experimental for Chapter 5.3

Synthesis of 3,5-dimethylphenyl 2-ethylhexanoate **5.3.2**



3,5-Dimethylphenol (1.5 g, 12.5 mmol) was dissolved in dry THF (10 mL) whereupon pyridine (0.8 mL, 10 mmol) and 2-ethylhexanoyl chloride (1.7 mL, 10 mmol) were added portionwise. The reaction mixture was stirred at room temperature for 2 h and then partitioned between CH₂Cl₂ (50 mL) and 2N HCl (80 mL). The organic extract was collected and the aqueous fraction was extracted further with CH₂Cl₂ (2 x 40 mL). The organic extracts were combined, washed with brine and dried over Na₂SO₄. The suspension was filtered and the solvent was removed under reduced pressure. The resulting crude product was purified by column chromatography (10 % CH₂Cl₂/hexane) to afford 3,5-dimethylphenyl 2-ethylhexanoate **5.3.2** as a colourless oil (2.2 g, 90 %). [Found: (HNESP⁺) [M+H]⁺ 249.1848. C₁₆H₂₅O₂ (M+H)⁺ requires 249.1849]; ν_{\max} (neat/cm⁻¹) 2960, 2931, 1753, 1618, 1591, 1460, 1136, 902; δ_{H} (500 MHz, CDCl₃) 0.93-0.95 (3H, m, CH₂CH₃), 1.02 (3H, t, *J* 7.4, CH₂CH₃), 1.40-1.41 (4H, m, 2 x CH₂), 1.57-1.65 (2H, m, CH₂), 1.75-1.81 (2H, m, CH₂), 2.33 (6H, s, ArCH₃), 2.50 (1H, m, C(O)CH), 6.69 (2H, s, ArH), 6.86 (1H, s, ArH); δ_{C} (125 MHz, CDCl₃) 11.8, 13.9, 21.2, 22.6, 25.5, 29.6, 31.8, 47.4, 119.2, 127.4, 139.2, 150.7, 175.0.

Reduction of 3,5-dimethylphenyl 2-ethylhexanoate **5.3.2** with **4.1.15**

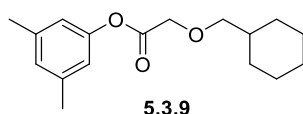


The general procedure for UV-activated reductions was applied to the substrate (125 mg, 0.5 mmol) using SED **4.1.15** (853 mg, 3.0 mmol) for 72 h at room temperature.

The reaction mixture was then subjected to the general acidic workup procedure and the resulting crude material was purified by column chromatography (5 % EtOAc/hexane) to afford 3,5-dimethylphenol **5.3.1** as a low melting off-white solid (54 mg, 88 %). δ_{H} (500 MHz, CDCl_3) 2.28 (6H, s, CH_3), 6.50 (2H, bs, ArH), 6.57 (1H, bs, ArH); δ_{C} (125 MHz, CDCl_3) 22.5, 111.3, 122.5, 139.7, 155.5; (GCMS EI) 122 (M^+ , 100 %), 107.5 (96), 91.2 (21). The spectral data were consistent with the literature data.^{235, 236}

Blank reactions: i) SED-free, UV-active and ii) SED (6 eq.), UV-free experiments were performed following the general procedure. For the first blank reaction, the starting material **5.3.2** was recovered (113 mg, 95 %). For the second blank reaction, the starting material **5.3.2** was recovered (118 mg, 90 %) along with 3,5-dimethylphenol **5.3.1** (6 mg, 10 %). The spectral data for the starting material **5.3.2** and 3,5-dimethylphenol **5.3.1** were as previously reported.

Synthesis of 3,5-dimethylphenyl 2-(cyclohexylmethoxy)acetate **5.3.9**

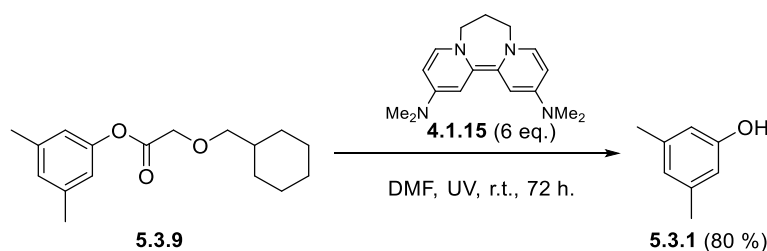


The general procedure for the *in situ* generation of acyl chloride followed by esterification was employed.

Reagents: 2-(cyclohexylmethoxy)acetic acid **5.2.56** (1.0 g, 6.0 mmol), oxalyl chloride (0.58 mL, 6.6 mmol), pyridine (0.53 mL, 6.6 mmol), 3,5-dimethylphenol (880 mg, 7.0 mmol), dry CH_2Cl_2 (30 mL). The reaction mixture was left to stir for 16 h after which it was quenched with H_2O (50 mL) and extracted with EtOAc (4 x 30 mL). The organic layers were combined, washed with brine (20 mL), dried over Na_2SO_4 , filtered and then concentrated under reduced pressure. The crude product was purified by column chromatography (35 % CH_2Cl_2 /hexane) to afford 3,5-dimethylphenyl 2-(cyclohexylmethoxy)acetate **5.3.9** as a colourless oil (200 mg, 12 %). [Found: (HNES P^+) $[\text{M}+\text{H}]^+$ 277.1792. $\text{C}_{17}\text{H}_{25}\text{O}_3$ ($\text{M}+\text{H})^+$ requires 277.1798]; ν_{max} (neat)/ cm^{-1} 2921, 2851, 1776, 1618, 1449, 1291, 1138, 1119, 841, 682; δ_{H} (500

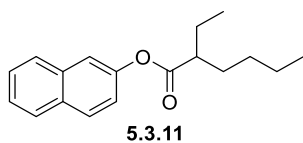
MHz, CDCl₃) 0.95-0.96 (2H, m, CH₂CH₂), 1.17-1.33 (3H, m, CH₂CH₂ and CH₂CH), 1.73-1.85 (6H, m, 3 x CH₂CH₂), 2.34 (6H, s, ArCH₃), 3.44 (2H, d, *J* 6.6, OCH₂CH), 4.31 (2H, s, ArCO₂CH₂), 6.75 (2H, s, ArH), 6.89 (1H, s, ArH); δ_C (125 MHz, CDCl₃) 21.2, 25.8, 26.6, 29.9, 38.0, 68.5, 77.8, 118.9, 127.7, 139.3, 150.1, 169.4.

Reduction of 3,5-dimethylphenyl 2-(cyclohexylmethoxy)acetate **5.3.9** with **4.1.15**



The general procedure for UV-activated reductions was applied to 3,5-dimethylphenyl 2-(cyclohexylmethoxy)acetate **5.3.9** (110 mg, 0.4 mmol) using SED **4.1.15** (683 mg, 2.4 mmol) for 72 h at room temperature. The reaction mixture was then subjected to the general acidic workup procedure and the resulting crude material was purified by column chromatography (5 % EtOAc/hexane) to afford 3,5-dimethylphenol **5.3.1** as a pale yellow solid (39 mg, 80 %). The spectral data were as previously reported. ¹H NMR spectrum analysis of the crude material after workup had revealed complete conversion of the starting material.

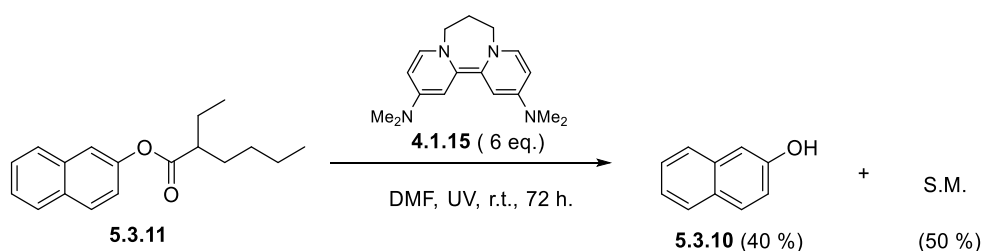
Synthesis of naphthalen-2-yl 2-ethylhexanoate **5.3.11**



2-Naphthol (2.2 g, 15 mmol) was dissolved in dry THF (15 mL) whereupon pyridine (1.6 mL, 19.5 mmol) and 2-ethylhexanoyl chloride (3.5 mL, 19.5 mmol) were added portionwise. The reaction mixture was stirred at room temperature for 3 h and then partitioned between CH₂Cl₂ (50 mL) and 2N HCl (100 mL). The organic phase was collected and the aqueous phase was extracted further with CH₂Cl₂ (2 x 50 mL). The

organic extracts were combined, washed with brine and dried over Na₂SO₄. The suspension was filtered and the solvent was removed under reduced pressure. The resulting crude was purified by column chromatography (15 % CH₂Cl₂/hexane) to afford naphthalen-2-yl 2-ethylhexanoate **5.3.11** as a colourless oil (3.8 g, 94 %). [Found: (HNESP⁺) [M+H]⁺ 271.1694. C₁₈H₂₃O₂ (M+H)⁺ requires 271.1698]; ν_{\max} (neat/cm⁻¹) 2958, 2931, 1751, 1510, 1462, 1381, 1209, 1124, 964, 800; δ_{H} (500 MHz, CDCl₃) 0.97 (3H, t, *J* 7.2, CH₂CH₃), 1.09 (3H, t, *J* 7.2, CH₂CH₃), 1.44-1.46 (4H, m, 2 x CH₂), 1.42-1.48 (2H, m, CH₂), 1.83-1.85 (2H, m, CH₂), 2.61 (1H, m, C(O)CH), 7.24 (1H, dd, *J* 8.7, 2.5, ArH), 7.56-7.57 (3H, m, ArH), 7.88-7.91 (3H, m, ArH); δ_{C} (125 MHz, CDCl₃) 11.4, 13.5, 22.2, 25.0, 29.2, 31.3, 46.9, 117.9, 120.8, 125.0, 126.0, 127.1, 127.2, 128.8, 130.9, 133.3, 148.0, 174.5.

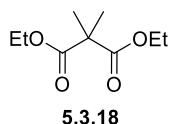
Reduction of naphthalen-2-yl 2-ethylhexanoate **5.3.11** with **4.1.15**



The general procedure for UV-activated reductions was applied to naphthalen-2-yl 2-ethylhexanoate **5.3.11** (125 mg, 0.5 mmol) using SED **4.1.15** (853 mg, 3.0 mmol) for 72 h at room temperature. The reaction mixture was then subjected to the general acidic workup procedure and the resulting crude material was purified by column chromatography (3 % EtOAc/hexane) to afford 2-naphthol **5.3.10** (40 mg, 40 %) and the starting material **5.3.11** (67 mg, 50 %). The spectral data for the starting material **5.3.11** were as previously reported.

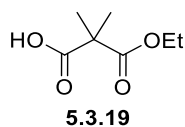
2-Naphthol **5.3.10**: white solid; M.pt. 121-122 °C (lit. 122-124 °C)²⁴²; δ_{H} (400 MHz, CDCl₃) 7.16 (1H, dd, *J* 8.2, 2.5, ArH), 7.19 (1H, bs, ArH), 7.33 (1H, t, *J* 7.5, ArH), 7.44 (1H, t, *J* 7.5, ArH), 7.69 (1H, d, *J* 8.2, ArH), 7.71-7.80 (m, 2H, ArH); δ_{C} (100 MHz, CDCl₃) 109.5, 117.8, 125.3, 126.4, 126.5, 127.0, 128.3, 130.2, 135.7, 154.1; The spectral data were consistent with the literature data.²⁴²

Synthesis of diethyl 2,2-dimethylmalonate **5.3.18**



Pre-washed and dried NaH (60 % dispersion in mineral oil, 4.4 g, 0.18 mol) was suspended in dry THF (50 mL) and cooled to 0 °C whereupon diethyl malonate (9.6 g, 0.06 mol) was added dropwise over 30 min using a dropping funnel. The reaction was then warmed to room temperature and stirred for 30 min during which effervescence ceased. The slurry was cooled to 0 °C and methyl iodide (18 mL, 0.3 mol) was added dropwise. After complete addition, the reaction mixture was stirred at room temperature for 18 h and then quenched with H₂O at 0 °C. The reaction mixture was then partitioned between CH₂Cl₂ (80 mL) and H₂O (150 mL). The organic phase were collected and the aqueous fraction was extracted further with CH₂Cl₂ (2 x 80 mL). The organic extracts were combined, washed with brine and then dried over Na₂SO₄. The suspension was filtered and solvent was removed under reduced pressure. The crude material was purified by column chromatography (5 % EtOAc/hexane) to afford diethyl 2,2-dimethylmalonate **5.3.18** as a colourless oil (10.7 g, 95 %). δ_{H} (500 MHz, CDCl₃) 1.29 (6H, t, *J* 7.4, (CH₂CH₃)₂), 1.43 (6H, s, 2 x CH₃), 4.19 (4H, q, *J* 7.4, (OCH₂)₂); δ_{C} (125 MHz, CDCl₃) 13.9, 22.7, 49.7, 61.2, 172.9; *m/z* (GCMS, CI, CH₄) 189.1 (M+H⁺, 70 %), 143.1 (100), 115.1 (25), 87.1 (30). The spectral data were consistent with the literature data.²⁴³

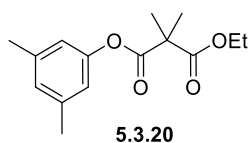
Synthesis of 3-ethoxy-2,2-dimethyl-3-oxopropanoic acid **5.3.19**



A solution of diethyl 2,2-dimethylmalonate **5.3.18** (3.4 g, 18 mmol) in EtOH (20 mL) was stirred vigorously whereupon a solution of KOH (1 g, 18 mmol) in EtOH (20 mL) was added portionwise. The reaction mixture was warmed to reflux for 2 h and then left to stir for a further 16 h at room temperature after which the solvent was

removed under reduced pressure. The crude product was then dissolved in 2N HCl (50 mL) and extracted with Et₂O (3 x 20 mL). The organic extracts were combined and the solvent removed under reduced pressure. The resulting crude material was purified by vacuum distillation (135-138 °C @ 19 mmHg) to yield 3-ethoxy-2,2-dimethyl-3-oxopropanoic acid **5.3.19** as a colourless oil (1.8 g, 62 %). ν_{\max} (neat/cm⁻¹) 3286 (br), 2985, 2939, 1725, 1710, 1469, 1388, 1265, 1138, 1026, 860; δ_{H} (500 MHz, CDCl₃) 1.29 (3H, t, *J* 7.4, CH₂CH₃), 1.49 (6H, s, (C)CH₃), 4.24 (2H, q, *J* 7.4, CH₂CH₃), 10.15 (1H, bs, CO₂H); δ_{C} (125 MHz, CDCl₃) 13.4, 22.2, 49.3, 61.1, 172.0, 178.4. The spectral data were consistent with the literature data.²⁴⁴

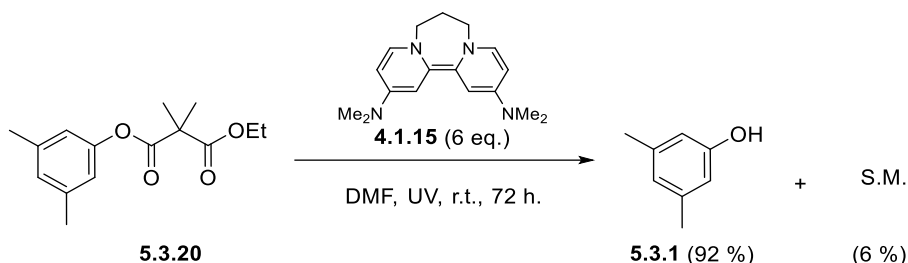
Synthesis of 1-(3,5-dimethylphenyl) 3-ethyl 2,2-dimethylmalonate **5.3.20**



3-Ethoxy-2,2-dimethyl-3-oxopropanoic acid **5.3.19** (2.5 g, 15 mmol) was dissolved in dry CH₂Cl₂ (15 mL) and cooled to 0 °C whereupon oxalyl chloride (1.7 mL, 20 mmol) was added. 5 drops of dry DMF was added to the solution and the reaction mixture was left to stir at 0 °C under a steady stream of argon for 30 min. The reaction was then warmed to room temperature and a solution of 3,5-dimethylphenol (2.0 g, 16.7 mmol) in dry CH₂Cl₂ (10 mL) was added. Dry pyridine (10 mL) was delivered and the reaction was stirred for 16 h after which the reaction mixture was partitioned between CH₂Cl₂ (30 mL) and 1N NaOH (50 mL). The organic phase was collected and the aqueous phase was extracted further with CH₂Cl₂ (2 x 30 mL). The organic fractions were combined, washed with brine and then dried over Na₂SO₄. The suspension was filtered and solvent was removed under reduced pressure. The crude material was purified by column chromatography (10 % EtOAc/hexane) to yield 1-(3,5-dimethylphenyl) 3-ethyl 2,2-dimethylmalonate **5.3.20** as a colourless oil (3.3 g, 82 %). [Found: (HNESP⁺) [M+H]⁺ 265.1433. C₁₅H₂₁O₄ (M+H)⁺ requires 265.1434]; ν_{\max} (neat/cm⁻¹) 2983, 1764, 1735, 1619, 1591, 1467, 1386, 1267, 1246, 1159, 1134, 1105, 1026, 860; δ_{H} (500 MHz, CDCl₃) 1.32 (3H, t, *J* 7.5, OCH₂CH₃), 1.58 (6H, s, (C)CH₃), 2.32 (6H, s, ArCH₃), 4.28 (2H, q, *J* 7.5 Hz, OCH₂CH₃), 6.69 (2H, s, ArH),

6.87 (1H, s, ArH); δ_C (125 MHz, CDCl₃) 13.6, 20.8, 22.4, 49.5, 61.0, 118.4, 127.2, 138.8, 150.1, 171.1, 171.2.

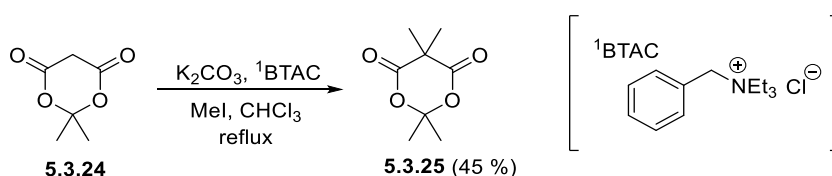
Reduction of 1-(3,5-dimethylphenyl) 3-ethyl 2,2-dimethylmalonate **5.3.20** with SED **4.1.15**



The general procedure for UV-activated reductions was applied to 1-(3,5-dimethylphenyl) 3-ethyl 2,2-dimethylmalonate **5.3.20** (132 mg, 0.5 mmol) using SED **4.1.15** (853 mg, 3.0 mmol) for 72 h at room temperature. The reaction mixture was then subjected to the general acidic workup procedure and the resulting crude material was purified by column chromatography (5 % EtOAc/hexane) to afford 3,5-dimethylphenol **5.3.1** (58 mg, 92 %) and the starting material **5.3.20** (8 mg, 6 %) with data for both compounds as previously reported.

Blank reactions: i) SED-free, UV-active and ii) SED (6 eq.), UV-free experiments were performed following the general procedure. For the first blank reaction, the starting material **5.3.20** was recovered (125 mg, 95 %). For the second blank reaction, the starting material **5.3.20** was recovered (115 mg, 89 %) along with 3,5-dimethylphenol **5.3.1** (5 mg, 8 %). The spectral data for the starting material **5.3.20** and 3,5-dimethylphenol **5.3.1** were as previously reported.

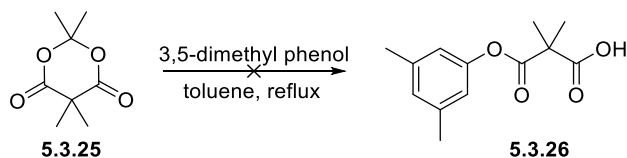
Synthesis of 2,2,5,5-tetramethyl-1,3-dioxane-4,6-dione **5.3.25**



Granulated K_2CO_3 (14.5 g, 105 mmol) and benzyltriethylammonium chloride (24 g, 105 mmol) were added portionwise to a solution of Meldrum's acid **5.3.24** (5 g, 35 mmol) in $CHCl_3$ (10 mL). The resulting suspension was stirred at 50 °C for 15 min, cooled to room temperature whereupon methyl iodide was added dropwise over 15 min using a dropping funnel. The reaction mixture was then refluxed for 4 h, cooled to room temperature and partitioned between $CHCl_3$ (30 mL) and H_2O (50 mL). The organic phase was collected and the aqueous layer was extracted further with $CHCl_3$ (2 x 30 mL). The organic extracts were combined, washed with brine and dried over Na_2SO_4 . The suspension was filtered and solvent was removed under reduced pressure to yield 2,2,5,5-tetramethyl-1,3-dioxane-4,6-dione **5.3.25** as a crystalline solid (15.5 g, 45 %). M.pt 60-61 °C (lit 60 °C)²⁴⁵; ν_{max} (neat/cm⁻¹) 1775, 1728, 1399, 1382, 1376; δ_H (500 MHz, $CDCl_3$) 1.66 (6H, s, $C(O)C(CH_3)_2$), 1.76 (6H, s, $O(C)(CH_3)_2$); δ_C (125 MHz, $CDCl_3$) 25.0, 28.3, 44.0, 104.2, 170.5. The spectral data were consistent with the literature data.²⁴⁵

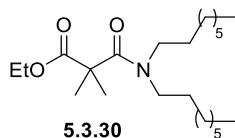
Attempted synthesis of 3-(3,5-dimethylphenoxy)-2,2-dimethyl-3-oxopropanoic acid

5.3.26



2,2,5,5-Tetramethyl-1,3-dioxane-4,6-dione **5.3.25** (2.7 g, 16 mmol) was dissolved in toluene (25 mL). 3,5-Dimethylphenol (1.95 g, 16 mmol) and KOH (895 mg, 16 mmol) were added to the solution and the reaction mixture was refluxed for 24 h after which the reaction was cooled to room temperature and the solvent was removed under reduced pressure. The resulting crude material was dissolved in CH_2Cl_2 (80 mL) and washed with 2N HCl (2 x 20 mL). The organic phase was washed with brine, dried over Na_2SO_4 , filtered and solvent removed under reduced pressure. The material recovery was poor (200 mg) and the 1H NMR spectrum showed no desired product.

Synthesis of ethyl 3-(dioctylamino)-2,2-dimethyl-3-oxopropanoate **5.3.30**

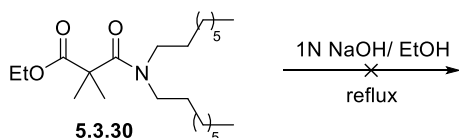


The general procedure for the *in situ* generation of acyl chloride followed by amide formation was employed.

Reagents: 3-ethoxy-2,2-dimethyl-3-oxopropanoic acid **5.3.19** (1.4 g, 8.6 mmol), oxalyl chloride (1.0 mL, 11.2 mmol), dry pyridine (2 mL), *N,N*-dioctylamine (2.7 g, 11.2 mmol), dry CH₂Cl₂ (20 mL). The resulting solution was then stirred for 4 h and then poured into 2 N HCl (50 mL). The aqueous collection was extracted with EtOAc (3 x 40 mL) and the organic collections were combined, washed with brine and dried over anhydrous Na₂SO₄. The solution was filtered and the solvent was removed under reduced pressure. The resulting crude was purified by column chromatography (5 % EtOAc/hexane) on silica gel to afford ethyl 3-(dioctylamino)-2,2-dimethyl-3-oxopropanoate **5.3.30** as a colourless oil (1.75 g, 53 %). ν_{\max} (neat/cm⁻¹) 2924, 2854, 1730, 1643, 1465, 1419, 1259, 1143, 1118, 1026, 723; δ_{H} (500 MHz, CDCl₃) 0.90 (6H, bs, CH₃), 1.29 (23H, m, OCH₂CH₃, CH₂), 1.43 (6H, s, CH₃), 1.52-1.55 (4H, m, (NCH₂CH₂)₂), 3.04 (2H, m, NCH₂CH₂), 3.31 (2H, m, NCH₂CH₂), 4.18 (2H, q, *J* 7.1, OCH₂CH₃); δ_{C} (125 MHz, CDCl₃) 13.5, 22.1, 24.0, 27.7, 28.7, 28.8, 28.9, 31.2, 45.0, 46.8, 48.5, 60.6, 170.6, 174.7; *m/z* (CI⁺ corona) 384 [(M+H)⁺, 100 %], 338 [(M-OCH₂CH₃)⁺, 30 %].

Attempted hydrolysis of ethyl 3-(dioctylamino)-2,2-dimethyl-3-oxopropanoate.

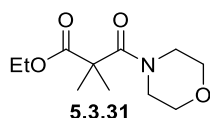
5.3.30



Ethyl 2,2-dimethyl-3-morpholino-3-oxopropanoate **5.3.30** (1.75 g, 4.6 mmol) was dissolved in EtOH (20 mL). A freshly prepared solution of 1N NaOH (380 mg, 9.2 mmol) in EtOH was added to the reaction mixture which was then brought to reflux

for 1 h. A small sample was taken from the reaction and partitioned between EtOAc (10 mL) and 2N HCl (10 ml). The resulting crude material was analysed by GC (CI) which showed only starting material. Another 2 eq. of 1N NaOH/EtOH was added to the reaction mixture and refluxed for 16 h. A sample was then retrieved from the reaction mixture and analysed as before. No reaction had occurred. The reaction was re-attempted in separate experiments using DMF (20 mL) and THF (20 mL) as solvents but no desired product was observed.

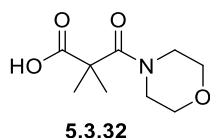
Synthesis of ethyl 2,2-dimethyl-3-morpholino-3-oxopropanoate.5.3.31



The general procedure for the *in situ* generation of acyl chloride followed by amide formation was employed.

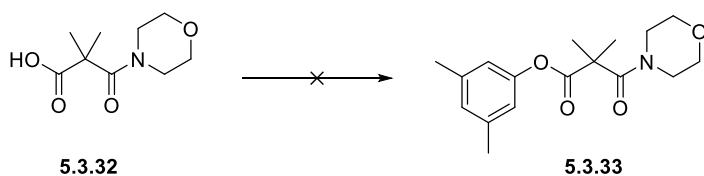
Reagents: 3-ethoxy-2,2-dimethyl-3-oxopropanoic acid **5.3.19** (704 mg, 4.4 mmol), oxalyl chloride (0.5 mL, 5.7 mmol), pyridine (2 mL), morpholine (496 mg, 5.7 mmol), dry CH₂Cl₂ (20 mL). The resulting solution was then stirred for 4 h and then poured into 2 N HCl (50 mL). The aqueous collection was extracted with EtOAc (3 x 40 mL) and the organic collections were then combined, washed with brine and dried over anhydrous Na₂SO₄. The solution was filtered and the solvent was removed under reduced pressure. The resulting crude was purified by column chromatography (30 % EtOAc/hexane) on silica gel to afford ethyl 2,2-dimethyl-3-morpholino-3-oxopropanoate **5.3.31** as a colourless oil (1.05 g, 91 %). [Found: [M+Na]⁺ 252.1202. C₁₁H₁₉NaNO₄ (M+Na)⁺ requires 252.1206; ν_{\max} (neat/cm⁻¹) 2983, 2856, 1726, 1643, 1423, 1267, 1138, 1113, 1035, 862; δ_{H} (500 MHz, CDCl₃) 1.27 (3H, t, *J* 7.0 Hz, OCH₂CH₃), 1.45 (6H, s, CH₃), 3.46 (4H, bs, CH₂), 3.65 (4H, bs, CH₂), 4.20 (2H, q, *J* 7.0 Hz, OCH₂CH₃), δ_{C} (125 MHz, CDCl₃) 13.6, 23.7, 48.1, 60.9, 66.0, 170.1, 174.4; *m/z* (CI⁺ corona) 230 [(M+H)⁺, 80 %], 184 [(M-OEt)⁺, 100 %].

Synthesis of 2,2-dimethyl-3-morpholino-3-oxopropanoic acid 5.3.32



Ethyl 2,2-dimethyl-3-morpholino-3-oxopropanoate **5.3.31** (1.0 g, 4.6 mmol) was dissolved in ethanol (20 mL) whereupon a solution of KOH (773 mg, 13.8 mmol) in ethanol (10 mL) was added. The reaction was then warmed to reflux for 3 days and then cooled to room temperature. Solvent was removed under reduced pressure and the crude product was partitioned between 2N NaOH (15 mL) and EtOAc (30 mL). The organic phase was further extracted with 2N NaOH (2 x 15 mL). The aqueous collections were combined, re-acidified with 6N HCl (50 mL) and then extracted with CH₂Cl₂ (3 x 20 mL). The organic extracts were combined, washed with brine and dried over anhydrous Na₂SO₄. The solution was filtered and the solvent was removed under reduced pressure to yield an off-white solid. The material was recrystallised from toluene/EtOAc to afford 2,2-dimethyl-3-morpholino-3-oxopropanoic acid **5.3.32** as white needles (545 mg, 60 %); M.pt. 159-160 °C; [Found: [M+H]⁺ 202.1071. C₉H₁₆NO₄ (M+H)⁺ requires 202.1074; ν_{\max} (neat/cm⁻¹) 3000, 2727, 1720, 1677, 1585, 1467, 1276, 1238, 1139, 1035, 896, 711; δ_{H} (500 MHz, CDCl₃) 1.50 (s, 6H, 2 x CH₃), 3.54 (bs, 4H, 2 x CH₂), 3.69 (m, 4H, 2 x CH₂), 8.74 (bs, 1H, CO₂H); δ_{C} (125 MHz, CDCl₃) 23.7, 48.1, 65.6, 65.9, 169.8, 178.6; m/z (CI⁺ corona) 156 [(M-CO₂H)⁺, 100 %], 88 [(M-(CH₃CH₃CO₂H)⁺, 40].

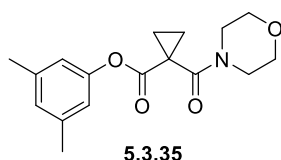
Attempted synthesis of 3,5-dimethylphenyl 2,2-dimethyl-3-morpholino-3-oxopropanoate **5.3.33**



The general procedure for the *in situ* generation of acyl chloride followed by ester formation was employed.

Reagents: 2,2-dimethyl-3-morpholino-3-oxopropanoic acid **5.3.32** (500 mg, 2.5 mmol), oxalyl chloride (0.40 mL, 4.3 mmol), pyridine (0.5 mL, 6.3 mmol), 3,5-dimethylphenol (460 mg, 3.8 mmol), dry CH₂Cl₂ (30 mL). After 12 h, the reaction mixture was partitioned between 2N HCl (20 mL) and CH₂Cl₂ (15 mL). The aqueous layer was extracted further with CH₂Cl₂ (2 x 20 mL) and the organic extracts were combined, washed with brine, and dried over Na₂SO₄. The suspension was filtered and the solvent was removed under reduced pressure. The mass recovery was very poor and no further purification was attempted.

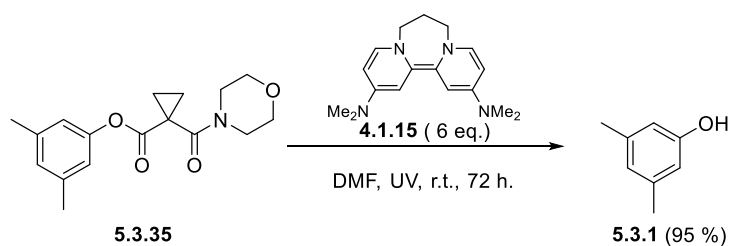
Synthesis of 3,5-dimethylphenyl 1-(morpholine-4-carbonyl)cyclopropane-1-carboxylate **5.3.35**



Cyclopropane-1,1-dicarbonyl dichloride (450 mg, 3.0 mmol) was diluted with dry CH₂Cl₂ (5 mL) and cooled to 0 °C whereupon a solution of 3,5-dimethylphenol (330 mg, 3.0 mmol) in dry CH₂Cl₂ (10 mL) and Hünig's base (0.53 mL, 3.0 mmol) were added portionwise to the reaction mixture. The reaction was stirred at 0 °C for 2 h, whereupon a solution of morpholine (280 mg, 3.2 mmol) in dry CH₂Cl₂ (10 mL) and Hünig's base (0.53 mL, 3.0 mmol) were added. The reaction mixture was warmed to room temperature and stirred for 16 h, after which it was partitioned between CH₂Cl₂ (20 mL) and H₂O (40 mL). The organic phase was separated and the aqueous layer was extracted further with CH₂Cl₂ (2 x 30 mL). The organic fractions were combined, washed with brine and dried over Na₂SO₄. The suspension was filtered and the solvent was removed under reduced pressure. The resulting crude material was purified by column chromatography (50 % EtOAc/hexane) to afford 3,5-dimethylphenyl 1-(morpholine-4-carbonyl)cyclopropane-1-carboxylate **5.3.35** as a white solid (530 mg, 58 %). M.pt. 149-150 °C; [Found: (HNESP⁺) [M+H]⁺ 304.1544. C₁₇H₂₂NO₄ (M+H)⁺ requires 304.1543]; ν_{max} (neat/cm⁻¹) 3100, 2974, 1739, 1633, 1460, 1431, 1273, 1139, 1111, 873, 686; δ_H (500 MHz, CDCl₃) 1.49-1.51 [2H, m, (C)(CH₂)], 1.66-1.69 [(2H, m, (C)(CH₂)], 2.33 (6H, s, ArCH₃), 3.70-3.76 [8H, m,

$N(CH_2)_2$ and $N(CH_2CH_2)_2$, 6.69 (2H, s, ArH), 6.90 (1H, s, ArH); δ_C (125 MHz, $CDCl_3$) 16.3, 20.0, 27.9, 42.2, 45.9, 65.8, 66.1, 118.2, 127.4, 138.9, 149.8, 165.9, 169.9.

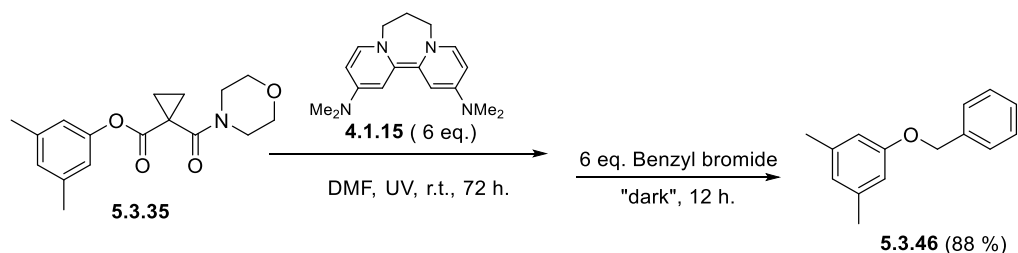
Reduction of 1-(morpholine-4-carbonyl)cyclopropane-1-carboxylate **5.3.35** with **4.1.15**



The general procedure for UV-activated reductions was applied to the substrate (152 mg, 0.5 mmol) using SED **4.1.15** (853 mg, 3.0 mmol) for 72 h at room temperature. The reaction mixture was then subjected to the general acidic workup procedure and the resulting crude material was purified by column chromatography (5 % EtOAc/hexane) to afford 3,5-dimethylphenol **5.3.1** (58 mg, 95 %) with data as previously reported. 1H NMR analysis of the crude material revealed full conversion of the starting material.

Blank reactions: i) SED (6 eq.), UV-free and ii) SED-free, UV-active experiments were performed following the general procedure. For the first blank reaction, the starting material **5.3.35** was recovered (144 mg, 95 %). For the second blank reaction, the starting material **5.3.35** was recovered (130 mg, 85 %) along with 3,5-dimethylphenol **5.3.1** (6 mg, 9 %). The spectral data for the starting material **5.3.35** and 3,5-dimethylphenol **5.3.1** were as previously reported.

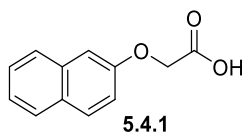
• **With subsequent trapping using benzyl bromide**



The general procedure for UV-activated reductions was applied to the substrate (152 mg, 0.5 mmol) using SED **4.2.15** (853 mg, 3.0 mmol) for 72 h at room temperature. The reaction mixture was then removed from the UV setup and benzyl bromide (0.5 mL, 3.0 mmol) was syringed into the reaction mixture. The reaction mixture was then stirred for 12 h and then subjected to the general acidic workup procedure and the resulting crude material was purified by column chromatography (20 % EtOAc/hexane) to afford 1-(benzyloxy)-3,5-dimethylbenzene **5.3.46** as a colourless oil (86 mg, 88 %). ν_{max} (neat)/ cm^{-1} 3062, 3032, 2916, 1612, 1596, 1452, 1321, 1294, 1151, 1058, 825, 732, 686; δ_{H} (500 MHz, CDCl_3) 2.33 (6H, s, ArCH_3), 5.07 (2H, s, OCH_2), 6.66 (3H, bs, ArH), 7.35-7.46 (5H, m, ArH); δ_{C} (125 MHz, CDCl_3) 20.9, 63.33, 122.0, 122.2, 126.9, 127.3, 128.0, 136.8, 138.7, 158.4; m/z (CI^+ corona) 213.2 $[(\text{M}+\text{H})^+$, 35 %], 135 $[(\text{M}-\text{C}_6\text{H}_5)^+$, 30], 91.1 $[(\text{M}-\text{C}_8\text{H}_9\text{O})^+$, 100]. The spectral data were consistent with the literature data.²⁴⁶

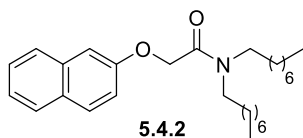
7.6 Experimental for Chapter 5.4

Synthesis of 2-(naphthalen-2-yloxy)acetic acid **5.4.1**



A slurry of pre-washed and dried NaH (760 mg, 31.5 mmol) in dry THF (15 mL) was made up in an oven-dried 250 ml round-bottomed flask under argon and then cooled to 0 °C whereupon a solution of 2-naphthol (2.17 g, 15.0 mmol,) in dry THF (20 mL) was added portionwise. After the addition, the resulting suspension was warmed to 35 °C for 30 min, whereupon a solution of bromoacetic acid (2.50 g, 18.0 mmol) in dry THF (20 mL) was added portionwise. The reaction mixture was then refluxed for 10 h, cooled to room temperature and then partitioned between 2 N HCl (80 mL) and CH₂Cl₂ (50 mL). The organic phase was separated and the aqueous phase was further extracted with CH₂Cl₂ (2 x 50 mL). The organic fractions were combined, washed with brine (40 mL), dried over Na₂SO₄, filtered and solvent removed under reduced pressure. The crude product was recrystallised from toluene to give 2-(naphthalen-2-yloxy)acetic acid **5.4.1** as a white solid (2.95 g, 100 %). M.pt. 154-155 °C (lit. 155 °C)²⁴⁷; ν_{\max} (ATR)/cm⁻¹ 3671, 3059, 2912, 2586, 1735, 1598, 1508, 1429, 1246, 1182, 1076, 908; δ_{H} (400 MHz, DMSO-d₆); 4.81 (2H, s, ArOCH₂), 7.22-7.27 (2H, dd, *J* 8.3, 2.6, Ar*H*), 7.35-7.38 (1H, m, Ar*H*), 7.45 (1H, t, *J* 7.5, Ar*H*), 7.47 (1H, t, *J* 7.5, Ar*H*), 7.79-7.86 (3H, m, Ar*H*), 13.01 (1H, bs, CO₂H); δ_{C} (100 MHz, DMSO-d₆) 62.5, 106.9, 118.4, 123.7, 126.4, 126.7, 127.4, 128.6, 129.3, 134.0, 155.6, 170.0; *m/z* (EI) 202.1 (M⁺, 100 %), 157 (40), 144 (25); The spectral data were consistent with the literature data.²⁴⁷

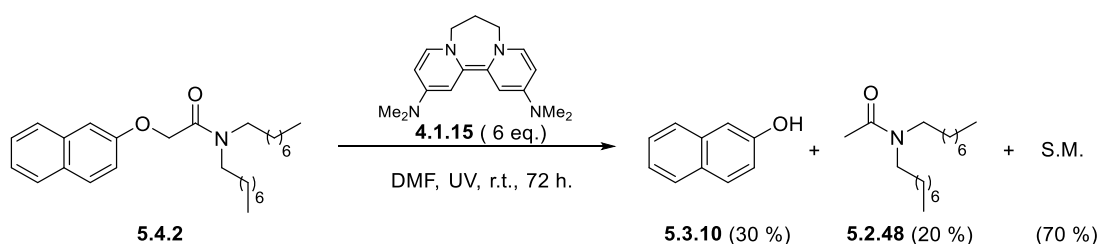
Synthesis of 2-(naphthalen-2-yloxy)-*N,N*-dioctylacetamide **5.4.2**



The general procedure for the *in situ* generation of acyl chloride followed by amide formation was employed.

Reagents: 2-(naphthalen-2-yloxy)acetic acid **5.4.1** (1.62 g, 8 mmol), oxalyl chloride (0.83 mL, 9.6 mmol), pyridine (0.78 mL, 9.6 mmol), dioctylamine (2.90 g, 12.0 mmol), dry CH₂Cl₂ (30 mL). After 12 h, the reaction mixture was partitioned between 2N HCl (50 mL) and CH₂Cl₂ (30 mL). The aqueous layer was extracted further with CH₂Cl₂ (30 mL) and the organic extracts were combined, washed with brine and dried over Na₂SO₄. The suspension was filtered and the solvent was removed under reduced pressure. The resulting crude material was purified by column chromatography (10 % EtOAc/hexane) to afford the desired product 2-(naphthalen-2-yloxy)-*N,N*-dioctylacetamide **5.4.2** as a colourless oil (2.17 g, 64 %). [Found: (HNESP⁺) (M+H)⁺, 426.3364. C₂₈H₄₄NO₂⁺ (M+H)⁺, requires 426.3367]; ν_{\max} (ATR)/cm⁻¹ 2953, 2852, 1647, 1600, 1465, 1253, 1215, 1176, 1045, 833; δ_{H} (400 MHz, CDCl₃) 0.89-0.90 (6H, m, 2 x CH₃), 1.31-1.32 (20H, m, 10 x CH₂), 1.57-1.63 (4H, m, 2 x NCH₂CH₂), 3.36-3.37 (m, 4H, 2 x NCH₂), 4.82 (2H, s, ArOCH₂), 7.20-7.24 (2H, m, ArH), 7.39 (1H, t, *J* 7.6, ArH), 7.44 (1H, t, *J* 7.6, ArH), 7.74-7.79 (3H, m, ArH); δ_{C} (100 MHz, CDCl₃) 13.6, 22.2, 26.4, 26.5, 26.9, 28.5, 28.7, 28.8, 28.9, 31.2, 31.3, 45.5, 46.9, 67.2, 106.8, 118.0, 123.4, 125.9, 126.4, 127.1, 128.8, 129.0, 133.9, 155.6, 166.8.

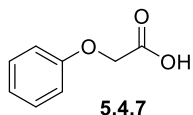
Reduction of 2-(naphthalen-2-yloxy)-*N,N*-dioctylacetamide **5.4.2** with **4.1.15**



The general procedure for UV-activated reductions was applied to substrate **5.4.2** (213 mg, 0.5 mmol) using SED **4.1.15** (853 mg, 3.0 mmol) for 72 h at room temperature. The reaction mixture was then subjected to the general acidic workup procedure and the resulting crude product was purified by column chromatography

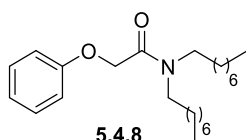
(5-10 % EtOAc/hexane) to afford 2-naphthol **5.3.10** (22 mg, 30 %), *N,N*-dioctylacetamide **5.2.48** (25 mg, 20 %) and the starting material **5.4.2** (150 mg, 70 %). The spectral data for the three compounds were as previously reported.

Synthesis of 2-phenoxyacetic acid **5.4.7**



A slurry of pre-washed and dried NaH (735 mg, 30.5 mmol), in dry THF (15 mL) was made up in an oven-dried 250 mL round-bottomed flask under argon and then cooled to 0 °C whereupon a solution of phenol (1.35g, 14.5 mmol,) in dry THF (20 mL) was added portionwise. After the addition, the resulting suspension was warmed to 35 °C for 30 min whereupon a solution of bromoacetic acid (2.0 g, 14.5 mmol) in dry THF (20 mL) was added portionwise. The reaction mixture was then refluxed for 10 h, cooled and then partitioned between 2 N HCl (80 mL) and CH₂Cl₂ (50 mL). The organic phase was separated and the aqueous layer was further extracted with CH₂Cl₂ (2 x 50 mL). The organic extracts were combined, washed with brine, dried over Na₂SO₄, filtered and solvent removed under reduced pressure to afford the 2-phenoxyacetic acid **5.4.7** as a white solid (2.2 g, 100 %). M.pt. 100-102 °C (lit. 98-100 °C)²⁴⁸; ν_{\max} (ATR)/cm⁻¹ 3060, 3020, 2920, 2794, 2574, 1697, 1595, 1487, 1265, 1089, 960, 752; δ_{H} (400 MHz, CDCl₃) 4.72 (2H, s, ArOCH₂), 6.97 (2H, d, *J* 7.3, ArH), 7.05 (1H, t, *J* 7.3, ArH), 7.34 (2H, t, *J* 7.3, ArH); δ_{C} (100 MHz, CDCl₃) 64.3, 114.2, 121.6, 129.2, 156.9, 173.8; *m/z* (APCI) 152.0 (M⁺, 60%), 107 (40), 77 (100); The spectral data were consistent with the literature data²⁴⁸

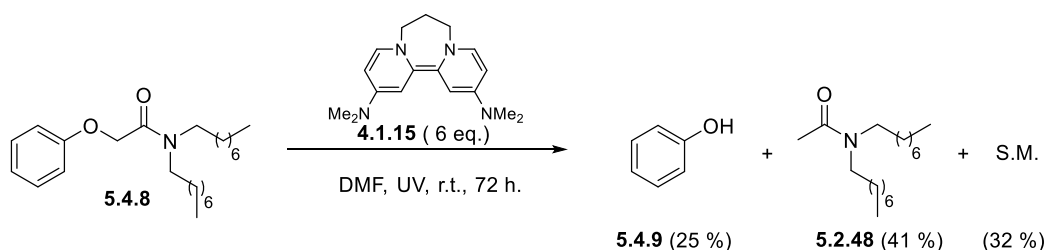
Synthesis of *N,N*-dioctyl-2-phenoxyacetamide **5.4.8**



The general procedure for the *in situ* generation of acyl chloride followed by amide formation was employed.

Reagents: 2-phenoxyacetic acid **5.4.7** (760 mg, 5 mmol), oxalyl chloride (0.52 mL, 6.0 mmol), pyridine (0.41 mL, 5.1 mmol), *N,N*-dioctylamine (2.26 g, 7.5 mmol), dry CH_2Cl_2 (30 mL). The reaction mixture was left to stir for 16 h after which it was quenched with H_2O (50 mL) and extracted with EtOAc (4 x 30 mL). The organic layers were combined, washed with brine, dried over Na_2SO_4 , filtered and then concentrated under reduced pressure. The crude product was purified by column chromatography (5 % EtOAc/hexane) and afforded *N,N*-dioctyl-2-phenoxyacetamide **5.4.8** as a colourless oil (1.50 g, 80 %). [Found: (HNESP⁺) (M+H)⁺ 376.3208. $\text{C}_{24}\text{H}_{42}\text{NO}_2$ (M+H)⁺ requires 376.3210]; ν_{max} (ATR)/ cm^{-1} 2954, 2924, 2854, 1647, 1598, 1494, 1232, 1172, 1082, 750; δ_{H} (400 MHz, CDCl_3) 0.90-0.91 (6H, m, 2 x CH_3), 1.28-1.32 (20 H, m, 10 x CH_2), 1.51-1.62 (4H, m, 2 x NCH_2CH_2), 3.30-3.37 (4H, m, 2 x NCH_2), 4.70 (2H, s, ArOCH_2), 6.95-7.01 (3H, m, ArH), 7.28-7.32 (2H, m, ArH); δ_{C} (100 MHz, CDCl_3) 13.6, 22.1, 26.4, 26.5, 26.9, 28.5, 28.7, 28.8, 28.9, 31.2, 31.3, 45.4, 46.9, 67.1, 114.2, 120.9, 129.0, 157.7, 166.9.

Reduction of *N,N*-dioctyl-2-phenoxyacetamide **5.4.8** with **4.1.15**

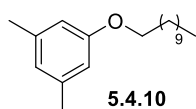


The general procedure for UV-activated reductions was applied to the substrate **5.4.8** (188 mg, 0.5 mmol) using SED **4.1.15** (853 mg, 3.0 mmol) for 72 h at room temperature. The reaction mixture was then subjected to the general acidic workup procedure and the resulting crude material was purified by column chromatography (5-10 % EtOAc/hexane) to afford *N,N*-dioctylacetamide **5.2.48** (51.3 mg, 41 %), the starting material **5.4.9** (60 mg, 32 %) and phenol **5.4.9** (11.8 mg, 25 %). The spectral data for *N,N*-dioctylacetamide **5.2.48** and the starting material **5.4.9** were as previously reported.

Phenol **5.4.9**: white solid; M.pt. 40-41 °C (lit. 38.5-41.5 °C)²⁴⁹; δ_{H} (400 MHz, CDCl₃) 4.87 (1H, bs, ArOH), 6.85-6.87 (2H, m, ArH), 6.95 (1H, tt, *J* 7.5, 1.1, ArH), 7.27 (2H, t, *J* 7.5, ArH); δ_{C} (100 MHz, CDCl₃) 113.5, 120.3, 130.4, 152.1; *m/z* (GCMS, CI, CH₄) 95.2 (M+H⁺, 100 %); The spectral data were consistent with the literature data.²⁴⁹

Blank reactions: i) SED-free, UV-active and ii) SED (6 eq.), UV-free experiments were performed following the general procedure. For the first blank reaction, the starting material **5.4.8** was recovered (178 mg, 95 %). For the second blank reaction, the starting material **5.4.8** was recovered (173 mg, 90 %). The spectral data for the starting material **5.4.8** were as previously reported.

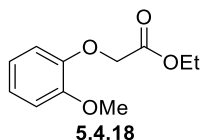
Synthesis of 1,3-dimethyl-5-(undecyloxy)benzene **5.4.10**



Potassium carbonate (1.2 g, 8.8 mmol) was added to a solution of 3,5-dimethylphenol (980 mg, 8.0 mmol) in acetone (15 mL). The suspension was stirred at room temperature for 30 min and then 1-bromoundecane (1.7 g, 7.5 mmol) was added to the reaction mixture portionwise. The reaction mixture was refluxed for 12 h, cooled to room temperature and then partitioned between H₂O (50 mL) and Et₂O (30 mL). The aqueous layer was extracted further with Et₂O (2 x 30mL) and the organic extracts were combined. The organic fraction was washed with brine, dried over Na₂SO₄ and filtered. The solvent was removed under reduced pressure and the resulting crude material was purified by column chromatography (100 % hexane) on silica gel to afford 1,3-dimethyl-5-(undecyloxy)benzene **5.4.10** as a colourless oil (1.05 g, 51 %). [Found: [M+H]⁺ 277.2531. C₁₉H₃₃O (M+H)⁺ requires 277.2526]; ν_{max} (neat/cm⁻¹) 2922, 2852, 1595, 1465, 1323, 1294, 1167, 1155, 1066, 825, 686; δ_{H} (500 MHz, CDCl₃) 0.90-0.92 (3H, m, CH₂CH₃), 1.30 (14H, bs, 7 x CH₂), 1.45-1.49 (2H, m, OCH₂CH₂CH₂), 1.75-1.82 (2H, m, OCH₂CH₂). 2.31 (6H, s, ArCH₃), 3.95 (2H, t, *J* 6.7, OCH₂), 6.56 (2H, s, ArH), 6.61 (1H, s, ArH); δ_{C} (125 MHz, CDCl₃) 13.6, 20.9,

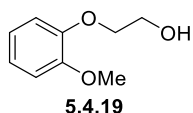
22.2, 25.6, 28.8, 28.9, 29.0, 29.1, 29.2, 31.5, 67.3, 111.7, 121.8, 138.6, 158.7; m/z (Cl^+ corona) 277 $[(\text{M}+\text{H})^+]$, 100 %], 195 (10), 123 (15).

Synthesis of ethyl 2-(2-methoxyphenoxy)acetate **5.4.18**



To a solution of 2-methoxyphenol (1.6 g, 12.5 mmol) in DMF (20 mL) was added finely crushed potassium carbonate (4.2 g, 30.0 mmol). The resulting suspension was stirred at 50 °C for 0.5 h whereupon a solution of ethyl 2-bromoacetate (3.3 mL, 30.0 mmol) in DMF (10 mL) was added portionwise. The reaction mixture was stirred at 80 °C for 16 h, cooled to room temperature and then partitioned between Et_2O (80 mL) and 2N HCl (100 mL). The organic phase was collected and the aqueous layer was extracted further with Et_2O (2 x 30 mL). washed with brine and dried over Na_2SO_4 . The suspension was filtered and concentrated under reduced pressure. The crude material was then purified by column chromatography (15 % EtOAc/hexane) to afford ethyl 2-(2-methoxyphenoxy)acetate **5.4.18** as a colourless oil (2.4 g, 92 %). [Found: (HNESP^+) $[(\text{M}+\text{H})^+]$ 211.0962. $\text{C}_{11}\text{H}_{15}\text{O}_4$ $(\text{M}+\text{H})^+$ requires 211.0965]; ν_{max} (neat)/ cm^{-1} 3060, 2980, 2937, 2837, 1755, 1732, 1502, 1456, 1249, 1174, 1024, 740; δ_{H} (500 MHz, CDCl_3) 1.30 (3H, t, J 7.2, OCH_2CH_3), 3.90 (3H, s, ArOCH_3), 4.28 (2H, q, J 7.2, OCH_2CH_3), 4.70 (2H, s, ArOCH_2COO), 6.86-7.02 (4H, m, ArH); δ_{C} (125 MHz, CDCl_3) 13.7, 55.4, 60.7, 66.1, 111.7, 114.0, 120.2, 122.0, 146.8, 149.2, 168.6. The spectral data were consistent with the literature data.²⁵⁰

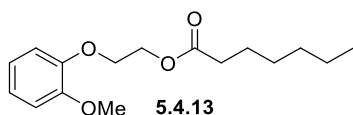
Synthesis of ethyl 2-(2-methoxyphenoxy)ethan-1-ol **5.4.19**



A solution of ethyl 2-(2-methoxyphenoxy)acetate **5.4.18** (1.0 g, 5.0 mmol) in dry THF (10 mL) was added dropwise to a suspension of LiAlH_4 (150 mg, 4.0 mmol) in dry THF (10 mL) at 0 °C. The reaction mixture was stirred at 0 °C for 0.5 h and then warmed to reflux for 2 h. The reaction mixture was then carefully quenched with

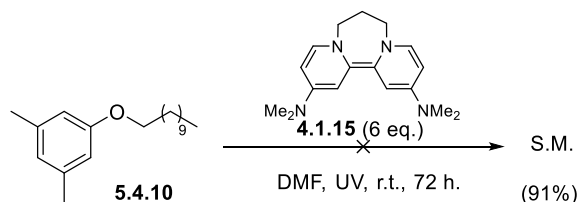
MeOH and 2N HCl at 0 °C and partitioned between Et₂O (20 mL) and 2N HCl (50 mL). The organic phase was collected and the aqueous layer was extracted further with Et₂O (2 x 30 mL). washed with brine and dried over Na₂SO₄. The suspension was filtered and concentrated under reduced pressure. The crude material was then purified by column chromatography (35 % EtOAc/hexane) to afford ethyl 2-(2-methoxyphenoxy)ethan-1-ol **5.4.19** as a colourless oil (795 mg, 94 %). ν_{\max} (neat)/cm⁻¹ 3421(br), 2933, 2873, 1593, 1504, 1452, 1249, 1220, 1122, 912, 740; δ_{H} (500 MHz, CDCl₃) 3.3 (1H, bs, OH), 3.88 (3H, s, ArOCH₃), 3.95 (2H, t, *J* 4.5 Hz, CH₂CH₂OH), 4.13 (2H, t, *J* 4.5 Hz, CH₂CH₂OH), 6.91-7.01 (4H, m, ArH); δ_{C} (125 MHz, CDCl₃) 55.3, 60.7, 70.9, 111.4, 114.6, 120.6, 121.6, 147.6, 140.4; *m/z* (GCMS, CI, CH₄) 160.0 [(M+H)⁺, 30 %], 151.0 (75), 125.0 (100). The spectral data were consistent with the literature data.²⁵¹

Synthesis of 2-(2-methoxyphenoxy)ethyl heptanoate **5.4.13**



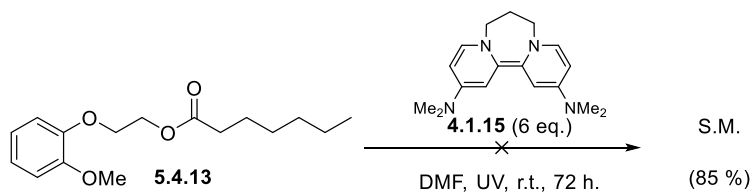
Heptanoyl chloride (0.87 mL, 5.7 mmol) and pyridine (0.5 mL, 6.2 mmol) were added portionwise to a solution of ethyl 2-(2-methoxyphenoxy)ethan-1-ol **5.4.19** (800 mg, 4.8 mmol) in dry THF (15 mL). The reaction mixture was then refluxed for 16 h, cooled to room temperature and partitioned between Et₂O (20 mL) and H₂O (50 mL). The organic phase was collected and the aqueous layer was extracted further with Et₂O (2 x 10 mL). washed with brine and dried over Na₂SO₄. The suspension was filtered and concentrated under reduced pressure. The crude material was then purified by column chromatography (15 % EtOAc/hexane) to afford 2-(2-methoxyphenoxy)ethyl heptanoate **5.4.13** as a pale yellow oil (865 mg, 65 %). [Found: (HNESP⁺) [(M+H)⁺ 281.1746. C₁₆H₂₅O₄ (M+H)⁺ requires 281.1747]; ν_{\max} (neat)/cm⁻¹ 2929, 1734, 1504, 1454, 1251, 1165, 1126, 1028, 740; δ_{H} (500 MHz, CDCl₃) 0.89 (3H, t, *J* 7.3, CH₂CH₃), 1.30-1.32 (6H, m, 3 x CH₂), 1.63-1.66 (2H, m, COCH₂CH₂), 2.37 (2H, t, *J* 7.5, COCH₂), 3.88 (3H, s, ArOCH₃), 4.26 (2H, t, *J* 5.0, CH₂), 4.47 (2H, t, *J* 5.0, CH₂), 6.93-7.10 (4H, m, ArH); δ_{C} (125 MHz, CDCl₃) 13.5, 21.9, 24.3, 28.2, 30.9, 33.7, 55.4, 62.1, 66.9, 111.8, 114.2, 120.3, 121.5, 147.5, 149.4, 173.3.

Attempted reduction of 1,3-dimethyl-5-(undecyloxy)benzene **5.4.10**



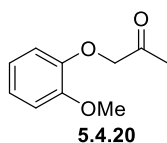
The general procedure for UV-activated reductions was applied to the substrate (188 mg, 0.5 mmol) using SED **4.1.15** (853 mg, 3.0 mmol) for 72 h at room temperature. The reaction mixture was then subjected to the general acidic workup procedure and the resulting crude material was purified by column chromatography (5-10 % EtOAc/hexane) to afford the starting material **5.4.10** (125 mg, 91 %) with spectral data as previously reported.

Attempted reduction of 2-(2-methoxyphenoxy)ethyl heptanoate **5.4.13** with **4.1.15**



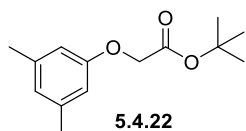
The general procedure for UV-activated reductions was applied to the substrate (140 mg, 0.5 mmol) using SED **4.1.15** (853 mg, 3.0 mmol) for 72 h at room temperature. The reaction mixture was then subjected to the general acidic workup procedure and the resulting crude material was purified by column chromatography (10 % EtOAc/hexane) to afford the starting material **5.4.13** (120 mg, 85 %) with data as previously reported.

Synthesis of 1-(2-methoxyphenoxy)propan-2-one **5.4.20**



Potassium carbonate (1.0 g, 7.5 mmol) was added to a solution of guaiacol (620 mg, 5.0 mmol) in acetone (15 mL). The suspension was stirred at room temperature for 30 min and then 1-chloropropan-2-one (693 mg, 7.5 mmol) was syringed into the reaction mixture portionwise. The reaction mixture was refluxed for 15 h, cooled to room temperature and then partitioned between H₂O (50 mL) and Et₂O (30 mL). The aqueous layer was extracted further with Et₂O (2 x 30mL) and the organic extracts were combined. The organic fraction was washed with brine, dried over Na₂SO₄ and filtered. The solvent was removed under reduced pressure and the resulting crude material was purified by column chromatography (10 % EtOAc/hexane) on silica gel to afford 1-(2-methoxyphenoxy)propan-2-one **5.4.20** as a colourless oil (900 mg, 84 %). [Found: [M+H]⁺ 181.0858. C₁₀H₁₃O₃ (M+H)⁺ requires 181.0859; ν_{\max} (neat/cm⁻¹) 3064, 2937, 1716, 1593, 1502, 1250, 1126, 1024, 810; δ_{H} (500 MHz, CDCl₃) 2.31 (3H, s, OCH₂COCH₃), 3.91 (3H, s, ArOCH₃), 4.61 (2H, s, OCH₂COCH₃), 6.80 (1H, dd, *J* 8.0, 1.5, Ar*H*), 6.88-6.96 (2H, m, Ar*H*), 6.99-7.03 (1H, m, Ar*H*); δ_{C} (125 MHz, CDCl₃) 23.0, 52.5, 71.1, 108.9, 110.9, 117.5, 119.2, 144.0, 146.3, 203.0; *m/z* (CI⁺ corona) 203 [(M+Na)⁺, 100 %], 181 [(M+H)⁺, 60 %] 163 (10).

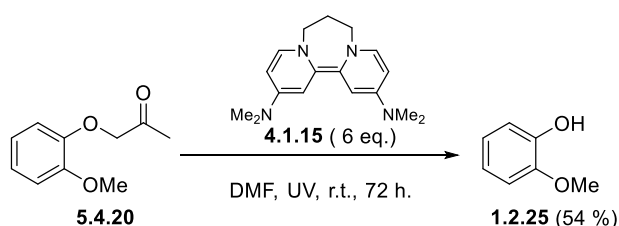
Synthesis of *tert*-butyl 2-(3,5-dimethylphenoxy)acetate **5.4.22**



3,5-Dimethylphenol (3.0 g, 25 mmol) was dissolved in DMF (10 mL). A solution of *tert*-butyl bromoacetate (9.7 g, 50 mmol) was added portionwise to the reaction followed by potassium carbonate (4.1 g, 30 mmol). The reaction was then warmed to 80 °C for 20 h, cooled to room temperature and partitioned between EtOAc (100 mL) and 2N HCl (150 mL). The aqueous layer was extracted further with EtOAc (2 x 80 mL) and the organic extracts were combined, washed with brine and dried over Na₂SO₄. The suspension was filtered and the solvent was removed under reduced pressure. The resulting crude material was purified by column chromatography (5 % EtOAc/hexane) on silica gel to afford *tert*-butyl 2-(3,5-dimethylphenoxy)acetate

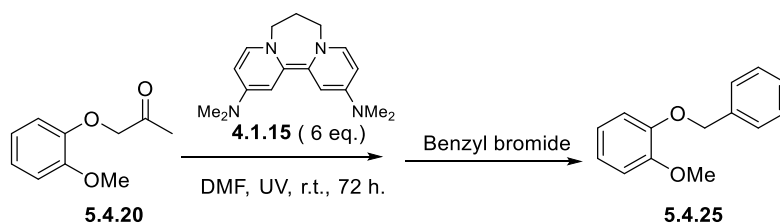
5.4.22 (5.9 g, 98 %) as a white crystalline solid. M.pt 52-53 °C; [Found: [M+Na]⁺ 259.1305. C₁₄H₂₀O₃Na (M+Na)⁺ requires 259.1305]; ν_{\max} (neat/cm⁻¹) 2980, 2854, 1755, 1598, 1436, 1328, 1220, 1141, 1093, 844, 759; δ_{H} (500 MHz, CDCl₃) 1.40 (9H, s, 3 x CH₃), 2.28 (6 H, s, 2 x CH₃), 5.05 (2H, s, ArOCH₂), 6.46 (2H, bs, ArH), 6.60 (1H, bs, ArH); δ_{C} (125 MHz, CDCl₃) 21.4, 28.0, 65.7, 82.1, 112.4, 123.3, 139.2, 157.9, 168.2; *m/z* (CI⁺ corona) 180 [(M-^tBu)⁺, 100 %], 135 (80).

Reduction of 1-(2-methoxyphenoxy)propan-2-one **5.4.20** with **4.1.15**



The general procedure for UV-activated reductions was applied to substrate **5.4.20** (90 mg, 0.5 mmol) using SED **4.1.15** (853 mg, 3.0 mmol) for 72 h at room temperature. The reaction mixture was then subjected to the general acidic workup procedure and the resulting crude material was purified by column chromatography (5 % EtOAc/hexane) to afford guaiacol **1.2.25** as a colourless oil (60 mg, 54 %); δ_{H} (500 MHz, CDCl₃) 3.92 (3H, s, ArOCH₃), 5.63 (1H, bs, ArOH), 6.88-6.92 (3H, m, ArH), 6.94-6.97 (1H, m, ArH); δ_{C} (125 MHz, CDCl₃) 57.1, 111.0, 114.5, 119.3, 121.3, 145.7, 146.5; (GCMS, CI, CH₄) 125.0 [(M+H)⁺, 100 %] The spectral data were consistent with the literature data.²⁵²

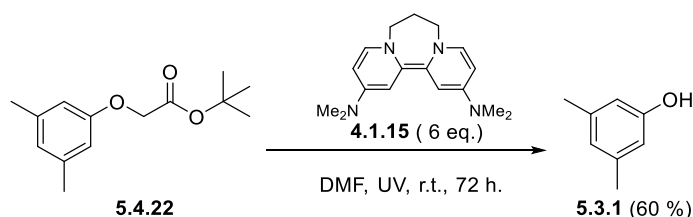
- **With subsequent trapping with benzyl bromide**



The general procedure for UV-activated reductions was applied to the substrate (90 mg, 0.5 mmol) using SED **4.1.15** (853 mg, 3.0 mmol) for 72 h at room temperature. The reaction mixture was then removed from the UV setup and benzyl bromide (0.5

mL, 3.0 mmol) was syringed into the reaction mixture. The reaction mixture was stirred for 12 h, quenched with 2N HCl (20 mL) and extracted with Et₂O (3 x 30 mL). The organic extracts were combined, washed with brine and dried over Na₂SO₄. The suspension was filtered and the solvent was removed under reduced pressure. The resulting crude product was purified by column chromatography (100 % hexane) on silica gel to afford 1-(benzyloxy)-2-methoxybenzene **5.4.25** as a colourless oil (76 mg, 71 %). [Found: [M+NH₄]⁺ 232.1333. C₁₄H₁₈NO₂ (M+NH₄)⁺ requires 232.1332; ν_{\max} (neat/cm⁻¹) 3032, 2931, 1591, 1502, 1249, 1219, 1122, 1024, 736; δ_{H} (500 MHz, CDCl₃) 3.90 (3H, s, ArOCH₃), 5.17 (2H, s, ArOCH₂), 6.90-6.93 (4H, m, ArH), 7.2-7.36 (5H, m, ArH); δ_{C} (125 MHz, CDCl₃) 55.9, 71.1, 112.0, 114.3, 120.8, 121.5, 127.3, 127.8, 128.5, 137.3, 148.3, 149.8, m/z (CI⁺ corona) 232 [(M+NH₄)⁺, 100 %], 215 (40). The spectral data were consistent with the literature data.²⁵³

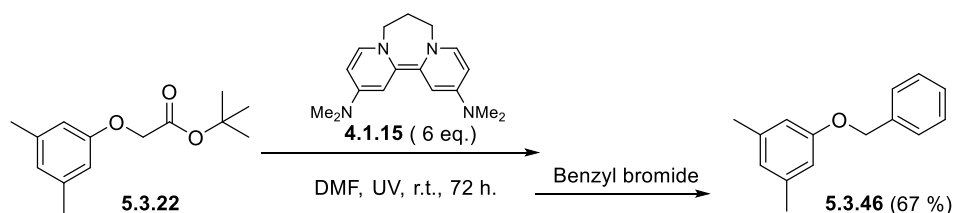
Reduction of *tert*-butyl 2-(3,5-dimethylphenoxy)acetate **5.4.22** with **4.1.15**



The general procedure for UV-activated reductions was applied to substrate **5.4.22** (118 mg, 0.5 mmol) using SED **4.1.15** (853 mg, 3.0 mmol) for 72 h at room temperature. The reaction mixture was then subjected to the general acidic workup procedure and the resulting crude material was purified by column chromatography (100 % hexane) to afford 3,5-dimethylphenol **5.3.1** as a pale yellow solid (37 mg, 60 %) with spectral data as previously reported.

Blank reactions: i) SED-free, UV-active and ii) SED (6 eq.), UV-free experiments were performed following the general procedure. For the first blank reaction, the starting material **5.4.22** was recovered (103 mg, 87 %). For the second blank reaction, the starting material **5.4.22** was recovered (89 mg, 75 %). The spectral data for the starting material **5.4.22** were as previously reported.

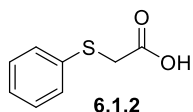
- **With subsequent trapping with benzyl bromide**



The general procedure for UV-activated reductions was applied to the substrate (118 mg, 0.5 mmol) using SED **4.1.15** (853 mg, 3.0 mmol) for 72 h at room temperature. The reaction mixture was then removed from the UV setup and benzyl bromide (0.5 mL, 3.0 mmol) was syringed into the reaction mixture. The reaction mixture was stirred for 12 h, then quenched with 2N HCl (20 mL) and extracted with Et₂O (3 x 30 mL). The organic fractions were combined, washed with brine and dried over Na₂SO₄. The suspension was filtered and the solvent was removed under reduced pressure. The resulting crude product was purified by column chromatography (100 % hexane) on silica gel to afford 1-(benzyloxy)-3,5-dimethylbenzene **5.3.46** as a colourless oil (71 mg, 67 %) with data as previously reported.

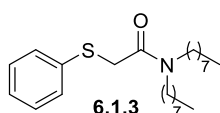
7.7 Experimental for Chapter 6.1

Synthesis of 2-(phenylsulfanyl)acetic acid **6.1.2**



Thiophenol (5.1 mL, 50 mmol) was dissolved in DMF (50 mL) whereupon potassium carbonate (15.2 g, 110 mmol) was added portionwise to the solution. The reaction mixture was warmed to 60 °C for 0.5 h then cooled to room temperature. Bromoacetic acid (7.6 g, 55 mmol) was then added whereupon a white emulsion was formed. The reaction mixture was diluted with DMF (50 mL) to allow easier stirring, stirred for 48 h at 80 °C and then cooled to room temperature during which crystallisation occurred. The crystals were filtered from the solvent and then recrystallised (CH₂Cl₂/hexane 1:9) to yield 2-(phenylthio)acetic acid **6.1.2** as colourless crystals (8.2 g, 98 %). M.pt. 61-62 °C (lit. 62-64 °C)²⁵⁴; ν_{\max} (ATR)/cm⁻¹ 3057, 2953, 2852, 1710, 1643, 1479, 1438, 1113, 736; δ_{H} (400 MHz, DMSO-d₆); 3.80 (2H, s, SCH₂), 7.20-7.22 (1H, m, ArH), 7.34-7.35 (4H, m, ArH), 12.75 (1H, bs, CO₂H); δ_{C} (100 MHz, DMSO-d₆) 34.9, 125.8, 127.7, 128.9, 135.7, 170.6; m/z (ESI): 167 [(M-H)⁻, 100 %]. The spectral data were consistent with the literature data.²⁵⁵

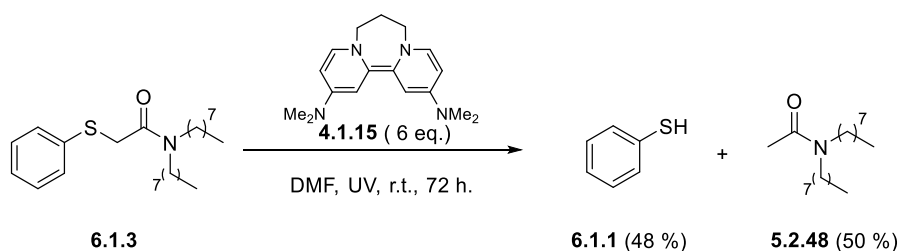
Synthesis of *N,N*-dioctyl-2-(thiophenyl)acetamide **6.1.3**



To a solution of phenyl(sulfanyl)acetic acid **6.1.2** (3.4 g, 20 mmol) in CH₂Cl₂ (40 mL) was added oxalyl chloride (2.1 mL, 24 mmol) dropwise at 0 °C. A few drops of dry DMF were added slowly and the resulting solution was left to stir at 0 °C for 0.5 h after which a solution of *N,N*-dioctylamine (7.25 g, 30 mmol) in pyridine (15 mL) was added in one portion. The resulting red suspension was then warmed to room temperature and then stirred for 3 h. The reaction mixture was then diluted with 2N HCl (50 mL) and extracted with Et₂O (3 x 30 mL). The organic fractions were

combined, washed with brine and then dried over Na₂SO₄. The suspension was filtered and concentrated under reduced pressure. The crude was then purified by column chromatography (5 % EtOAc/hexane) to afford *N,N*-dioctyl-2-(thiophenyl)acetamide **6.1.3** as a red oil (5.10 g, 55%). [Found: (HNESP⁺) (M+H)⁺ 392.2983. C₂₄H₄₂NOS (M+H)⁺, requires 392.2983]; ν_{\max} (ATR)/cm⁻¹ 3057, 2924, 2853, 1643, 1586, 1477, 1456, 1438, 1378, 1300, 1116, 1026, 737; δ_{H} (400 MHz, CDCl₃); 0.90-0.91 (6H, m, CH₂CH₃), 1.28-1.30 (20H, m, CH₂), 1.52-1.58 (4H, m, NCH₂CH₂), 3.23 (2H, t, *J* 7.7, NCH₂), 3.25 (2H, t, *J* 7.7, NCH₂), 3.75 (2H, s, SCH₂), 7.23 (1H, t, *J* 7.7, Ar*H*), 7.33 (2H, t, *J* 7.7, Ar*H*), 7.45-7.48 (2H, m, Ar*H*); δ_{C} (100 MHz, CDCl₃) 13.6, 22.1, 22.2, 26.4, 26.5, 27.1, 28.6, 28.7, 28.8, 28.9, 31.2, 31.3, 36.6, 45.6, 48.0, 126.3, 128.4, 129.8, 135.0, 167.4.

Reduction of *N,N*-dioctyl-2-(thiophenyl)acetamide **6.1.3** with **4.1.15**

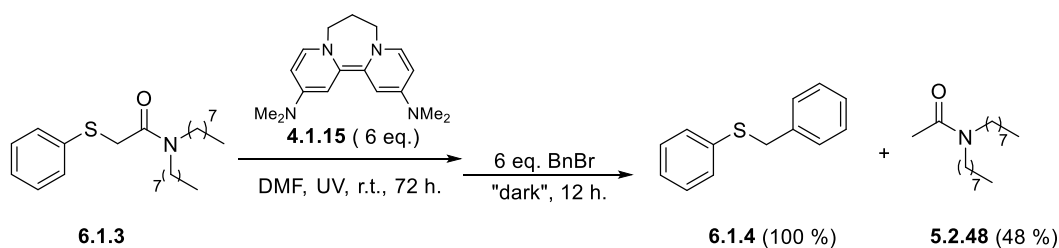


The general procedure for UV-activated reductions was applied to the substrate (196 mg, 0.5 mmol) using SED **4.1.15** (853 mg, 3.0 mmol) for 72 h at room temperature. The reaction mixture was then subjected to the general acidic workup procedure and the resulting crude material was purified by column chromatography (5-25 % EtOAc/hexane) to afford thiophenol **6.1.1** (26 mg, 48 %) and *N,N*-dioctylacetamide **5.2.48** (62 mg, 50 %) with data as previously reported. GCMS and ¹H NMR analysis of the crude material after workup showed full conversion of the starting material.

Thiophenol **6.1.1**: yellow liquid; ν_{\max} (ATR)/cm⁻¹ 3061, 2565, 1581, 1477, 1440, 1024, 731, 686; δ_{H} (400 MHz, CDCl₃) 3.45 (1H, s, ArSH), 7.16-7.18 (2H, m, Ar*H*), 7.28-7.30 (3H, m, Ar*H*); δ_{C} (100 MHz, CDCl₃) 125.1, 128.6, 128.9, 130.2. The spectral data were consistent with the literature data.²⁵⁶

Blank reactions: i) SED-free, UV-active and ii) SED (6 eq.), UV-free experiments were performed following the general procedure. For the first blank reaction, the starting material **6.1.3** was recovered (192 mg, 98 %). For the second blank reaction, the starting material **6.1.3** was recovered (184 mg, 94 %). The spectral data for the starting material **6.1.3** were as previously reported.

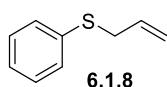
- **With subsequent trapping using benzyl bromide**



The general procedure for UV-activated reductions was applied to *N,N*-dioctyl-2-(thiophenyl)acetamide **6.1.3** (196 mg, 0.5 mmol) using SED **4.1.15** (853 mg, 3.0 mmol) for 72 h at room temperature. The reaction mixture was then removed from the UV setup and benzyl bromide (0.5 mL, 3.0 mmol) was syringed into the reaction mixture. The reaction mixture was stirred for 12 h, subjected to the general acidic workup procedure and the resulting crude product was purified by column chromatography (5 % EtOAc/hexane) to afford the trapped product benzyl(phenyl)sulfane **6.1.4** (86 mg, 100 %) and *N,N*-dioctylacetamide **5.2.48** (60 mg, 48 %). The spectral data for **5.2.48** were as previously reported.

Benzyl(phenyl)sulfane **6.1.4**: pale yellow oil; ν_{max} (ATR)/ cm^{-1} 3050, 2900, 1466, 1412, 1233, 1096, 924; δ_{H} (500 MHz, CDCl_3) 4.15 (2H, s, ArCH_2), 7.19-7.35 (10H, m, ArH); δ_{C} (125 MHz, CDCl_3) 38.5, 125.9, 126.7, 128.0, 128.3, 129.3, 135.9, 136.9; m/z (Cl^+ corona) 200.1 [$(\text{M})^+$, 10 %], 122.9 (30), 91.0 (100). The spectral data were consistent with the literature data.²⁵⁷

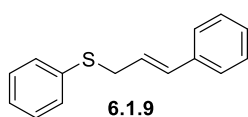
Synthesis of allyl(phenyl)sulfane **6.1.8**



washed with brine (80 mL) and dried over Na_2SO_4 . The suspension was filtered and concentrated under reduced pressure. The crude material was then purified by

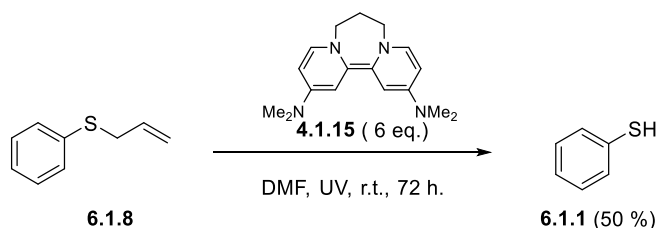
column chromatography (1 % CH₂Cl₂/hexane) followed by distillation to afford allyl(phenyl)sulfane **6.1.8** ν_{\max} (ATR)/cm⁻¹ 3077, 2989, 2912, 2345, 1634, 1577, 1481, 1437, 1238, 1089, 984, 918, 734, 686; δ_{H} (400 MHz, CDCl₃) 3.58 (2H, dt, *J* 6.8, 1.2, SCH₂), 5.10 (1H, dt, *J* 10.0, 1.0, SCH₂CHCH₂), 5.19 (1H, m, SCH₂CHCH₂), 5.91 (1H, m, SCH₂CH), 7.21 (1H, tt, *J* 7.2, 2.1, ArH), 7.31 (2H, t, *J* 7.5, ArH), 7.37 (2H, m, ArH); δ_{C} (100 MHz, CDCl₃) 36.6, 117.2, 125.7, 129.3, 133.1, 135.4; *m/z* (GCMS, CI, CH₄) 150.9 [(M+H)⁺, 100 %], 122.9 (30). The spectral data were consistent with the literature data.²⁵⁸

Synthesis of cinnamyl(phenyl)sulfane **6.1.9**



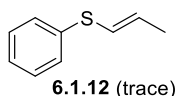
Potassium carbonate (9.1 g, 66 mmol) was added to a solution of thiophenol (6.2 mL, 60 mmol) in DMF (20 mL). The resulting suspension was stirred at 80 °C for 0.5 h, cooled to room temperature and a solution of cinnamyl bromide (13 g, 66 mmol) in DMF (20 mL) was added portionwise. The reaction mixture was stirred at 90 °C for 16 h, cooled to room temperature and partitioned between Et₂O (50 mL) and H₂O (200 mL). The organic phase was collected and the aqueous phase was extracted further with Et₂O (2 x 50 mL). The organic fractions were combined, washed with brine and then dried over Na₂SO₄. The suspension was filtered and concentrated under reduced pressure. The crude material was then purified by column chromatography (5 % EtOAc/hexane) to afford cinnamyl(phenyl)sulfane **6.1.9** as colourless crystals (12.2 g, 90 %). M.pt. 75-76 °C (lit. 73-76 °C)²⁵⁹; ν_{\max} (ATR)/cm⁻¹ 3083, 3030, 2910, 1640, 1579, 1477, 962, 734, 688; δ_{H} (400 MHz, CDCl₃) 3.74 (2H, dd, *J* 7.1, 1.2, SCH₂), 6.28 (1H, dt, *J* 15.7, 7.2, ArSCH₂CH), 6.45 (1H, d, *J* 15.7, ArSCH₂CHCH), 7.21-7.36 (8H, m, ArH), 7.40-7.43 (2H, m, ArH); δ_{C} (100 MHz, CDCl₃) 36.6, 124.5, 125.8, 125.9, 127.0, 128.0, 128.3, 129.7, 132.3, 135.3, 136.2; (GCMS, EI) 109 (10 %), 115 (50), 117 (100), 226 [(M)⁺, 10 %], 117 (100), 115 (50), 109 (10). The spectral data were consistent with the literature data.^{258,260}

Reduction of allyl(phenyl)sulfane **6.1.8** with **4.1.15**



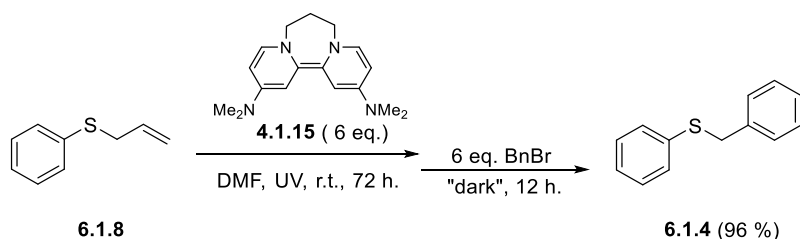
The general procedure for UV-activated reductions was applied to the substrate (75 mg, 0.5 mmol) using SED **4.1.15** (853 mg, 3.0 mmol) for 72 h at room temperature. The reaction mixture was then subjected to the general acidic workup procedure and the resulting crude material was purified by column chromatography (5% CH₂Cl₂/hexane) to afford thiophenol **6.1.1** (36 mg, 50 %) with data as previously reported. Initial ¹H NMR and GCMS spectra of the crude material after workup had revealed complete conversion of the starting material.

Blank reactions: i) SED-free, UV-active and ii) SED (6 eq.), UV-free experiments were performed following the general procedure. For the first blank reaction, the starting material **6.1.8** was recovered (74 mg, 98 %). For the second blank reaction, the starting material **6.1.7** was recovered (65 mg, 86 %). The spectral data were as previously reported. Additionally the ¹H NMR spectrum and GCMS analyses of the crude material obtained revealed the presence of phenyl(1-propenyl)sulfane **6.1.12**.



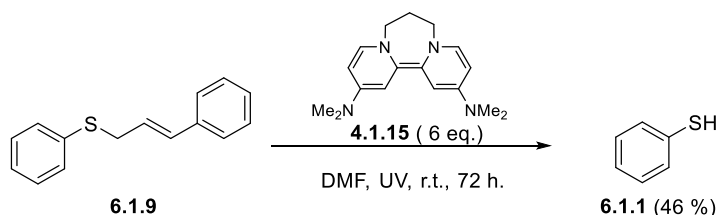
This product was likely due to deprotonation of allyl(phenyl)sulfane **6.1.8** by the SED **4.1.15** at the allylic position resulting in isomerisation. Based on the ¹H NMR of the crude material, signals corresponding to **6.1.12** are presented; δ_{H} (400 MHz, CDCl₃) 1.83 (3H, d, *J* 6.8, CH₃), 5.7-6.3 (2H, m, 2 x CH), 7.1-7.35 (5H, m, ArH); *m/z* (GCMS, Cl⁺, CH₄) 150.9 [(M+NH₄⁺), 100 %], 122.9 (25). The spectral data were consistent with the literature data.²⁶¹

- With subsequent trapping using benzyl bromide

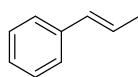


The general procedure for UV-activated reductions was applied to the substrate (75 mg, 0.5 mmol) using SED **4.1.15** (853 mg, 3.0 mmol) for 72 h at room temperature. The reaction mixture was then removed from the UV setup and benzyl bromide (0.5 mL, 3.0 mmol) was syringed into the reaction mixture. The reaction mixture was stirred for 12 h and then subjected to the general acidic workup procedure and the resulting crude material was purified by column chromatography (5 % EtOAc/hexane) to afford the trapped product benzyl(phenyl)sulfane **6.1.4** (83 mg, 96 %) with data as previously reported.

Reduction of cinnamyl(phenyl)sulfane **6.1.9** with **4.1.15**



The general procedure for UV-activated reductions was applied to the substrate (114 mg, 0.5 mmol) using SED **4.1.15** (853 mg, 3.0 mmol) for 72 h at room temperature. The reaction mixture was then subjected to the general acidic workup procedure and the resulting crude material was purified by column chromatography (5 % CH₂Cl₂/hexane) to afford thiophenol **6.1.1** (25 mg, 46 %) with data as previously reported. ¹H NMR and GCMS analyses of the crude material after workup had revealed complete conversion of the starting material. Additionally the ¹H NMR spectrum analysis of the crude material obtained revealed the presence of trans-2-methylstyrene **6.1.11**

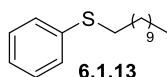


6.1.11 (trace)

Based on the ^1H NMR of the crude material, signals corresponding to **6.1.11** δ_{H} (400 MHz, CDCl_3) 1.93-1.95 (3H, dd, J 6.5, 1.5, CH_3), 6.25-6.30 (1H, dq, J 16.0, 6.5, $\text{C}=\text{CHCH}_3$), 6.47-6.50 (1H, d, J = 16.0, $\text{ArCH}=\text{CH}$), 7.28-7.42 (5H, m, ArH). The spectral data were consistent with the literature data.²⁶²

Blank reaction: SED (6 eq.), UV-free experiment was performed following the general procedure. The starting material **6.1.9** was recovered (105 mg, 92 %) The spectral data were as previously reported.

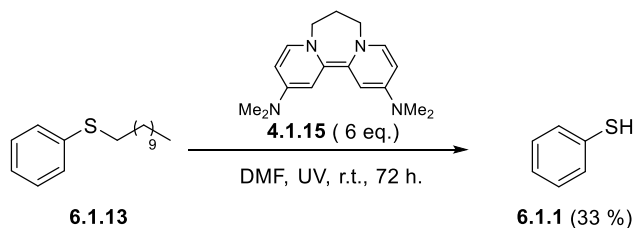
Synthesis of undecyl(phenyl)sulfane **6.1.13**



6.1.13

Thiophenol (1.6 g, 15 mmol) and NaOH (720 mg, 18 mmol,) were suspended in DMF (50 mL). The suspension was stirred at 50 °C for 2 h whereupon 1-bromoundecane (3.9 g, 16.5 mmol) was added portionwise. The reaction mixture was stirred at 80 °C for 18 h after which it was cooled to room temperature and then partitioned between 2N HCl (50 mL) and Et_2O (3 x 50 mL). The organic fractions were combined, washed with brine and dried over Na_2SO_4 . The suspension was filtered and the solvent was removed under reduced pressure. The crude material was then purified by column chromatography (100 % hexane) to yield phenyl(undecyl)sulfane **6.1.13** as a white solid (3.18 g, 80 %). M.pt. 33-34 °C; [Found: (HNESP^+) ($\text{M}+\text{H}$) $^+$ 265.1982. $\text{C}_{17}\text{H}_{29}\text{S}^+$ ($\text{M}+\text{H}$) $^+$, requires 265.1982]; ν_{max} (ATR)/ cm^{-1} 3082, 3057, 2954, 2918, 2850, 2357, 2015, 1585, 1480, 1464, 1440, 1375, 1309, 1252, 1186, 1099, 1023, 889, 733, 697, 685; δ_{H} (400 MHz, CDCl_3) 0.89-0.92 (3H, m, CH_3), 1.29 (14H, bs, CH_2), 1.43-1.46 (2H, m, CH_2), 1.68-1.71 (2H, m, CH_2), $\text{C}\delta_{\text{C}}$ (100 MHz, CDCl_3) 13.6, 22.2, 28.3, 28.6, 28.7, 28.8, 29.0, 29.1, 31.4, 33.1, 125.1, 128.3, 136.6.

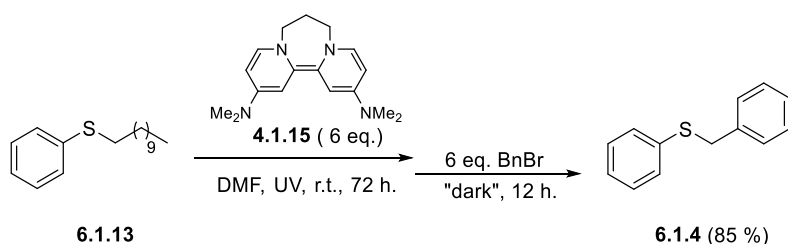
Reduction of allyl(phenyl)sulfane **6.1.13** with SED **4.1.15**



The general procedure for UV-activated reductions was applied to the substrate (132 mg, 0.5 mmol) using SED **4.1.15** (853 mg, 3.0 mmol) for 72 h at room temperature. The reaction mixture was then subjected to the general acidic workup procedure and the resulting crude material was purified by column chromatography (5% CH₂Cl₂/hexane) to afford thiophenol **6.1.1** (26 mg, 33 %) with data as previously reported. Initial ¹H NMR and GCMS spectra of the crude material after workup had revealed complete conversion of the starting material.

Blank reactions: i) SED-free, UV-active and ii) SED (6 eq.), UV-free experiments were performed following the general procedure. For the first blank reaction, the starting material **6.1.13** was recovered (129 mg, 98 %). For the second blank reaction, the starting material **6.1.13** was recovered (130 mg, 99 %). The spectral data for the starting material **6.1.13** were as previously reported.

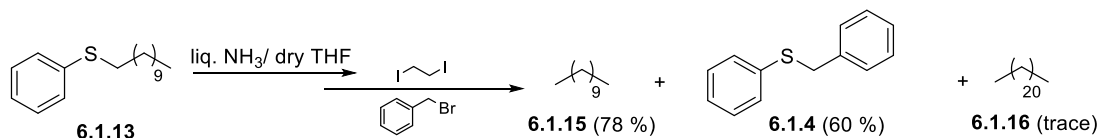
- **With subsequent trapping with benzyl bromide**



The general procedure for UV-activated reductions was applied to the substrate (132 mg, 0.5 mmol) using SED **4.1.15** (853 mg, 3.0 mmol) for 72 h at room temperature. The reaction mixture was then removed from the UV setup and benzyl bromide (0.5 mL, 3.0 mmol) was syringed into the reaction mixture. The reaction mixture was then stirred for 12 h and then subjected to the general acidic workup procedure. The resulting crude material was purified by column chromatography (5 %

EtOAc/hexane) to afford the trapped product benzyl(phenyl)sulfane **6.1.4** (85 mg, 85 %) with data as previously reported.

Birch reduction of phenyl(undecyl)sulfane **6.1.13**



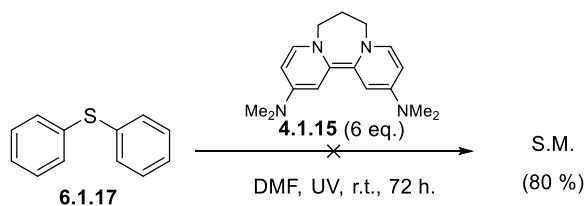
An oven-dried three-necked flask was charged phenyl(undecyl)sulfane **6.1.13** (265 mg, 1.0 mmol) and then fitted with a dry-ice condenser (cold finger). The flask was sealed and then flushed with argon before ammonia (60 mL) was condensed into the reaction vessel. Dry THF (30 mL) was syringed into the reaction vessel to encourage the substrate to dissolve. Freshly cut sodium (28 mg, 1.2 mmol) was then added to the flask causing the clear solution to turn blue. The reaction mixture was refluxed for 4.5 h after which 1,2-diiodoethane (0.20 mL, 1.5 mmol) was added portionwise to quench the reaction. This resulted in the formation of a thick white emulsion which was stirred vigorously for 5 mins. The cold finger was also detached and a strong stream of argon was applied onto the reaction mixture to assist in the evaporation of ammonia. Benzyl bromide (0.9 mL, 8 mmol) was then added to the reaction in one portion and left to stir vigorously for 16 h. Thereafter, the reaction mixture was partitioned between Et₂O (50 mL) and sat. NH₄Cl (50 mL). The aqueous layer was extracted further with Et₂O (2 x 30 mL). The organic collections were combined, washed with brine, dried over anhydrous Na₂SO₄, filtered and the solvent removed under reduced pressure. The crude material was analysed by GCMS and a trace amount of docosane **6.1.16** was detected. The crude material was purified by column chromatography (10-40 % CH₂Cl₂/hexane) on silica gel to afford undecane **6.1.15** (122 mg, 78 %) and benzyl(phenyl)sulfane **6.1.4** (120 mg, 60 %). The spectral data for benzyl(phenyl)sulfane **6.1.4** were as previously reported.

Undecane **6.1.24**: as a colourless oil; ν_{\max} (neat/cm⁻¹) 2914, 2848, 2339, 1469, 1377, 891, 715; δ_{H} (500 MHz, CDCl₃) 0.90 (6H, t, *J* 7.2, CH₃), 1.28 (18H, bs); δ_{C} (125 MHz, CDCl₃) 14.1, 22.7, 29.3, 29.6, 29.6, 31.9; *m/z* (CI⁺ corona) retention time of

8.60 min, 155[(M-H)⁺, 30 %], 113[(M-C₃H₇)⁺, 40 %], 85[(M-C₅H₁₁)⁺, 100 %], 57[(M-C₇H₁₅)⁺, 95 %]. The spectral data were consistent with the literature data.²⁶³

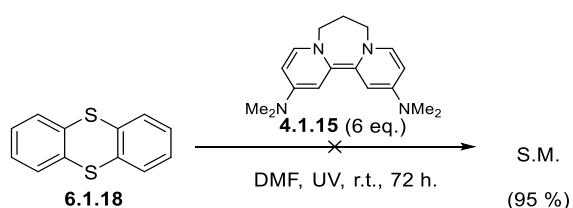
Docosane **6.1.25**; *m/z* (CI⁺ corona) retention time of 15.0 min, 308.4 [(M-H)⁺ 70 %], 253.3 [(M-C₄H₉)⁺, 5 %], 239.3 [(M-C₅H₁₁)⁺, 10 %], 225.3 [(M-C₆H₁₃)⁺, 15 %], 197.2 [(M-C₈H₁₇)⁺, 20 %], 85.2 [(M-C₁₆H₃₃)⁺, 100 %].

Attempted reduction of diphenyl sulfide **6.1.17**



The general procedure for UV-activated reductions was applied to the commercially available substrate **6.1.17** (93 mg, 0.5 mmol) using SED **4.1.15** (853 mg, 3.0 mmol) for 72 h at room temperature. The reaction mixture was then subjected to the general acidic workup procedure and the resulting crude material was purified by column chromatography (2 % EtOAc/hexane) to recover the starting material **6.1.17** as a colourless oil (75 mg, 80 %). δ_{H} (400 MHz, CDCl₃) 7.25-7.38 (10 H, m, ArH); δ_{C} (125 MHz, CDCl₃) 126.99, 129.14, 129.20, 130.9, 135.8. The spectral data were consistent with the literature data.²⁶⁴

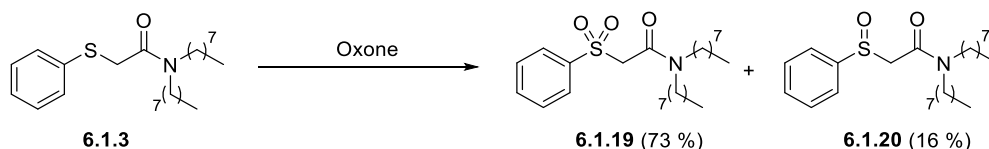
Attempted reduction of thianthrene **6.4.18**



The general procedure for UV-activated reductions was applied to the commercially available substrate **6.1.18** (108 mg, 0.5 mmol) using SED **4.1.15** (853 mg, 3.0 mmol) for 72 h at room temperature. The reaction mixture was then subjected to the general acidic workup procedure and the resulting crude material was purified by column

chromatography (5 % EtOAc/hexane) to afford the starting material **6.1.18** as a colourless oil (105 mg, 95 %). δ_{H} (400 MHz, CDCl_3) 7.20-7.28 (4H, m, ArH), 7.43-7.52 (4H, m, ArH); δ_{C} (125 MHz, CDCl_3) 127.9, 128.5, 135.7. The spectral data were consistent with the literature data.²⁶⁵

Synthesis of *N,N*-dioctyl-2-(phenylsulfonyl)acetamide **6.1.19** and *N,N*-dioctyl-2-(phenylsulfinyl)acetamide **6.1.20**



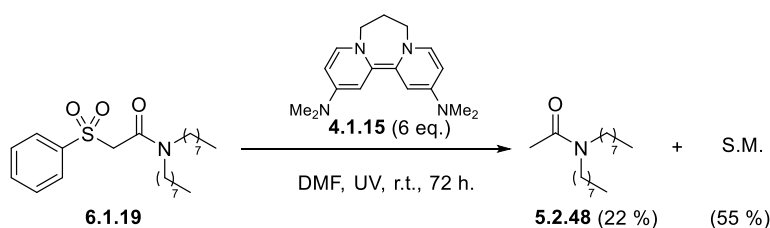
N,N-dioctyl-2-(thiophenyl)acetamide **6.1.3** (1.30 g, 3.3 mmol) was dissolved in EtOH/H₂O (1:1, 80 mL) whereupon Oxone (5.2 g, 16.5 mmol) was added in one portion. The resulting suspension was heated to steady reflux and stirred for 16 h, cooled to room temperature and then partitioned between H₂O (50 mL) and Et₂O (40 mL). The organic phase was separated and the aqueous phase was extracted further with Et₂O (2 x 40 mL). The organic extracts were combined, washed with brine and then dried over Na₂SO₄. The suspension was filtered and the solvent was removed under reduced pressure. The crude was then purified by column chromatography (25 % EtOAc/hexane) to afford *N,N*-dioctyl-2-(phenylsulfonyl)acetamide **6.1.19** (1.0 g, 73 %) and *N,N*-dioctyl-2-(phenylsulfinyl)acetamide **6.1.20** (210 mg, 16 %).

N,N-dioctyl-2-(phenylsulfonyl)acetamide **6.1.19**: yellow solid; M.pt. 42-43 °C; [Found: (APCI⁺) (M+H)⁺ 424.2877. C₂₄H₄₂NO₃S (M+H)⁺, requires 424.2880; ν_{max} (ATR)/cm⁻¹ 3000, 2917, 2866, 1638, 1584, 1445, 1373, 1306, 1153, 1087, 901, 756, 685; δ_{H} (400 MHz, CDCl_3); 0.89-0.92 (6H, m, CH₃), 1.29 (20H, bs, CH₂), 1.50-1.58 (4H, m, CONCH₂CH₂), 3.27-3.29 (2H, t, *J* 7.8, NCH₂), 3.39 (2H, t, *J* 7.8, NCH₂), 4.22 (2H, s, PhSO₂CH₂), 7.56-7.58 (2H, tt, *J* 7.5, 1.3, ArH), 7.67-7.69 (1H, m, ArH), 7.93 (2H, m, ArH); δ_{C} (100 MHz, CDCl_3) 13.6, 22.1, 22.2, 26.3, 26.4, 26.9, 28.6, 28.7, 28.8, 28.9, 29.0, 31.2, 31.3, 46.0, 48.4, 59.3, 128.1, 128.5, 133.6, 138.3, 160.2.

N,N-dioctyl-2-(phenylsulfinyl)acetamide **6.1.20**: yellow oil; [Found: (HNESP⁺) (M+H)⁺ 408. 2926. C₂₄H₄₂NO₂S (M+H)⁺, requires 408.2931; ν_{max} (ATR)/cm⁻¹ 3485,

3059, 2950, 2854, 1631, 1443, 1375, 1306, 1086, 1051, 745, 689; δ_{H} (400 MHz, CDCl_3); 0.88-0.92 (6H, t, J 7.1, CH_3), 1.27 (20H, bs, CH_2), 1.42-1.46 (4H, m, CH_2), 3.02-3.18 (2H, m, CH_2), 3.27-3.29 (2H, m, CH_2). 3.73-3.76 (1H, d, J 12.0, PhSOCH_2), 4.05-4.08 (1H, d, J 12.0, PhSOCH_2), 7.54-7.55 (3H, m, ArH), 7.76-7.79 (2H, m, ArH); δ_{C} (100 MHz, CDCl_3) 13.5, 13.6, 22.1, 22.2, 26.2, 26.4, 27.1, 28.5, 28.6, 28.7, 28.8, 31.2, 31.3, 45.9, 48.0, 61.8, 123.9, 128.7, 130.9, 143.4, 163.2.

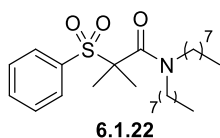
Reduction of *N,N*-dioctylamine-2-(phenylthioacetamide) **6.1.19** with **4.1.15**



The general procedure for UV-activated reductions was applied to the substrate (212 mg, 0.5 mmol.) using SED **4.1.15** (853 mg, 3.0 mmol) for 72 h at room temperature. The reaction mixture was then subjected to the general acidic workup procedure and the resulting crude material was purified by column chromatography (10 % EtOAc/hexane) to afford *N,N*-dioctylamine acetamide **5.2.48** (34 mg, 22 %) and the starting material **6.1.19** (116 mg, 55 %). The spectral data for both compounds were as previously reported.

Blank reaction: SED (6 eq.), UV-free experiment was performed following the general procedure. The starting material **6.1.19** was recovered (205 mg, 97 %). The spectral data were as previously reported.

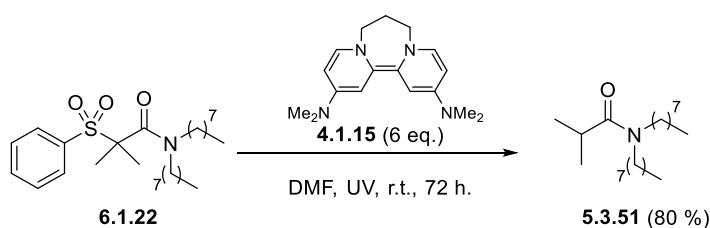
Synthesis of *N,N*-dioctyl-2-methyl-2-(phenylsulfonyl)propanamide **6.1.22**



A solution of *N,N*-dioctyl-2-(phenylsulfonyl)acetamide **6.1.19** (590 mg, 1.4 mmol) in dry THF (10 mL) was cooled to $-78\text{ }^\circ\text{C}$ whereupon *n*-BuLi (2.5 M, 1.4 mL, 3.5 mmol)

was added dropwise to the reaction mixture. The reaction mixture was stirred at -78 °C for 0.5 h whereupon methyl iodide (0.2 mL, 3.1 mmol) was added dropwise. The reaction mixture was stirred at room temperature for 0.5 h and then partitioned between EtOAc (20 mL) and H₂O (50 mL). The organic phase was separated and the aqueous phase was extracted further with Et₂O (2 x 40 mL). The organic extracts were combined, washed with brine and then dried over Na₂SO₄. The suspension was filtered and the solvent was removed under reduced pressure. The crude material was then purified by column chromatography (10 % EtOAc/hexane) to afford *N,N*-dioctyl-2-methyl-2-(phenylsulfonyl)propanamide **6.1.22** as a colourless oil (330 mg, 53 %). [Found: (APCI⁺) [M+H]⁺ 452.3191. C₂₆H₄₆NO₃S (M+H)⁺ requires 452.3193]; ν_{\max} (neat/cm⁻¹) 2924, 2854, 1625, 1463, 1417, 1303, 1157, 1132, 1078, 754, 721, 688; δ_{H} (500 MHz, CDCl₃) 0.89-0.93 (6H, m, 2 x CH₂CH₃), 1.31 (20H, bs, 10 x CH₂), 1.53-1.61 (4H, m, 2 x NCH₂CH₂), 1.70 (6H, s, 2 x N(CO)C(CH₃)₂), 3.23 (2H, bs, NCH₂), 3.74 (2H, bs, NCH₂), 7.53 (2H, t, *J* 7.5 Hz, Ar*H*), 7.65 (1H, t, *J* 7.5 Hz, Ar*H*), 7.82 (2H, d, *J* 7.5 Hz, Ar*H*); δ_{C} (125 MHz, CDCl₃) 13.6, 22.1, 22.2, 23.0, 26.6, 28.7, 28.8, 28.9, 31.3, 48.5, 69.9, 76.2, 128.1, 129.6, 133.5, 135.4, 165.7.

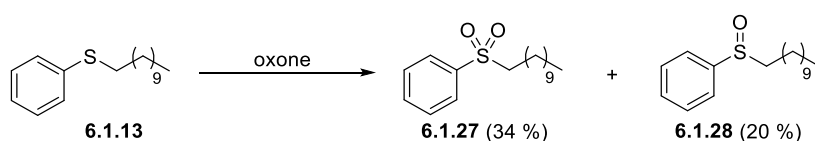
Reduction of *N,N*-dioctyl-2-methyl-2-(phenylsulfonyl)propanamide **6.1.22** with **4.1.15**



The general procedure for UV-activated reductions was applied to the substrate (180 mg, 0.5 mmol.) using SED **4.1.15** (853 mg, 3.0 mmol) for 72 h at room temperature. The reaction mixture was then subjected to the general acidic workup procedure and the resulting crude material was purified by column chromatography (5 % EtOAc/hexane) to afford *N,N*-dioctylisobutyramide **5.3.51** as a colourless oil (100 mg, 80 %). [Found: (HNESP⁺) (M+H)⁺ 312.3257. C₂₀H₄₂NO⁺ (M+H)⁺, requires 312.3261; ν_{\max} (ATR)/cm⁻¹ 2956, 2924, 2854, 2370, 1643, 1467, 1423, 1377, 1304,

1134, 750; δ_{H} (400 MHz, CDCl_3) 0.89-0.91 (6H, m, CH_3), 1.13 (6H, d, J 7.0 Hz, CH_3), 1.29 (20 H, m, CH_2), 1.53 (4H, m, CH_2), 2.75 (1H, m, NCOCH), 3.24 (2H, t, J 7.8, NCH_2), 3.30 (2H, t, J 7.8, NCH_2); δ_{C} (100 MHz, CDCl_3) 13.6, 19.2, 22.1, 26.4, 26.5, 27.3, 28.6, 28.7, 28.8, 28.9, 29.1, 29.6, 31.2, 31.3, 45.5, 47.3, 176.3. ^1H NMR analysis of the crude material after workup had revealed complete conversion of the starting material.

Synthesis of (undecylsulfonyl)benzene **6.1.27** and (undecylsulfinyl)benzene **6.1.28**



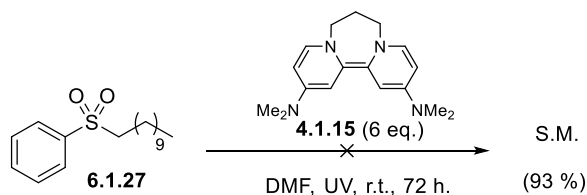
Phenyl(undecyl)sulfane **6.1.13** (1.33 g, 5 mmol) was suspended in acetonitrile/water (1:1, 50 mL) and Oxone (7.7 g, 25 mmol) was added portionwise to the reaction mixture. The reaction mixture was stirred for 18 h and then partitioned between EtOAc (40 mL) and H_2O (50 mL). The organic phase was collected and the aqueous phase was further extracted with EtOAc (2 x 40 mL). The organic fractions were combined, washed with brine and dried over Na_2SO_4 . The suspension was filtered and concentrated under reduced pressure. The crude material was then purified by column chromatography (5-20 % EtOAc/hexane) to yield (undecylsulfonyl)benzene **6.1.27** (500 mg, 34 %) and (undecylsulfinyl)benzene **6.1.28** (278 mg, 20 %).

(Undecylsulfonyl)benzene **6.1.27**: white solid; M.pt. 42-43 °C; [Found: (APCI⁺) (M+H)⁺ 297.1882. $\text{C}_{17}\text{H}_{29}\text{O}_2\text{S}$ (M+H)⁺, requires 297.1882; ν_{max} (ATR)/ cm^{-1} 2965, 2916, 2868, 2850, 1586, 1471, 1446, 1406, 1317, 1300, 1280, 1257, 1226, 1144, 1085, 1072, 1026, 999, 862, 796, 771, 752, 690; δ_{H} (500 MHz, CDCl_3) 0.90 (3H, t, J 7.0, CH_2CH_3), 1.26 (14H, bs, 7 x CH_2), 1.35-1.37 (2H, m, $\text{SO}_2\text{CH}_2\text{CH}_2\text{CH}_2$), 1.71-1.75 (2H, m, $\text{SO}_2\text{CH}_2\text{CH}_2$), 3.08-3.12 (2H, m, PhSO_2CH_2), 7.59-7.61 (2H, m, ArH), 7.67-7.68 (1H, m, ArH), 7.93 (2H, d, J 8.5, ArH); δ_{C} (100 MHz, CDCl_3) 13.6, 22.1, 22.2, 27.7, 28.5, 28.7, 28.8, 28.9, 29.0, 31.4, 55.8, 127.6, 128.7, 133.1, 138.7.

(Undecylsulfinyl)benzene **6.1.28**: white solid; M.pt. 36-37 °C; [Found: (APCI⁺) (M+H)⁺ 281.1934. $\text{C}_{17}\text{H}_{29}\text{OS}$ (M+H)⁺ requires 281.1934]; ν_{max} (neat/ cm^{-1})

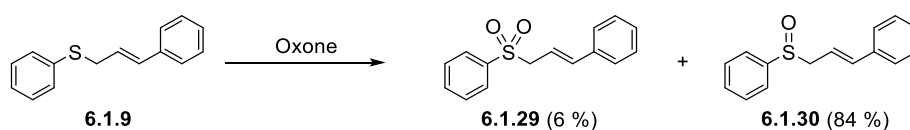
3059, 2964, 2914, 2846, 1471, 1440, 1018, 744, 686; δ_{H} (500 MHz, CDCl_3) 0.90 (3H, t, J 6.8, CH_2CH_3), 1.26-1.38 (14H, m, 7 x CH_2), 1.41-1.45 (2H, m, $\text{SOCH}_2\text{CH}_2\text{CH}_2$), 1.62-1.79 (2H, m, SOCH_2CH_2), 2.78-2.82 (2H, m, SOCH_2), 7.49-7.54 (3H, m, ArH), 7.63-7.65 (2H, m, ArH); δ_{C} (125 MHz, CDCl_3) 13.6, 21.6, 22.1, 28.1, 28.6, 28.7, 28.8, 28.9, 29.0, 31.3, 56.9, 123.5, 128.7, 130.3, 143.6.

Attempted reduction of phenyl(undecylsulfonyl)benzene **6.1.27** with **4.1.15**



The general procedure for UV-activated reductions was applied to the substrate **6.1.27** (150 mg, 0.5 mmol) using SED **4.1.15** (853 mg, 3.0 mmol) for 72 h at room temperature. The reaction mixture was then subjected to the general acidic workup procedure and the resulting crude material was purified by column chromatography (20 % EtOAc/hexane) to afford the starting material **6.1.27** as a white solid (140 mg, 93 %). The spectral data were as previously reported.

Synthesis of cinnamyl(sulfonyl)benzene **6.1.29** and cinnamyl(sulfinyl)benzene **6.1.30**



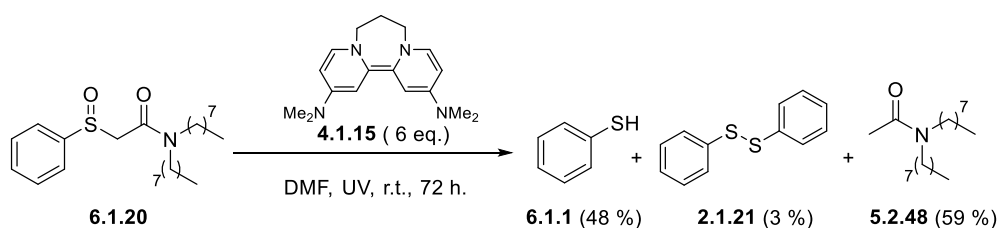
Cinnamyl(phenyl)sulfane **6.1.9** (885 mg, 4 mmol) was suspended in acetonitrile/water (1:1, 50 mL) and Oxone (6.0 g, 19.0 mmol) was added portionwise to the reaction mixture. The reaction mixture was stirred for 18 h after which the suspension was partitioned between EtOAc (40 mL) and H_2O (50 mL). The organic phase was collected and the aqueous phase was extracted further with EtOAc (2 x 40 mL). The organic fractions were combined, washed with brine and dried over Na_2SO_4 . The organic fraction was filtered and concentrated under reduced pressure.

The crude material was then purified by column chromatography (30 % EtOAc/hexane) to afford cinnamyl(sulfonyl)benzene **6.1.29** (63 mg, 6 %) and cinnamyl(sulfinyl)benzene **6.1.30** (860 mg, 84 %).

Cinnamyl(sulfonyl)benzene **6.1.29**: white solid; M.pt. 110-111 °C (lit. 111-112 °C)²⁶⁶; ν_{\max} (ATR)/cm⁻¹ 3153, 3080, 3058, 3033, 2957, 2906, 1956, 1888, 1814, 1666, 1494, 1475, 1443, 1084, 1030, 968, 914, 747, 689; δ_{H} (400 MHz, CDCl₃) 3.96 (2H, d, *J* 7.6, SO₂CH₂), 6.07-6.13 (1H, m, SO₂CH₂CH), 6.36 (1H, d, *J* 15.7, ArCH), 7.30-7.39 (5H, m, ArH), 7.55 (2H, t, *J* 7.6, ArH), 7.63 (1H, t, *J* 7.6, ArH), 7.91 (2H, d, *J* 7.8 Hz, ArH); δ_{C} (100 MHz, CDCl₃) 60.5, 115.1, 126.6, 128.5, 128.6, 128.8, 129.0, 133.7, 135.7, 138.4, 139.2; *m/z* (ESI⁺) 259.3 ([M+H]⁺, 100 %). The spectral data were consistent with the literature data.²⁶⁶

Cinnamyl(sulfinyl)benzene **6.1.30**: white solid; M.pt. 82-83 °C (not reported in literature); ν_{\max} (ATR)/cm⁻¹ 3100, 3058, 3029, 2974, 2904, 2851, 1950, 1890, 1815, 1596, 1580, 1444, 1317, 1290, 1134, 1084, 1025, 737, 688; δ_{H} (400 MHz, CDCl₃) 3.68-3.70 (2H, m, CH₂), 5.96-6.04 (1H, m, SOCH₂CH), 6.42 (1H, d, *J* 16.0, SOCH₂CHCH), 7.26-7.31 (5H, m, ArH), 7.51-7.62 (5H, m, ArH); δ_{C} (100 MHz, CDCl₃) 60.8, 116.1, 124.4, 126.5, 128.2, 128.6, 129.0, 131.2, 136.1, 138.5, 143.0, *m/z* (ESI⁺) 243.4 [(M+H)⁺, 30 %], 117.0 (100). The spectral data were consistent with the literature data.²⁶⁷

Reduction of *N,N*-dioctyl-2-(phenylsulfinyl)acetamide **6.1.20** with **4.1.15**

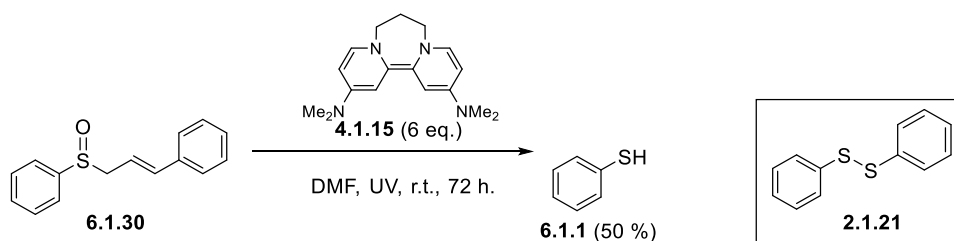


The general procedure for UV-activated reductions was applied to the substrate (196 mg, 0.5 mmol.) using SED **4.1.15** (853 mg, 3.0 mmol) for 72 h at room temperature. The reaction mixture was then subjected to the general acidic workup procedure and the resulting crude material was purified by column chromatography (8 %

EtOAc/hexane) to afford *N,N*-dioctylacetamide **5.2.48** (84 mg, 59 %), thiophenol **6.1.1** (26 mg, 48 %) and 1,2-diphenyldisulfane **2.1.21** (4 mg, 3 %). The spectral data for *N,N*-dioctylacetamide **5.2.48** and thiophenol **6.1.1** were as previously reported.

1,2-diphenyldisulfane **2.1.21**: colourless crystals; M.pt. 43-45 °C (lit. 45-46 °C)²⁶⁸; ν_{\max} (ATR)/cm⁻¹ 3057, 2954, 2852, 1573, 1473, 1436, 1296, 1072, 732, 684; δ_{H} (400 MHz, CDCl₃) 7.26-7.8 (2H, m, ArH), 7.31-7.35 (4H, m, ArH), 7.52 (4H, d, *J* 7.8, ArH); δ_{C} (100 MHz, CDCl₃) 127.8, 128.1, 129.7, 137.7; (GCMS, CI, CH₄) 219.0 [(M+H)⁺, 35 %], 140.9 (100), 110.9 (20). The spectral data were consistent with the literature data.²⁶⁹

Reduction of cinnamyl(sulfinyl)benzene **6.1.30** with **4.1.15**



The general procedure for UV-activated reductions was applied to the substrate (122 mg, 0.5 mmol) using SED **4.1.15** (853 mg, 3.0 mmol) for 72 h at room temperature. The reaction mixture was then subjected to the general acidic workup procedure and the resulting crude material was purified by column chromatography (3 % EtOAc/hexane) to afford thiophenol **6.1.1** (30 mg, 50 %). The spectral data were as previously reported.

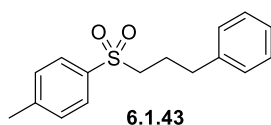
Blank reaction, 1st attempt: SED (6 eq.), UV-free experiment was performed following the general procedure. The reaction mixture was then subjected to the general acidic workup procedure and the crude material was purified by column chromatography (3 % EtOAc/hexane) to afford thiophenol **6.1.1** (31 mg, 51 %). The spectral data were previously reported.

Blank reaction, 2nd attempt: SED (6 eq.), UV-free experiment was performed following the general procedure. The reaction mixture was then subjected to the general acidic workup procedure and the crude material was purified by column

chromatography (3 % EtOAc/hexane) to afford thiophenol **6.1.1** (24 mg, 40 %) and 1,2-diphenyldisulfane **2.1.21** (5 mg, 4 %). The spectral data for thiophenol **6.1.1** and 1,2-diphenyldisulfane **2.1.21** were as previously reported.

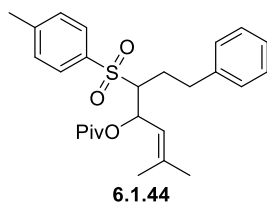
Blank reaction, SED-free, UV active was performed following the general procedure. After the general acidic workup procedure, a gum remained which was highly insoluble in CHCl₃, acetonitrile, DMF and DMSO. The product was rinsed with CDCl₃ and the liquid was transferred to a NMR tube for analysis. ¹H NMR showed no products were present in the solvent. A small portion of the liquid was used for GCMS analysis which also showed that no products were present.

Synthesis of 1-methyl-4-((3-phenylpropyl)sulfonyl)benzene **6.1.43**



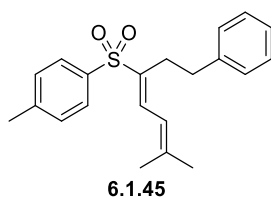
Sodium-*p*-toluenesulfinate (12 g, 44 mmol) was dissolved in a mixture of DMF/H₂O (2:1, 40 mL) whereupon 1-bromo-3-phenyl propane (8.8 g, 44 mmol) was added to the reaction mixture. The resulting solution was stirred for 16 h at 80 °C, cooled to room temperature and partitioned between Et₂O (50 mL) and sat.NH₄Cl (80 mL). The organic phase was collected and the aqueous layer was extracted further with Et₂O (2 x 30 mL). washed with brine (60 mL) and dried over Na₂SO₄. The suspension was filtered and concentrated under reduced pressure. The crude material was then purified by column chromatography (50 % CH₂Cl₂/Hexane) to afford 1-methyl-4-((3-phenylpropyl)sulfonyl)benzene **6.1.43** as colourless crystals (7.6 g, 63 %). M.pt. 93-94 °C; [Found: (HNESP⁺) [M+H]⁺ 275.1100. C₁₆H₁₉O₂S (M+H)⁺ requires 275.1100]; ν_{\max} (neat/cm⁻¹) 3057, 2947, 2872, 1600. 1497, 1446, 1303, 1286, 1145, 1085, 825, 771, 700; δ_{H} (500 MHz, CDCl₃) 2.02-2.10 (2H, m, SO₂CH₂CH₂CH₂), 2.47 (3H, s, ArCH₃), 2.72 (2H, t, *J* 7.5, SO₂CH₂CH₂), 3.06-3.10 (2H, m, SO₂CH₂), 7.11-7.13 (2H, m, ArH), 7.22-7.24 (1H, m, ArH), 7.28-7.31 (2H, m, ArH), 7.38 (2H, d, *J* 8.1, ArH), 7.79 (2H, d, *J* 8.1, ArH); δ_{C} (125 MHz, CDCl₃) 21.1, 23.8, 33.6, 55.0, 125.9, 127.5, 127.8, 128.0, 129.3, 135.7, 139.4, 144.1.

Synthesis of 2-methyl-7-phenyl-5-tosylhept-2-en-4-yl pivalate **6.1.44**¹⁹⁸



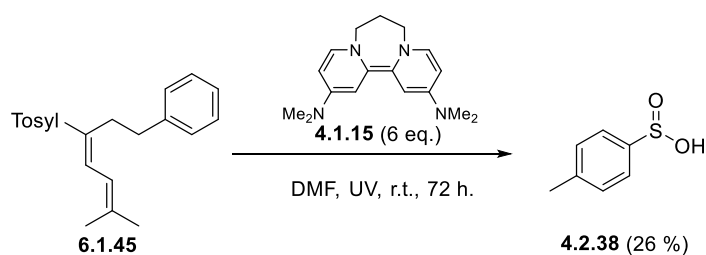
1-methyl-4-((3-phenylpropyl)sulfonyl)benzene **6.1.43** (2.8 g, 10 mmol) was dissolved in dry THF (20 mL), cooled to $-78\text{ }^{\circ}\text{C}$ whereupon *n*-BuLi (1.3 M in hexanes, 9.3 mL, 12 mmol) was added dropwise. The resulting yellow solution was stirred at $-78\text{ }^{\circ}\text{C}$ for 0.5 h whereupon 3-methyl-2-butenal (1.1 mL, 11 mmol) was added dropwise. The reaction was stirred for another 0.5 h and pivaloyl chloride (1.4 mL, 11 mmol) was then added in one portion. The reaction mixture was left to warm to room temperature overnight (16 h), cooled to $0\text{ }^{\circ}\text{C}$ and quenched with H_2O (5 mL). The reaction mixture was then partitioned between H_2O (20 mL) and Et_2O (10 mL). The organic phase was collected and the aqueous layer was extracted further with Et_2O (2 x 10 mL). washed with brine and dried over Na_2SO_4 . The suspension was filtered and concentrated under reduced pressure. The crude material was then purified by column chromatography (5 % EtOAc/hexane) to afford 2-methyl-7-phenyl-5-tosylhept-2-en-4-yl pivalate **6.1.44** as a colourless oil (1.1 g, 25 %). δ_{H} (500 MHz, CDCl_3) 1.14-1.15 (9H, s), 1.41 (3H, d, J 1.2, $\text{CH}=\text{CCH}_3$), 1.60 (3H, d, J 1.2, $\text{CH}=\text{CCH}_3$), 2.43 (3H, s, ArCH_3), 2.46-2.47 (4H, m, 2 x CH_2), 3.04-3.06 (1H, m, SO_2CH), 4.96-4.98 (1H, m, SO_2CHCH), 5.88-5.95 (1H, m, $\text{CH}=\text{C}$), 7.08-7.37 (7H, m, ArH), 7.76-7.78 (2H, m, ArH); (GCMS, CI, CH_4) 341.1 [(M-PivO)⁻, 100 %], 185.1 (50). This intermediate was immediately used in the next step of synthesis.

The synthesis of (*E*)-1-methyl-4-((6-methyl-1-phenylhepta-3,5-dien-3-yl)sulfonyl)benzene **6.1.45**



2-Methyl-7-phenyl-5-tosylhept-2-en-4-yl pivalate **6.1.44** (1.1 g, 2.5 mmol) was dissolved in dry THF (10 mL) whereupon 1,8-diazabicyclo[5.4.0]undec-7-ene (3.8 mL, 25 mmol) was added in one portion. The reaction mixture was stirred for 16 h after which solvent was removed and the crude material was partitioned between EtOAc (50 mL) and sat. NaHCO₃ (50 mL). The organic phase was collected and the aqueous layer was extracted further with EtOAc (2 x 30 mL). washed with brine (50 mL) and dried over Na₂SO₄. The suspension was filtered and concentrated under reduced pressure. The crude material was purified by column chromatography (5 % EtOAc/hexane) to yield (*E*)-1-methyl-4-((6-methyl-1-phenylhepta-3,5-dien-3-yl)sulfonyl)benzene 2-(3,5-dimethylphenoxy)-1-phenylethan-1-one **6.1.45** as a colourless oil (690 mg, 81 %). [Found: (HNESP⁺) [M+H]⁺ 341.1564. C₂₁H₂₅O₂S (M+H)⁺ requires 341.1570]; ν_{\max} (neat/cm⁻¹) 3016, 2924, 2358, 1635, 1593, 1494, 1454, 1288, 1139, 1089, 817, 731; δ_{H} (500 MHz, CDCl₃) 1.87 (3H, s, CH=CCH₃), 1.93 (3H, s, CH=CCH₃), 2.43 (3H, s, ArCH₃), 2.57-2.60 (2H, m, ArCH₂), 2.81-2.83 (2H, m, ArCH₂CH₂), 5.81 (1H, dt, *J* 11.9, 1.3, CH=C(CH₃)₂), 7.11-7.33 (7H, m, ArH), 7.57 (1H, d, *J* 11.7, Tosyl-C=CH), 7.79 (2H, d, *J* 8.2, ArH); δ_{C} (125 MHz, CDCl₃) 19.0, 21.6, 27.0, 28.8, 35.4, 118.8, 126.1, 127.2, 128.0, 128.4, 129.8, 134.0, 136.3, 137.4, 141.4, 143.8, 148.1.

Attempted reduction of (*E*)-1-methyl-4-((6-methyl-1-phenylhepta-3,5-dien-3-yl)sulfonyl)benzene 2-(3,5-dimethylphenoxy)-1-phenylethan-1-one **6.1.45** with **4.1.15**



The general procedure for UV-activated reductions was applied to substrate **6.1.45** (170 mg, 0.5 mmol) using SED **4.1.15** (853 mg, 3.0 mmol) for 72 h at room temperature. The reaction mixture was then subjected to the general acidic workup procedure and the resulting crude material was purified by column chromatography

(5-20 % EtOAc/hexane) to afford toluenesulfinic acid **4.2.38** as yellow crystals (20 mg, 26 %). M.pt. 82-84 °C. (lit. 81 °C); $\nu_{\max}(\text{neat}/\text{cm}^{-1})$ 2799, 2450, 1596, 1486, 1300, 1080, 1065, 1024, 800; δ_{H} (500 MHz, CDCl_3) 2.44 (3H, s, ArCH_3), 4.22 (1H, bs, SO_2H), 7.33 (2H, d, J 8.1, ArH), 7.60 (2H, d, J 8.1, ArH); δ_{C} (125 MHz, CDCl_3) 21.3, 128.5, 129.3, 129.9, 130.5, 131.2, 134.5; m/z (ESI): 155 ($[\text{M}-\text{H}]^-$). The spectral data were consistent with the literature data.¹⁴¹ The ^1H NMR and GCMS spectra of the crude material after workup had revealed that no starting material was present.

Blank reaction: SED (6 eq.), UV-free experiment was performed following the general procedure. The starting material **6.1.45** was recovered (128 mg, 77 %) with spectral data as previously reported.

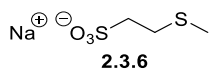
Blank reaction: SED-free, UV-active experiment was performed following the general procedure. The starting material **6.1.45** was recovered (150 mg, 90 %) with spectral data as previously reported.

7.8 Experimental for Chapter 6.2

General procedure for the Birch reduction

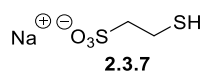
All glassware was dried overnight in an oven. A three-necked 25 mL round-bottomed flask equipped with a stirrer bar was charged with the substrate. One neck was attached to a dry-ice condenser, a second neck was attached to a vacuum line and the third neck was subsealed. The flask was evacuated and back-filled with argon thrice. Then, the vacuum line was disconnected and replaced with an inlet for liq. NH₃. The condenser was then filled with dry ice and acetone upon which liq. NH₃ was condensed out until the flask was about 3/4 filled and the substrate was fully dissolved. Meanwhile, in the glovebox, the required metal was cut and weighed into a vial which was then capped and brought out of the glovebox. The subseal was detached from the reaction flask while ensuring a steady argon flow and the sodium was added portionwise. The metal pieces were cut again just before addition to expose a fresh surface.

Synthesis of Methyl-coenzyme M sodium salt **2.3.6**



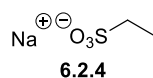
Coenzyme M sodium salt **2.3.7** (12.5 mmol, 1.0 eq) was dissolved in a solution of NaOMe in methanol (0.5 M, 1.0 eq.). Methyl iodide was then added portionwise with vigorous stirring at room temperature which resulted in the formation of a white emulsion. The reaction was then refluxed for 15 h. After evaporation of the solvent, the crude product was dissolved in water and precipitated with acetone. The precipitate was collected and crystallised thrice from hot EtOH/H₂O to yield methyl coenzyme M **2.3.6** as colourless plates (355 mg, 15 %). δ_{H} (500 MHz, D₂O) 2.09 (s, 3H, SCH₃), 2.80 (m, 2H, CH₂SCH₃), 3.10 (m, 2H, CH₂SO₃⁻); δ_{C} (125 MHz, D₂O) 14.3, 27.6, 50.6; MALDI (ESI) 154.90 ([M-Na]⁻, 70 %), 25.99 (100). The spectral data were consistent with the literature data.⁷⁷

Analysis of commercially available coenzyme M sodium salt **2.3.7**



δ_{H} (500 MHz, D₂O) 2.83 (2H, m, AA'BB' splitting pattern, SHCH₂), 3.12 (2H, m, AA'BB' splitting pattern, CH₂SO₃⁻); δ_{C} (500 MHz, D₂O) 17.9, 53.9; MALDI (ESI) 140.9 ([M-Na]⁻, 25 %), 108.9 (20)].

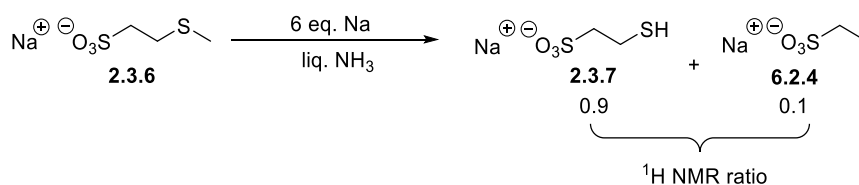
Analysis of commercially available sodium ethyl sulfonate **6.2.4**



δ_{H} (500 MHz, D₂O) 1.18 (3H, t, *J* 7.6, CH₂CH₃), 2.80 (2H, q, *J* 7.6, CH₂CH₃); δ_{C} (500 MHz, D₂O) 7.9, 44.9; MALDI (ESI) 109.0 ([M-Na]⁻, 100 %).

Birch reduction of Methyl coenzyme M sodium salt **2.3.6** using sodium

1st attempt (using workup and freeze-dry apparatus)

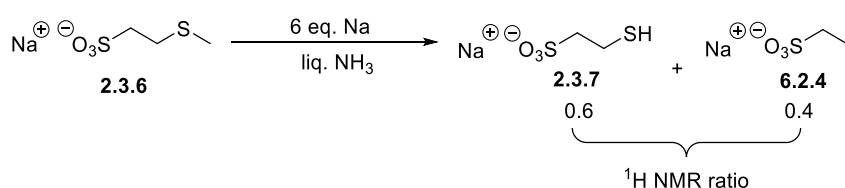


A 3-necked 100 mL RB flask equipped with a stirrer bar was charged with methyl-coenzyme M (299.0 mg, 1.68 mmol), evacuated and then flushed with argon. A dry-ice condenser was then attached to the flask and liq. NH₃ (60 mL) was condensed into the reaction. It was ensured that the starting material was completely dissolved before the addition of Na (10.1 mmol, 6.0 eq.). The reaction was left to reflux for 1 h, stirred for another 7 h before quenching with MeOH (5 mL) and 6N HCl (20 mL). The quenched reaction mixture was left to stir overnight before conducting a work up with CH₂Cl₂ (3 x 10 mL). The organic extracts were combined, washed with brine, dried over Na₂SO₄. The suspension was filtered and the solvent was removed under reduced pressure. The crude product was analysed by ¹H NMR and showed no potential product from the reaction. After repeated attempts, water and other volatile compounds were removed from the aqueous phase using the freeze-dry technique

which resulted in large amounts of white salt. Analysis of the white salt by ^1H NMR (500 MHz, D_2O) showed sodium coenzyme M **2.3.7** and sodium ethyl sulfonate **6.2.4** in a 0.9:0.1 product ratio based on integration of the ^1H NMR spectrum. The spectral data were consistent with those of the commercial product.

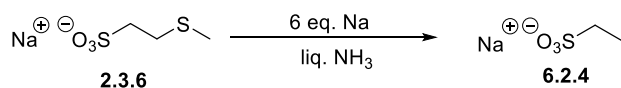
Broad peaks potentially due to the large amounts of NH_4^+ salts were also observed in the ^1H NMR spectrum (500 MHz, D_2O , 7.18-7.44 ppm). A second attempt at the Birch reduction was conducted.

2nd attempt (immediate analysis of the reaction mixture after solvent was evaporated)



The standard procedure for the Birch reduction experiments was adopted using methyl coenzyme M sodium salt **2.3.6** (180.0 mg, 1.0 mmol) and sodium (140 mg, 6.0 mmol). The reaction was refluxed for 1 h and then left to stir at room temperature for 7 h. A white powder remained when the solvent was evaporated. A small portion of the residue (10 mg) was then used for analysis. Analysis of the white powder by ^1H NMR showed a mixture of co-enzyme M sodium salt **2.3.7** and sodium ethanesulfonate **6.2.4** as the main components of the crude material with 0.6:0.4 product ratio based on integration of the ^1H NMR spectrum. The spectral data were consistent with those of the commercial products.

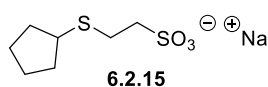
3rd attempt (immediate analysis of the reaction mixture after solvent was evaporated)



The Birch reduction was repeated in a similar fashion as the second attempt. In the event, ^1H NMR analysis of the crude product revealed that coenzyme M sodium salt **2.3.7** was not present. Nevertheless, sodium ethanesulfonate **6.2.4** was present as the

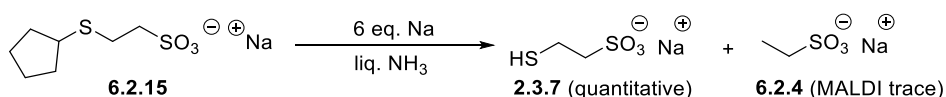
The reaction was refluxed for 1 h and then left to stir at room temperature for 7 h. A white residue remained when the solvent was evaporated. A small portion of the residue was then used for analysis. Analysis of the white powder by ^1H NMR (500 MHz, D_2O) showed a mixture of coenzyme M sodium salt **2.3.7** and sodium ethanesulfonate **6.2.4**. The Birch reduction was attempted twice; each yielded similar results. The product distribution of **2.3.7:6.2.4** based on ^1H NMR spectra analysis are as follows: 1st attempt: 0.6:0.4. 2nd attempt: 0.5:0.5. The spectral data were consistent with those of the commercial products.

Synthesis of Cyclopentyl coenzyme M **6.2.15**



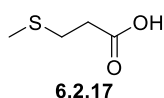
A freshly made solution of 2N NaOH in MeOH (540 mg, 13.5 mmol) was added to a suspension of coenzyme M sodium salt (1 g, 6.1 mmol) and stirred vigorously at room temperature for 0.5 h during which the suspension turned to a pale red solution. The reaction was then cooled to 0 °C and cyclopentyl bromide (2.0 mL, 19.0 mmol) was added portionwise whereupon a suspension formed. MeOH (10 mL) was added to aid stirring and the reaction was left for 16 h after which the solvent was removed under reduced pressure. The crude material was dissolved in minimal hot water and precipitated using acetone. The resulting solid was filtered off and the purification repeated. The resulting product was then dried under vacuum with desiccant to afford cyclopentyl coenzyme M sodium salt **6.2.15** (960 mg, 68 %). Decomp. 290-292 °C; [Found: $[\text{M}-\text{Na}]^-$ 209.0313. $\text{C}_7\text{H}_{13}\text{O}_3\text{S}_2$ ($\text{M}-\text{Na}$)⁻ requires 209.0312; ν_{max} (neat/ cm^{-1}) 3600 (br), 2958, 2868, 1448, 1423, 1172, 1047, 798; δ_{H} (500 MHz, D_2O) 1.46-1.68 (6H, m), 2.00-2.02 (2H, m) 2.89-2.91 (2H, m, CH_2SO_3^-), 3.12-3.14 (2H, m, SCH_2), 3.21 (1H, m, SCH (cyclopentyl)); δ_{C} (125 MHz, D_2O) 23.9, 24.9, 32.7, 42.9, 50.7.

Birch reduction of cyclopentyl coenzyme M sodium salt **6.2.15** using sodium



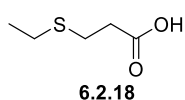
The standard procedure for the Birch reduction experiments was adopted using cyclopentyl coenzyme M sodium salt **6.2.15** (233 mg, 1.0 mmol) and sodium (140 mg, 6.0 mmol). The reaction was refluxed for 1 h and then left to stir at room temperature for 7 h. A white residue remained when the solvent was evaporated. A small portion of the residue was then used for analysis. Analysis of the white powder by ^1H NMR showed only coenzyme M sodium salt **2.3.7** with data as previously reported. A trace of sodium ethanesulfonate **6.2.4** was detectable only by MALDI (i.e., not observed by ^1H NMR). MALDI (ESI) 109.0 ($[\text{M}-\text{Na}]^-$, 40 %). This trace of **6.2.4** could be a result of fragmentation of coenzyme M sodium salt **2.3.7** during the analysis and not necessarily resulting from the Birch reduction.

Synthesis of 3-(methylthio)propionic acid **6.2.17**



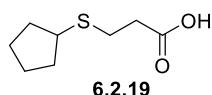
A freshly made solution of 2N NaOH in MeOH (601 mg, 15.0 mmol) was added to a suspension of 3-mercaptopropionic acid (0.44 mL, 5.0 mmol) and stirred vigorously at room temperature. The reaction was then cooled to 0 °C and methyl iodide (0.4 mL, 6.5 mmol) was added portionwise, whereupon a suspension formed. MeOH (5 mL) was added to aid stirring and the reaction was left for 12 h after which the solvent was removed under reduced pressure. The crude material was purified by column chromatography (20 % EtOAc/hexane) on silica gel to afford 3-(methylthiopropionic) acid **6.2.17** as a colourless oil (600 mg, 74 %). [Found: $[\text{M}+\text{H}]^+$ 121.0315. $\text{C}_4\text{H}_9\text{O}_2\text{S}$ requires 121.0318]; ν_{max} (neat/ cm^{-1}) 3026 (br), 1703, 1427, 1261, 933; δ_{H} (500 MHz, CDCl_3) 2.16 (3H, s, SCH_3), 2.70 (2H, t, J 7.3, $\text{CH}_3\text{SCH}_2\text{CH}_2$), 2.78 (2H, t, J 7.3, $\text{CH}_3\text{SCH}_2\text{CH}_2$), 10.22 (1H, bs, CO_2H); δ_{C} (125 MHz, CDCl_3) 15.0, 28.1, 33.7, 177.7.

Synthesis of 3-(ethylthio)propionic acid **6.1.18**



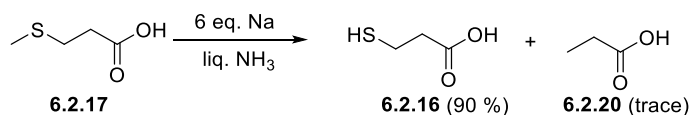
A freshly made solution of 2N NaOH in MeOH (601 mg, 15.0 mmol) was added to a suspension of 3-mercaptopropionic acid (0.44 mL, 5.0 mmol) and stirred vigorously at room temperature. The reaction was then cooled to 0 °C and ethyl bromide (0.56 mL, 7.5 mmol) was added portionwise whereupon a suspension formed. MeOH (8 mL) was added to aid stirring and the reaction was left for 12 h after which the solvent was removed under reduced pressure. The resulting crude material was purified by column chromatography (20 % EtOAc/hexane) on silica gel to afford 3-(ethylthiopropionic) acid **6.2.18** as a colourless oil (595 mg, 89 %). [Found: $[M+H]^+$ 135.0471. $C_5H_{11}O_2S$ requires 135.0474]; ν_{\max} (neat/ cm^{-1}) 3026 (br), 1705, 1411, 1259, 923; δ_H (500 MHz, $CDCl_3$) 1.29 (3H, t, J 7.4, SCH_2CH_3), 2.58 (2H, q, J 7.4, SCH_2CH_3), 2.69 (2H, t, J 7.4, $SCH_2CH_2CO_2H$), 2.80 (2H, t, J 7.4, $SCH_2CH_2CO_2H$), 9.52 (1H, bs, CO_2H), δ_C (125 MHz, $CDCl_3$) 14.1, 25.5, 25.6, 34.1, 177.6.

Synthesis of 3(cyclopentylthio)propionic acid **6.2.19**



A freshly made solution of 2N NaOH in MeOH (601 mg, 15.0 mmol) was added to a suspension of 3-mercaptopropionic acid (0.44 mL, 5.0 mmol) and stirred vigorously at room temperature. The reaction was then cooled to 0 °C and cyclopentyl bromide (0.81 mL, 7.5 mmol) was added portionwise whereupon a suspension formed. MeOH (10 mL) was added to aid stirring and the reaction was left for 12 h after which the solvent was removed under reduced pressure. The crude material was purified by column chromatography (20 % EtOAc/hexane) on silica gel to afford 3-(cyclopentylthio)propionic acid **6.2.19** as a colourless oil (610 mg, 70 %). [Found: $[M+H]^+$ 175.0783. $C_8H_{11}O_2S$ requires 175.0787]; ν_{\max} (neat/ cm^{-1}) 3021 (br), 1704, 1412, 1261, 1242, 1197, 1141, 929; δ_H (500 MHz, $CDCl_3$) 1.48-1.62 (4H, m, 2 x CH_2 (Cyp)), 1.72-1.80 (2H, m, CH_2 (Cyp)), 1.99-2.07 (2H, m, CH_2 (Cyp)), 2.68 (2H, t, J 7.2, $SCH_2CH_2CO_2H$), 2.83 (2H, t, J 7.2, $SCH_2CH_2CO_2H$), 3.12 (1H, quintet, J 7.2, CH (Cyp)); δ_C (125 MHz, $CDCl_3$) 24.2, 25.9, 33.3, 34.2, 43.4, 177.3.

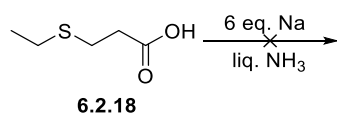
Birch reduction of 3-(methylthio)propionic acid **6.2.17** using sodium



The standard procedure for the Birch reduction experiments was adopted using 3-(methylthio)propionic acid **6.2.17** (120 mg, 1.0 mmol) and sodium (140 mg, 6.0 mmol). The reaction was refluxed for 1 h and then left to stir at room temperature for 7 h. A white residue remained when the solvent was evaporated. A small portion of the residue was then used for analysis. Analysis of the white powder by ^1H NMR showed full conversion of the starting material with 3-mercaptopropionic acid **6.2.16** as the major product and a trace of propionic acid **6.2.20**. The white powder was dissolved in 2N HCl (10 mL) and extracted with CH_2Cl_2 (3 x 5 mL). The organic extractions were combined, washed with brine, and dried over Na_2SO_4 and filtered. Solvent was removed under reduced pressure and the crude material was purified by column chromatography (5 % EtOAc/hexane) to afford 3-mercaptopropionic acid **6.2.16** as a colourless oil (98 mg, 90 %). ν_{max} (neat/ cm^{-1}) 3020 (br), 2670, 2581, 1711, 1423, 1270, 1208, 1160, 1045, 990; δ_{H} (500 MHz, CDCl_3) 1.70 (1H, t, J 7.2, CH_2SH), 2.73-2.79 (4H, m, $\text{SCH}_2\text{CH}_2\text{CO}_2\text{H}$), 10.94 (1H, bs, CO_2H); δ_{C} (125 MHz, CDCl_3) 20.2, 39.0, 177.2; (GCMS, CI, CH_4) 106.2 (100 %), 88.0 (50), 61.4 (70). The spectral data were consistent with the literature data.²⁷⁰

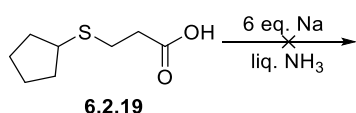
^1H NMR of the white powder after the reaction showed both **6.2.16** and **6.2.20**. For **6.2.16**: δ_{H} (500 MHz, D_2O) 2.29 (2H, m, SCH_2CH_2), 2.55 (2H, m, SCH_2CH_2). For **6.2.20**: δ_{H} (500 MHz, D_2O) 0.99 (3H, t, J 7.8, $\text{CH}_3\text{CH}_2\text{CO}_2\text{H}$), 2.12 (2H, q, J 7.8, $\text{CH}_2\text{CO}_2\text{H}$).

Attempted Birch reduction of 3-(ethylthio)propionic acid **6.2.18** using sodium



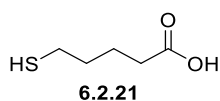
The standard procedure for the Birch reduction experiments was adopted using 3-(ethylthio)propionic acid **6.2.18** (135 mg, 1.0 mmol) and sodium (140 mg, 6.0 mmol). The reaction was refluxed for 1 h and then left to stir at room temperature for 7 h. A white residue remained when the solvent was evaporated. A small portion of the residue was then used for analysis. Analysis of the white powder by ^1H NMR showed only starting material **6.2.18**. The white powder was dissolved in 2N HCl (10 mL) and extracted with CH_2Cl_2 (3 x 5 mL). The organic extractions were combined, washed with brine, dried over Na_2SO_4 and filtered. Solvent was removed under reduced pressure and the crude material was purified by column chromatography (5 % EtOAc/hexane) to recover the starting material **6.2.18** as a colourless oil (116 mg, 88 %) with data as previously reported.

Attempted Birch reduction of 3-(cyclopentylthio)propionic acid **6.2.19** using sodium



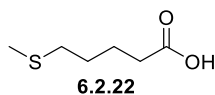
The standard procedure for the Birch reduction experiments was adopted using 3-(cyclopentylthio)propionic acid **6.2.19** (174 mg, 1.0 mmol) and sodium (140 mg, 6.0 mmol). The reaction was refluxed for 1 h and then left to stir at room temperature for 7 h. A white residue remained when the solvent was evaporated. A small portion of the residue was then used for analysis. Analysis of the white powder by ^1H NMR showed only starting material. The white powder was dissolved in 2N HCl (10 mL) and extracted with CH_2Cl_2 (3 x 5 mL). The organic extractions were combined, washed with brine, and dried over Na_2SO_4 and filtered. Solvent was removed under reduced pressure and the crude material was purified by column chromatography (5 % EtOAc/hexane) to recover the starting material **6.2.19** as a colourless oil (128 mg, 95 %) with data as previously reported.

Synthesis of 5-mercaptopentanoic acid **6.2.21**



A solution of 5-bromovaleric acid (12.1 mmol, 1.0 eq) in EtOH (20 mL) was stirred vigorously whereupon a solution of thiourea (18.4 mmol, 1.5 eq) in EtOH (15 mL) was added portionwise. The reaction was then warmed to reflux during which the solution became faint yellow. After refluxing for 20 h, the reaction was cooled to room temperature and a solution of NaOH (7.5M, 25 mL) was added portionwise with stirring. The reaction was then stirred at 90 °C for 19 h, cooled to 0 °C and then treated with 2M H₂SO₄ until pH 1 was reached. The reaction mixture was then extracted with CH₂Cl₂ (3 x 50 mL). The organic extracts were combined, washed with brine, dried over Na₂SO₄ and filtered. Solvent was removed under reduced pressure to give 5-mercaptopentanoic acid **6.2.21** as a pale yellow oil (1.5 g, 97 %). ν_{\max} (neat/cm⁻¹) 3200 (br), 2933 (br), 2572 (br), 1701, 1411, 1228, 929; δ_{H} (500 MHz, CDCl₃) 1.38 (t, 1H, *J* 8.0, CH₂SH), 1.68-1.80 (m, 4H, 2 x CH₂), 2.40 (t, 2H, *J* 6.3, CH₂CO₂H), 2.58 (q, 2H, *J* 6.7, CH₂SH); δ_{C} (125 MHz, CDCl₃) 22.8, 23.7, 32.7, 32.9, 179.0; (GCMS, CI, CH₄) 134.9 (10 %), 117.1 (100), 101.0 (90), 89.2 (40) The spectral data were consistent with the literature data.²⁷¹

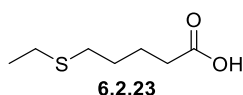
Synthesis of 5-(methylthio)pentanoic acid **6.2.22**



A solution of 2N NaOH (2.1 mL, 4.3 mmol) was added dropwise to a solution of 5-mercaptopentanoic acid (190 mg, 1.4 mmol) in EtOH (5 mL) at 0 °C. The reaction was stirred at 0 °C for 0.5 h whereupon methyl iodide (0.12 mL, 1.84 mmol) was added to the reaction in one portion. The reaction was left to stir at room temperature for 12 h after which the solvent was removed from the reaction mixture and the crude material was partitioned between 2N HCl (10 mL) and CH₂Cl₂ (15 mL). The aqueous layer was extracted further with CH₂Cl₂ (2 x 15 mL). The organic extracts were combined, washed with brine, dried over Na₂SO₄ and filtered. Solvent was removed under reduced pressure and the crude material was purified by column chromatography (20 % EtOAc/hexane) on silica gel to afford 5-(methylthio)pentanoic acid **6.2.22** as colourless crystals (115 mg, 55 %). M.pt. 21-22 °C; [Found: [M-H]⁻ 147.0487. C₆H₁₁O₂S (M-H) requires 147.0485]; ν_{\max} (neat)/cm⁻¹

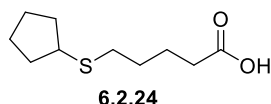
3400 (br), 3030, 2937, 2916, 1703, 1411, 1280, 1230, 931; δ_{H} (500 MHz, CDCl_3) 1.65-1.67 (2H, m, SCH_2CH_2), 1.74-1.76 (2H, m, $\text{SCH}_2\text{CH}_2\text{CH}_2$), 2.10 (3H, s, SCH_3), 2.40 (2H, t, J 7.0, CH_3SCH_2), 2.52 (2H, t, J 7.0, $\text{CH}_2\text{CO}_2\text{H}$), 11.20 (1H, bs, CO_2H); δ_{C} (125 MHz, CDCl_3) 15.5, 23.7, 28.4, 33.5, 33.8, 179.2.

Synthesis of 5-(ethylthio)pentanoic acid **6.2.23**



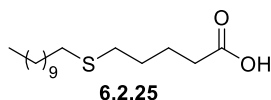
A solution of 2N NaOH (173 mg, 7.5 mmol) in EtOH (5 mL) was added dropwise to a solution of 5-mercaptopentanoic acid (403 mg, 3.0 mmol) in EtOH (5mL) at 0 °C. The reaction was stirred at 0 °C for 0.5 h whereupon ethyl bromide (0.45 mL, 6.0 mmol) was added to the reaction in one portion. The reaction was left to stir at temperature for 12 h after which solvent was removed from the reaction mixture and the crude material was partitioned between 2N HCl (10 mL) and CH_2Cl_2 (15 mL). The aqueous layer was extracted further with CH_2Cl_2 (2 x 15 mL). The organic extractions were combined, washed with brine, dried over Na_2SO_4 and filtered. Solvent was removed under reduced pressure and the crude material was purified by column chromatography (20 % EtOAc/hexane) on silica gel to afford 5-(ethylthio)pentanoic acid **6.2.23** as a colourless oil (242 mg, 50 %). [Found: $[\text{M}-\text{H}]^-$ 161.0645. $\text{C}_7\text{H}_{13}\text{O}_2\text{S}$ (M-H) requires 161.0642]; ν_{max} (neat/ cm^{-1}) 3150 (br), 2929 (br), 2667, 1703, 1411, 1282, 931; δ_{H} (500 MHz, CDCl_3) 1.28 (3H, t, J 7.4, SCH_2CH_3), 1.63-1.81 (4H, m, 2 x CH_2), 2.41 (2H, t, J 7.4, $\text{CH}_2\text{CO}_2\text{H}$), 2.57 (4H, m, 2 x CH_2); δ_{C} (125 MHz, CDCl_3) 14.3, 23.3, 25.4, 28.4, 30.7, 32.9, 178.6. The spectral data were consistent with the literature data.²⁷²

Synthesis of 5-(cyclopentyl)pentanoic acid **6.2.24**



A solution of 2N NaOH (173 mg, 7.5 mmol) in EtOH (5 mL) was added dropwise to a solution of 5-mercaptopentanoic acid **6.2.21** (403 mg, 3.0 mmol) in EtOH (5 mL) at 0 °C. The reaction was stirred at 0 °C for 0.5 h whereupon cyclopentyl bromide (0.65 mL, 6.0 mmol) was added to the reaction in one portion. The reaction was left to stir at temperature for 12 h after which solvent was removed from the reaction mixture and the crude material was partitioned between 2N HCl (10 mL) and CH₂Cl₂ (15 mL). The aqueous layer was extracted further with CH₂Cl₂ (2 x 15 mL). The organic extracts were combined, washed with brine, dried over Na₂SO₄ and filtered. Solvent was removed under reduced pressure and the crude material was purified by column chromatography (20 % EtOAc/hexane) on silica gel to afford 5-(cyclopentylthio)pentanoic acid **6.2.24** as a colourless oil (490 mg, 81 %). [Found: [M-H]⁻ 201.0956. C₁₀H₁₇O₂S (M-H) requires 201.0955]; $\nu_{\max}(\text{neat}/\text{cm}^{-1})$ 3026 (br), 1705, 1411, 1282, 1230, 933; δ_{H} (500 MHz, CDCl₃) 1.50-1.72 (10H, m, 5 x CH₂), 2.00-2.02 (2H, m, CH₂), 2.40 (2H, t, *J* 7.0, SCH₂CH₂), 2.57 (2H, t, *J* 7.0, SCH₂CH₂), 3.09 (1H, m, *J* 7.0, Cyp(CH)); δ_{C} (125 MHz, CDCl₃) 23.5, 24.3, 28.6, 30.9, 33.0, 33.3, 43.4, 178.9.

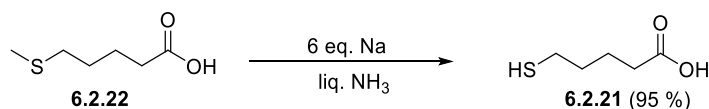
Synthesis of 5-(dodecylthio)pentanoic acid **6.2.25**



A solution of 2N NaOH (9.0 mL, 3.0 eq) was added dropwise to a solution of 5-mercaptopentanoic acid **6.2.21** (5.0 mmol, 1.0 eq) in EtOH (10 mL) at 0 °C. The reaction was stirred at 0 °C for 0.5 h and undecyl bromide (3.3 eq, 20 mmol) was added in one portion. The reaction was left to stir at room temperature for 12 h after which the solvent was removed from the reaction mixture and the crude material was partitioned between 2N HCl (50 mL) and CH₂Cl₂ (30 mL). The aqueous layer was extracted further with CH₂Cl₂ (2 x 30 mL). The organic extracts were combined, washed with brine, dried over Na₂SO₄ and filtered. Solvent was removed under reduced pressure and the crude material was purified by column chromatography (20 % EtOAc/hexane) on silica gel to afford 5-(undecylthio)pentanoic acid **6.2.25** as a white solid (1.8 g, 92 %). M.pt. 54-55 °C; Found: [M-H]⁻ 301.2203. C₁₇H₃₃O₂S (M-

H) requires 301.2207]; ν_{\max} (neat)/ cm^{-1} 3042 (br), 2916, 1689, 1469, 1282, 1226, 1182, 914 (br), 717; δ_{H} (500 MHz, CDCl_3) 0.90 (3H, t, J 7.2, CH_2CH_3), 1.28 (16H, bs, 8 x CH_2), 1.40 (2H, m, CH_2), 1.55-1.79 (4H, m, 2 x CH_2), 1.80-1.81 (2H, m, CH_2), 2.41 (2H, t, J 7.3, CH_2), 2.50-2.56 (4H, m, 2 x CH_2); δ_{C} (125 MHz, CDCl_3) 14.1, 22.7, 23.8, 28.9, 29.2, 29.3, 29.4, 29.5, 29.6, 29.7, 31.6, 31.9, 32.2, 33.6, 179.7.

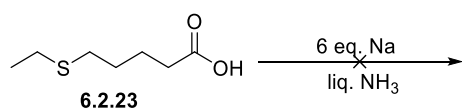
Birch reductions of 5-(methylthio)pentanoic acid **6.2.22** using sodium



The general procedure for Birch reductions was applied to 5-(methylthio)pentanoic acid **6.2.22** (82 mg, 0.55 mmol) with sodium (80 mg, 3.3 mmol). The reaction was refluxed for 1 h and then left to stir at room temperature for 7 h. A white residue remained when the solvent was evaporated. The ^1H NMR analysis of the white residue revealed that the crude material was mainly 5-mercaptopentanoic acid **6.2.21**. The crude material was carefully quenched with 2N HCl (5 mL) and the aqueous layer was extracted with CH_2Cl_2 (3 x 5 mL). The organic fractions were combined, washed with brine, dried over Na_2SO_4 and filtered. The crude material was then purified by column chromatography (20 % EtOAc/hexane) to afford 5-mercaptopentanoic acid **6.2.21** (86 mg, 95 %) with data as previously reported.

A second attempt of the Birch reduction using sodium yielded a similar result; 5-mercaptopentanoic acid **6.2.21** (86 mg, 95 %) with data previously reported. (Reflux time and duration of the reaction were kept constant).

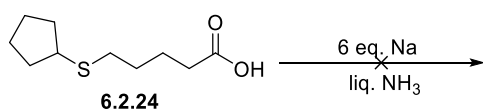
Attempted Birch reduction of 5-(ethylthio)pentanoic acid **6.2.23** using sodium



The general procedure for Birch reductions was applied to 5-(ethylthio)pentanoic acid **6.2.23** (90 mg, 0.55 mmol) with sodium (80 mg, 3.3 mmol). The reaction was

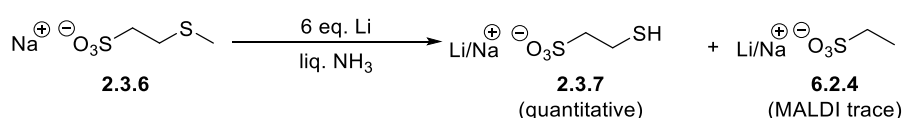
refluxed for 1 h and then left to stir at room temperature for 8 h. A white residue remained when the solvent was evaporated. The ^1H NMR analysis revealed that the crude material was mainly starting material. The crude material was carefully quenched with 2N HCl (5 mL) and the aqueous layer was extracted with CH_2Cl_2 (3 x 5 mL). The organic fractions were combined, washed with brine, dried over Na_2SO_4 and filtered. Solvent was removed under reduced pressure and the crude material was purified by column chromatography (5-20 % EtOAc/hexane) to afford quantitative recovery of the starting material **6.2.23** (85 mg, 94 %) with data as previously reported.

Attempted Birch reduction of 5-(cyclopentylthio)pentanoic acid **6.2.24** using sodium



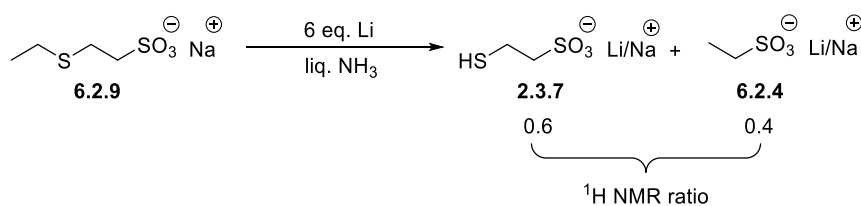
The general procedure for Birch reductions was applied to 5-(cyclopentylthio)pentanoic acid **6.2.24** (202 mg, 1.0 mmol) with sodium (180 mg, 6.0 mmol). The reaction was refluxed for 1 h and then left to stir at room temperature for 8 h. A white residue remained when the solvent was evaporated. The ^1H NMR analysis revealed that the crude material was mainly starting material **6.2.24**. The crude material was carefully quenched with 2N HCl (5 mL) and the aqueous layer was extracted with CH_2Cl_2 (3 x 5 mL). The organic fractions were combined, washed with brine, dried over Na_2SO_4 and filtered. Solvent was removed under reduced pressure and the crude material was purified by column chromatography (5-20 % EtOAc/hexane) to afford quantitative recovery of the starting material **6.2.24** (186 mg, 92 %) with data as previously reported.

Birch reduction of Methyl coenzyme M sodium salt **2.3.6** using lithium



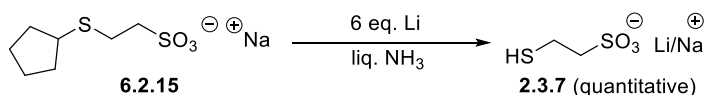
The standard procedure for the Birch reduction experiments was adopted using methyl coenzyme M sodium salt **2.3.6** (180.0 mg, 1.0 mmol) and lithium (42 mg, 6.0 mmol). The reaction was refluxed for 1 h and then left to stir at room temperature for 8 h. A white powder remained when the solvent was evaporated. A small portion of the residue was then used for analysis. Analysis of the white powder by ^1H NMR (500 MHz, D_2O) showed full conversion of the starting material and coenzyme M metal salt **2.3.7** as the only product with data consistent with that of the commercially available product previously reported. The Birch reduction was repeated which yielded similar results. MALDI spectra for both experiments showed that ethanesulfonate **6.2.4** was also present in small traces. MALDI (ESI) 109.0 ($[\text{M}-\text{Na}]^-$, 45 %). However, this trace of **6.2.4** could be a result of fragmentation of coenzyme M **2.3.7** during the analysis and not necessarily resulting from the Birch reduction.

Birch reduction of Ethyl coenzyme M sodium salt **6.2.9** using lithium



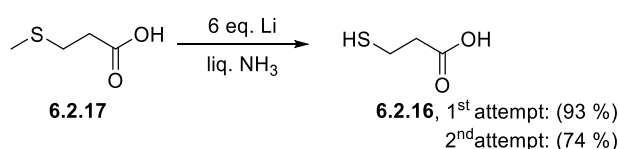
The standard procedure for the Birch reduction experiments was adopted using ethyl coenzyme M sodium salt **6.2.9** (191.0 mg, 1.0 mmol) and lithium (42 mg, 6.0 mmol). The reaction was refluxed for 1 h and then left to stir at room temperature for 7 h. A white residue remained when the solvent was evaporated. A small portion of the residue was then used for analysis. Analysis of the white powder by ^1H NMR (500 MHz, D_2O) showed a mixture of coenzyme M metal salt **2.3.7** and ethanesulfonate **6.2.4**, with 0.6:0.4 product ratio based on the integration of the spectrum. The ^1H NMR data for sodium co-enzyme M **2.3.7** and ethanesulfonate **6.2.4** were consistent with that of the commercially available product previously reported.

Birch reduction of cyclopentyl coenzyme M sodium salt **6.2.15** using lithium



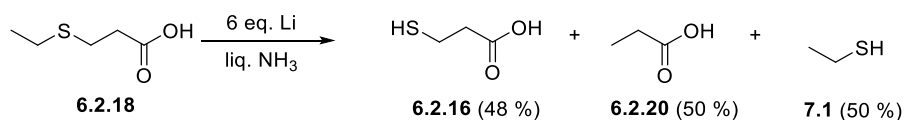
The standard procedure for the Birch reduction experiments was adopted using cyclopentyl coenzyme M sodium salt **6.2.15** (233 mg, 1.0 mmol) and lithium (42 mg, 6.0 mmol). The reaction was refluxed for 1 h and then left to stir at room temperature for 8 h. A white residue remained when the solvent was evaporated. A small portion of the residue was then used for analysis. Analysis of the white powder by ^1H NMR (500 MHz, D_2O) showed coenzyme M sodium salt **2.3.7** as the sole product with the data consistent with that of the commercially available product previously reported.

Birch reduction of 3-(methylthio)propionic acid **6.2.17** using lithium



The standard procedure for the Birch reduction experiments was adopted using 3-(methylthio)propionic acid **6.2.17** (120 mg, 1.0 mmol) and lithium (42 mg, 6.0 mmol). The reaction was refluxed for 1 h and then left to stir at room temperature for 7 h. A white residue remained when the solvent was evaporated. A small portion of the residue was then used for analysis. Analysis of the white powder by ^1H NMR showed 3-mercaptopropionic acid **6.2.16** as the sole product. The white powder was dissolved in 2N HCl (10 ml) and extracted with CH_2Cl_2 (3 x 5 mL). The organic extracts were combined, washed with brine, dried over Na_2SO_4 and filtered. Solvent was removed under reduced pressure and the crude material was purified by column chromatography (5 % EtOAc/hexane) to afford 3-mercaptopropionic acid **6.2.16** (98 mg, 93 %) with data as previously reported. The Birch reduction was repeated which afforded 3-mercaptopropionic acid **6.2.16** (78 mg, 74 %) as the sole product.

Attempted Birch reduction of 3-(ethylthio)propionic acid **6.2.18** using lithium

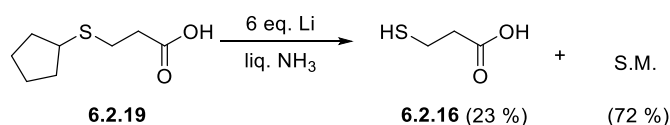


The standard procedure for the Birch reduction experiments was adopted using 3-(ethylthio)propionic acid **6.2.18** (135 mg, 1.0 mmol) and lithium (42 mg, 6.0 mmol). The reaction was refluxed for 1 h and then left to stir at room temperature for 7 h. A white residue remained when the solvent was evaporated. A small portion of the residue was then used for analysis. Analysis of the white powder by ^1H NMR (500 MHz, D_2O) showed compounds **6.2.16**, **6.2.20** and **7.1** were present. Integration of the spectrum estimated these products to be in equal distribution. The white powder was dissolved in 2N HCl (10 mL) and extracted with CH_2Cl_2 (3 x 5 mL). The organic extracts were combined, washed with brine, dried over Na_2SO_4 and filtered. Solvent was removed under reduced pressure and the crude material was purified by column chromatography (5 % EtOAc/hexane) to afford 3-mercaptopropionic acid **6.2.16** (65 mg, 48 %) with data as previously reported.

From the ^1H NMR of the crude material; **6.2.20**: δ_{H} (500 MHz, D_2O) 0.99 (3H, t, J 7.3, $\text{CH}_3\text{CH}_2\text{CO}_2\text{H}$), 2.45 (2H, q, J 7.3, $\text{CH}_3\text{CH}_2\text{CO}_2\text{H}$).

From the ^1H NMR of the crude material; **7.1**: δ_{H} (500 MHz, D_2O) 1.09 (3H, t, J 7.3, $\text{CH}_3\text{CH}_2\text{SH}$), 2.33 (2H, q, J 7.2, CH_2SH).

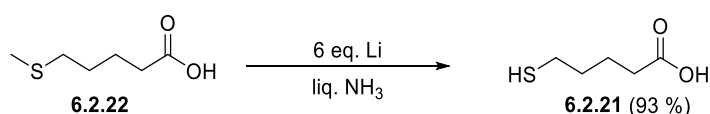
Attempted Birch reduction of 3-(cyclopentylthio)propionic acid **6.2.19** using lithium



The standard procedure for the Birch reduction experiments was adopted using 3-(cyclopentylthio)propionic acid **6.2.19** (174 mg, 1.0 mmol) and lithium (42 mg, 6.0 mmol). The reaction was refluxed for 1 h and then left to stir at room temperature for 7 h. A white residue remained when the solvent was evaporated. A small portion of the residue was then used for analysis. Analysis of the white powder by ^1H NMR (500 MHz, D_2O) showed that both 3-mercaptopropionic acid **6.2.16** and the starting

material **6.2.19** were present. The white powder was dissolved in 2N HCl (10 mL) and extracted with CH₂Cl₂ (3 x 5 mL). The organic extracts were combined, washed with brine, dried over Na₂SO₄ and filtered. Solvent was removed under reduced pressure and the crude material was purified by column chromatography (5 % EtOAc/hexane) to recover the starting material **6.2.19** (99 mg, 72 %) and 3-mercaptopropionic acid **6.2.16** (17 mg, 23 %). The data for both compounds were as previously reported.

Birch reduction of 5-(methylthio)pentanoic acid **6.2.22** using lithium



The general procedure for Birch reductions was applied to 5-(methylthio)pentanoic acid **6.2.22** (82 mg, 0.55 mmol) with lithium (25 mg, 3.3 mmol). The reaction was refluxed for 1 h and then left to stir at room temperature for 7 h. A white residue remained when the solvent was evaporated. A small portion of the residue was then used for analysis. Analysis of the white powder by ¹H NMR (500 MHz, D₂O) showed full conversion of the starting material and **6.2.21** as the only product. The crude material was carefully quenched with 2N HCl (5 mL) and the aqueous was extracted with CH₂Cl₂ (3 x 5 mL). The organic extracts were combined, washed with brine, dried over Na₂SO₄ and filtered. The crude material was then purified by column chromatography (20 % EtOAc/hexane) to afford 5-mercaptopentanoic acid **6.2.21** (85 mg, 93 %) with data as previously reported.

Attempted Birch reduction of 5-(ethylthio)pentanoic acid **6.2.23** using lithium



The general procedure for Birch reductions was applied to 5-(ethylthio)pentanoic acid **6.2.23** (90 mg, 0.55 mmol) with lithium (25 mg, 3.3 mmol). The reaction was

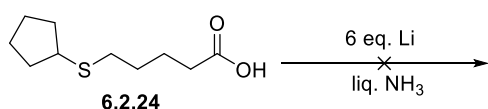
refluxed for 1 h and then left to stir at room temperature for 7 h. A white residue remained when the solvent was evaporated. A small portion of the residue was then used for analysis. Analysis of the white powder by ^1H NMR (500 MHz, D_2O) revealed that the crude material contained compounds **6.2.21**, **6.6.26**, and **6.2.23**. This was confirmed by GCMS(CI) in which three distinct peaks with the related mass ions were detected. The crude material was carefully quenched with 2N HCl (5 mL) and then aqueous was extracted with CH_2Cl_2 (3 x 5 mL). The organic extracts were combined, washed with brine, dried over Na_2SO_4 and filtered. Solvent was removed under reduced pressure and the crude material was purified by column chromatography (5-20 % EtOAc/hexane) to afford the starting material **6.2.23** (32 mg, 36 %), 5-mercaptopentanoic acid **6.2.21** (50 mg, 45 %) and pentanoic acid **6.2.26** (10 mg, 18 %). The spectral data for **6.2.23** and **6.2.21** were as previously reported.

Pentanoic acid **6.2.26**: colourless oil; δ_{H} (500 MHz, CDCl_3) 0.90-0.95 (3H, m, CH_3), 1.15-1.72 (4H, m, $\text{CH}_3\text{CH}_2\text{CH}_2$), 2.32-2.38 (2H, m, $\text{CH}_2\text{CO}_2\text{H}$); δ_{C} (125 MHz, CDCl_3) 13.5, 22.1, 26.6, 33.7, 180.3; (GCMS, CI, CH_4) 103.0 (100), 85.1 (20 %). The spectral data were consistent with the literature data.²⁷³

From the GCMS (CI, CH_4) of the crude material:

- i) pentanoic acid **6.2.26**; retention time of 7.50 min, 103.0 ($[\text{M}+\text{H}]^+$, 100 %), 85.1 (20).
- ii) 5-mercaptopentanoic acid **6.2.21**; retention time of 10.1 min, 157.0 ($[\text{M}+\text{Na}]^+$, 10 %), 135.1 (5), 117.0 (100).
- iii) 5-(ethylthio)pentanoic acid **6.2.23**; retention time of 11.5 min, 163.0 ($[\text{M}+\text{H}]^+$, 5 %), 145.0 (100), 117.1 (30).

Attempted Birch reduction of 5-(cyclopentylthio)pentanoic acid **6.2.24** using lithium



The general procedure for Birch reductions was applied to 5-(cyclopentylthio)pentanoic acid (202 mg, 1.0 mmol) with lithium (42 mg, 6.0 mmol). The reaction was refluxed for 1 h and then left to stir at room temperature for 7 h. A white residue remained when the solvent was evaporated. A small portion of the residue was then used for analysis. Analysis of the white powder by ^1H NMR (500 MHz, D_2O) revealed that the crude material was mainly starting material. The crude material was carefully quenched with 2N HCl (5 mL) and the aqueous was extracted with CH_2Cl_2 (3 x 5 mL). The organic fractions were combined, washed with brine, dried over Na_2SO_4 and filtered. Solvent was removed under reduced pressure and the crude material was purified by column chromatography (5-20 % EtOAc/hexane) to afford quantitative recovery of the starting material (190 mg, 94 %) with data as previously reported.

Chapter 8 References

- (1) S.A. Weissman, D. Zewge, *Tetrahedron* **2005**, *61*, 7833.
- (2) B.C. Ranu, S. Bhar, *Organic Preparations and Procedures International* **1996**, *28*, 371.
- (3) *Protective Groups in Organic Chemistry*; 4th ed.; T.W. Greene, P.G.M. Wuts, Wiley, **2006**.
- (4) S.S. Kim, H.C. Jung, *Synthesis* **2003**, *2003*, 2135.
- (5) L. Syper, *Tetrahedron Lett.* **1966**, *7*, 4493.
- (6) S. Torii, H. Tanaka, T. Inokuchi, S. Nakane, M. Akada, N. Saito, T.J. Sirakawa, *J. Org. Chem.* **1982**, *47*, 1647.
- (7) Y. Oikawa, T. Tanaka, K. Horita, T. Yoshioka, O. Yonemitsu, *Tetrahedron Lett.* **1984**, *25*, 5393.
- (8) F.G. Mann, M.J. Pragnell, *J. Chem. Soc.* **1965**, *52*, 4120.
- (9) E. Alonso, D.J. Ramón, M. Yus, *Tetrahedron*, **1997**, *53*, 14355.
- (10) E.A. Mayeda, L.L. Miller, J.F. Wolf, *J. Am. Chem. Soc.* **1972**, *94*, 6812.
- (11) Hartung, W. H.; Simonoff, R. In *Organic Reactions*; John Wiley & Sons, Inc.: 2004.
- (12) L.L. Miller, J.F. Wolf, E.A. Mayeda, *J. Am. Chem. Soc.* **1971**, *93*, 3306.
- (13) E.A. Mayeda, L.L. Miller, J.F. Wolf, *J. Am. Chem. Soc.* **1972**, *94*, 6812.
- (14) W. Schmidt, E. Steckhan, *Angew. Chem., Int. Ed.* **1978**, *17*, 673.
- (15) D. Sahu, C.H. Tsai, H.Y. Wei, K.C. Ho, F.-C.; Chang, C.-W. Chu, *J. Mater. Chem.* **2012**, *22*, 7945.
- (16) H.B. Goodbrand, N.X. Hu, *J. Org. Chem.* **1998**, *64*, 670.
- (17) W. Schmidt, E. Steckhan, *Angew. Chem., Int. Ed.* **1979**, *18*, 802.
- (18) W. Schmidt, E. Steckhan, *Angew. Chem., Int. Ed.* **1979**, *18*, 801.
- (19) R.I. Walter, *J. Am. Chem. Soc.* **1966**, *88*, 1923.
- (20) H.J. Liu, J. Yip, K.S. Shia, *Tetrahedron Lett.* **1997**, *38*, 2253.
- (21) B. Wang, Z. Yin, Y. Li, T.X. Yang, X.-B. Meng, Z.-J. Li, *J. Org. Chem.* **2011**, *76*, 9531.

- (22) K. Ishihara, Y. Hiraiwa, H. Yamamoto, *Synlett.* **2000**, 48, 80.
- (23) J.R. Falck, D.K. Barma, R. Baati, C. Mioskowski, *Angew. Chem., Int. Ed.* **2001**, 40, 1281.
- (24) F.A. Anet, E. Leblanc, *J. Am. Chem. Soc.* **1957**, 79, 2649.
- (25) T. Green, P.B.M. Wuts, *Protective Groups in Organic Synthesis*; 2nd ed.; New York, 1991.
- (26) H.G. Weinig, P. Passacantilli, M. Colapietro, G. Piancatelli, *Tetrahedron Lett.* **2002**, 43, 4613.
- (27) Y. Kato, T. Mase, *Tetrahedron Lett.* **1999**, 40, 8823.
- (28) K. Kusuda, J. Inanaga, M. Yamaguchi, *Tetrahedron Lett.* **1989**, 30, 2945.
- (29) K.C. Nicolaou, S.P. Ellery, J.S. Chen, *Angew. Chem., Int. Ed.* **2009**, 48, 7140.
- (30) T. Ankner, G. Hilmersson, *Tetrahedron*, **2009**, 65, 10856.
- (31) E. Furimsky, *Appl. Catal., A.* **2000**, 199, 147.
- (32) D.G. Levine, R.H. Schlosberg, B.G. Silbernagel, *PNAS*, **1982**, 79, 3365.
- (33) A.L. Marshall, P.J. Alaimo, *Chem. Eur. J.* **2010**, 16, 4970.
- (34) J. Zakzeski, P.C.A. Bruijninx, A.L. Jongerius, B.M. Weckhuysen, *Chem. Rev.* **2010**, 110, 3552.
- (35) T.H. Parsell, B.C. Owen, I. Klein, T.M. Jarrell, C.L. Marcum, L.J. Hauptert, L.M. Amundson, H.I. Kenttamaa, F. Ribeiro, J.T. Miller, M.M. Abu-Omar, *Chem.Sci.* **2013**, 4, 806.
- (36) J.D. Nguyen, B.S. Matsuura, C.R.J. Stephenson, *J. Am. Chem. Soc.* **2013**, 136, 1218.
- (37) J.D. Nguyen, B. Reiss, C. Dai, C.R.J. Stephenson, *Chem. Commun.* **2013**, 49, 4352.
- (38) A.G. Sergeev, J.F. Hartwig, *Science*, **2011**, 332, 439.
- (39) E. Wenkert, E.L. Michelotti, C.S. Swindell, M. Tingoli, *J. Org. Chem.* **1984**, 49, 4894.
- (40) E. Wenkert, E.L. Michelotti, C.S. Swindell, *J. Am. Chem. Soc.* **1979**, 101, 2246.

- (41) A. Fedorov, A.A. Toutov, N.A. Swisher, R.H. Grubbs, *Chem Sci.* **2013**, *4*, 1640.
- (42) A.A. Toutov, W.B. Liu, K.N. Betz, A. Fedorov, B.M. Stoltz, R.H. Grubbs, *Nature* **2015**, *518*, 80.
- (43) H. Gilman, D. Aoki, D.J. Wittenberg, *Am. Chem. Soc.* **1959**, *81*, 1107.
- (44) S. Son, F.D. Toste, *Angew. Chem., Int. Ed.* **2010**, *49*, 3791.
- (45) C. Fabbri, M. Bietti, O. Lanzalunga, *J. Org. Chem.* **2005**, *70*, 2720.
- (46) C.K. Prier, D.A. Rankic, D.W.C. MacMillan, *Chem. Rev.* **2013**, *113*, 5322.
- (47) E. Jahn, U. Jahn, *Angew. Chem., Int. Ed.* **2014**, *49*, 13326
- (48) T.P. Yoon, M.A. Ischay, J. Du, *Nat. Chem.* **2010**, *2*, 527.
- (49) C.S. Lancefield, O.S. Ojo, F. Tran, N.J. Westwood, *Angew. Chem., Int. Ed.* **2015**, *54*, 258.
- (50) K. Lam, I.E. Marko, *Chem. Commun.* **2009**, *1*, 95.
- (51) K. Lam, I.E. Marko, *Org. Lett.* **2008**, *10*, 2773.
- (52) K. Lam, I.E. Marko, *Tetrahedron* **2009**, *65*, 10930.
- (53) D. Rackl, V. Kais, P. Kreitmeier, O. Reiser, O. Beilstein *J. Org. Chem* **2014**, *10*, 2157.
- (54) S.W. Ragsdale, *J. Biol. Chem.* **2009**, *284*, 18571.
- (55) Y. Shimazaki, O. Yamauchi, *Chem. Biodiv.* **2012**, *9*, 1635.
- (56) R. Mazingo, D.E. Wolf, S.A. Harris, K.J. Folkers, *J. Am. Chem. Soc.* **1943**, *65*, 1013.
- (57) N. Barbero, R. Martin, *Org. Lett.* **2012**, *14*, 796.
- (58) F. Dénès, M. Pichowicz, G. Povie, P. Renaud, *Chem. Rev.* **2014**, *114*, 2587.
- (59) W.B. Gara, B.P. Roberts, *Organomet. Chem.* **1977**, *135*, 20.
- (60) B.P. Roberts, *Chem. Soc. Rev.* **1999**, *28*, 25.
- (61) S.J. Cole, J.N. Kirwan, B.P. Roberts, C.R. Willis, *J. Chem. Soc., Perkin Trans. 1*, **1991**, *1*, 103.
- (62) D.H.R. Barton, D. Crich, A. Löbberding, S.Z. Zard, *Tetrahedron*, **1986**, *42*, 2329

- (63) A.V. Burasov, C.A. Paddon, F.L. Bhatti, T.J. Donohoe, R.G. Compton, *J. Phys. Org. Chem.* **2007**, *20*, 144.
- (64) M.G. Severin, M.C. Arevalo, G. Farnia, E. Vianello, *J. Phys. Org. Chem.* **1987**, *91*, 466.
- (65) M.G. Severin, M.C. Arevalo, F. Maran, E. Vianello, *J. Phys. Org. Chem* **1993**, *97*, 150.
- (66) N.C.L. Wood, C.A. Paddon, F.L. Bhatti, T.J. Donohoe, R.G. Compton, *J. Phys. Org. Chem.* **2007**, *20*, 732.
- (67) E. Baciocchi, T. Del Giacco, P. Giombolini, O. Lanzalunga, *Tetrahedron* **2006**, *62*, 6566.
- (68) E. Baciocchi, T.D. Giacco, F. Elisei, M.F. Gerini, M. Guerra, A. Lapi, P. Liberali, *J. Am. Chem. Soc.* **2003**, *125*, 16444.
- (69) D. Dondi, P. Cimino, V. Barone, A. Buttafava, O. Lanzalunga, A. Faucitano, *Tetrahedron Lett.* **2011**, *52*, 4097.
- (70) B. Jaun, R.K. Thauer, *Met. Ions Life Sci.* **2007**, *2*, 323.
- (71) T.J. Lie, K.C. Costa, B. Lupa, S. Korpole, W.B. Whitman, J.A. Leigh, *PNAS* **2012**, *109*, 15473.
- (72) W.E. Balch, G.E. Fox, L.J. Magrum, C.R. Woese, R.S. Wolfe, *Microbiol. Mol. Biol. Rev.* **1979**, *43*, 260.
- (73) R.S. Wolfe, *Microbiol. Res.* **1991**, *45*, 1.
- (74) R.K. Thauer, *Microbiol. Res.* **1998**, *144*, 2377.
- (75) D.A. Livingston, A. Pfaltz, J. Schreiber, A. Eschnmoser, D. Ankel-Fuchs, J. Moll, R. Jaenchen, R.K. Thauer, *Helv. Chim. Acta.* **1984**, *67*, 334.
- (76) Y. Ahn, J.A. Krzycki, H.G. Floss, *J. Am. Chem. Soc.* **1991**, *113*, 4700.
- (77) S. Scheller, M. Goenrich, S. Mayr, R.K. Thauer, B. Jaun, *Angew. Chem., Int. Ed.* **2010**, *49*, 8112.
- (78) Y.C. Horng, D.F. Becker, S.W. Ragsdale, *Biochem.* **2001**, *40*, 12875.
- (79) L.G. Bonacker, S. Baudner, E. Mörschel, R. Böcher, R.K. Thauer, *FEBS Lett.* **1993**, *217*, 587.
- (80) R.K. Thauer, *Angew. Chem., Int. Ed.* **2010**, *49*, 6712.
- (81) W.L. Ellefson, R.S. Wolfe, *J. Biol. Chem.* **1981**, *256*, 4259.

- (82) U. Ermler, W. Grabarse, S. Shima, M. Goubeaud, R.K. Thauer, *Science* **1997**, 278, 1457.
- (83) N. Yang, M. Reiher, M. Wang, J. Harmer, E.C. Duin, *J. Am. Chem. Soc.* **2007**, 129, 11028.
- (84) J. Harmer, C. Finazzo, R. Piskorski, S. Ebner, E.C. Duin, M. Goenrich, R.K. Thauer, M. Reiher, A. Schweiger, D. Hinderberger, B. Jaun, *J. Am. Chem. Soc.* **2008**, 130, 10907.
- (85) D. Hinderberger, R. Piskorski, M. Goenrich, R.K. Thauer, A. Schweiger, J. Harmer, B. Jaun, *Angew. Chem., Int. Ed.* **2006**, 45, 3602.
- (86) R. Sarangi, M. Dey, S.W. Ragsdale, *Biochem.* **2009**, 48, 3146.
- (87) B. Jaun, R.K. Thauer, *Met. Ions Life Sci.* **2009**; 6, 115.
- (88) W. Grabarse, F. Mahlert, S. Shima, E.C. Duin, M. Goubeaud, S. Sima, R.K. Thauer, V. Lamzin, U. Ermler, *J. Mol. Biol.* **2001**, 309, 315.
- (89) S. Shima, M. Goubeaud, D. Vinzenz, R.K. Thauer, U.J. Ermler, *Biochem.* **1997**, 121, 829.
- (90) J. Ellermann, S. Rospert, R.K. Thauer, M. Bokranz, A. Klein, M. Voges, A. Berkessel, *FEBS Lett.* **1989**, 184, 63.
- (91) C. Kratky, A. Fassler, A. Pfaltz, B. Krautler, B. Jaun, A. Eschenmoser, *J. Chem. Soc. Chem. Commun* **1984**, 1368.
- (92) U. Ermler, W. Grabarse, S. Shima, M. Goubeaud, R.K. Thauer, *Science* **1997**, 278, 1457.
- (93) S. Rospert, R. Boecher, S.P.J. Albracht, R.K. Thauer, *FEBS Lett.* **1991**, 291, 371.
- (94) M. Goubeaud, G. Schreiner, R.K. Thauer, *FEBS Lett.* **1997**, 243, 110.
- (95) J. Telser, R. Davydov, Y.C. Horng, S.W. Ragsdale, B.M. Hoffman, *J. Am. Chem. Soc.* **2001**, 123, 5853.
- (96) S.L. Chen, M.R. Blomberg, P.E. Siegbahn, *PCCP.* **2014**, 16, 14029.
- (97) J. Telser, Y.C. Horng, D.F. Becker, B.M. Hoffman, S.W. Ragsdale, *J. Am. Chem. Soc.* **1999**, 122, 182.
- (98) S.L. Chen, M.R. Blomberg, P.E. Siegbahn, *Chem.Eur. J.* **2012**, 18, 6309.

- (99) M. Goubeaud, G. Schreiner, R.K. Thauer, *Eur. J. Biochem.* **1997**, *243*, 110.
- (100) E.C. Duin, M.L. McKee, *J. Phys. Chem. B* **2008**, *112*, 2466.
- (101) G. Färber, W. Keller, C. Kratky, B. Jaun, A. Pfaltz, C. Spinner, A. Kobelt, A. Eschenmoser, *Helv. Chim. Acta* **1991**, *74*, 697.
- (102) A. Berkessel, R.K. Thauer, *Angew. Chem., Int. Ed.* **1995**, *34*, 2247.
- (103) B. Jaun, *Helv. Chim. Acta* **1990**, *73*, 2209.
- (104) Q. Tang, P.E. Carrington, Y.C. Horng, M.J. Maroney, S.W. Ragsdale, D.F. Bocian, *J. Am. Chem. Soc.* **2002**, *124*, 13242.
- (105) L.G. Bonacker, S. Baudner, E. Moerschel, R. Boecher, R.K. Thauer, *Eur. J. Biochem.* **1993**, *217*, 587.
- (106) J. Ellermann, R. Hedderich, R. Böcher, R.K. Thauer, *Eur. J. Biochem.* **1988**, *172*, 669.
- (107) S. Scheller, M. Goenrich, R.K. Thauer, B. Jaun, *J. Am. Chem. Soc.* **2013**, *135*, 14975.
- (108) *Metal Ions in Biological Systems*; ed. H. Sigel, S. Astrid, Dekker Inc., 1993; Vol. 29., Chapter 2, pg 52.
- (109) V. Pelmeshnikov, M.R. Blomberg, P.E. Siegbahn, R.H. Crabtree, *J. Am. Chem. Soc.* **2002**, *124*, 4039.
- (110) W. Buckel, R. Keese, *Angew. Chem., Int. Ed.* **1995**, *34*, 1502.
- (111) W. Buckel, *FEBS Letters* **1996**, *389*, 20.
- (112) S.L. Chen, V. Pelmeshnikov, M.R.A. Blomberg, P.E. Siegbahn, *J. Am. Chem. Soc.* **2009**, *131*, 9912.
- (113) V. Pelmeshnikov, P.E. Siegbahn, *J. Biol. Inorg. Chem.* **2003**, *8*, 653.
- (114) A. Berkessel, *Bioorganic Chemistry* **1991**, *19*, 101.
- (115) U. Ermler, *J. Chem. Soc., Dalton Trans.* **2005**, *21*, 3451.
- (116) S. Rospert, M. Voges, A. Berkessel, S.P.J. Albracht, R.K. Thauer, *Eur. J. Biochem.* **1992**, *210*, 101.
- (117) F. Wudl, G.M. Smith, E.J. Hufnagel, *Chem. Commun.* **1970**, 1453.
- (118) P.R. Ashton, V. Balzani, J. Becher, A. Credi, M.C.T. Fyfe, G. Mattersteig, S. Menzer, M.B. Nielsen, F.M. Raymo, J.F. Stoddart, M. Venturi, D.J. Williams, *J. Am. Chem. Soc.* **1999**, *121*, 3951.

- (119) V. E. Kampar, V. R. Kokars, O. Neiland, *Zh. Obshch. Khim.* **1980**, 50, 2057.
- (120) R.J. Fletcher, C. Lampard, J.A. Murphy, N. Lewis, *J. Chem. Soc., Perkin Trans. I* **1995**, 623.
- (121) O. Callaghan, C. Lampard, A.R. Kennedy, J.A. Murphy, *J. Chem. Soc., Perkin Trans. I* **1999**, 995.
- (122) G.V. Tormos, M.G. Bakker, P. Wang, M.V. Lakshmikantham, M.P. Cava, R.M. Metzger, *J. Am. Chem. Soc.* **1995**, 117, 8528.
- (123) R.L. Pruett, J.T. Barr, K.E. Rapp, C.T. Bahner, J.D. Gibson, R.H. Lafferty, *J. Am. Chem. Soc.* **1950**, 72, 3646.
- (124) C. Burkholder, W.R. Dolbier, M. Médebielle, *J. Org. Chem* **1998**, 63, 5385.
- (125) W. Carpenter, *J. Org. Chem* **1965**, 30, 3082.
- (126) O. Amiri-Attou, T. Terme, P. Vanelle, *Synlett* **2005**, 20, 3047.
- (127) Y. Nishiyama, A. Kobayashi, *Tetrahedron Lett.* **2006**, 47, 5565.
- (128) M. Mahesh, J.A. Murphy, F. LeStrat, H.P. Wessel, *Beilstein J Org. Chem.* **2009**, 5, 1.
- (129) S. Hünig, D. Scheutzow, H. Schlaf, H. Quast, *Liebigs Ann. Chem.* **1973**, 765, 110.
- (130) R.P. Thummel, V. Gouille, B. Chen, *J. Org. Chem.* **1989**, 54, 3057.
- (131) Z. Shi, R.P. Thummel, *J. Org. Chem.* **1995**, 60, 5935.
- (132) T.A. Taton, P. Chen, *Angew. Chem. Int. Ed. Engl.* **1996**, 35, 1011.
- (133) J.A. Murphy, T.A. Khan, S.Z. Zhou, D.W. Thomson, M. Mahesh, *Angew. Chem. Int. Ed. Engl.* **2005**, 44, 1356.
- (134) J.R. Ames, M.A. Houghtaling, D.L. Terrian, T.P. Mitchell, *Can. J. Chem* **1997**, 75, 28.
- (135) J.A. Murphy, S.Z. Zhou, D.W. Thomson, F. Schoenebeck, M. Mahesh, S.R. Park, T. Tuttle, L.E.A. Berlouis, *Angew. Chem. Int. Ed. Engl.* **2007**, 46, 5178.
- (136) J. Garnier, J.A. Murphy, S.Z. Zhou, A.T. Turner, *Synlett* **2008**, 14, 2127.

- (137) J. Garnier, E.A. Leonard, Berlouis, Andrew T. Turner, J. A. Murphy, *Beilstein J. Org. Chem* **2010**, *6*, 73.
- (138) C.P. Andrieux, J. Pinson, *J. Am. Chem. Soc.* **2003**, *125*, 14801.
- (139) E. Doni, S. O'Sullivan, J.A. Murphy, *Angew. Chem., Int. Ed.* **2013**, *52*, 2239.
- (140) L.A. Paquette, G.D. Maynard, *J. Org. Chem* **1989**, *54*, 5054.
- (141) S. O'Sullivan, E. Doni, T. Tuttle, J.A. Murphy, *Angew. Chem., Int. Ed.* **2014**, *53*, 474.
- (142) P. Maslak, R.D. Guthrie, *J. Am. Chem. Soc.* **1986**, *108*, 2628.
- (143) J. Mortensen, J. Heinze, *Angew. Chem., Int. Ed.* **1984**, *23*, 84.
- (144) A.P. Davis, A.J. Fry, *J. Phys. Chem. A.* **2010**, *114*, 12299.
- (145) E. Cahard, F. Schoenebeck, J. Garnier, S.P.Y. Cutulic, S.Z. Zhou, J.A. Murphy, *Angew. Chem., Int. Ed.* **2012**, *51*, 3673.
- (146) J. Garnier, Ph.D. Thesis, University of Strathclyde. **2009**.
- (147) S.Z. Zhou, J.A. Murphy, *Unpublished results*.
- (148) E.J. Corey, P.L. Fuchs, *Tetrahedron Lett.* **1972**, *13*, 3769.
- (149) P.E. Pfeffer, L.S. Silbert, J.M. Chirinko, *J. Org. Chem.* **1972**, *37*, 451
- (150) Salmon. R.; *Encyclopedia of Reagents for Organic Synthesis*; 4th ed.; John Wiley & Sons, Ltd, **2001**.
- (151) H.B. Gray, J.R. Winkler, *PNAS.* **2005**, *102*, 3534.
- (152) E. Doni, B. Mondal, S. O'Sullivan, T. Tuttle, J.A. Murphy, *J. Am. Chem. Soc.* **2013**, *135*, 10934.
- (153) S. O'Sullivan, Thesis, University of Strathclyde, **2014**
- (154) S.P.Y. Cutulic, J.A. Murphy, H. Farwaha, S.Z. Zhou, E. Chrystal, *Synlett.* **2008**, *2008*, 2132.
- (155) T.K. Hutton, K. Muir, D.J Procter, *J. Org. Lett.* **2002**, *4*, 2345.
- (156) T.K. Hutton, K. Muir, D.J Procter, *J. Org. Lett.* **2003**, *5*, 4811.
- (157) M. Szostak, M. Spain, D. Parmar, D.J. Procter, *Chem. Commun.* **2012**, *48*, 330.
- (158) K.G. Liu, M.H. Lambert, L.M. Leesnitzer, W. Oliver Jr, R.J. Ott, K.D. Plunket, L.W. Stuart, P.J. Brown, T.M. Willson, D.D. Sternbach, *Bioorganic & Medicinal Chemistry Letters*, **2001**, *11*, 2959.

- (159) D. Parmar, H. Matsubara, K. Price, M. Spain, D.J. Procter, *J. Am. Chem. Soc.* **2012**, *134*, 12751.
- (160) K. K. Georgieff, *Can. J. Chem.* **1952**, *30*, 332.
- (161) C. D. Hurd, F.H. Blunck, *J. Am. Chem. Soc.* **1938**, *60*, 2419.
- (162) H. Werner, P. Joachim, V. F. Karl, S. Hardo, P. Sigberg *US Patent No: US3996246*, **1976**.
- (163) M.A. Casadei, A.D. Martino, C. Galli, L. Mandolini, *Gazzetta Chimica Italiana* **1986**, *116*, 659
- (164) R.M. Beesley, C.K. Ingold, J.F. Thorpe, *J. Chem. Soc. Trans.* **1915**, *107*, 1080.
- (165) T.C. Bruice, U.K. Pandit, *J. Am. Chem. Soc.* **1960**, *82*, 5858.
- (166) M.E. Jung, M. Kiankarimi, *J. Org. Chem* **1998**, *63*, 2968.
- (167) R. Salvio, L. Mandolini, C. Savelli, *J. Org. Chem.* **2013**, *78*, 7259.
- (168) M.Y. Yeh, H.C. Lin, T.S. Lim, S.L. Lee, C.H. Chen, W. Fann, T.Y. Luh, *Macromolecules* **2007**, *40*, 9238.
- (169) M.D. Forbes, J.T. Patton, T.L. Myers, H.D. Maynard, D.W. Smith, G.R. Schulz, K.B. Wagener, *J. Am. Chem. Soc.* **1992**, *114*, 10978.
- (170) J. Jager, T. Graafland, H. Schenk, A.J. Kirby, J.B.F.N Engberts, *J. Am. Chem. Soc.* **1984**, *106*, 139.
- (171) P. von Ragué Schleyer, *J. Am. Chem. Soc.* **1961**, *83*, 1368.
- (172) S. Searles, E.F. Lutz, M. Tamres, *J. Am. Chem. Soc.* **1960**, *82*, 2932.
- (173) H.B. Gray, J. Halpern, *PNAS* **2005**, *102*, 3533.
- (174) S.S. Skourtis, I.A. Balabin, T. Kawatsu, D.N. Beratan, *PNAS* **2005**, *102*, 3552.
- (175) R.H. Goldsmith, L.E. Sinks, R.F. Kelley, L.J. Betzen, W. Liu, E.A. Weiss, M.A. Ratner, M.R. Wasielewski, *PNAS* **2005**, *102*, 3540.
- (176) C.C. Page, C.C. Moser, X. Chen, P.L. Dutton, *Nature* **1999**, *402*, 47.
- (177) R. Zhao, J. Lind, G. Merenyi, T.E. Eriksen, *J. Am. Chem. Soc.* **1994**, *116*, 12010.
- (178) P.S. Surdhar, D.A. Armstrong, *The Journal of Physical Chemistry* **1987**, *91*, 6532.
- (179) A. Harriman, *J. Phys. Chem. A.* **1987**, *91*, 6102.

- (180) M.R. DeFelippis, C.P. Murthy, M. Faraggi, M.H. Klapper, *Biochem.* **1989**, 28, 4847.
- (181) C.L. Hawkins, M. Davies, J. *Biochimica et Biophysica Acta (BBA) - Bioenergetics*, **2001**, 1504, 196.
- (182) S. Rustgi, P. Riesz, *Int. J. Radiat. Biol.* **1978**, 34, 449.
- (183) J.B. D'Arcy, M.D. Sevilla, *Radiat. Phys. Chem* **1979**, 13, 119.
- (184) M. Faraggi, J.L. Redpath, Y. Tal, *Radiat. Res.* **1975**, 64, 452.
- (185) H. Fischer, *Chem. Rev.* **2001**, 101, 3581.
- (186) A. Studer, *Chem. Soc. Rev.* **2004**, 33, 267.
- (187) C. Wetter, K. Jantos, K. Woithe, A. Studer, *Org. Lett.* **2003**, 5, 2899.
- (188) E.C. Juenge, M.D. Corey, D.A. Beal, *Tetrahedron* **1971**, 27, 2671.
- (189) H.B. Burgi, J.D. Dunitz, E. Shefter, *J. Am. Chem. Soc.* **1973**, 95, 5065.
- (190) Y. Ryu, A.I. Scott, *Tetrahedron Lett.* **2003**, 44, 7499.
- (191) S.V. More, T.T. Chang, Y.-P. Chiao, S.C. Jao, C.K. Lu, W.S. Li, *Eur. J. Med. Chem.* **2013**, 64, 169.
- (192) C.J. Hayes, N.M.A. Herbert, N.M. Harrington-Frost, G. Pattenden, *Org. Biol. Chem.* **2005**, 3, 316.
- (193) J. Grimshaw, *Electrochemical Reactions and Mechanisms in Organic Chemistry*; Grimshaw, J., 2nd Ed.; Elsevier Science B.V.: Amsterdam, 2000, pg 100.
- (194) *Organic Sulfur Chemistry: Structure and Mechanism*; 2nd ed. B. Raton; CRC Press, 1992.
- (195) M. Julia, J.M, Paris, *Tetrahedron Lett.* **1973**, 14, 4833.
- (196) P.J. Kocienski, B. Lythgoe, S. Ruston, *J. Chem. Soc. Perkin Trans. I*, **1978**, 829.
- (197) P.R. Blakemore, *J. Chem. Soc. Perkin Trans. I*, **2002**, 2563.
- (198) G.E. Keck, K.A. Savin, M.A. Weglarz, *J. Org. Chem* **1995**, 60, 3194.
- (199) J.I. Seeman, *Journal of Chemical Education*, **1986**, 63, 42.
- (200) H.E. Zimmerman, *Acc. Chem. Res.* **2011**, 45, 164.
- (201) P.P. Edwards, in *Advances in Inorganic Chemistry*; ed.; H.J. Emeléus, A.G. Sharpe, Academic Press: 1982; Vol. 25, pg 135.

- (202) C.A. Kraus, *J. Am. Chem. Soc.* **1907**, 29, 1557.
- (203) J.L. Dye, *Science* **2003**, 301, 607.
- (204) J.L. Dye, M.J. Wagner, G. Overney, R.H. Huang, T.F. Nagy, D. Tománek, *J. Am. Chem. Soc.* **1996**, 118, 7329.
- (205) N. Mammano, M.J. Sienko, *J. Am. Chem. Soc.* **1968**, 90, 6322.
- (206) A.M. Stacy, D.C. Johnson, M.J. Sienko, *J. Chem. Phys.* **1982**, 76, 4248.
- (207) D.J. Singh, H. Krakauer, C. Haas, W.E. Pickett, *Nature* **1993**, 365, 39.
- (208) S. Matsuishi, Y. Toda, M. Miyakawa, K. Hayashi, T. Kamiya, M. Hirano, I. Tanaka, H. Hosono, *Science* **2003**, 301, 626.
- (209) E. Zurek, P.P. Edwards, R. Hoffmann, *Angew. Chem., Int. Ed.* **2009**, 48, 8198.
- (210) P. Edwards, *J. Supercond. Nov. Magn.* **2000**, 13, 933.
- (211) E. Duval, P. Rigny, G. Lepoutre, *Chem. Phys. Lett.* **1968**, 2, 237.
- (212) J. Jortner, *J. Chem. Phys.* **1959**, 30, 839.
- (213) U. Olsher, R.M. Izatt, J.S. Bradshaw, N.K. Dalley, *Chem. Rev.* **1991**, 91, 137.
- (214) T.E. Salter, V. Mikhailov, A.M. Ellis, *J. Phys. Chem. A.* **2007**, 111, 8344.
- (215) I.V. Hertel, C. Hüglin, C. Nitsch, C.P. Schulz, *Phys. Rev. Lett.* **1991**, 67, 1767.
- (216) G. Grue-Sorenson, E. Kelstrup, A. Kjaer, J.O. Madsen, *J. Chem. Soc., Perkin Trans. 1*, **1984**, 1091.
- (217) A.S. Bommarius, K. Drauz, K. Günther, G. Knaup, M. Schwarm, *Tetrahedron Assym.* **1997**, 8, 3197.
- (218) J.A. Murphy, J. Garnier, S.R. Park, F. Schoenebeck, S.Z. Zhou, A.T. Turner, *Org. Lett.* **2008**, 10, 1227.
- (219) C.T. Chen, J.H. Kuo, V.D. Pawar, Y.S. Munot, S.S. Weng, C.H. Ku, C.Y. Liu, *J. Org. Chem* **2005**, 70, 1188.
- (220) C.T. Chen, J.H. Kuo, C.H. Li, N.B. Barhate, S.W. Hon, T.W. Li, S.D. Chao, C.C. Liu, Y.C. Li, I.H. Chang, J.S. Lin, C.J. Liu, Y.C. Chou, *Org. Lett.* **2001**, 3, 3729.

- (221) J.M. Grill, J.W. Ogle, S.A. Miller, *J. Org. Chem* **2006**, *71*, 9291.
- (222) M. Ananth Reddy, A. Thomas, G. Mallesham, B. Sridhar, V. Jayathirtha Rao, K. Bhanuprakash, *Tetrahedron Lett.* **2011**, *52*, 6942.
- (223) K. Sato, M. Aoki, J. Takagi, K. Zimmermann, R. Noyori, *Bull. Chem. Soc. Jpn.* **1999**, *72*, 2287.
- (224) K. Ishihara, M. Nakayama, S. Ohara, H. Yamamoto, *Tetrahedron* **2002**, *58*, 8179.
- (225) X.F. Wu, H. Neumann, M. Beller, *Chem. Commun.* **2011**, *47*, 7959.
- (226) L.R. Cafiero, T.S. Snowden, *Org. Lett.* **2008**, *10*, 3853.
- (227) Y. Sawama, Y. Yabe, M. Shigetsura, T. Yamada, S. Nagata, Y. Fujiwara, T. Maegawa, Y. Monguchi, H. Sajiki, *Adv. Synth. Cat.* **2012**, *354*, 777.
- (228) A. Watanabe, *Bull. Chem. Soc. Jpn.* **1963**, *36*, 336.
- (229) T. Ohta, M. Kamiya, M. Nobutomo, K. Kusui, I. Furukawa, *Bull. Chem. Soc. Jpn.* **2005**, *78*, 1856.
- (230) S.P.Y. Cutulic, N.J. Findlay, S.Z. Zhou, E.J.T. Chrystal, J.A. Murphy, *J. Org. Chem.* **2009**, *74*, 8713.
- (231) J.A. Murphy, F. Schoenebeck, N.J. Findlay, D.W. Thomson, S.Z. Zhou, J. Garnier, *J. Am. Chem. Soc.* **2009**, *131*, 6475.
- (232) L. Benati, G. Calestani, R. Leardini, M. Minozzi, D. Nanni, P. Spagnolo, S. Strazzari, *Org. Lett.* **2003**, *5*, 1313.
- (233) R.H. Taaning, L. Thim, J. Karaffa, A.G. Campaña, A.M.; Hansen, T. Skrydstrup, *Tetrahedron* **2008**, *64*, 11884.
- (234) N. Naulet, G.J. Martin, *Tetrahedron Lett.* **1979**, *20*, 1493.
- (235) J.S. Clark, A.G. Dossetter, Y.S. Wong, R.J. Townsend, W.G. Whittingham, C.A. Russell, *J. Org. Chem* **2004**, *69*, 3886.
- (236) C.A. Seizert, E.M. Ferreira, *Chem. Eur. J* **2014**, *20*, 4460.
- (237) L.Y. Jiao, M. Oestreich, *Chem. Eur. J* **2013**, *19*, 10845.
- (238) L. Wu, I. Fleischer, R. Jackstell, I. Profir, R. Franke, M. Beller, *J. Am. Chem. Soc.* **2013**, *135*, 14306.

- (239) S. Chakraborty, H. Dai, P. Bhattacharya, N.T. Fairweather, M.S. Gibson, J.A. Krause, H. Guan, *J. Am. Chem. Soc.* **2014**, *136*, 7869.
- (240) K. Kamata, T. Yamaura, N. Mizuno, *Angew. Chem., Int. Ed.* **2012**, *51*, 7275.
- (241) D.A. Otte, D.E. Borchmann, C. Lin, M. Weck, K.A. Woerpel, *Org. Lett.* **2014**, *16*, 1566.
- (242) Y.Q. Zou, J.R. Chen, X.P. Liu, L.Q. Lu, R.L. Davis, K.A. Jørgensen, W.J. Xiao, *Angew. Chem., Int. Ed.* **2012**, *51*, 784.
- (243) M. Long, D.W. Thornthwaite, S.H. Rogers, G. Bonzi, F.R. Livens, S.P. Rannard, *Chem. Commun.* **2009**, 6406.
- (244) A. Lascaux, G. Delahousse, J. Ghostin, J.P. Bouillon, I. Jabin, *Eur. J. Org. Chem.* **2011**, *2011*, 5272.
- (245) C.C. Chan, X. Huang, *Synthesis* **1982**, 452.
- (246) A.V. Vorogushin, X. Huang, S.L. Buchwald, *J. Am. Chem. Soc.* **2005**, *127*, 8146.
- (247) K.V. Sashidhara, G.R. Palnati, R.P. Dodda, R. Sonkar, A.K. Khanna, G. Bhatia, *Eur. J. Med. Chem.* **2012**, *57*, 302.
- (248) F. Jiménez, M.D. Cruz, C. Zúñiga, M. Martínez, G. Chamorro, F. Díaz, J. Tamariz, *Med. Chem. Res.* **2010**, *19*, 33.
- (249) G.H. Posner, K.A. Canella, *J. Am. Chem. Soc.* **1985**, *107*, 2571.
- (250) J. Buendia, J. Mottweiler, C. Bolm, *Chem. Eur. J* **2011**, *17*, 13877.
- (251) M. Ahmad, J.N. Roberts, E.M. Hardiman, R. Singh, L.D. Eltis, T.D. Bugg, *Biochem.* **2011**, *50*, 5096.
- (252) H.J. Xu, Y.F. Liang, Z.Y. Cai, H.X. Qi, C.Y. Yang, Y.S. Feng, *J. Org. Chem* **2011**, *76*, 2296.
- (253) H. Wang, Y. Ma, H. Tian, A. Yu, J. Chang, Y. Wu, *Tetrahedron* **2014**, *70*, 2669
- (254) M. Zarei, M. Mohamadzadeh, *Tetrahedron* **2011**, *67*, 5832.
- (255) J.B. Lambert, S.M. Wharry, *J. Am. Chem. Soc.* **1982**, *104*, 5857.
- (256) I.W. Still, I. D. Watson, *Synth. Commun.* **2001**, *31*, 1355.
- (257) S. Banerjee, L. Adak, B.C. Ranu, *Tetrahedron Lett.* **2012**, *53*, 2149.

- (258) M.S. Holzwarth, I. Alt, B. Plietker, *Angew. Chem., Int. Ed.* **2012**, *51*, 5351.
- (259) N. Arnau, M. Moreno-Mañas, R. Pleixats, *Tetrahedron* **1993**, *49*, 11019.
- (260) N.M. Yoon, J. Choi, J.H. Ahn, *J. Org. Chem* **1994**, *59*, 3490.
- (261) K. Kobayashi, M. Kawakita, K. Yokota, T. Mannami, K. Yamamoto, O. Morikawa, H. Konishi, *Bull. Chem. Soc. Jpn.* **1995**, *68*, 1401.
- (262) C. Chen, T.R. Dugan, W. Brennessel, D.J. Weix, P.L. Holland, *J. Am. Chem. Soc.* **2014**, *136*, 945.
- (263) G.P. Boldrini, D. Savoia, E. Tagliavini, C. Trombini, A. Umani, *J. Org. Chem* **1985**, *50*, 3082.
- (264) J.H. Cheng, C. Ramesh, H.L. Kao, Y.J. Wang, C.C. Chan, C.F. Lee, *J. Org. Chem.* **2012**, *77*, 10369.
- (265) H. Morita, Y. Oida, T. Ariga, S. Fukomoto, M.C. Sheikh, T. Fujii, T. Yoshimura, *Tetrahedron*, **2011**, *67*, 4672.
- (266) X.S. Wu, Y. Chen, M.B. Li, M.G. Zhou, S.K. Tian, *J. Am. Chem. Soc.* **2012**, *134*, 14694.
- (267) A.A. Lindén, M. Johansson, N. Hermanns, J.E. Bäckvall, *J. Org. Chem.* **2006**, *71*, 3849.
- (268) R.H. Zhu, X.X. Shi, *Synth. Commun.* **2012**, *42*, 1108.
- (269) A. Latorre, I. López, V. Ramírez, S. Rodríguez, J. Izquierdo, F.V. González, C. Vicent, *J. Org. Chem* **2012**, *77*, 5191.
- (270) C. Hedfors, E. Östmark, E. Malmström, K. Hult, M. Martinelle, *Macromolecules* **2005**, *38*, 647.
- (271) Y. Lu, M. Tanasova, B. Borhan, G.E. Reid, *Analytical Chemistry* **2008**, *80*, 9279.
- (272) M. Node, K. Nishide, M. Ochiai, K. Fuji, E. Fujita, *J. Org. Chem* **1981**, *46*, 5163.
- (273) T.M. Shaikh, F.E. Hong, *Tetrahedron* **2013**, *69*, 8929.